SERI/STR-211-2363
UC Category: 63
DE84013002

SERI/STR--211-2363

DE84 013002

Sputtered Amorphous Silicon Solar Cells

Final Report
22 July 1982 - 22 July 1983

A Subcontract Report

T. D. Moustakas
H. P. Maruska
C. R. Wronski

Exxon Research and Engineering Company
Annandale, New Jersey

September 1984

Prepared under Subcontract No. ZB-3-02166-01

SERI Technical Monitor: E. Sabisky

Solar Energy Research Institute
A Division of Midwest Research Institute

1617 Cole Boulevard
Golden, Colorado 80401

Prepared for the
U.S. Department of Energy
Contract No. DE-AC02-83CH10093

Printed in the United States of America
Available from:
National Technical Information Service
U.S. Department of Commerce
5285 Port Royal Road
Springfield, VA 22161
Price:
Microfiche A01
Printed Copy A11

NOTICE

TABLE OF CONTENTS

TABLE OF CONTENTS (cont.)

I. PROGRAM OBJECTIVES

The objective of this years program was to further develop reactive sputtering of amorphous silicon for solar cell applications. The major goals of the program were:

- To develop intrinsic material capable of generating a J_{SC} of 12 to 13 mA/cm^2 and V_{oc} of 0.9 Volts
- To investigated the mechanism of doping of sputtered a-SiH_x and μc-SiHx films and develop methods to dope such layers from silicon doped targets
- To investigate the origin of the low Fill Factor
- To demonstrate a complete P-I-N solar cell structure fabricated totally from silicon targets, without the use of any gas phase toxic dopants
- To fabricate P-I-N solar cells having efficiencies of 6% or larger

II. RESULTS AND DISCUSSION

The studies conducted during this contract year cover the areas of thin film growth, doping, correlation between deposition parameters and photovoltaic properties and device fabrication. In this section we give a brief summary of these results and more detail studies are presented in the Appendices.

1. Thin Film Growth Studies

A number of physical and chemical effects in sputter deposition of α-SiH have been investigated and models for the thin film growth of both amorphous and partially crystallized films have been developed.

A. Amorphous Films

The common experience in reactive sputtering is that, at very low reactive gas partial pressure and high target sputtering rate, virtually all of the compound formation occur at the substrate. As the reactive gas partial pressure is increased or the sputtering rate is decreased, a threshold is reached at which the rate of target compound formation exceeds the removal rate of compound, and thus most of the compound synthesis occur at the target.

We find that films produced with up to 20 to 40% of hydrogen in the discharge and deposition rates in the range of 1 to 5 A/sec most of the compound formation occurs at the substrate and the Si and H reactions are kinetically controlled. These film are found by x-rays to be amorphous. The Si and H reactions were investigated by studying the density of states in the middle of the gap and the hydrogen content in the films. From these studies we find that there are two sites in the silicon network for hydrogen attachment. The sticking coefficient of hydrogen to these two sites has been

measured. Besides these reactive sputtering effects the importance of etching of the growing films by the H-plasma has been investigated through indirect etching studies of already formed SiH films.

The evolution and control of structural and compositional inhomogeneities in these films were also investigated. The major conclusions of this study can be summarized as follows:

- In agreement with Ross and Messier (1), we demonstrated that the coalescence of the island structure is influenced primarily by charged rather than neutral particle bombardment. However, in disagreement with these authors, we proposed that the beneficial effects arise from the electron bombardment, while Ar^+ ion bombardment leads to undesirable effects, such as Ar incorporation and void formation.
- We demonstrated that control of the hydrogen bonding, and thus the formation of compositionally homogeneous films can be accomplished through bias sputtering. Postive substratre bias (electron bombardment) favors hydrogen in the 2000 cm^{-1} mode while negative substrate bias (Ar^+ ion bombardment) favors the hydrogne in the 2100 cm^{-1} mode. This mode is correlated with Ar incorporation and microvoid formation in the films.
- We have shown that the density of states in the middle of the gap, and related phenomena, such as recombination, do not depend on the bonding of hydrogen in the 2000 or 2100 cm^{-1} modes but they depend on the total amount of hydrogen in the film.

Details of these studies are presented in Appendices A and B.

B. Microcrystalline Films

The effect of a number of deposition parameters on the degree of crystallization of amorphous silicon films has been investigated. Such parameters include the partial pressure of hydrogen in the discharge the total pressure of Ar + H_2, the substrate temperature and the power in the discharge. The films were characterized through x-rays, Raman, IR and optoelectronic studies. We find that the crystallization is controlled by the amount of atomic hydrogen in the discharge, which affects the etching of the growing film. The other deposition parameters (power, temperature) affect the crystallization indirectly by affecting the amount of atomic hydrogen or the etching rate. Microcrystalline films have been doped P or N-type either by gas phase doping or by sputtering from a boron doped targets. These doped films are highly transparent and conductive and are most suitable as P and N-Contacts in P-I-N solar cells. A preliminary report on these studies is given in Appendix C.

2. Doping Studies

Amorphous Silicon films have been doped P- or N-type either by gas phase doping or by sputtering from heavily doped P or N-type targets. These studies indicate that the amount of hydrogen in the films affects the electrical activity of the dopant atoms. Preliminary reports on these studies are given in Appendices D,E,F.

3. Photovoltaic Studies

A. Correlation between deposition parameters and the photovoltaic properties of the intrinsic films

Correlations between deposition parameters and photovoltaic properties of the intrinsic films were investigated through studies

of Pt-Schottky barrier structures. These studies indicate strong correlations between photovoltaic properties and structural and compositional inhomogeneities, amount of incorporated hydrogen and contamination by low levels of dopant impurities. These results can be summarized as follows:

Structural inhomogeneities in sputtered amorphous silicon films are correlated with bombardment of the growing film by charged particles. Deposition parameters, which were found to afect such inhomogeneities, are the pressure of the sputtering gas, and the target and substrate bias. Structural inhomogeneities influence the photovoltaic properties through the introduction of defects which control recombination and possibly through the modification of the structural disorder, which affects the width of the band tails, and thus carrier transport and optical properties. Compositional inhomogeneities were found to affect the optical properties, suggesting that such inhomogeneities introduce additional disorder, which broadens the band tails. Our studies do not indicate that compositional inhomogeneities introduce defects in the middle of the gap.

Opto-electronic and photovoltaic studies of films produced at different hydrogen concentrations suggest that the dual role of hydrogen in removing dangling bond related defects and simultaneously increasing the optical gap is an unfortunate trade-off. We suggested that since the current is independent of hydrogen content the large gap material has an advantage for photovoltaic applications because it leads to solar cells with higher V_{oc}.

The introduction of low levels (<1 ppm) of PH_3 and B_2H_6 in the discharge has a significant effect on the photovoltaic properties of the films. Some of the effects may be related to the introduction of structural defects by these impurities or to the shift of the Fermi level towards the conduction or valance bands. Details on these studies are presented in Appendices G,H.I.

B. Device fabrication and performance

Solar cell structures were fabricated in the configurations: SS/N-I-P/ITO and SS/P-I-N/ITO. The deposition chamber was cleaned beteen N and I or P and I depositions to minimize the phosphorus and boron contamination effects, which were discussed previously. Since boron contamination was found to be far more severe than phosphorus contamination the most efficient cells were fabricated with the first configuration. Besides contamination effects, the optical and transport properties of the doped layers were found to have a significant effect on the device performance. For example, devices fabricated with amorphous P and N layers were reported to have an efficieincy of about 4% (2). This performance can be improved significantly upon using microcrystalline P and N layers, due to their high conductivity and reduced optical absorption in the visible spectral region. As an example, we show in Figs. 1 and 2 the I-V characteristics and the spectral dependence of the collection efficiency of one such device. The I-layer of this device was produced at 5 mTorr of Ar + H_2 (H_2/Ar = 0.18), at target voltage of -800 volts and deposition temperature of 325^{o}C. The P and N layers were deposited under the conditions described in Appendix C. This solar cell structure generates a J_{sc} of 13$^{mA}/cm^2$ and V_{oc} of 0.86 Volts. The efficiency of this device, 5.5%, is limited by the low FF

of 0.49. In the following we discuss the factors which limit the efficiency of these devices and suggests methods for further improvments.

The low value of the FF is partly due to the degradation of the N-I interface which results from the need to clean the chamgber between N and I depositions. It has been shown in another paper (3) that the FF increases from 0.49 to 0.57 as the evacuation time between N and I depositions decreases from 24h to 20 min. Also studies of the wavelength dependence of the FF were accounted for in terms of surface recombination at the N-I interface (4). Therefore, the low value of the FF is not inherent, to the sputtered devices. Sequential deposition of all layers in interlocked dedicated sputtering chambers should lead to FF's equivalent to those found in cells prepared by the glow discharge decomposition of silane process.

The J_{sc} can be increased by further improvements in the film's structural and compositional homogeneity and by improvements in the device design. As an example, we show in Fig. 3 how the incorporation of back reflective contacts can improve the red portion of the spectrum. The two devices have the configurations: substrate/N-I-P/ITO. In the one device the substrate is SS and in the other is SS/Ag/TiO_2. The TiO_2 layer, approximately 30 A thick, acts to prevent diffusion of silver into the amorphous silicon. Incorporation of highly transparent a-SiC hetercontact should result in significant improvement in the blue part of the spectrum. Therefore, upon implementation of these device design concepts the J_{sc} should approach the values of cells produced by the glow discharge process.

Th V_{oc} value is also expected to increase upon minimizing cross contamination and improving the device design. Values of V_{oc} as high as 0.95 Volts have already been observed in devices having the configuration: SS/N-I-P/ITO.

To further test the potential of this technology we fabricated tandem solar cell structures having the configuration: SS/N-I-P-N-I-P/ITO. The I-layers in both solar cells was made under the same conditions, and their thickness was not adjusted for current matching. The P and N layers were microcrystalline. The I-V haracteristics of this device, shown in Fig. 4, suggests good junction characteristics. In particular, the tunneling between the microcrystalline P and N layers appears to be satisfactory. These initial results suggest that high efficiency tandem cells can be fabricated by the method of sputtering if a smaller gap material, made for example from α-SiGe alloys, is used as a back solar cells.

A PIN solar cell structure fabricated totally from silicon targets, without the use of gas phase toxic dopants is shown in Fig. 5. This structure has the configuration SS/NIP/Pt. The phosphorus and boron doped targets were fabricated in single crystal form by the Czochralski method. The phosphorus and boron impurities were added to the melt during the growth. The analysis of the single crystals indicate that the doped targets contan about 1×10^{19} (200 ppm) of phosphorus or boron. The insufficient doping of these P and N-layer would explain the relatively small value of the open circuit voltage of the device.

More details on these studies can be found in Appendices J and K.

C. Studies of the FF

The FF of the devices reported in the previous section is the efficiency limiting factor in these devices. To understand the origin or the low Ff we investigated the wavelength dependence of the Shunt conductance and FF of a number of either N-I-Pt or N-I-P solar cell structures. From these studies we found that the FF has lower values in both the red and the blue portion of the spectrum. The decreased values of the FF at the ends of the spectrum were ascribed to recombination of the photogenerated carriers at both the front and the back contacts to the I-layer. Preparation of the N, I and P layers at sequential dedicated chambers is expected to lead to better interfaces and hence higher performance. Details of these studies are presented in Appendix L.

D. Opto-electronic properties of boron compensated amorphous silicon solar cells

The effect of boron compensation on the properties of the intrinsic films was investigated by studying the optical absorption, dual beam photoconductivity and collection efficiency of Pt Schottky barrier structures. We find that small amounts of B is beneficial, however, more the 0.4 ppm of B_2H_6 in the discharge dopes the intrinsic layer p-type and also introduce approximately 1×10^{17} states/cm^3.eV in the middle of the gap. A preliminary report on these studies is given in Appendix M.

III. CONCLUSIONS

The studies presented in this paper showed that the properties of both the intrinsic and doped sputtered amorphous silicon films can be optimizied to produce high efficiency solar cells.

The photovoltaic properties of the intrinsic films were found to depend sensitively on structural and compositional inhomogeneities, amount of incorporated hydrogen and low levels of dopant impurities.

Conditions for depositon of both amorphous as well as microcrystalline phosphorus and boron doped films have been identified. These films were characterized through studies of their optical and transport properties and the superiority of the microcrystaline films for photovoltaic applications has been demonstrated.

The combination of the best intrinsic and doped films led to the fabrication of P-I-N solar cell structures with efficiency 5.5%. We showed that this efficiency can be improved even further by depositing the three layers in sequential dedicated chambers and by implementing device design concepts such as back reflective contacts and highly transparent a-SiC front contacts. Finally, the photovoltaic potential of this technology was demonstrated through the fabrication of efficient tandem solar cell structures.

REFERENCES

1. R. C. Ross and R. Messier, J. Appl. Phys. 52, 5381 (1981).

2. T. D. Moustakas and R. Friedman, Appl. Phys. Lett. 40, 587 (1982).

3. T. D. Moustakas, R. Friedman and B. R. Weinberger, Appl. Phys. Lett. 40, 587 (1982).

4. H. P. Maruska and T. D. Moustakas, IEEE Trans. Electron Devices (to be published).

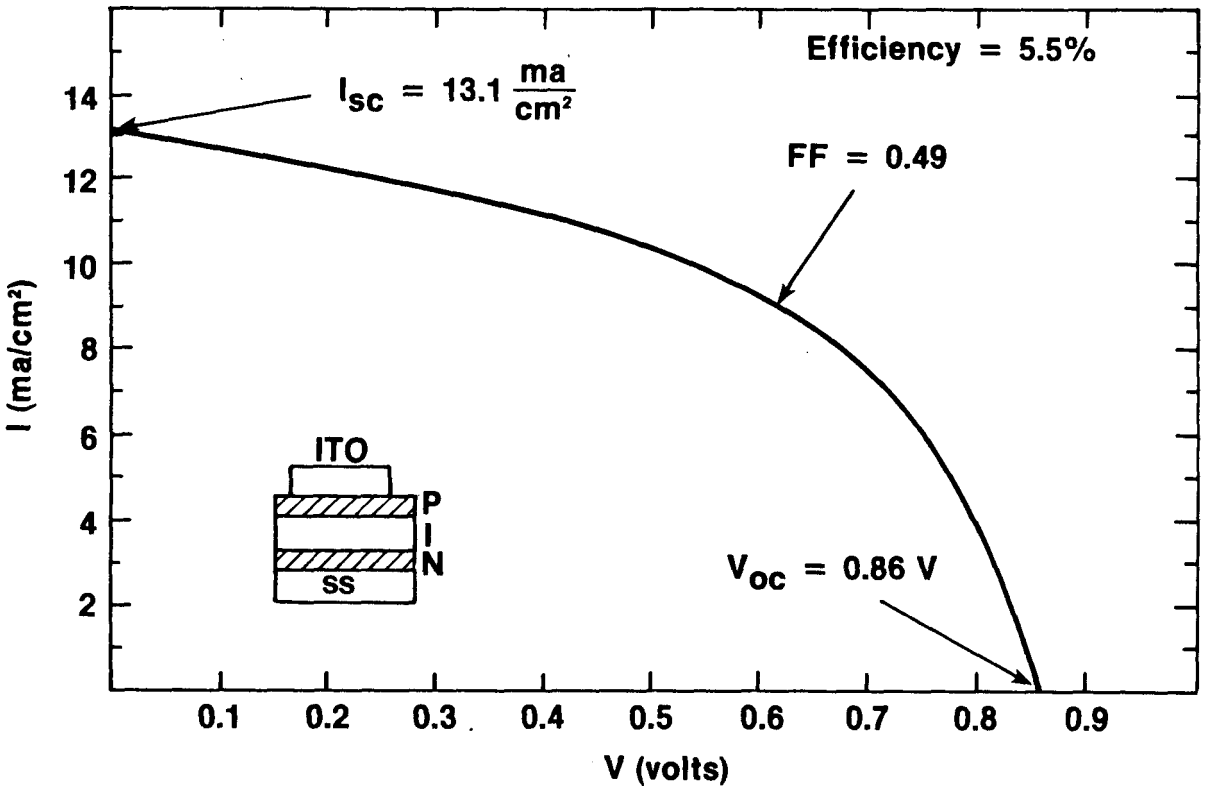

Figure 1. I-V Characteristics of a Sputtered SS/NIP/ITO Solar Cell Structure.

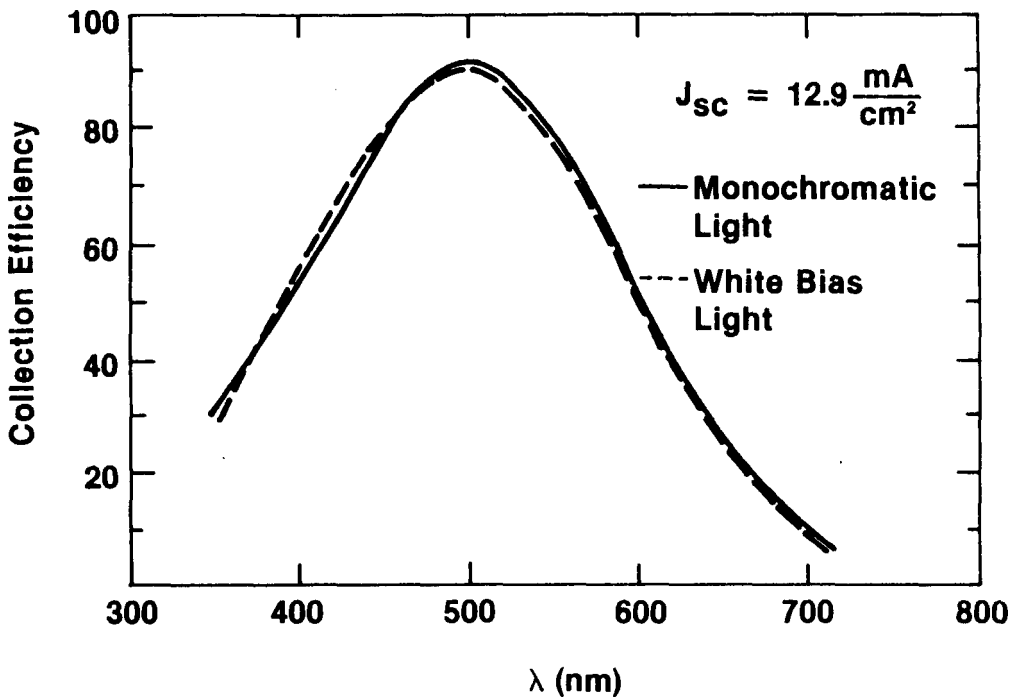

Figure 2. Spectral Dependence of the Collection Efficiency of the Device Shown in Figure 7.

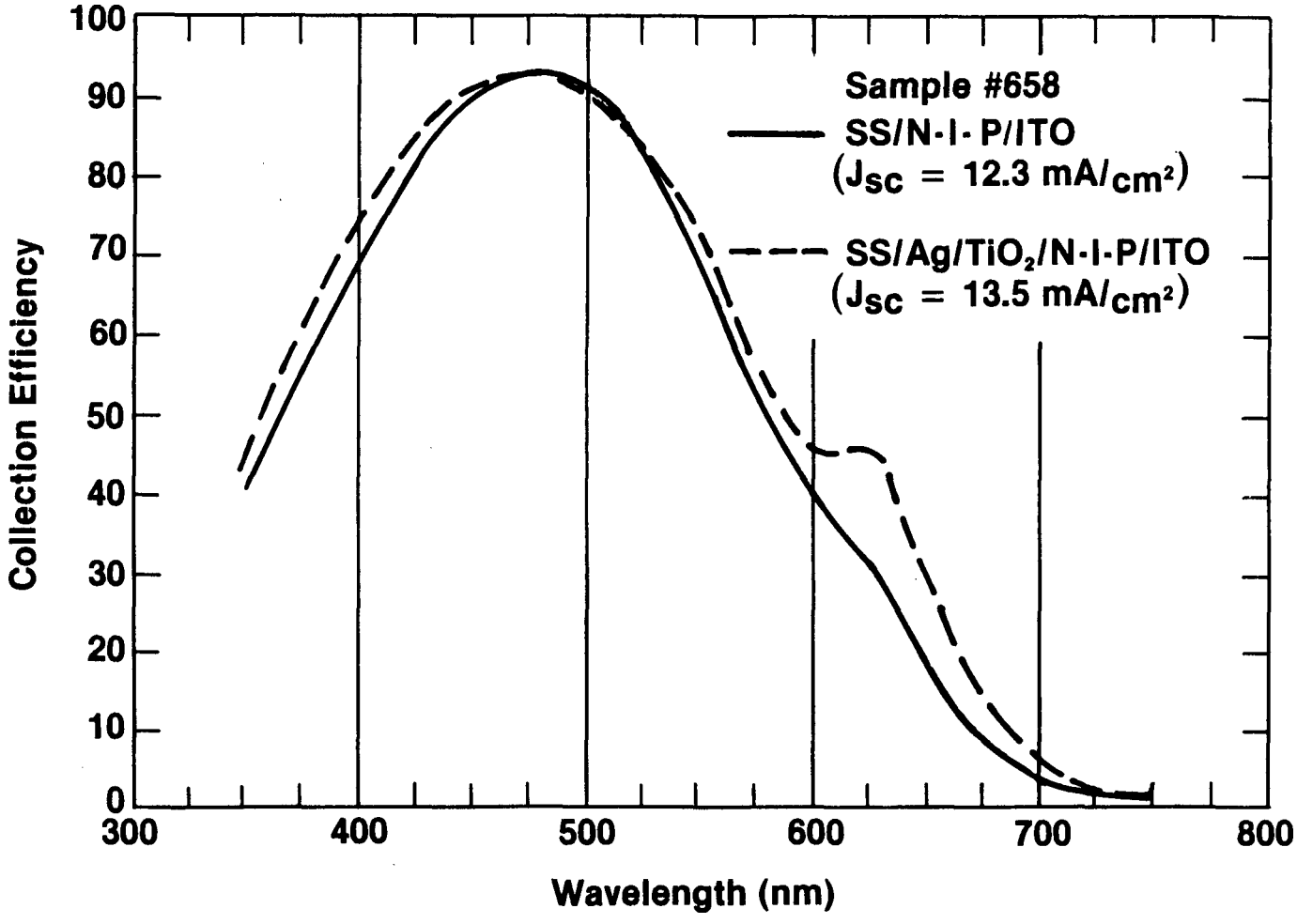

Figure 3. The Effect of Substrate Reflectivity on the Spectral Dependence of the Collection Efficiency of Sputtered Solar Cells

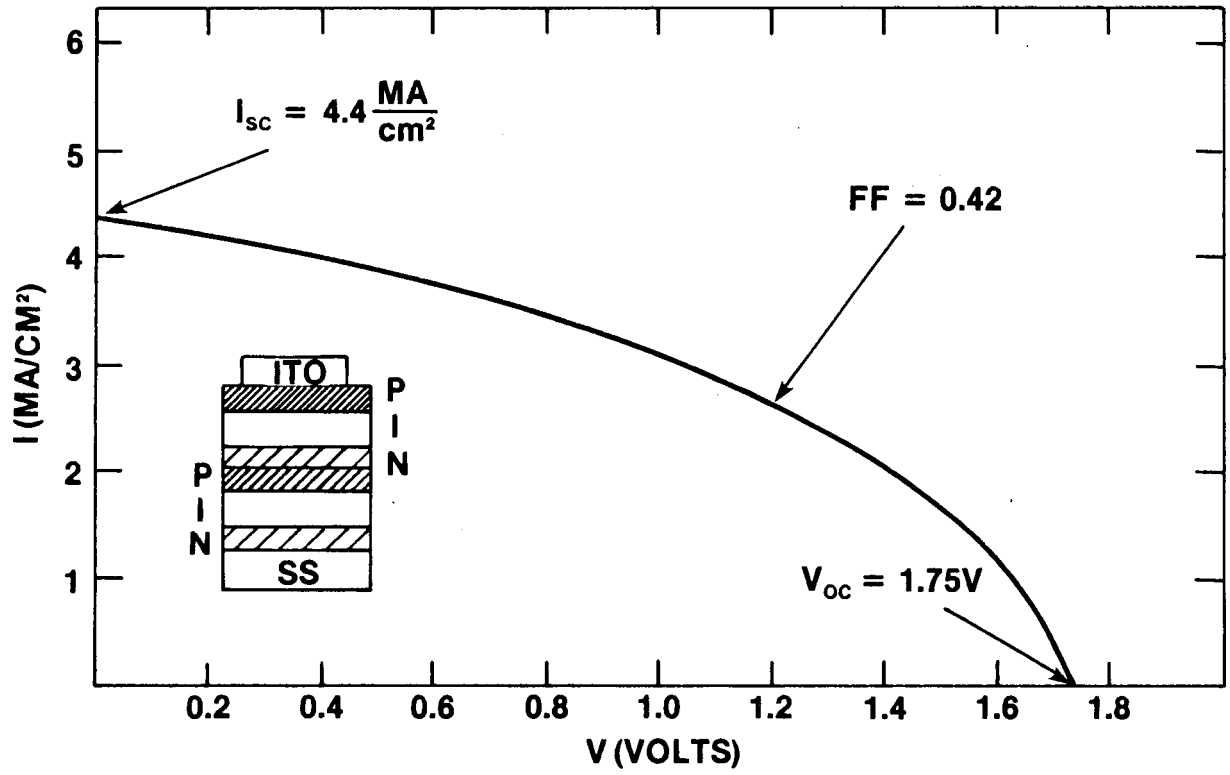

Figure 4 . I-V Characteristics of a Sputtered SS/NIP NIP/ITO Solar Cell Structure

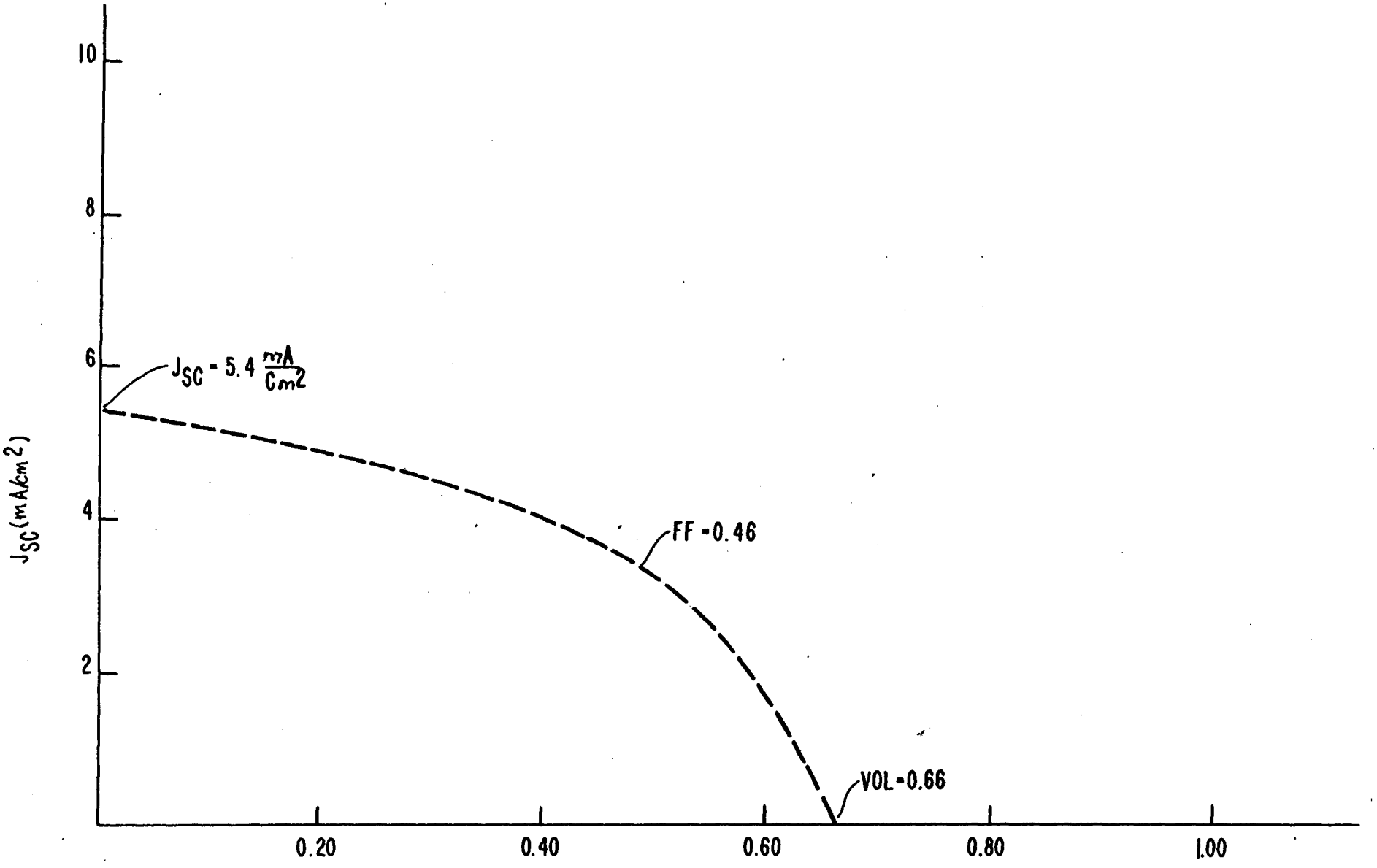

Figure 5. I-V Characteristics of a SS/NIP/Pt solar cell structure. The N and P layer were deposited from doped targets as described in the text.

APPENDIX A. Studies of Thin-Film Growth of Sputtered Hydrogenated Amorphous Silicon

Solar Energy Materials 8 (1982) 187-204
North-Holland Publishing Company

STUDIES OF THIN-FILM GROWTH OF SPUTTERED HYDROGENATED AMORPHOUS SILICON

T.D. MOUSTAKAS

Corporate Research Laboratory, Exxon Research and Engineering Co., P.O. Box 45, Linden, NJ 07036, USA

The role of a number of physical and chemical sputtering effects in the thin film growth of hydrogenated amorphous silicon has been investigated. Charged particle bombardment was found to affect the film microstructure more than neutral particle bombardment. The roles of electron and Ar^+ ion bombardment have been identified. Control of the hydrogen bonding is accomplished through bias sputtering. Positive substrate bias (electron bombardment) favors hydrogen in the 2000 cm^{-1} mode. Negative substrate bias (Ar^+ ion bombardment) favors the hydrogen in the 2100 cm^{-1} mode. However, the density of states in the middle of the gap and the recombination properties do not depend on the mode of the hydrogen bonding, but rather on the total amount of hydrogen in the film. Experimental evidence is produced that the SiH_x compound formation moves progressively from the substrate to the target as the hydrogen pressure in the discharge increases. Evidence of the importance of chemical etching of the growing film by H-plasma is produced.

1. Introduction

The anticipated potential use of hydrogenated amorphous silicon (a-SiH_x), or other related materials, for large area thin film device applications, has stimulated extensive research of these materials at a number of laboratories. Of the two plasma methods (glow discharge decomposition of silane, and sputtering from a silicon target in an $Ar + H_2$ plasma), the former has attracted considerably more attention since it was perceived as a more suitable technology for surface sensitive devices, and was assumed to lead to films with better optoelectronic properties. As a result this material has been extensively investigated through structural, optical, transport and recombination studies, which led to solar cell structures with efficiencies up to 8% [1]. Recent reviews in the physics and device areas have been published by Fritzsche [2] and Carlson [3].

It is widely believed that this rapid progress in the device area is the result of the understanding of the thin film growth conditions, which lead to material with much less structural and compositional inhomogeneity. Towards this end one needs to conceptualize and develop diagnostic tools to study the complex reactions in the plasma and in the surface of the growing film, and also develop an understanding of

0165-1633/82/0000-0000/$02.75

the thin film growth habit by studying the film's structure. Progress towards the first goal, which unravels the mechanism of hydrogen elimination, is slowly emerging [4], and towards the second goal the structural studies of Knights and Lujan [5] have led to the discovery that plasma deposition of a-SiH$_x$ films proceeds via nucleation and growth of island structures (average lateral dimensions $\approx$100 Å). The coalescence of these islands, if imperfect, leads to columnar morphology in subsequent growth. These authors report that growth of the films in pure silane, at low deposition rates, at large substrate negative biases, and deposition temperatures between 200 to 300 °C leads to much more perfect coalescence of the islands. The structural inhomogeneities, revealed by these studies, have been invoked to also interpret compositional inhomogeneities observed in NMR, neutron scattering and infrared vibrational studies [6–8]. Films showing columnar morphology are unstable upon exposure to atmosphere. The interstitial regions between the columns can be penetrated by active atmospheric impurities leading to post-deposition contamination effects. The electronic properties of such films are poor since the low density interstitial regions are correlated with electronically active defects [8].

The development of the reactive sputtering technology in depositing such films is proceeding along the same lines, namely through structural and optoelectronic studies of films deposited under a variety of deposition conditions. The properties of such films have recently been reviewed by Paul and Anderson [9] and earlier by the present author [10]. The device potential of this material has also come to age since films with very low density of states in the middle of the gap ($<10^{15}$ cm^{-3} eV^{-1}) and large collection widths [11, 12], as well as multilayer PIN devices with efficiencies up to 4% have been reported [13]. Although there is evidence that part of this lower value of the solar cell efficiency is related to practical problems, such as cross-contamination between the layers of the device [14], further optimization of the optoelectronic properties requires a better understanding of the critical parameters, which control the film growth.

The growth habit of the sputtered a-SiH$_x$ films is also columnar, as has been revealed by the extensive structural studies of Ross and Messier [15]. These authors find that films produced at high argon pressure have columnar microstructure, while those produced at low argon pressure show no noticeable microstructure. Their preferred interpretation for the lack of microstructure for the low argon pressure films is bombardment of the films by *positive Ar^+ ions* due to the substrate negative floating potential. However, these authors admit that the beneficial effects of this ion bombardment are partly offset by the simultaneous creation of atomic-scale electronically active defects. The Harvard group [16] attributes the microstructural changes with the pressure of argon to the bombardment of the film by the *neutral sputtered Si species* from which the film grows. They suggest that weak bombardment of the growing film might be beneficial in removing loosely bound material from the surface. At high argon pressures, this desirable bombardment is removed due to the thermalization of the Si species. Besides, the controversy

between these two models, the data indicate that even films which do not show microstructural imhomogeneity do show compositional inhomogeneity as revealed by Si-H vibrational studies. For example, the Si-H stretching vibration was found to be a doublet for films produced under a variety of deposition conditions [17, 18].

In this paper we present data which clearly indicate that charged particle bombardment rather than neutral particle bombardment is the cause of the observed microstructural changes as a function of argon pressure. In addition, we show how bias sputtering can be used to control compositional inhomogeneity through selective charged bombardment. Films produced with positively biased substrates (electron bombardment) have the Si-H stretching mode centered at 2000 cm^{-1}, while negative substrate bias (positive ion bombardment) favors the 2100 cm^{-1} mode. We also discuss experimental evidence that at low partial pressure of hydrogen, the SiH$_x$ compound is synthesized at the surface of the substrate, while at high partial pressure there is evidence of compound formation at the surface of the target. The importance of H-plasma etching effects of the growing film and target is also briefly addressed.

2. Deposition system and experimental methods

The deposition system used in this study has stainless steel walls, held at ground potential, and electrically insulated cathode and anode assemblies. The water cooled target is a polycrystalline silicon disk, 5" (13 cm) in diameter and $\frac{1}{4}$" (0.64 cm) thick, and is supplied with an rf power at a frequency 13.56 MHz. The anode assembly was held 5 cm below the target and can be grounded, floated or supplied with rf or dc electrical bias. The substrates (quartz glass and high purity silicon single crystal wafer) were fastened with a stainless steel frame and molybdenum springs on the top of the anode assembly. An 0.005 cm thick Al foil is inserted between the anode and substrates to improve the thermal contact. The system was pumped by a combination of turbomolecular and mechanical pumps to a base pressure of about $1\text{–}2 \times 10^{-7}$ Torr and routinely checked for atmospheric leaks with a mass spectrometer. The systems total leak rate was approximately $1\text{–}2 \times 10^{-5}$ Torr $l\,s^{-1}$.

The parameter space investigated involved variation of the substrate temperature, the argon pressure, the hydrogen pressure, the substrate bias (self-induced or externally applied) and the power in the discharge.

Microstructural changes in the films were investigated through measurements of the index of refraction, post deposition oxidation effects and SEM microscopy. All of these properties are very sensitive to microstructural changes, and in particular the index of refraction and post deposition contamination effects can be measured accurately on thin films ($\simeq 1\,\mu$m). The index of refraction was determined by studying the optical densities of the films deposited on the quartz substrates in a Carry 17 spectrophotometer, using a 2 mm aperture to eliminate the possibility of

thickness gradients. The magnitude, ΔOD, of the interference fringes, which are displayed at wavelengths longer than the absorption edge, was used to calculate the refractive index at given wavelength. The post-oxidation effects were investigated by studying the optical densities of the films, deposited on the silicon substrates, using a Digilab FT Spectrophotometer set at a resolution of 4 cm^{-1}. Both type of measurements were made immediately after the films were removed from the deposition system and aging effects were followed up by repeating the measurements as a function of time.

The hydrogen contents of the films were measured by the nuclear reaction $^{15}N + {}^{1}H \rightarrow {}^{12}C + {}^{4}He + \gamma$ [19, 20]. These measurements were also correlated with the integrated intensities under the Si-H vibrational modes [20]. These modes were also used in identifying different bonding configurations of hydrogen.

The films were also characterized by measuring their optoelectronic properties such as, optical absorption constant, conductivity, photoconductivity, photoluminescence and density of states. Such data will be mentioned in this paper only to support observed trends in the film's growth.

3. Relation between microstructural changes and film bombardment by charged and neutral particles

In order to investigate the relation between the film's microstructure and bombardment by different particles in the discharge we deposited a number of films at fixed hydrogen partial pressure ($P_H = 0.7$ mTorr) and argon pressure varying between 5 to 40 mTorr. The substrates were electrically floated and held at a temperature of 275 °C. The target was supplied with a constant power of 200 W, which resulted in a deposition rate increasing monotonically with the pressure of argon from 2.2 to 2.7 Å/s. The hydrogen content of the films was found to be between 22 to 20 at%. The optical gaps of the films, measured immediately after removing the substrates from the deposition system, were found to decrease with the argon of pressure from 1.85 to 1.77 eV. The optical constants of the film produced at 40 mTorr were found to change with the length of time of air exposure.

Fig. 1 shows the dependence of index of refraction, n, measured immediately after the film deposition at wavelength $\lambda \approx 2.0\ \mu$m, on the argon pressure in the discharge. The value of n remains constant up to about 20 mTorr of argon and then it drops rather abruptly. The reduction of the index of refraction at high argon pressures is accompanied by post-deposition contamination. Fig. 2 shows the infrared vibrational spectral for samples deposited at 5, 10, 20 and 40 mTorr of argon. The films deposited at 5 and 10 mTorr of argon show the usual Si-H vibrations [17], while the samples deposited at 20 and 40 mTorr of argon additionally show Si-O ($\approx$1100 cm^{-1}), Si-N (880 cm^{-1}) and C-H ($\approx$3000 cm^{-1}) vibrations. In agreement with Freeman and Paul [18], we find that these additional vibrations are due to post-

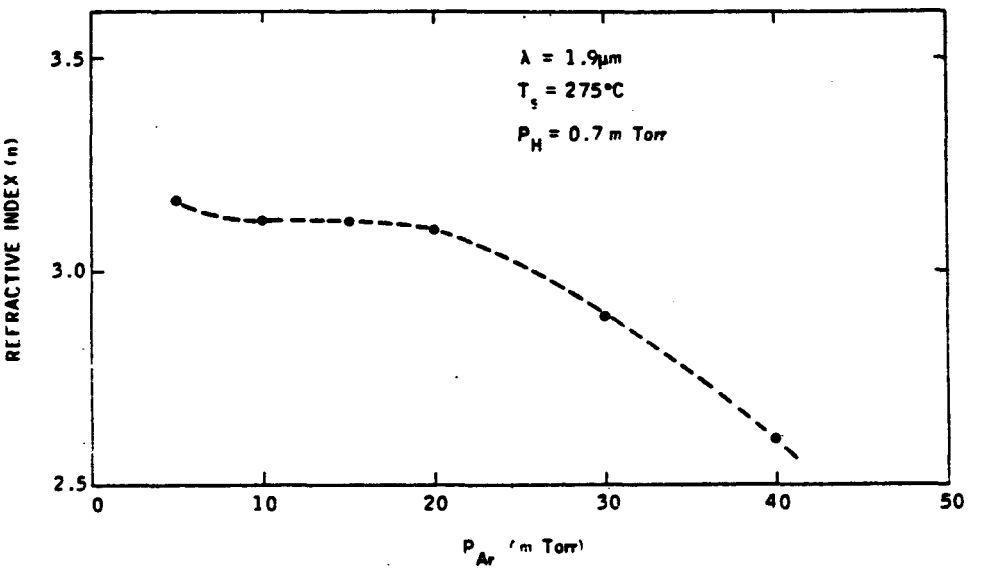

Fig. 1. The index of refraction, measured at $\lambda \approx 2.0\,\mu$m, vs. the argon pressure in the discharge.

deposition contamination and they grow as a function of time.

The reduction of the index of refraction for the films produced at high argon pressure can be accounted for as the result of the film's porosity (since n depends on

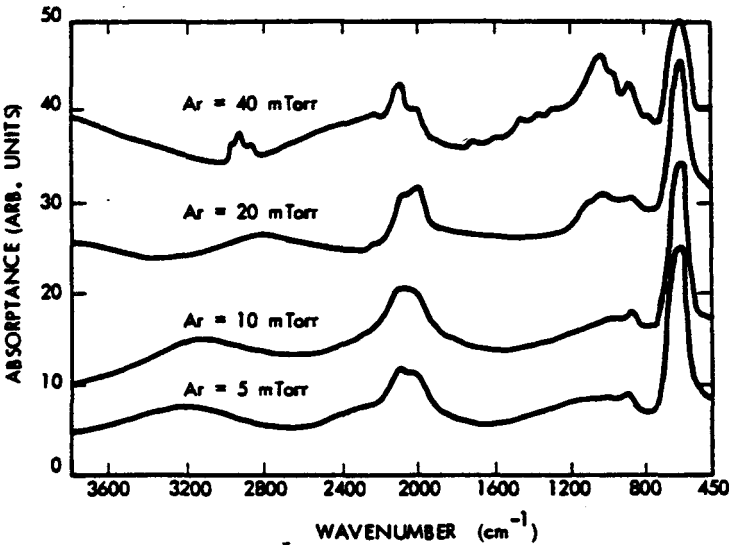

Fig. 2. Infrared vibrational spectra of sample deposited at argon pressure of 5, 10, 20 and 40 mTorr.

the density of the valence electrons), and the formation of low index of refraction coatings (SiO_x, SiN_x) in the internal surfaces of the voids. Therefore, the results of figs. 1 and 2 are consistent with the observations of Ross and Messier [15] that films grown at high argon pressure have a columnar morphology, and that under the described preparation conditions the coalescence of the island structure is imperfect for films grown at argon pressure higher than 20 mTorr.

In agreement with Knights [8] and Anderson et al. [10] we find that the films produced at high argon pressures have poor photoelectronic properties. As an illustration, fig. 3 shows the photoconductivity under AM1 illumination vs. the argon pressure in the discharge. The photoconductivity of the film produced at 40 mTorr

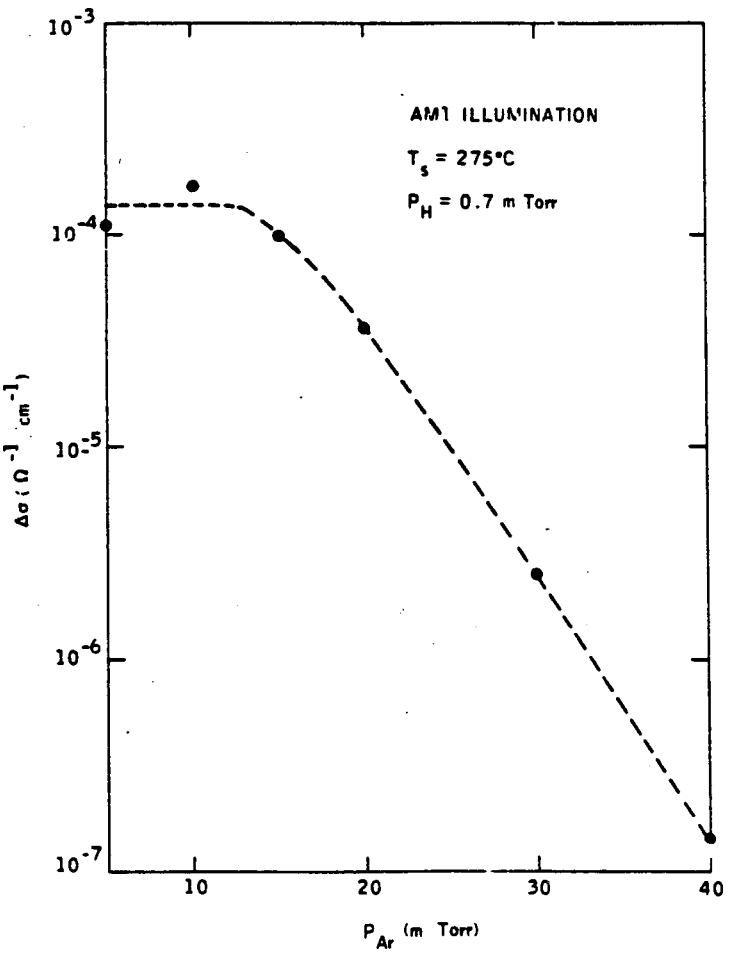

Fig. 3. The photoconductivity, measured under AM1 illumination, vs. the argon pressure in the discharge.

of argon is lower by three orders of magnitude from that of the films produced at low argon pressures.

In order to investigate whether these structural changes are the result of bombardment or lack of bombardment of the film by neutral or charged particles we determined the dependence of the self-bias potential of the substrates on the partial pressure of argon. The substrate self-bias voltage was measured with respect to the ground in a separate experiment, which simulated the conditions of the sample deposition. Fig. 4 shows the substrate self-bias potential, with respect to the ground, vs. the partial pressure argon in the discharge. The substrates are negatively biased at low argon pressures, because they are bombarded by more electrons than ions due to the higher electron mobility. At high argon pressures, on the other hand, the substrates have the same potential as the plasma (positive), and charged particles do not bombard but migrate to the substrates by thermal diffusion [21]. Ross and Messier [15] have measured, in addition, the plasma potential with a Lagmuir probe and they were able to calculate the floating potential of the substrates with respect to the plasma. Their data have the same functional behavior observed in fig. 4. We conclude from the data of figs. 1–4 that the change in the sign of self-bias potential with respect to the ground, occurs at exactly the same argon pressure where significant changes in the film's microstructure have been observed. Therefore, these data sug-

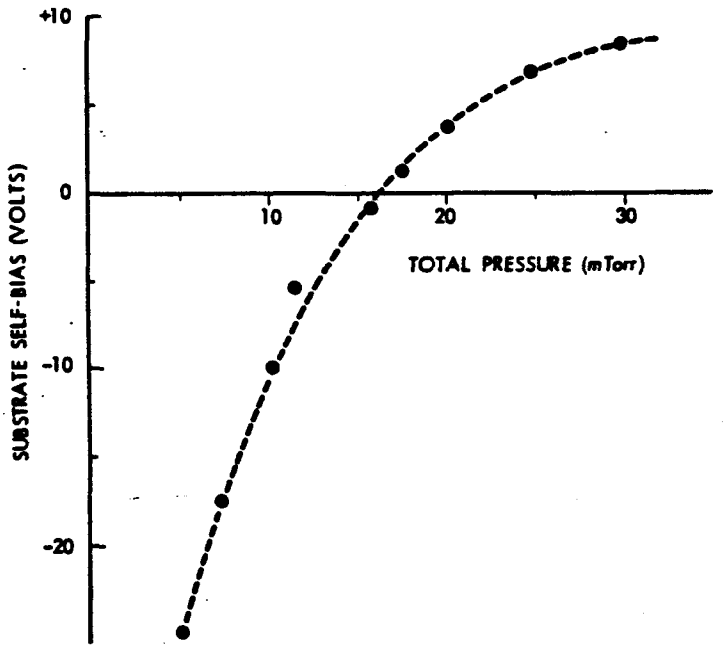

Fig. 4. The substrate self-bias voltage, measured with respect to the ground vs. the total pressure in the discharge.

gest that the coalescence of the island structure is the result of atomic rearrangement due to the bombardment of the growing film by charged particles. However, these data cannot differentiate the relative roles of electron or Ar^+ bombardment in the growth of the film. Ross and Messier [15] attribute the structural changes to the Ar^+ ion bombardment. However, in the next section we will show that electron bombardment may be as important in inducing structural changes. The correlations observed in figs. 1–4 cannot be explained on the basis of film bombardment by neutral species, as suggested by the Harvard group [16], since such species are unaffected by substrate bias.

4. Control of Si–H bonding through substrate biasing

In this section we address two issues concerning the Si–H bonding configuration in reactively sputtered a-SiH$_x$ films. The first issue deals with the ability to control the bonding of hydrogen in these materials, through external deposition parameters, and the second deals with the correlation between the hydrogen bonding and electronic properties of the films.

The Si–H vibrational spectra in reactively sputtered a-SiH$_x$ films were first reported by Brodsky et al. [17] and by Freeman and Paul [18]. Both of these extensive studies indicate that the Si–H stretching vibration is always a doublet for films produced under a variety of deposition conditions. This should be contrasted with the ease of controlling the H-bonding in a-SiH$_x$ films produced by the method of glow discharge decomposition of silane [17]. Although there are multiple opinions [22] as to the type of Si–H local environments which give rise to this doublet, it is evident that its existence indicates that these films are compositionally inhomogeneous. This appears to be the case even for films produced at low argon pressures, which do not show structural inhomogeneity. The inability to control the bonding of hydrogen in the sputtered material has led to the widespread belief that the sputtered films are inferior to those produced by decomposition of silane.

Jeffrey and co-workers [23] have demonstrated that sputtered a-SiH$_x$ films having only the 2000 cm^{-1} Si–H stretching mode can be made, if the substrates are inserted inside the plasma below the edge of the dark space. Based on photoconductivity studies, these authors report that films having only the 2000 cm^{-1} Si–H stretching mode have superior electronic properties than films with the Si–H stretching mode at 2100 cm^{-1}. The Harvard group [24], by adopting Jeffrey's method of film deposition, recently produced films having the Si–H stretching vibration at 2000 cm^{-1}. However, this group concluded that sputtered films having the stretching mode at 2000 cm^{-1} have inferior electonic properties than films having the stretching mode at 2100 cm^{-1}.

At our laboratory we have developed [25] bias sputtering as a means of controlling the bonding of hydrogen. We find that the maximum effect of external bias on

the films' microstructure occurs under deposition conditions which lead to substrate self-bias close to zero. We also find that positive bias favors the 2000 cm^{-1} Si-H stretching mode, while negative bias favors the 2100 cm^{-1} Si-H stretching mode. Fig. 5 shows the Si-H stretching vibrations of a number of films produced at substrate bias +50 V and at other deposition conditions as indicated in figure caption. Indicated next to the sample number is the hydrogen content in the films. Note that most of the hydrogen, up to 14 at%, is bonded in the 2000 cm^{-1} mode. The 2100 cm^{-1} mode acquires the same strength as the 2000 cm^{-1} mode for films having more than 20 at% H. For contrast we show in fig. 6 the Si-H stretching vibrations for a number of films produced under negative biasing conditions. The negative bias in these films is self-induced (−25 V), by sputtering the films at low argon pressure, $P_{Ar} = 5$ mTorr, and having all other deposition parameters the same. Note that although the hydrogen content of these films covers the same range as those of fig. 5, the 2100 cm^{-1} mode is present even at the lowest hydrogen content films and becomes progressively stronger as the hydrogen content increases.

These structural variations associated with the substrate biasing can now be accounted for in the following way. Biasing the substrates to a positive voltage has two effects. One is electronic bombardment of the growing film, and the second is minimization of Ar^+ ion bombardment. Although electronic bombardment is thought to be undesirable in the growth of semiconductor material, our findings

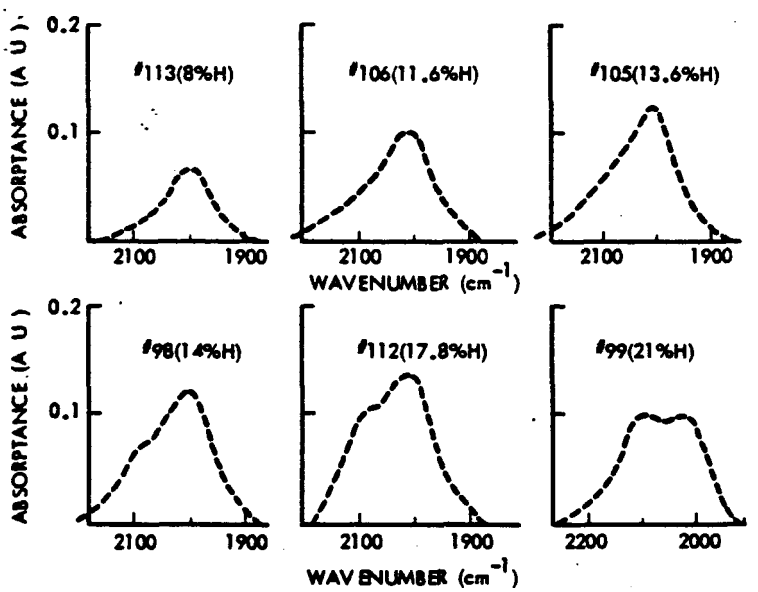

Fig. 5. The Si-H stretching vibrations for a number of films produced at positive substrate bias. Indicated next to the sample number is the hydrogen content in the films. (These films were produced at $T_s = 275$ °C, power = 200 W and $P_{Ar} = 15$ mT.)

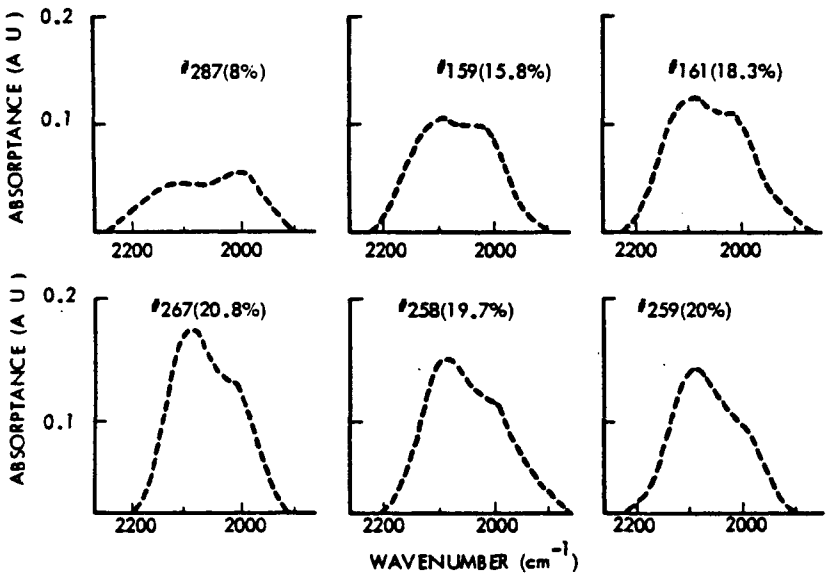

Fig. 6. The Si-H stretching vibrations for a number of films produced under negative bias conditions. Indicated next to the sample number is the hydrogen content in the films.

indicate that some electronic bombardment can have a favorable effect on the growth of structurally and compositionally homogeneous sputtered a-SiH$_x$ films. Under typical sputtering conditions, there are low energy and high energy electrons arriving at the substrate. The high-energy electrons have a sharp cut-off which corresponds to the cathode potential, and are the secondary electrons ejected from the target. Bombardment by these electrons can have profound effects on the film's chemistry and structure because it enhances adatom surface mobility through surface heating. We believe that this electron bombardment is responsible for the perfect coalescence of the island structure which leads to films having both structural and compositional homogeneity. The second effect of the positive bias, namely the minimization of the Ar^+ ion bombardment, is also highly desirable. These films contain much less argon since the Ar^+ ions require a certain threshold ($\approx$15 to 20 eV) in order to be implanted into the film [26]. Resputtering is also minimized under these conditions of film growth. Since resputtering by Ar^+ ions is likely to be anisotropic, i.e., with higher sputtering yield at the low density intercolumnar regions, there is a high possibility of microvoid formation during the film re-growth in these regions. Both argon incorporation and void formation lead to films with structural and compositional inhomogeneity. In fact there is some evidence [27, 28] that argon inhabits voids. We believe that such structural inhomogeneities result in the formation of a stretching vibration doublet.

Regarding the second issue, namely the correlation between hydrogen bonding

and electronic properties of the films, our data do not substantiate either the claims of Jeffrey et al. [23] or those of the Harvard group [24]. More specifically, we find that the states in the middle of the gap [11] and properties which are related to these states (recombination), do not depend on the hydrogen bonding, but rather on the total amount of bonded hydrogen. To illustrate this point we show in figs. 7 and 8 the photoconductivity and the density of states in the middle of the gap of the same films, whose Si-H stretching vibrations have been discussed in figs. 5 and 6 correspondingly.

The data of fig. 7 indicate that the photoconductivity increases by four orders of magnitudes as the hydrogen content increases from 8 to 14 at%. Sample #98 has as high photoconductivity as the best reported for glow discharge films [29]. This is contrary to the claim [24] that sputtered films with the 2000 cm^{-1} mode have inferior electronic properties. The second point to be made is that sample #99, in which the 2000 and 2100 cm^{-1} modes have the same strength, has exactly the same photoconductivity as sample #98. This contradicts the alternative claim [23] that films with the 2000 cm^{-1} mode have superior photoconductivity than those with the 2100 cm^{-1} mode.

The data of fig. 8, which were published earlier [11], demonstrate the same point through a direct measurement of the density of states in the middle of the gap by *C-V* and ESR techniques. The film with the lowest density of states (7×10^{14} cm^{-3} eV^{-1}) has a significant fraction of its hydrogen bonded in the 2100 cm^{-1} mode.

From these studies we conclude that in good electronic quality sputtered material (no visible microstructure), most of the defects, which contribute states in the middle of the gap, are coordination type defects and can be eliminated through hydrogen incorporation into the films. However, films with more structural inhomogeneity require more hydrogen in order to accomplish the same result. This point as well as other differences between films with the 2000 and 2100 cm^{-1} modes will be discussed in another paper [30].

5. The role of reactive sputtering effects in the synthesis of SiH_x compounds

In this section we discuss experimental results related to the synthesis of the SiH_x compound. Of the three possible places (target, gas phase, substrate) where the Si and H can react, the gas phase reaction can be ruled out. This is because the heat liberated in the chemical reaction cannot be dissipated in a two body collision. Simultaneous conservation of energy and momentum requires the reaction to occur at a surface [21]. The common experience in reactive sputtering is that, at very low reactive gas partial pressure and high target sputtering rate, virtually all of the compound synthesis occurs at the substrate. As the reactive gas partial pressure is increased or the sputtering rate is decreased, a threshold is reached at which the rate of target compound formation exceeds the removal rate of compound, and thus most

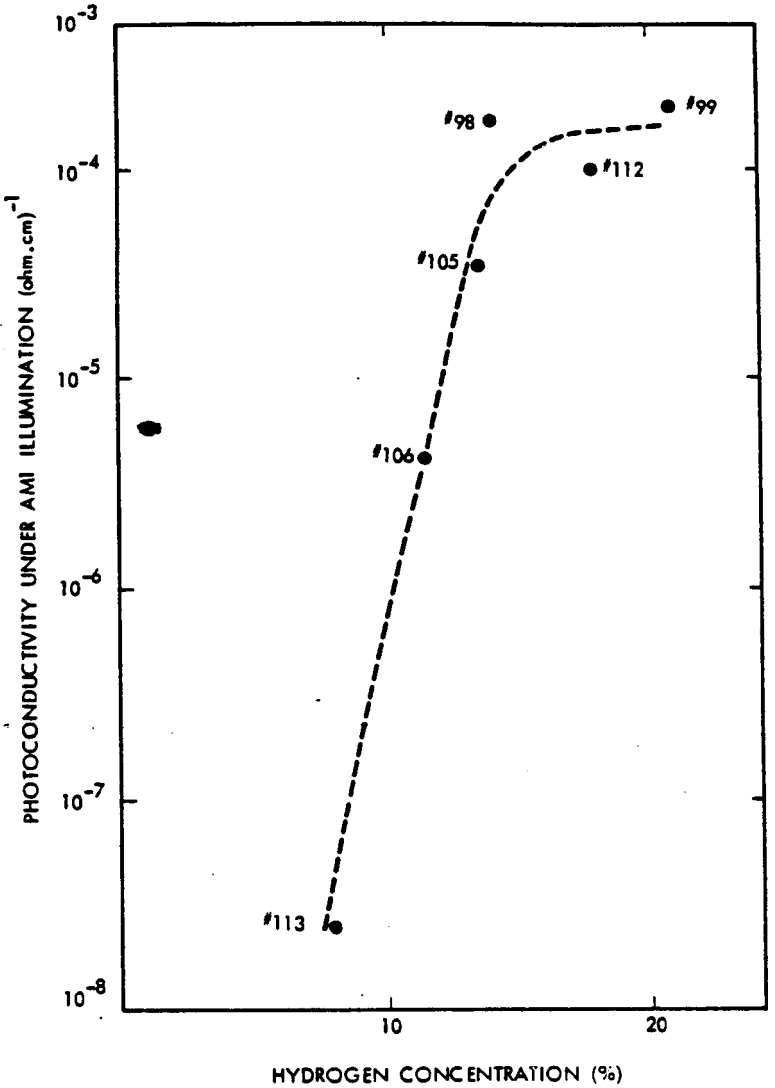

Fig. 7. The photoconductivity under AM1 illumination vs. hydrogen content for films produced under positive substrate bias. The infrared vibrational spectra of these films are shown in fig. 5.

of the compound synthesis occurs at the target [21].

In earlier papers [11, 20] we have published experimental results suggesting that, for films produced up to 20 to 30% hydrogen in the discharge, with deposition rates in the range of 1 to 4 Å/s, most of the compound formation occurs at the substrate. In this paper we give only a brief summary of these results. In order to investigate

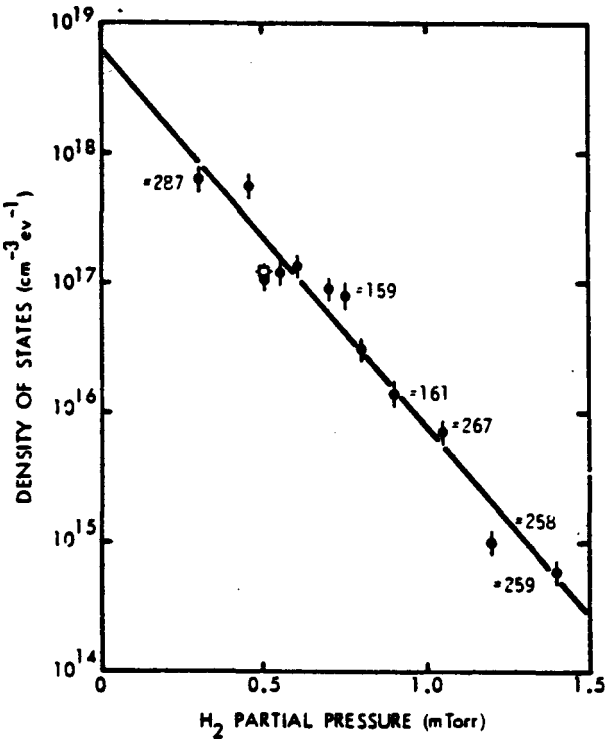

Fig. 8. Density of states in the middle of the gap as a function of hydrogen partial pressure in the discharge. The point indicated by the symbol (☼) is the ESR spin density (1.1×10^{17} cm^{-3}). The infrared vibrational spectra of some of these films are shown in fig. 6.

the Si and H reactions, we studied the density of states in the middle of the gap, which is related to Si dangling bonds, and the hydrogen content of the films. We find that both the density of states and the hydrogen content depend exponentially on the ratio of the flux of hydrogen atoms impinging on the substrate, and the deposition rate. These results are summarized in figs. 8 and 9. These data clearly indicate that the composition of the film depends on the relative rates of arrival at the substrate of Si and H atoms. In the substrate temperature range of 200 to 400 °C, where the electronic quality material is produced, we find that the Si and H reactions are kinetically controlled and that there is no evidence of thermodynamic equilibrium between the hydrogen in the film and the hydrogen in the plasma. From the kinetic model, for the Si and H reactions, we have deduced that there are two sites for hydrogen attachment and the hydrogen bonds to these sites with different efficiency. One site has been identified as a potential Si dangling bond and the second site has been speculated to be a potential reconstructed dangling bond in internal surfaces. The sticking coefficient of hydrogen to the second site is likely to

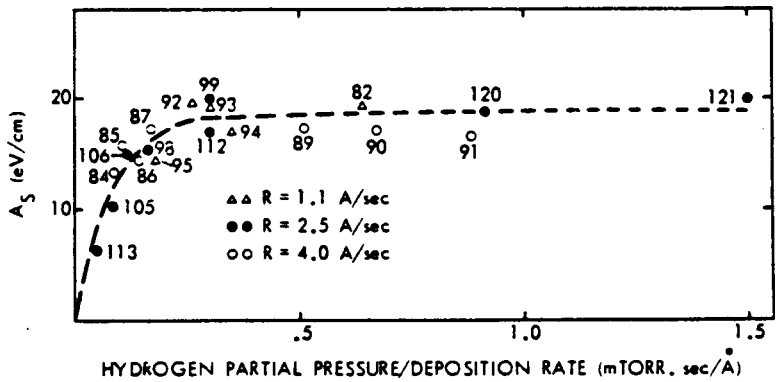

Fig. 9. Integrated infrared absorption under the Si-H stretching vibration vs. the P_H/R (deposition rate) for a number of films, deposited at $P_H \ll P_{Ar}$.

be smaller than for a true dangling bond, because the hydrogen incorporation involves bond breaking. The data also indicate that from the different species of hydrogen in the discharge (molecule, atom, ion) the atomic hydrogen incorporates far more efficiently than the most abundant molecular hydrogen.

We next discuss experimental data indicating that the SiH_x compound formation occurs at the target as the partial pressure of hydrogen increases. Fig. 10 shows the substrate self-bias potential vs. the total gas pressure in the discharge, as the ratio of H_2/Ar in the discharge increases from zero to ten. Note that the substrates are self-biased to more negative voltages as the hydrogen pressure in the discharge increases. In addition, the deposition rate decreases by about an order of magnitude with the hydrogen pressure in the discharge, even at a constant target voltage.

These results can now be accounted for as follows. The increase of the negative value of the self-bias voltage implies that the substrates are bombarded by more electrons as the hydrogen content in the discharge increases. This indeed is expected to be the case if the SiH_x compound formation occurs at the surface of the target. Compounds have higher secondary-electron emission yields than metal. The same effect can partly account also for the drop in the deposition rate since most of the energy of the incoming ions is used to produce and accelerate secondary electrons. The drop in the deposition rate could also partly be accounted for by the fact that compounds have generally lower sputtering yields than metals and by the fact that hydrogen as a lighter ion will carry a large fraction of the discharge current although contributing very little to the sputtering rate [21]. Therefore, this model of data interpretation suggests that the SiH_x compound formation moves gradually from the substrate to the target as the hydrogen pressure in the discharge increases or the deposition rate decreases. It should be emphasized, however, that the SiH_x compound in the target may or may not sputter stoichiometrically, because ion bombardment can result in chemical dissociation. The film growth under such conditions

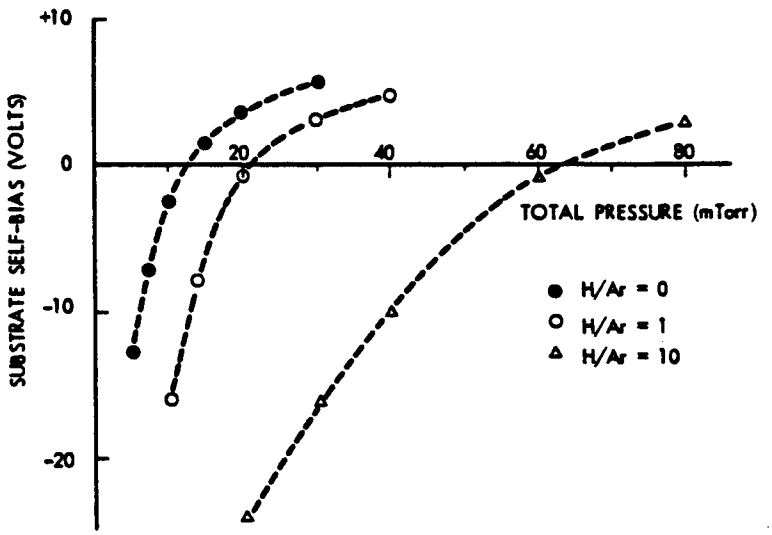

Fig. 10. The substrate self-bias voltage, measured with respect to the ground, vs. the total gas pressure in the discharge. The three curves correspond to H/Ar ratios of 0, 1 and 10.

would be greatly influenced by the fluxes of the products of the chemical dissociation arriving at the substrate.

This model of SiH_x compound formation could perhaps account for the controversial results of the two existing spectroscopic studies of the sputtering plasmas [31, 32]. In one study the results suggest that SiH_x molecules exist in the sputtering plasma, while in the other study SiH_x species have not been detected.

6. The role of chemical sputtering effects in the synthesis of SiH_x compounds

Up to this point we have discussed the effects of physical sputtering processes on the growth of a-SiH_x films. There is a high possibility, however, that in addition to these processes the film growth is influenced by chemical sputtering effects of the target or the growing film. As an example, the H-plasma may react with the surface of the target or the growing film and forms volatile SiH_x compounds, which may either be pumped out or may undergo plasma decomposition. Since such etching process of the growing film may be anisotropic, its influence on film structure may be significant.

Since direct observation of such processes are difficult, we have investigated this effect indirectly. We have first grown an a-SiH_x film and then exposed it to a hydrogen plasma. The surface morphology of this film, as revealed by SEM microscopy, is shown in fig. 11. Details of these etching studies will be published elsewhere [33]. At this point we want to emphasize that such processes participate during the film

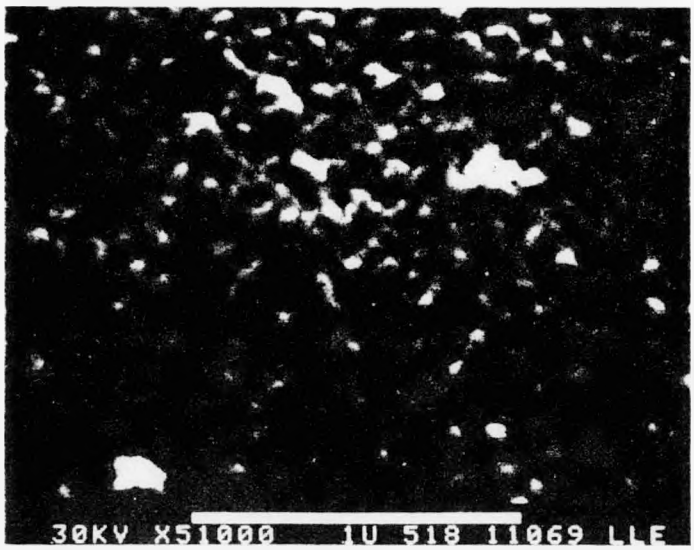

Fig. 11. SEM micrograph of the surface morphology of an a-SiH$_x$ film exposed to a hydrogen plasma [33].

growth. Of course they become far more important as the hydrogen pressure in the discharge increases.

7. Conclusions

In conclusion we have presented experimental results showing the role of different physical sputtering and chemical sputtering effects on the growth of hydrogenated a-SiH$_x$ films. These results can be summarized as follows:

In agreement with Ross and Messier [15], we demonstrated that the coalescence of the island structure is influenced primarily by charged rather than neutral particle bombardment. However, in disagreement with these authors, we proposed that the beneficial effects arise from the electron bombardment, while Ar^+ ion bombardment leads to undesirable effects, such as Ar incorporation and void formation.

We demonstrated that control of the hydrogen bonding, and thus the formation of compositionally homogeneous films can be accomplished through bias sputtering. Positive substrate bias (electron bombardment) favors hydrogen in the 2000 cm^{-1} mode while negative substrate bias (Ar^+ ion bombardment) favors the hydrogen in the 2100 cm^{-1} mode. This mode is correlated with Ar incorporation and microvoid formation in the film.

We have shown that the density of states in the middle of the gap, and related phenomena, such as recombination, do not depend on the bonding of hydrogen in the 2000 or 2100 cm^{-1} modes but they depend on the total amount of hydrogen in the film.

We produced evidence that the SiH_x compound formation occurs in the substrate at low hydrogen partial pressures, while at high hydrogen pressure, compound formation at the target becomes important.

Finally, the effects of etching of the growing film by the H-plasma have been pointed out through indirect etching studies of already formed SiH_x films.

Acknowledgements

The author is indebted to B. Abeles, R. Chimenti, M. Cohen, H.P. Maruska, J. Shropshire and T. Tiedje for a number of technical discussions and to R. Friedman and K. Rodgers for technical assistance. The work was partially supported by the US Department of Energy through a Solar Energy Research Institute Contract (Contract #XZ-0-9219).

References

[1] Y. Tawada, M. Kondo, H. Okamoto and Y. Hamakawa, Solar Energy Mater. 6 (1982) 299.
[2] H. Fritzsche, Solar Energy Mater. 3 (1980) 447.
[3] D.E. Carlson, Solar Energy Mater. 3 (1980) 503.
[4] F.J. Kampas and R.W. Griffith, Appl. Phys. Lett. 39 (1981) 407.
[5] J.C. Knights and R.A. Jujan, Appl. Phys. Lett. 35 (1979) 244.
[6] J.A. Reimer, R.W. Vaughan and J.C. Knights, Phys. Rev. Lett. 44 (1980) 193.
[7] T.A. Postol, C.M. Falco, R.T. Campwirth, I.K. Schuller and W.B. Yelon, Phys. Rev. Lett. 45 (1980) 648.
[8] J.C. Knights, Japan. J. Appl. Phys. 18 (1979) 101.
[9] W. Paul and D.A. Anderson, Solar Energy Mater. 5 (1981) 229.
[10] T.D. Moustakas, J. Electron. Mater. 8 (1979) 391.
[11] T. Tiedje, T.D. Moustakas and J.M. Cebulka, Phys. Rev. B23 (1981) 5634.
[12] T.D. Moustakas, C.R. Wronski and T. Tiedje, Appl. Phys. Lett. 39 (1981) 721.
[13] T.D. Moustakas and R. Friedman, Appl. Phys. Lett. 40 (1982) 515.
[14] T.D. Moustakas, R. Friedman and B.R. Weinberger, Appl. Phys. Lett. 40 (1982) 587.
[15] R.C. Ross and R. Messier, J. Appl. Phys. 52 (1981) 5329; Tetrahedrally Bonded Amorphous Semiconductors, eds. R.A. Street, D.K. Biegelsen and J.C. Knights, AIP Conf. Proc. no. 73 (1981) 53.
[16] D.A. Anderson, G. Moddel, M.A. Paesler and W. Paul, J. Vac. Sci. Technol. 16 (1979) 906.
[17] M.H. Brodsky, M. Cardona and J.J. Cuomo, Phys. Rev. B16 (1977) 3556.
[18] E.C. Freeman and W. Paul, Phys. Rev. B18 (1978) 4288.
[19] J.P. deNeufville, T.D. Moustakas, A.F. Ruppert and W.A. Lanford, J. Non-Crystalline Solids 35-36 (1980) 481.
[20] T.D. Moustakas, T. Tiedje and W.A. Lanford, Tetrahedrally Bonded Amorphous Semiconductors, eds. R.A. Street, D.K. Biegelsen and J.C. Knights, AIP Conf. Proc. no. 73 (1981) 20.
[21] J.L. Voson and W. Kern, Thin Film Processes (Academic Press, New York, 1978).
[22] W. Paul, Solid State Commun. 34 (1980) 283.
[23] F.R. Jeffrey, H.R. Shanks and G.C. Danielson, J. Appl. Phys. 50 (1979) 7034.
[24] S. Oguz, D.K. Paul, J. Blake, R.W. Collins, A. Lachter, B.G. Yacobi and W. Paul, J. de Phys. Colloq. C4 suppl. no. 10, Tome 42 (1981) C4-679.

[25] T.D. Moustakas, Patent Appl., US Ser. no. 108469 (31 Dec. 1979); Patent Appl., US Ser. no. 213034 (4 Dec. 1980).
[26] J. Comas and E.A. Wolicki, J. Electrochem. Soc. 117 (1970) 1197.
[27] W. Paul, G.A.N. Connell and R.J. Temkin, Advan. Phys. 22 (1973) 529.
[28] D.J. Kalnicky and T.D. Moustakas, Anal. Chem. 53 (1981) 1972.
[29] D.E. Carlson and C.R. Wronski, Amorphous Semiconductors, ed. M.H. Brodsky (Springer-Verlag, New York, 1979) p. 287.
[30] T.D. Moustakas, to be published.
[31] A. Matsuda, K. Nakagawa, K. Tanaka, M. Matsumura, S. Yamasaki, H. Okushi and S. Iizima, J. Non-Crystalline Solids 35-36 (1980) 183.
[32] M.A. Paesler, T. Okumura and W. Paul, J. Vac. Sci. Technol. 17 (1980) 1332.
[33] T.D. Moustakas, US Patent 4285762 (25 August 1981); to be published.

APPENDIX B. Preparation of Hydrogenated Amorphous Silicon by Sputtering

2.3 PREPARATION BY SPUTTERING

T. D. Moustakas
Corporate Research Laboratories
Exxon Research and Engineering Company
Linden, New Jersey 07036

TABLE OF CONTENTS

I. INTRODUCTION

There are two plasma methods for depositing hydrogenated amorphous silicon; glow discharge decomposition of silane, and reactive sputtering from a silicon target in a mixture of inert gas and hydrogen. Of the two, glow discharge has attracted considerably more attention. The extensive investigation of this deposition process, through plasma diagnostic studies, and of the resulting films through structural, optical, transport, recombination and device studies, has led to the fabrication by Catalano et al. (1982) of solar cell structures with efficiency up to 10%. It is widely believed that this rapid progress in the device area resulted from the identification of thin film growth conditions, which lead to material with the lowest structural and compositional inhomogeneities.

The alternative technology of reactive sputtering, inherently, has many advantages as a deposition process. Principal among these is the ability to uncouple the two source materials, Si and H, and to independently optimize the role that each plays in forming the network and in determining the ensuing electro-optical properties. This type of control is not possible for glow discharge decomposition of silane because the source materials are initially chemically bonded in the feed gas SiH_4. In addition, sputtered films in general, are mechanically strong (good film-substrate adhesion) and the process is easily scalable. Despite these obvious advantages, this process has not been pursued as vigorously as the glow discharge process, primarily because early work suggested that sputtered α-Si:H films are inferior in their electronic properties to those produced by the glow discharge process. In addition, there is a widespread belief that sputtering is an unsuitable technology for surface sensitive devices.

In the past two years significant progress has been made in the understanding of thin film growth process of the sputtered material, and this was followed by progress in the device area. Solar cell structures with efficiency up to 5.5% have recently been announced (Moustakas 1983).

This chapter reviews progress made over the past few years in the preparation of α-Si:H films by the method of RF diode reactive sputtering. The material is organized to include a brief historical background of the evolution of this method, and sections on physical and chemical effects in sputter-deposition of a-Si:H films, on the mechanisms of film growth and on methods to control structural and compositional inhomogeneities. Finally we comment on the device potential of this method and on future research directions.

II. HISTORICAL BACKGROUND

The development of amorphous silicon by sputtering can be divided historically into two eras. Prior to 1974 sputtering was widely used for the deposition of pure tetrahedrally-coordinated amorphous semiconductors. Structural studies on such materials by Moss and Graczyk (1969), Shevchik and Paul (1972) and Temkin et. al. (1973) have revealed that such films contain microvoids of the order of 5 to 10Å in diameter. Optical, transport and electron spin resonance measurements have been plausibly and self-consistently interpreted by Brodsky et al. (1970) and Paul et al. (1973) on a model which assumed that these structural defects give rise to a large density of states in the gap of the semiconductor. At the same time, the studies of Spear (1974) indicated that a-Si produced by glow-discharge decomposition of SiH_4 has a considerably smaller density of states in the gap and exhibited electronic properties typical of semiconducting behavior. It has been speculated by Brodsky et al. (1970) that the difference between sputtered and glow-discharge a-Si might be caused by hydrogen contamination.

Against this background Lewis, et al. (1974) have produced the first sputtered hydrogenated amorphous germanium films by sputtering from a germanium target in a mixture of argons and hydrogen. This initial study and subsequent studies of such material by Lewis (1976), Connell and Pawlik (1976), Moustakas and Connell (1976) and Moustakas and Paul (1977a) indicated that hydrogen incorporation reduced the density of spins by orders of magnitude with corresponding changes in the optical, transport and recombination properties.

Hydrogen incorporation was found to have far more dramatic effects in amorphous silicon than in amorphous germanium. Following the

discovery by Spear and LeComber (1975), that glow discharge material could be doped n-type and p-type, Paul et al. (1976) have demonstrated that sputtered hydrogenated amorphous silicon could also be doped n-type and p-type and that semiconductor junctions could be formed. Subsequent studies of this material by Moustakas et al. (1977b,), Anderson et al. (1977, 1979) and Moustakas (1979), suggested that careful optimization of the deposition parameter space could lead to material with similar electronic properties as that produced by glow discharge decomposition of silane.

Following these initial discoveries, the focus shifted to understanding the bonding configuration of hydrogen in the amorphous silicon network and to identify those deposition parameters that control hysrogen bonding. Experimental tools used in these studies include Si-H vibrational studies, photoemission, hydrogen evolution and nuclear magnetic resonance. Such studies have recently been reviewed by Paul and Anderson (1981).

The vibrational studies of Brodsky et al. (1977) and Freeman and Paul (1978) identified the stretching modes in the 2000-2100 cm^{-1} region, the bending modes in the 800-900 cm^{-1} region and the rocking and wagging modes at 630 cm^{-1}. These studies indicated that in sputtered material, produced under a variety of deposition conditions, the stretching vibration is always a doublet. It is generally accepted that the mode at 2000 cm^{-1} is due to isolated Si-H units. The assignment of the mode at 2100 cm^{-1} is still controversial. Brodsky et al. (1977) suggested that it is due to SiH_2 units. Paul (1980) and Shanks et al. (1980) have proposed that this mode could also arise from Si-H units in particular local environments. Jeffrey et al. (1979, 1980) demonstrated that sputtered α-Si:H films having only the 2000 cm^{-1} stretching mode can be made by sputtering at high power

with the substrates located below the edge of the dark space. Oguz et al. (1981a) also reported that films grown on substrates located next to the dark space have the Si-H stretching vibration at 2000 cm^{-1}. Moustakas (1982c) developed bias sputtering as a means of controlling the bonding of hydrogen. This method will be discussed in greater detail in Section V.

Photoemission studies on sputtered α-Si:H were first reported by VonRoedern et al. (1979). These studies revealed the existence of a number of peaks in the valence band density of states which were correlated with SiH, SiH_2 and SiH_3 configurations.

Information regarding the bonding of H in the Silicon network can also be obtained by hydrogen evolution studies. Such studies on sputtered α-Si:H films were performed by Oguz et al. (1980a, 1980b). These authors find that samples produced at low hydrogen partial pressure show a single evolution peak near 600°C while those produced at high partial pressure of hydrogen have also a second peak near 375°c. Although these data suggest the existence of two sites for hydrogen attachment, their interpretation is not firm yet. For more details the reader is refered to works by Oguz (1981b) and Bruyere et al. (1980).

Nuclear magnetic resonance measurements in sputtered α-Si:H films were reported by Jeffrey et al. (1981) and Carlos et al. (1981). These studies revealed two superposed resonance lines of different widths as was also observed for glow discharge a-Si:H by Reimer et al. (1980). The narrower line contains about 2-4 at % H and was attributed to monohydride configurations. The width of this line suggests that some of the monohydride units are clustered rather than randomly distributed. The broader line contains the rest of the hydrogen and is associated with densely clustered monohydrides or polyhydrides. The interpretation of

these data and their correlation with the results obtained from other hydrogen probing experimental techniques is not firm yet.

In parallel with these studies, a large volume of work on optical transport and recombination properties has been generated in a number of laboratories. These properties were found to be sensitive to the hydrogen content and to the microstructure of the films. A comprehensive review on these properties was published by Paul and Anderson (1981).

Methods have been developed to probe the states in the gap of the semiconductor. Such methods include ESR, field effect, capacitance-voltage optical absorption and drift mobility. These studies indicated that device quality material, having density of states in the middle of the gap of 10^{15} or lower can be fabricated by the method of sputtering (Tiedje et al. 1981).

Thin film growth and microstructural studies have been reported by Anderson et al. (1979), Moustakas (1979, 1982c), Jeffrey et al. (1979), Tiedje et al. (1981), Moustakas et al. (1981a), Martin and Pawlewicz (1981), Turner et al. (1981) and Ross and Messier (1981a, 1981b). In these studies the kientics of the film growth and the influence of physical and chemical sputtering effects in controlling structural and compositional inhomogeneities have been investigated. These studies will be discussed in greater detail in the rest of the text.

Photovoltaic studies in this material were first reported by Thomson et al. (1978), Victorovitch et al. (1979), Moustakas et al. (1980) and Anderson et al. (1980). These studies were performed on Schottky barrier and Metal-Insulator-Semiconductor devices. The moderate performance of such devices (conversion efficiency ~2%) has reinforced the widespread belief that sputtered a-Si:H films are inferior to those

produced by glow discharge decomposition of silane. However, recent progress in identifying deposition parameters which control film growth and progress in doping and device studies (Tiedje et al. 1981, Moustakas et al. 1981a, 1981b, Morel and Moustakas 1981, Moustakas and Friedman 1982a, Moustakas et al. 1982b, Moustakas 1982c, Maruska et al. 1983) have led to the fabrication of solar cell structures with efficiencies up to 5.5% (Moustakas 1983).

III. PHYSICAL AND CHEMICAL EFFECTS IN SPUTTER-DEPOSITION OF α-Si:H FILMS

In this section we review physical and chemical effects which are likely to influence the growth mechanism of α-Si:H films produced by RF diode sputter deposition. We are going to explore phenomena occuring at the target, in the glow discharge and at the substrate. For a general reference on sputtering the reader is referred to the book by Vossen and Kern (1978).

A. Physical and Chemical effects at the Target

There are three types of phenomena which probably occur simultaneously at the Si target surface during sputtering in a mixture of Ar and H_2:

1. Bombardment By Ar^+ and H^+ Ions

During this process a number of effects may occur. (a) Some of the incident ions are neutralized and reflected as high energy neutrals. The probability for this elastic backscattering depends on the ratio of M_I/M_T, where M_I is the mass of the impinging ion and M_T is the mass of the target atom. Ross and Messier (1981a) have noticed that momentum transfer considerations favor backscattering from the Si target of H but not of Ar atoms. (b) The ion bombardment may cause the target to eject a secondary electron. These electrons are accelerated away from the target with an initial energy equal to the target potential. (c) The ion may be implanted into the target. Argon implantation into Si is substantial even at low ion energies (Comas and Carosellar 1968). (d) The target also emits UV and X-ray radiation. (e) Ion bombardment may damage and possibly disorder the surface of the target. (f) Ion bombardment removes neutral Si atoms by momentum transfer. This is the sputtering process which leads to the formation of the film. The threshold for sputtering single crystal silicon

is 10 to 15eV (Wolski and Zdanuk 1961). The sputtering yield by H^+ ions is probably very small. (g) A significant fraction of the energy of the bombarding ions is dissipated in the target in the form of heat (Maissel 1970).

2. Si:H Compound Formation

This process is favorable at high partial pressures of hydrogen ($H_2/Ar >> 1$) and low sputtering rates. It is well known in reactive sputtering (Schwartz 1964) that under these conditions compound formation (SiHx) occurs at the surface of the target as a solid state reaction. Later, some of this SiHx is sputtered off. As discussed in Section IV such a process results in a significant decrease in deposition rate, and in high secondary electron emission.

3. Chemical Sputtering

H-plasma etches crystalline Si (Veprek 1980). Therefore the hydrogen plasma may react with the surface of the target and form volatile SiH_x compounds. As discussed in Section IV the etching rate for such a process depends on the temperature of the Si target and on the concentration of atomic hydrogen. In the presence of such a process, the film grows by a combination of physical sputtering and glow discharge decomposition of silane.

B. Effects in the Glow Discharge Which Influence Film Growth

The density of the gas in the discharge controls the thermalization of the different particles (electrons, ions, neutrals) which are removed from the target. Depending on whether bombardment of the substrate by such particles is desirable or undesirable one may choose to work at low or high gas pressure.

In an RF discharge, neutral sputtered atoms can be positively

ionized by the Penning process (Coburn and Key 1972). In this process metastable discharge atoms (Ar^m) transfer their energy and ionize neutral sputtered species (X) according to the reaction:

$$Ar^m + X \longrightarrow X^+ + Ar + e$$

Silicon atoms will be readily ionized by such a process because their ionization potential (7eV) is significantly smaller than the energy of metastable Ar atoms (11.55 and 11.72 eV). Such positively ionized silicon atoms will provide another source for bombardment of the substrate.

C. Physical and Chemical Effects at the Substrate

The effects occuring at the substrate can be classified into the following categories.

1. Vapor Condensation and Network Formation

During this stage Si vapor from the target arrives at the substrate and condenses from an excited state. The atoms, utilize their heat of condensation or energy supplied by other means to move around to final low energy sites. This motion is influenced also by the binding energy of the atom to the substrate. Indeed, different results are obtained with different substrates. In the process of hopping from one adsorption site to another, the atom may re-evaporate or join with another atom to form a pair. This atomic pair has lower mobility. Therefore it is likely to be joined by other atoms, and the nucleation process of film growth has begun. This process leads initially to isolated islands, which as they grow in size coalesce to form a continuous film.

Movchan and Demshishin (1969) showed that the critical parameter in vacum deposition is the ratio of the substrate temperature to the

melting point of the evaporant (T_S/T_M). If this ratio is less than 0.45 the growth mode is columnar. Thornton (1974) has extended this model to the sputtering processes and included the role played by the sputtering gas. In this process, a decrease in gas pressure is equivalent to an increase in substrate temperature and vice versa. Such effects will be discussed in detail in Section V.

2. Substrate Bombardment by Energetic Particles and Radiation

In addition to sputtered neutral species from which the film is grown, the substrate is also bombarded by numerous other species arriving from the target or extracted from the glow discharge. For example, secondary electrons, and conceivably secondary negative ions, are accelerated away from the target and by bombarding the substrate may cause substrate heating and radiation damage. Many of these species may be thermalized by collisions within the gaseous ambient, but a substantial number arrives at the substrate with full target potential. Also, since the substrate in a glow discharge is negatively charged with respect to the plasma, it is also bombarded by positive species extracted from the discharge. Such species include Ar^+ and H^+ ions as well as Si atoms ionized positively by the Penning process.

In the case of RF glow discharge these bombardment effects by charged particles are also influenced by the systems geometry. It is known (Vossen and Cuomo 1978) that the ratio of the average potential on the target (V_T) to that of the grounded electrode (V_G) with respect to the plasma is given by:

$$V_T/V_G = (A_G/A_T)^4 \qquad (1)$$

where A_G and A_T are the areas of the grounded electrode and of the target, respectively. These areas refer to the areas in contact with the plasma. Therefore, the voltage of the substrate with respect to the plasma depends on the system geometry and can change for the same system by confining the discharge.

Bombardment effects by charged particles can also be influenced by an external bias intentionally applied to the substrate. The effects of both self-induced and externally supplied bias on the growth of a-Si:H films will be discussed in Sections V and VI.

In addition to bombardment by charged and neutral particles the substrate is also subjected to UV and X-radiation from the target and glow discharge. These effects may influence the kinetics of the Si and H reactions at the surface of the substrate and can also induce radiation damage.

3. Si:H Compound Formation

As was discussed earlier, at high partial pressures of hydrogen ($H_2/A_r \gg 1$) and low sputtering rates, Si:H compound formation is likely to occur at the surface of the target. In the opposite regime, low hydrogen partial pressure ($H_2/A_r \ll 1$) and high sputtering rate, compound formation is likely to occur at the surface of the substrate. This process and the kinetics of the Si and H reactions are discussed in Section IV.

4. H-Plasma Etching of the Film

H-plasma is known to etch amorphous silicon (Moustakas 1982c) and therefore the effect of such process is likely to influence the growth of

the thin film. A discussion of this process is given in Section IV.

IV. SYNTHESIS OF Si:H COMPOUNDS

The mechanism of synthesis of Si:H compounds by sputtering from a Si target in an atmosphere of Ar and H_2 is poorly understood. In classical reactive sputtering (Schwartz 1964, Vossen and Cuomo 1978), reactions between the target material and the reactive gas occur either at the surface of the substrate or the surface of the target, or both. Reactions in the gas phase are considered unfavorable because the simultaneous conservation of energy and momentum requires the presence of a third body. Whether the reaction occurs at the substrate or the target depends on the partial pressure of the reactive gas and the target sputtering rate. At low reactive gas partial pressure and high target sputtering rate, virtually all of the compound formation occurs at the substrate, whereas, in the opposite regime, high reactive gas partial pressure and low target sputtering rate the compound formation occurs at the target. The transition from one regime to the other occurs at a certain threshold value of the reactive gas partial pressure; for metallic targets, this is accompanied by a sharp decrease in the sputtering rate (Heller 1973, Vossen and Cuomo 1978). There are three factors which contribute to the decrease in the sputtering rate: (1) compounds, in general, have a lower sputtering yield than metals; (2) compounds have higher secondary electron emission yield than metals and therefore, the energy of the incoming ions is used to produce and accelerate secondary electrons; (3) sputtering by reactive gas ions is less efficient than by inert gas ions.

In addition to these reactive sputtering effects, the film growth may also be influenced by chemical sputtering effects. Hydrogen plasma is known to etch both crystalline silicon (Veprek 1980) and amorphous silicon (Moustakas 1982c). Since in RF diode sputtering both the surface of the

target and the surface of the growing film are in contact with the plasma, the possiblity that the hydrogen plasma attacks both and forms volatile SiH_x species is very likely. The etching rate of such processes was found to depend strongly on the density of atomic or ionic hydrogen and on the temperature of silicon. More specifically, the etching rate was found to attain a maximum value when the temperature of silicon is between 100 to 200°C and falls abruptly at lower and higher temperatures. This temperature dependence is probably related to the mobility of hydrogen atoms on the surface of silicon. These etching effects, particularly the etching of the growing film, may influence the film growth in a variety of ways. One possibility is that etching is anisotropic with higher rates at the intercolumnar low density regions. Therefore such processes could affect the film microstructure. Another possibility is the modification of the film chemistry since volatile SiH_x species are likely to form more easily by interaction of atomic hydrogen with polyhydride configurations.

These effects have been investigated through spectroscopic studies. One study by Matsuda et al. (1980) reports the presence of SiH_4 in their sputtering plasma while another by Paesler et al. (1980) reports that SiH_4 is not present in their sputtering plasmas. In the following I discuss the results of these studies and suggest a possible resolution of the controversy.

Based on their observation, Matsuda and co-workers suggest the following mechanism for the thin film growth: hydrogen gas introduced into the sputtering chamber is excited and decomposed into H atoms (or radicals) in the vicinity of the target where the electric field is the strongest. Such radicals react with sputtered Si atoms within the plasma close to the target, producing SiH_x molecules. After several collisons with other

species, SiH_x molecules reach the surface of the substrate and are solidified into a-Si:H through surface reaction. The authors recognize that an alternative mechanism of forming SiH_x molecules is by direct etching of the Si target by H atoms, but they suggest that this must be a secondary mechanism since the emission line intensity of SiH_4 is lowered in 100% H_2 gas.

In my view, the SiH_4 has been formed by H-plasma etching of the silicon target and of the film deposited on the substrate and on the surrounding walls. As mentioned earlier, this mechanism depends strongly on the temperature of the silicon. Unfortunately, the authors did not disclose the temperature of the target and that of the substrate platform in the description of their experimental conditions. However, based on the schematic diagrams of their experimental apparatus, it appears that neither the target nor the substrate platform were intentionally cooled or heated. If this suspicion is correct, then both the target and substrates may be heated to temperatures in excess of 100°C during the process of sputtering. It is estimated (Vossen and Cuomo 1978) that 1% of the energy incident on the target surface goes into ejection of sputtered particles, 75% into heating of the target, and the remainder is dissipated by secondary electrons that bombard and heat the substrates. Under such circumstances, the etching rate of silicon by the H-plasma is expected to have its maximum value. The observation by the authors that the amount of SiH_4 decreases in 100% H_2 gas can also be accounted for in this model. The etching rate of silicon is proportional to the amount of atomic hydrogen, which has been shown by the authors to decrease in the absence of argon.

Paesler and co-workers on the other hand operated their sputtering apparatus with water cooled target. As a result, the etching

rate of Si by the H-plasma should be very small and this should account for the lack of SiH_4 in their sputtering plasma.

On the basis of these observations, I propose the following model for film growth. If the target is water cooled and the substrate platform is held either close to room temperature or above 200°C, there is very little H-plasma etching of either the target or of the growing film. Under such experimental conditions, the kinetics of the Si and H reactions could be interpreted along the lines of classical reactive sputtering. If the target is held at temperatures between 100 to 200°C, then besides physical sputtering, the target is constantly etched by the H-plasma and forms SiH_4. Under such conditions, the film grows by a combination of physical sputtering and glow discharge decomposition of SiH_4. If the target is water-cooled and the substrates are held at temperatures between 100 to 200°C, the kinetics of the Si and H reactions are influenced not only by the physical sputtering processes but also by the etching of the growing film by the H-plasma.

To test this model we investigated the kientics of the Si and H reactions (Tiedje et al. 1981 and Moustakas et al. 1981a) under sputtering conditions which do not favor H-plasma etching of either the target or the growing film. (The target was water cooled and the substrate was held at temperatures higher than 200°C.) In these studies we deposited a number of films at low partial pressures of hydrogen ($H_2/Ar \ll 1$) and evaluated the Si and H reactions by measuring the density of states in the middle of the gap, which is related to Si dangling bonds and the hydrogen content in the films. Since these studies have been published we present only a brief summary of these results.

The samples were deposited at 275°C and argon pressure of 5

mTorr. The hydrogen pressure was varied from 0.3 to 1.4 mTorr. The density of states in the middle of the gap was measured by capacitance-voltage and ESR techniques (Tiedje et al. 1981). The results are shown in Figure 1 and clearly indicate that the density of states depends exponentially on the partial pressure of hydrogen in the discharge. The relative amount of bonded hydrogen in these films has been inferred from the integrated intensity under the Si-H stretching vibration (assumed to be proportional to the concentration of bonded hydrogen). The dependence of the integrated intensity of the Si-H stretching mode on the partial pressure of hydrogen is given in Figure 2.

To model the Si and H reactions from these data, we postulated that the measured gap states are due to dangling silicon bonds. During the film growth process, a potential dangling bond at the growing surface of the films will either capture an H atom or be covered up by a layer of silicon atoms. Once the dangling bond is covered, it is unlikely to capture a hydrogen and becomes an electronically active defect. The capture rate of hydrogen atoms by dangling bonds will be given by the product $\sigma\Theta FN$, of σ the capture cross section of the dangling bond for hydrogen, Θ the sticking coefficient, F the hydrogen flux onto the surface of the film and N the number of dangling Si bonds. For a given film growth rate R (monolayers/sec), the dangling bond will have on the average a time of 1/R in which to capture an H atom before it is sealed up by an overlayer of silicon. The time dependence of the number of dangling bonds N on the growing surface of the film will be given by:

$$\frac{dN}{dt} = - \sigma\theta F N \qquad (2)$$

If No is the number of dangling bonds present in the absence of hydrogen, then after the cutoff time 1/R the number surviving is given by:

$$N = No \exp(-\sigma\theta F/R) \qquad (3)$$

Equation (3) predicts an exponential decrease in the density of dangling bonds with increasing H partial pressure since the H flux, F, is expected to be proportional to the partial pressure of H_2.

In order to quantitatively fit the data of Figure 1 to Eq (3), one needs to know which species of hydrogen (molecule, atom, ion) is the important one for hydrogen attachment to the dangling bonds. Such information is not available. However, the density of all these species is expected to scale with the H partial pressure, provided the argon pressure is high compared to the H-pressure. For lack of more detailed information, we will use for F the flux of H_2 molecules in a hypothetical neutral gas at the same temperature and pressure. We find $F=Ap_H$ where $A = 1.1 \times 10^{18}$ cm^{-2} sec^{-1} $mTorr^{-1}$. If we use 10^{-16} cm^2 for σ and the experimental value of R of about 1 monolayer/sec, we find a sticking coefficient $\Theta = 0.06$. This small value of sticking coefficient is reasonable if we assume that the atomic hydrogen is the active species and that the more abundant molecular hydrogen is not expected to eliminate dangling bonds.

Since the density of dangling bonds in the absence of hydrogen is much smaller than the actual hydrogen content of the hydrogenated material, it is clear that only a small fraction of the incorporated hydrogen

eliminates potential dangling bonds. Most of the H bonds to other sites. We can estimate a sticking coefficient of these sites for H using the same kinetic model of thin film growth process. In this model the hydrogen concentration will be given by:

$$A = A_{max} [1 - \exp(-\sigma\theta' F/R)] \quad (4)$$

where A_{max} should reflect the maximum amount of H that can be incorporated into the lattice. By fitting the data in Figure 2 with Eq (4), we find that the H-sticking coefficient is $\theta' = 0.02$ if we use the same capture cross section (10^{16} cm^2) as for dangling bond sites.

The fact that the sticking coefficient inferred from the H content is smaller from that inferred from the density of gap states may mean that most of the hydrogen has a high probability of being displaced by Si during the film growth process or that the H is incorporated into reconstructed dangling bonds. The sticking coefficient for these sites is likely to be smaller than for true dangling bonds, because the hydrogen incorporation involves bond breaking. In this interpretation the bulk of the hydrogen is incorporated into sites that, in the absence of hydrogen, are reconstructed dangling bonds and do not have a spin or contribute states near midgap.

A further prediction of the model is that the hydrogen content in the films depends also on the deposition rate. To test this prediction we deposited three series of films at deposition temperature 275°C, argon pressure 15 mTorr, deposition rates between 1-4 A/sec and studied their hydrogen content (Moustakas et al. 1981a). The data of the hydrogen content in these films vs. the ratio P_H/R are shown in Figure 3. The

dashed curve is the fit to the data based on Eq (4) with a sticking coefficient 0.03. Therefore at these range of depositon rates the data are in good agreement with the model.

In the kinetic theory we have neglected thermal desorption of H from bonding sites, and assumed that the H and Si are far from thermodynamic equilibrium. This assumption can be checked by comparing the H content as a function of P_H, for films deposited at different substrate temperatures with other parameters held fixed. The results for two series of films, one deposited at 385°C and one at 225°C are shown in Fig. 4. The first thing to note is that the saturation H content at high P_H is higher for the low temperature films. A plausible explanation of this result is that the growing Si network anneals more at 385°C than at 225°C. At the high temperature the Si network is likely to be less defective and, as a result, may have fewer H bonding sites.

The data in Fig. 4 sugggest that the sticking coefficient θ at high temperature (385°C) is about equal to or larger than the sticking coefficient at 225°C. This observation rules out a thermodynamic equilibrium interpretation of the data. In this interpretation the effective sticking coefficient at a given P_H would be determined by the ratio of the H flux onto the surface to the rate of thermal desorption. The desorption process will involve bond breaking and hence should be thermally activated and strongly temperature dependent. In this case, the apparent sticking coefficient would decrease dramatically from 225 to 385°C, contrary to the experimental results in Fig. 4, where the sticking coefficient appears to go in the opposite direction. Thus we conclude that the system is far from thermal equilibrium and the kinetic model is appropriate.

These studies demonstrated that the compound formation of films, produced at low partial presure of hydrogen ($H_2/A_r << 1$) with substrate temperatures higher than 200°C and water cooled target, occurs at the surface of the substrate. The stoichiometry of these films was found to depend on the relative rates of arrival at the substrate of Si and H atoms, in agreement with the predictions of the reactive sputtering theories.

It has been shown in another paper (Moustakas 1982c) that for $H_2/A_r >> 1$) the Si:H compound formation occurs at the surface of the target. For details on these studies the reader is referred to the original work.

V. EVOLUTION AND CONTROL OF STRUCTURAL INHOMOGENEITIES

The structural studies of Knights and Lujan (1979) have led to the discovery that plasma deposition of a-Si:H films proceeds via nucleation and growth of island structures (average lateral dimensions ~100Å). The coalescence of these islands, if imperfect, leads to columnar morphology in subsequent growth. These authors report that growth of the films in pure silane, at low deposition rates, and deposition temperatures between 200 to 300°C leads to a more perfect coalescence of the islands. Films showing columnar morphology are unstable upon exposure to the atmosphere. The interstitial regions between the columns can be penetrated by active atmospheric impurities leading to post deposition contamination effects (Knights 1979). The electronic properties of such films are poor since the low density interstitial regions are correlated with electronically active defects (Biegelsen et al. 1979).

Evidence of microstructural changes as a function of deposition parameters of sputtered amorphous silicon were first reported by Freeman and Paul (1978). These authors observed that films produced at high argon pressure show post-deposition contamination effects, which they consider evidence of film porosity.

Another study by Paulewicz (1978) on unhydrogenated amorphous silicon correlated defect creation to bombardment by Ar atoms, backscattered from the silicon target. This study concluded that the best quality films (high resistivity) are those produced at high argon pressure (>150 mT). Moustakas (1979) reinterpreted Paulewicz's result in terms of post-oxidation contamination effects.

Anderson et al. (1979) studied in more detail the electronic properties of hydrogenated amorphous silicon films produced as a function

of argon and reported that high pressure films have poor electronic properties. These authors attributed the observed effects to the bombardment of the film by the neutral sputtered Si species from which the film grows. They argue that weak bombardment of the growing film might be beneficial in removing loosely bound material from the surface. At high argon pressures, this desirable bombardment is removed due to the faster collisional thermalization of the Si-species.

The most comprehensive study on the microstructure of sputtered a-Si:H films has been reported by Ross and Messier (1981a, 1981b). Their studies confirm that the growth habit of this material is also columnar, as in glow discharge decomposition of silane. Using TEM and SEM they demonstrated that films produced at high argon pressures have columnar microstructure, while those produced at low argon pressure show no noticeable microstructure.

Ross and Messier (1981a, 1981b) and Moustakas (1982c) correlated these microstructural changes with corresponding changes in the self-bias voltage of the substrates and attributed these structural changes to charged particle bombardment effects.

In the rest of this section I give some examples to illustrate the evolution and control of microstructure in sputtered or Si:H films (Moustakas 1982c). A number of films have been deposited at fixed hydrogen partial pressure (P_H = 0.7 mTorr) and argon pressure varying between 5 to 40 mTorr. The substrates were electrically floated and held at 275°C. The target was supplied with a constant power of 200 watts. The choice of this mode of operation resulted in a small but monotonic increase of the deposition rate from 2.1 to 2.7 A/sec, because the ion current increases as the pressure increases. As a result of that, the hydrogen content in the

films was found to decrease with the argon pressure from 21.5 to 19.5 at %. Microstructural changes in these films were inferred from measurements of the index of refraction and infrared vibrational spectra.

Figure 5 shows the dependence of the index of refraction, n, measured immediately after the film deposition at wavelength $\lambda \sim 2\mu m$, vs. the argon pressure in the discharge. The value of n remains constant up to about 20 mTorr of argon and then drops rather abruptly. The reduction of the index of refraction at high argon pressures is accompanied by post-deposition contamination. Figure 6 shows the infrared vibrational spectral for samples deposited at 5, 10, 20 and 40 mTorr of argon. The films deposited at 5 and 10 mTorr of argon show the usual Si-H vibrations, while the samples deposited at 20 and 40 mTorr of argon additionally show Si-O (~1100 cm^{-1}), Si-N (880 cm^{-1}) and C-H (~3000 cm^{-1}) vibrations. In agreement with Freeman and Paul (1978), we find that these additional vibrations are due to post-deposition contamination, and they grow as a function of time.

The reduction of the index of refraction for the films produced at high argon pressure can be accounted for as resulting from the film's porosity and from the formation of low index of refraction coatings (SiO_x, SiN_x) in the inter-columnar voids. Therefore, the results of Figs. 5 and 6 are consistent with the observations of Ross and Messier (1981a) that films grown at high argon pressure have a columnar morphology, and that under the described preparation conditions the coalescence of the island structure is imperfect for films grown at argon pressure higher than 20 mTorr.

In agreement with Knights (1979) and Anderson et al. (1979) we find that the films produced at high argon pressures have poor photoelectronic properties. As an illustration, Fig. 7 shows the

photoconductivity under AMI illumintion vs. the argon pressure in the discharge. The photoconductivity of the film produced at 40 mTorr of argon is lower by three orders of magnitude from that of the films produced at low argon pressures.

In order to investigate whether these structural changes are the result of bombardment or lack of bombardment of the film by neutral or charged particles we determined the dependence of the self-bias potential of the substrates on the partial pressure of argon. The substrate self-bias voltage was measured with respect to the ground in a separate experiment, which simulated the conditions of the sample deposition. Figure 8 shows the substrate self-bias potential, with respect to the ground, vs. the partial pressure of argon in the discharge. The substrates are negatively biased at low argon pressures, because they are bombarded by more electrons than ions due to the higher electron mobility. At high argon pressures, on the other hand, the substrates have approximately the same potential as the plasma (positive), and charged particles do not bombard but migrate to the substrates by thermal diffusion. Ross and Messier (1981b) have measured, in addition, the plasma potential with a Lagmuir probe and they were able to calculate the potential of the substrates with respect to the plasma. Their data have the same functional behavior observed in Fig. 8. We concluded from the data of Figs. 5-8 that the change in the sign of self-bias potential with respect to the ground, occurs at exactly the same argon pressure where significant changes in the film's microstructure have been observed. Therefore, these data suggest that the coalescence of the island structure is the result of atomic rearrangement due to the bombardment of the growing film by charged particles. However, these data cannot differentiate the relative roles of

electron or Ar^+ bombardment in the growth of the film. Ross and Messier (1981b) attribute the structural changes to the Ar^+ ion bombardment. However, in the next section we will show that electron bombardment may be as important in inducing structural changes. The correlations observed in Figs. 5-8 cannot be explained on the basis of film bombardment by neutral species, as suggested by Anderson et al. (1979) since such species are unaffected by substrate bias.

VI. COMPOSITIONAL INHOMOGENEITIES

Compositional inhomogeneities have been observed both in glow discharge and sputtered a-Si:H films through NMR, neutron scattering and infrared vibrational studies (Reimer et al. 1980, Jeffrey et al. 1981, Carlos et al. 1981, Postol et al. 1980, Freeman and Paul 1978 and Knights 1979). Some authors have attempted to correlate the observed compositional inhomogeneities with the type of structural inhomogeneities which were discussed in the previous section. However, such interpretations may not be totally correct, since films with no noticeable microstructure (low argon pressure sputtered films) do show two types of different local environments for hydrogen.

Compositional inhomogeneities are expected to influence the film properties because they introduce compositional disorder. This type of disorder together with other types of disorder, for example thermal and structural should in principle determine the extent of the band tails. Therefore compositional inhomogeneities are expected to affect carrier transport, optical properties and possibly carrier recombination. In view of this, understanding the origin of such inhomogeneities and developing methods to control them is of great importance.

In sputtered material, one type of compositional inhomogeneity is indicated by the stretching vibration, which is a doublet in the IR transmission spectrum (Brodsky et al. 1977, Freeman and Paul 1978). Although there are multiple opinions (Paul 1980) as to the type of Si-H local environments which give rise to this doublet, it is evident that its existence indicates that these films are compositionally inhomogeneous. The inability to control the bonding of hydrogen in the sputtered material and the experience from the glow discharge that films with the 2100 cm^{-1}

stretching mode generally have poorer electronic properties, led to the widespread belief that the sputtered films are inferior to those produced by decomposition of silane. In this section we discuss methods to control this type of inhomogeneity and try to identify correlations between hydrogen bonding and electronic properties of the films.

One method to control the bonding of hydrogen is through bias sputtering (Moustakas 1982c). We find that the maximum effect of external bias occurs under deposition conditions which lead to substrate self-bias close to zero. We also find that positive bias favors the 2000 cm^{-1} Si-H stretching mode, while negative bias favors the 2100 cm^{-1} Si-H stretching mode. Fig. 9 shows the Si-H stretching vibrations of a number of films produced at substrate bias +50 V and at other deposition conditions as indicated in the figure caption. Indicated next to the sample number is the hydrogen content in the film. Note that most of the hydrogen, up to 14 at %, is bonded in the 2000 cm^{-1} mode. The 2100 cm^{-1} mode acquires the same strength as the 2000 cm^{-1} mode for films having more than 20 at % H. For contrast we show in Fig. 10 the Si-H stretching vibrations for a number of films produced under negative biasing conditions. The negative bias in these films is self-induced (-25 V), by sputtering the films at low argon pressure, P_{Ar} = 5 mTorr, and having all other deposition parameters the same. Note that although the hydrogen content of these films covers the same range as those of Fig. 5, the 2100 cm^{-1} mode is present even in the lowest hydrogen content films and becomes progressively stronger as the hydrogen content increases.

The structural variations associated with the substrate biasing can now be accounted for in the following way. Biasing the substrates to a positive voltage has two effects. One is electronic bombardment of the

rowing film, and the second is minimization of Ar^+ and possibly Si^+ ion bombardment. Although electronic bombardment is thought to be undesirable in the growth of semiconductor material, our findings indicate that some electronic bombardment can have a favorable effect on the growth of structurally and compositionally homogeneous sputtered a-Si:H films. Under typical sputtering conditions, there are low energy and high energy electrons arriving at the substrate. Bombardment by these electrons can have profound effects on the film's chemistry and structure because it enhances adatom surface mobility through surface heating. We believe that this electron bombardment is responsible for the perfect coalescence of the island structure which leads to films having both structural and compositional homogeneity. The second effect of the positive bias, namely the minimization of the Ar^+ and possibly Si^+ ion bombardment is also highly desirable. These films contain much less argon since the Ar^+ ions require a certain threshold (~15 to 20 eV) in order to be implanted into the film (Comas and Carosella 1968). Resputtering is also minimized under these conditions of film growth. Since resputtering by Ar^+ ions is likely to be anisotropic, i.e., with higher sputtering yield at the low density intercolumnar regions, there is a high possibility of microvoid formation during the film re-growth in these regions. Both argon incorporation and void formation lead to films with structural and compositional inhomogeneity. In fact there is some evidence that argon inhabits voids (Paul et al. 1973). We believe that such structural inhomogeneities result in the formation of a stretching vibration doublet.

We now examine whether there is a correlation between the type of Si-H bonding and the electronic properties of the films. Such correlations were sought by studying the density of states in the middle of the gap, the

photoconductivity and the optical absorption constant.

The infrared data in Fig. 10 were measured on the films whose densities of states in the middle of the gap are given in Fig. 1. Note that the sample with the lowest density of states (7×10^{14} cm^{-3} ev^{-1}) has the most of its hydrogen bonded in the mode 2100 cm^{-1}. From these data we concluded that the states in the middle of the gap and properties which are related to these states (recombination) do not depend on the type of Si-H bonding but rather on the total amount of bonded hydrogen.

Next we compare the optical properties of films which have the Si-H stretching vibration primarily at 2000 cm^{-1} with others in which the 2100 cm^{-1} mode is the dominant one. For this study we deposited two series of films; in one series the substrates were electrically biased at +50 volts and in the other were electrically grounded. The hydrogen partial pressure in each series was adjusted so as to produce films with optical gaps in the range of 1.6 to 1.9 eV. All other deposition parameters were fixed. Namely, the deposition temperature was 275°C, the argon pressure 15 mTorr and the power in the discharge 1.5 watts/cm. The hydrogen content in these films was determined by the ^{15}N nuclear reaction (Moustakas et al. 1981a) and the Si-H bonding configuration was determined by studying the IR vibrational spectra. The stretching vibration spectrum for the biased samples centers at 2000 cm^{-1}, while for the grounded samples is a doublet with the 2100 cm^{-1} mode becoming progressively stronger as the hydrogen content increases. The optical gap of these films vs. the hydrogen content in the films are shown in Fig. 11. These data clearly indicate that structurally and compositionally inhomogeneous films require more hydrogen to attain the same optical gap. The fact that the more homogeneous films have larger gaps for the same amount of hydrogen, is consistent with the

model proposed by Cody et al. (1981a, 1981b) that the optical gap is related to disorder. Our data sugggest that in addition to structural and thermal disorder, which was proposed by Cody, compositional disorder is also important in determining the optical properties of a-Si:H alloys.

The studies we presented in this section suggest that compositional inhomogeneities in films with no noticeable microstructure do not affect the states in the middle of the gap but they do affect the band tails through the introduction of additional disorder.

VII. DEVICE POTENTIAL

The recent progress in fabricating high efficiency solar cells by sputtering (Moustakas 1983), suggests that sputtered a-Si:H films are not inferior in their electronic properties to those produced by the glow discharge process. Electron bombardment, which is generally unacceptable in crystalline surface sensitive devices, can be controlled and used to facilitate the coalescence of the island structure during the growth of the film.

These findings together with the fact that sputtering is a widely practiced fabrication technique with an extensive compendium of art, developed skills and available hardware suggest that this method will play a significant role in this emerging technology of amorphous materials. It should be pointed out that continuous processing plants using sputtering technology have proved successful for other materials. There is no intrinsic limit to size; scaling up increases deposition rates and improves film uniformity. The method is suitable also for depositing other amorphous semiconductors (Ge, GaAs) or their alloys and for forming chemically graded junctions and tendem solar cells.

VIII. FUTURE RESEARCH

In this review we presented data and models of interpretations of the different possible mechanisms of film growth. We also show that, low energy ion and electron bombardment of the growing film during deposition, affects the nucleation kinetics and improves structural and compositional inhomogeneities. The models of film growth, particularly the possibility that these films grow by a combination of physical sputtering and glow discharge decomposition of in-situ generated silane, need to be tested and refined. The electron and ion bombardment effects need to be studied in more detail and optimized for best results.

Another area which needs more research is the phenomenon of substitutional doping. Sputtering is a suitable technique for this type of studies because it can easily explore interactions between dopant atoms, natural defects and hydrogen atoms.

The concept of hydrogen insertion into a reconstructed dangling bond (a bridging H shared by two neighboring Si) should be tested by searching for its characteristic spin resonance that should differ from that of a single dangling bond.

Finally, other types of sputtering such as cylindrical magnetron (Thornton et al. 1981), planar magnetron (Stein et al. 1981) and ion beam sputtering (Kobayashi et al. 1981) need to be explored in more detail.

ACKNOWLEDGMENTS

The author gratefully acknowledges the partial support of the U.S. Department of Energy (Solar Energy Institute Contract No. ZB-3-02166-01) during the course of preparation of this chapter.

REFERENCES

Anderson, D. A., Moustakas, T. D. and Paul, W. (1977), "Amorphous and Liquid Semiconductors", (W. E. Spear, Ed.) pp. 334-8, University of Edinburgh.

Anderson, D. A., Moddel, G., Paesler, M. A. and Paul, W. (1979), J. Vac. Sci. Technol., 16, 906.

Anderson, D. A., Moddel, G. and Paul, W. (1980), J. Electronic Materials, 9, 141-52.

Biegelsen, D. K., Street, R. A., Tsai, C. C. and Knights, J. C. (1979), Phys. Rev. B, 20, 4839.

Brodsky, M. H., Title, R. S., Weiser, K. and Pettit, G. D. (1970), Phys. Rev. B., 1, 2632-41.

Brodsky, M. H., Cardona, M. and Cuomo, J. J. (1977), Phys. Rev. B, 16, 3556.

Bruyere, J. C., Deneuville, A., Mini, A., Fontenille, J. and Danielou, R. (1980), J. Appl. Phys., 51, 2199.

Carlos, W. E., Taylor, P. C., Oguz, S. and Paul, W. (1981), "Tetrahedrally Bonded Amorphous Semiconductors", (R. A. Street, D. K. Biegelsen and J. C. Knights, Eds.) pp. 67-72, American Institute of Physics, New York.

Catalano, A., D'Aiello, R. V., Dresner, J., Faughnan, B., Firester, A., Kane, J., Schade, H., Smith, Z. E., Swartz, G. and Triano, A. (1982), 16th IEEE Photovoltaic Specialists Conference, 1421-2.

Coburn, J. W. and Kay, E. (1972), J. Appl. Phys., 43, 4965.

Cody G. D., Tiedje, T., Abeles, B., Moustakas, T. D., Brooks, B. and Goldstein, Y. (1981a), J. de Phys., 42, Suppl. 10, C4-301-304.

Cody, G. D., Tiedje, T., Abeles, B., Brooks, B. and Goldstein, Y. (1981b),

Phys. Rev. Lett., 47, 1480.

Comas, J. and Carosella, C. A. (1968), J. Electrochem. Soc., 115, 974.

Connell, G. A. N. and Pawlik, J. R. (1976), Phys. Rev. B, 13, 787.

Freeman, E. C. and Paul, W. (1978), Phys. Rev. B, 18, 4288.

Heller, J. (1973), Thin Solid Films, 17, 163.

Jeffrey, F. R., Shanks, H. R. and Danielson, G. C. (1979), J. Appl. Phys., 50, 7034-8.

Jeffrey, F. R., Shanks, H. R. and Danielson, G. C. (1980), J. Non-Crystalline Solids, 35-36, 261-6.

Jeffrey, F. R., Lowry, M. E., Garcia, M. L. S., Barnes, R. G. and Torgeson, D. E. (1981), "Tetrahedrally Bonded Amorphous Semiconductors", (R. A. Street, D. K. Biegelsen and J. C. Knights, Eds.) pp. 83-8.

Knights, J. C. and Lujan, R. A. (1979), Appl. Phys. Lett., 35, 244.

Knights, J. C. (1979), Japan. J. Appl. Phys., 18, 101.

Kobayashi, M., Saraie, J. and Matsunami, H. (1981), Appl. Phys. Lett., 38, 696-697.

Lewis, A. J., Connell, G. A. N., Paul, W., and Pawlik, J. R. (1974), "Tetrahedrally Bonded Amorphous Semiconductors" (M. H. Brodsky and S. Kirkpatrick, Eds.) pp. 27-31, American Institute of Physics, New York.

Lewis, A. J. (1976), Phys. Rev. B, 14, 658-68.

Maissel, L. I. (1970), "Handbook of Thin Film Technology", (L. I. Maissel and R. Glang, Eds.), Ch. 4, McGraw-Hill, New York.

Martin, P. M. and Pawlewicz, W. T. (1981), J. Non-Crystalline Solids, 45, 15-27.

Maruska, H. P., Moustakas, T. D. and Hicks, M. C. (1983), Solar Cells, 9, 37-51.

Matsuda, A., Nakagawa, K., Tanaka, K., Matsumura, M., Yamasaki, S., Okushi,

H. and Iizima, S. (1980), J. Non-Crystalline Solids, 35-36, 183-8.

Morel, D. L. and Moustakas, T. D. (1981), Appl. Phys. Lett., 39, 612-4.

Moss, S. C. and Graczyk, J. F. (1969), Phys. Rev. Lett., 23, 1167.

Moustakas, T. D. and Connell, G. A. N. (1976), J. Appl. Phys., 47, 1322-6.

Moustakas, T. D. and Paul, W. (1977a), Phys. Rev. B, 16, 1564-76.

Moustakas, T. D., Anderson, D. A. and Paul, W. (1977b), Solid State Commun., 23, 155-8.

Moustakas, T. D. (1979), J. Electr. Mater., 8, 391-435.

Moustakas, T. D., Wronski, C. R. and Morel, D. L. (1980), J. Non-Cryst. Solids, 35-36, 719-24.

Moustakas, T. D., Tiedje, T. and Lanford, W. A. (1981a), "Tetrahedrally Bonded Amorphous Semiconductors", (R. A. Street, D. K. Biegelsen and J. C. Knights, Eds.), pp. 20-4, American Institute of Physics, New York.

Moustakas, T. D., Wronski, C. R. and Tiedje, T. (1981b), Appl. Phys. Lett., 39, 721-3.

Moustakas, T. D. and Friedman, R. (1982a), Appl. Phys. Lett., 40, 515-7.

Moustakas, T. D., Friedman, R. and Weinberger, B. R. (1982b), Appl. Phys. Lett., 40, 587-8.

Moustakas, T. D. (1982c), Solar Energy Materials, 8, 187-104.

Moustakas, T. D., (1983), "Proc. of SPIE Conference", (Arlington Va., April 1983).

Movchan, B. A. and Demshishin, A. V. (1969), Fiz. Met. Metalloved, 28, 653.

Oguz, S. and Paesler, M. A. (1980a), Phys. Rev. B, 22, 6213.

Oguz, S., Collins, R. W., Paesler, M. A. and Paul, W. (1980b), J. Non-Crystalline Solids, 35-36, 231.

Oguz, S. Paul, D. K., Blake, J., Collins, R. W., Lachter, A., Yacobi, B. G.

and Paul, W. (1981a), J. de Phys., 42, Suppl. 10, C4-679-82.

Oguz, S. (1981b), Thesis, Harvard University, Unpublished.

Paesler, M. A., Okumura, T. and Paul, W. (1980), J. Vac. Sci. Technol., 17, 1332

Paul, W., Connell, G. A. N. and Temkin, R. J. (1973), Advan. Phys., 22, 529-80.

Paul, W., Lewis, A. J., Connell, G. A. N. and Moustakas, T. D. (1976), Solid State Commun., 20, 969-72.

Paul W. (1980), Solid State Commun., 34, 283-5.

Paul, W. and Anderson, D. A. (1981), Solar Energy Materials, 5, 229-316.

Pawlewicz, W. T. (1978), J. Appl. Phys., 49, 5595-601.

Postol, T. A., Falco, C. M., Campwirth, R. T., Schuller, I. K. and Yelon, W. B. (1980), Phys. Rev. Lett., 45, 648.

Reimer, J. A., Vaughan, R. W. and Knights, J. C. (1980), Phys. Rev. Lett., 44, 193.

Ross, R. C. and Messier, R. (1981a), J. Appl. Phys., 52, 5329-39.

Ross, R. C. and Messier, R. (1981b), "Tetrahedrally Bonded Amorphous Semiconductors", (R. A. Street, D. K. Biegelsen and J. C. Knights, Eds.) pp. 53-57, American Institute of Physics, New York.

Sanks, H., Fang, C. J., Ley, L., Cardona, M., Demond, F. J. and Kalbitzer, S. (1980), Phys. Stat. Sol. (b), 100, 43.

Schwartz, N. (1964), Trans. Natl. Vac. Symp., 10th, Boston, 1963, p. 325.

Shevchik, N. J. and Paul, W. (1972), J. Non-Crystlaline Solids, 8-10, 381.

Spear, W. E. (1974), "Amorphous and Liquid Semiconductors", (J. Stuke and W. Brenig, Eds.) pp. 1-16, Taylor and Francis.

Spear, W. E. and L Comber, P. G. (1975), Solid State Commun., 17, 1193-6.

Stein, H. J., Peercy, P. S. and Peckerar, M. (1981), J. Electronic

Materials, 10, 797.

Temkin, R. J., Paul, W. and Connell, G. A. N. (1973), Advan. Phys., 22, 581.

Thornton, J. A. (1974), J. Var. Sci. Technol. II, 666-670.

Thornton, J. A. and Hoffman, D. W. (1981), J. of Vac. Sci. Technol., 18, 203-207.

Tiedje, T., Moustakas, T. D. and Cebulkar, J. M. (1981), Phys. Rev. B, 23, 5634-7.

Thompson, M. J., Allison, J., Al-Kaisi, M. M. and Thomas, I. P. (1978), Reuue de Physique Appliquee, 13, 625-8.

Turner, D. P., Thomas, I. P., Allison, J., Thompson, M. J., Rhodes, A. J., Austin, I. G. and Searle, T. M. (1981), "Tetrahedrally Bonded Amorphous Semiconductors", (R. A. Street, D. K. Biegelsen and J. C. Knights, Eds.) pp. 47-51, American Institute of Physics, New York.

Veprek, S. (1980), Chimia, 34, 489.

Victorovitch, P., Jousse, D., Chenevas-Paule, A. and Lieuz-Rocherz, L. (1979), Reveu de Phys. Appl., 14, 204.

Von Roedern, B., Ley, L., Cardona, M. and Smith, F. W. (1979), Philos. Mag. B, 40, 433-50

Vossen, J. L. and Cuomo, J. J. (1978), "Thin Film Processes", (J. L. Vossen and W. Kern, Eds.) Chapter 2, Academic Press, New York.

Vossen, J. L. and Kern, W., Eds., (1978), "Thin Film Processes", Academic Press, New York.

Wolski, S. P. and Zdanuk, E. J. (1961), J. Appl. Phys., 32, 782.

FIGURE CAPTIONS

Figure 1: Density of states in the middle of the gap as a function of hydrogen partial pressure. The error bars indicate the reproducibility of the measurements, and the solid line is a least-squares fit to the data. The point indicated by the symbol ( ) is the ESR spin density (1.1×10^{17} cm^{-3}). (After Tiedje et al. 1981.)

Figure 2: Dependence of the integrated intensity of the Si-H stretching mode on the partial pressure of hydrogen. The dashed line is a fit to the data based on Eq. (4) as discussed in the text (after Tiedje et al. 1981).

Figure 3: Dependence of the integrated intensity of the Si-H stretching mode on the ratio of the partial rpessure of hydrogen to the deposition rate. The dashed line is a fit to the data based on Eq. (4) as discussed in the text (after Moustakas et al. 1981a).

Figure 4: Depeendence of the integrated intensity of the Si-H stretching mode on the partial pressure of hydrogen for films produced at T_s = 225°C ( ) and T_s = 385°C ( ) (after Moustakas et al. 1981a).

Figure 5: Index of refraction, measured at $\lambda \simeq 2.0$ μm vs. the argon pressure in the discharge (after Moustakas 1982c).

Figure 6: Infrared vibrational spectra of samples deposited at argon pressure of 5, 10, 20 and 40 mTorr (after Moustakas 1982c).

Figure 7: Photoconductivity, measured under AMI illumination, vs. the argon pressure in the discharge (after Moustakas 1982c).

Figure 8: Substrate self-bias potential, measured with respect to the

ground vs. the total pressure in the discharge (after Moustakas 1982c).

Figure 9: Si-H stretching vibrations of films produced at positive substrate bias (+50 volts). Indicated next to the sample number is the hydrogen content in the film. (These films were produced at T_s = 275°C, power = 200 W and P_{Ar} = 15 mT.) (After Moustakas 1982c.)

Figure 10: Si-H stretching vibrations for a number of films produced under negative bias conditions as discussed in the text. Indicated next to the sample number is the hydrogen content in the film (after Moustakas 1982c).

Figure 11: Optical gap vs. hydrogen content for films produced on positively biased and electrically grounded substrates. [The optical gap, Eg, was defined by the relation $(\alpha h\nu)^{1/2} = B(h\nu - Eg)$.] (After Moustakas 1983.)

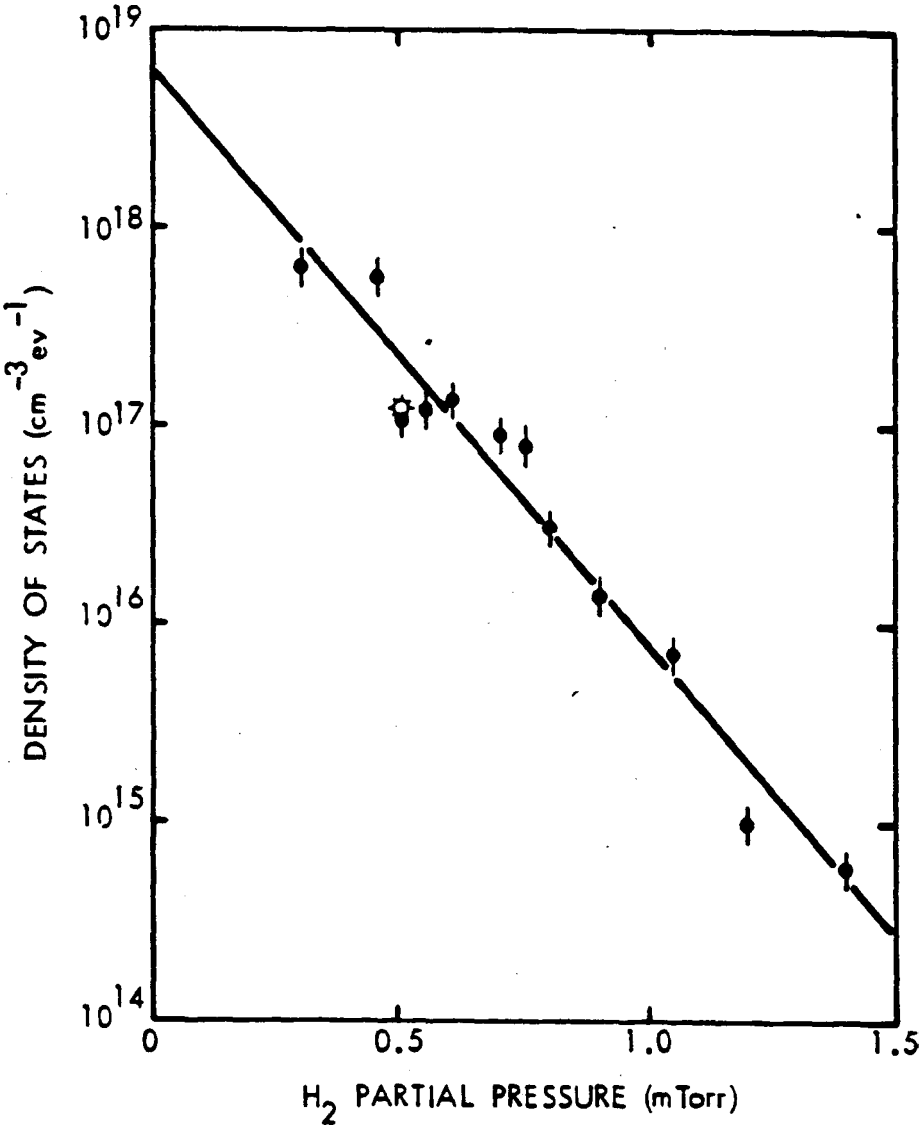
10^{19}
10^{18}
10^{17}
10^{16}
10^{15}
10^{14}
DENSITY OF STATES ($cm^{-3}_{ev}{}^{-1}$)
0
0.5
1.0
1.5
H_2 PARTIAL PRESSURE (mTorr)

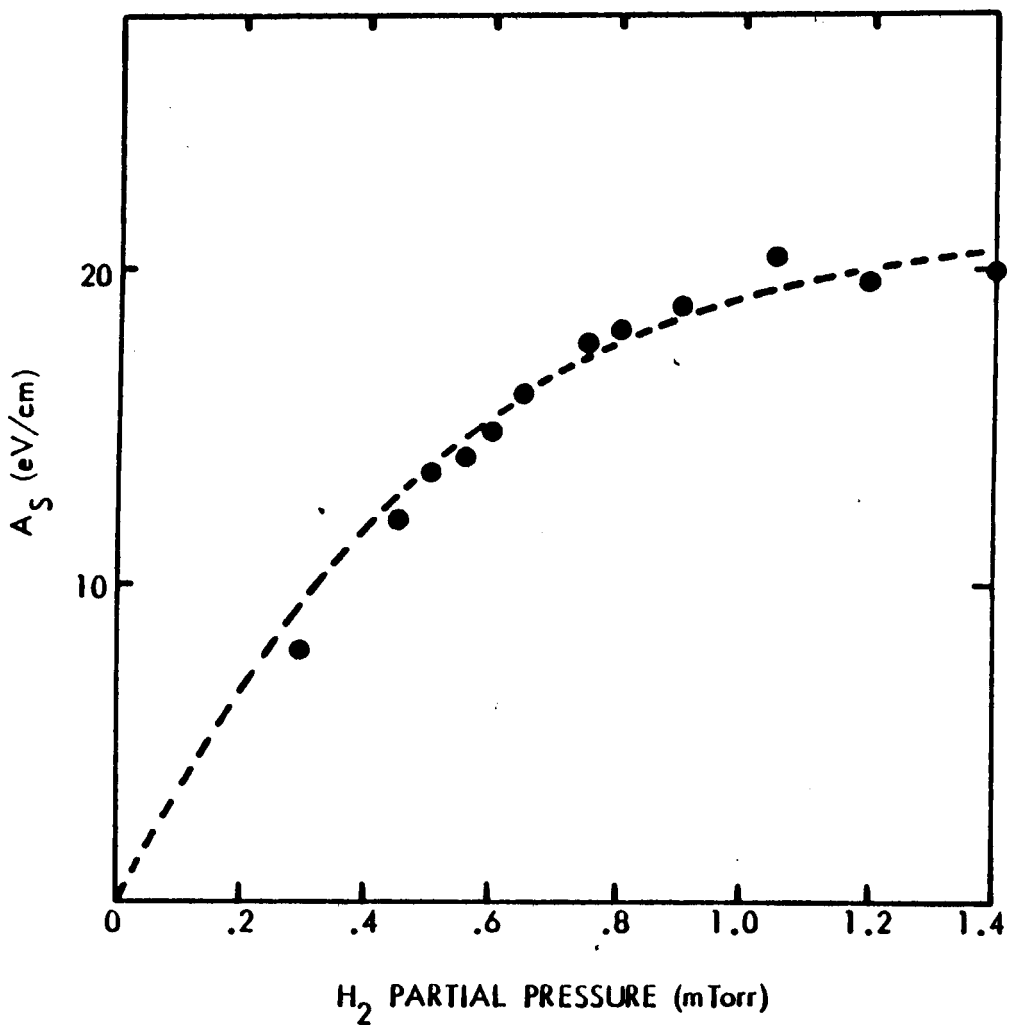
20
10
A_S (eV/cm)
0
.2
.4
.6
.8
1.0
1.2
1.4
H_2 PARTIAL PRESSURE (mTorr)

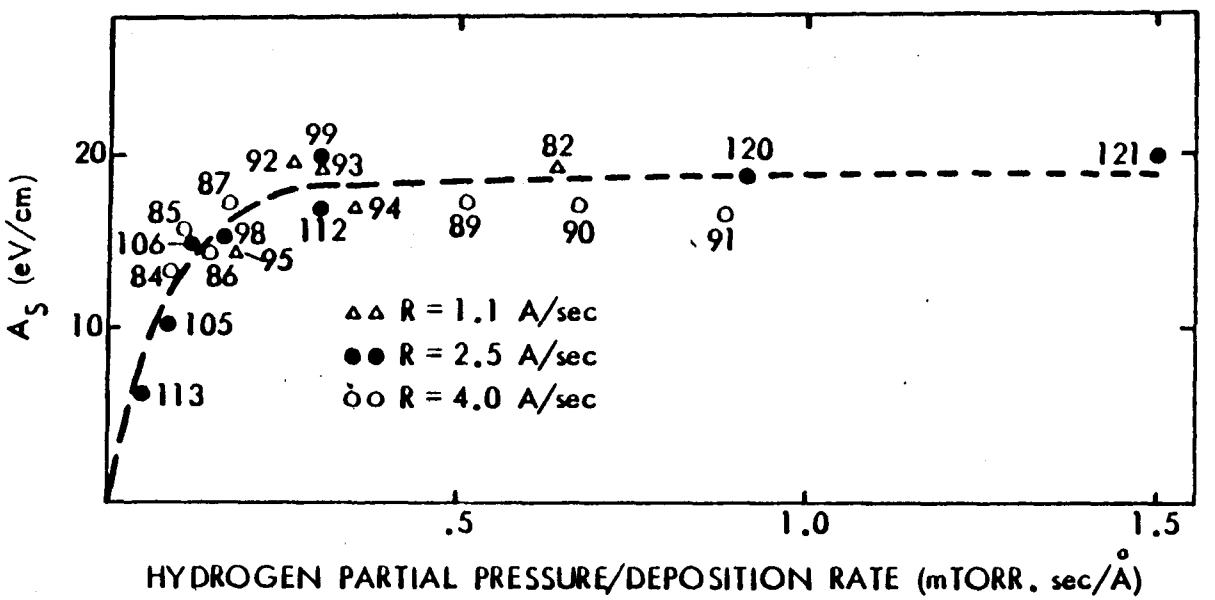
20
10
A_S (eV/cm)
99
92
93
82
120
121
87
85
106
98
112
94
89
90
91
84
86
95
105
113
△△ R = 1.1 A/sec
●● R = 2.5 A/sec
òo R = 4.0 A/sec
.5
1.0
1.5
HYDROGEN PARTIAL PRESSURE/DEPOSITION RATE (mTORR. sec/Å)

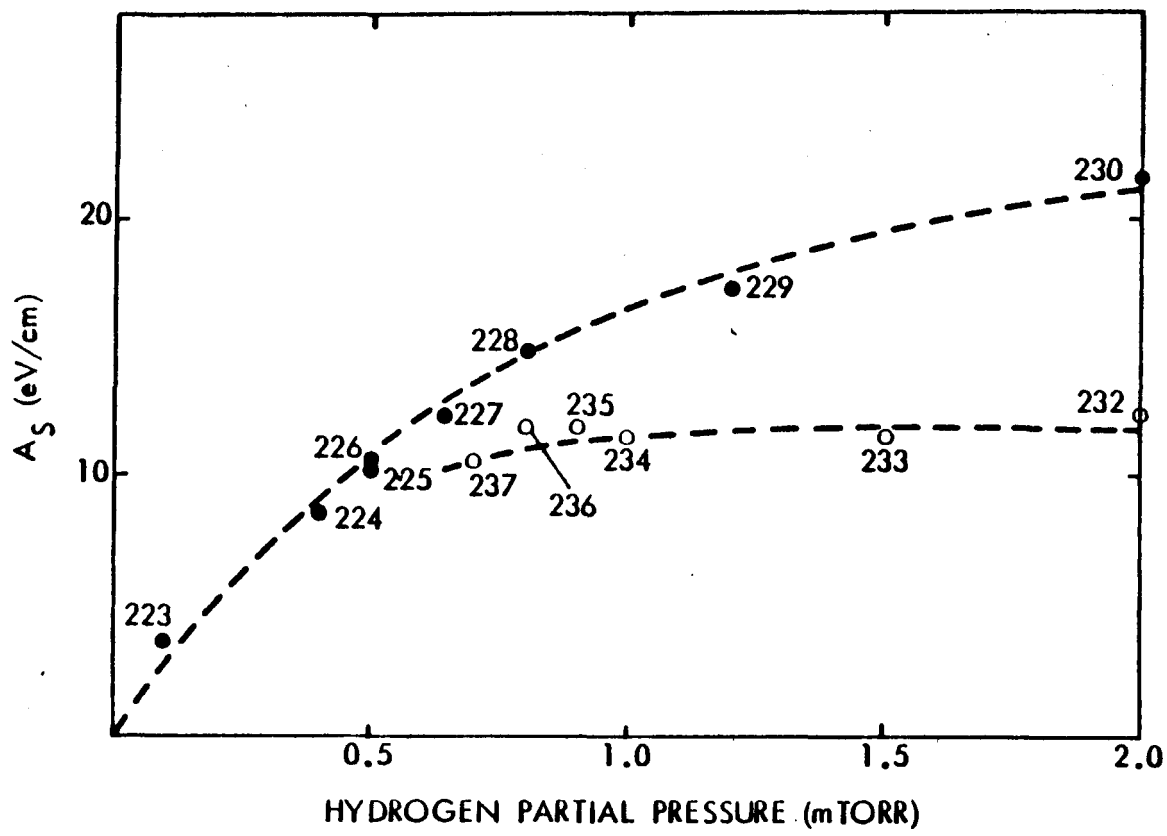
20
10
A_S (eV/cm)
230
229
228
227
235
232
226
225
237
234
233
236
224
223
0.5
1.0
1.5
2.0
HYDROGEN PARTIAL PRESSURE (mTORR)

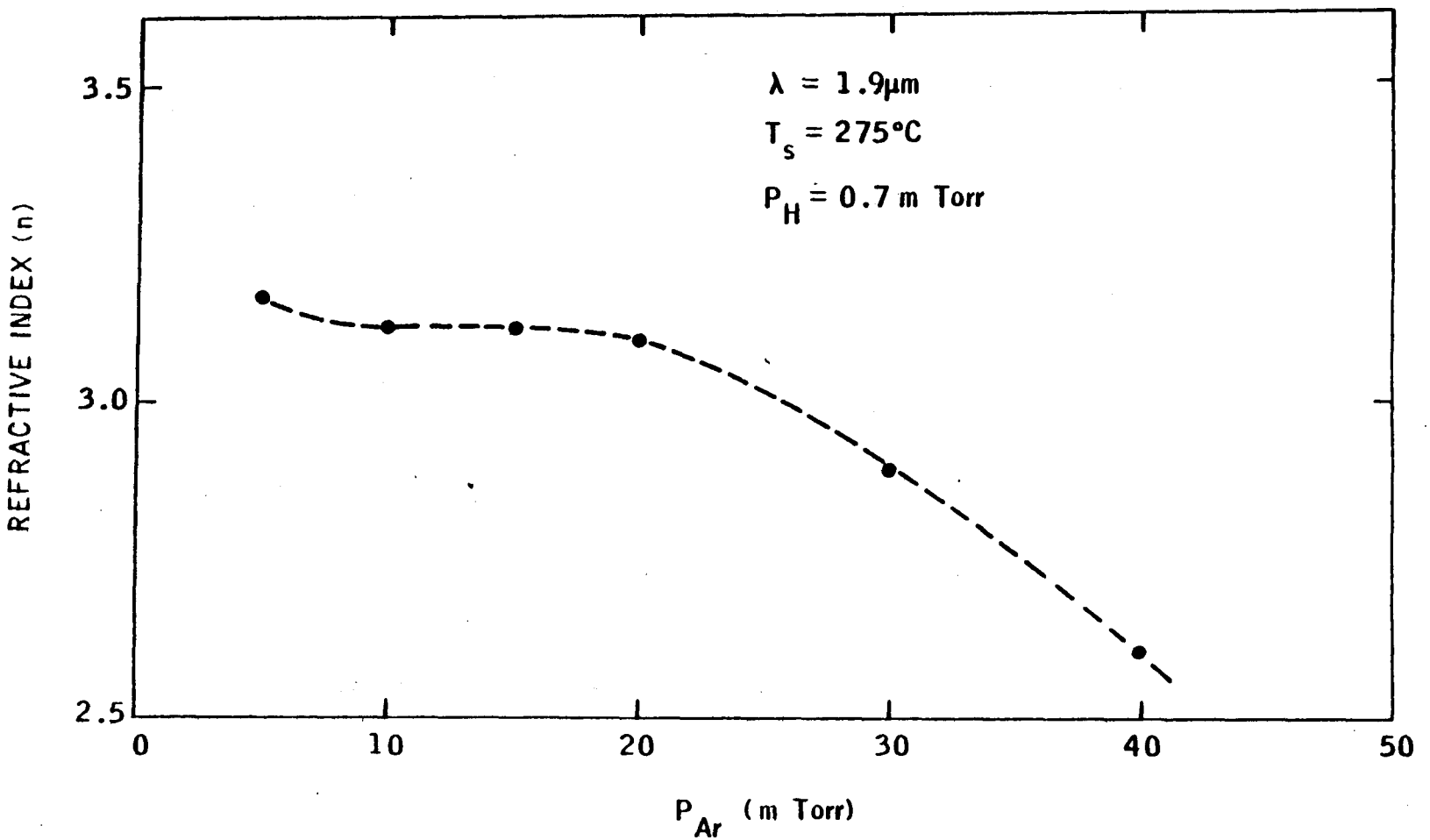
λ = 1.9μm
T_s = 275°C
P_H = 0.7 m Torr
REFRACTIVE INDEX (n)
3.5
3.0
2.5
0
10
20
30
40
50
P_{Ar} (m Torr)

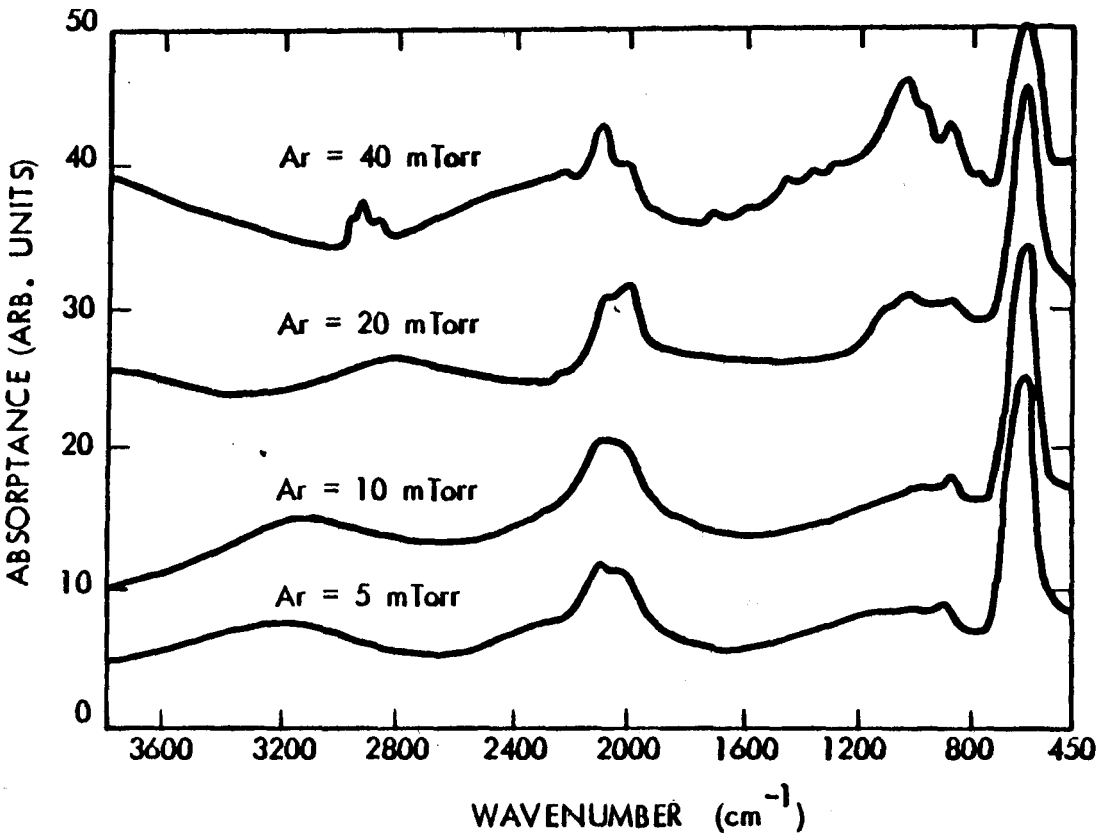
50
40
30
20
10
0
ABSORPTANCE (ARB. UNITS)
Ar = 40 mTorr
Ar = 20 mTorr
Ar = 10 mTorr
Ar = 5 mTorr
3600
3200
2800
2400
2000
1600
1200
800
450
WAVENUMBER (cm^{-1})

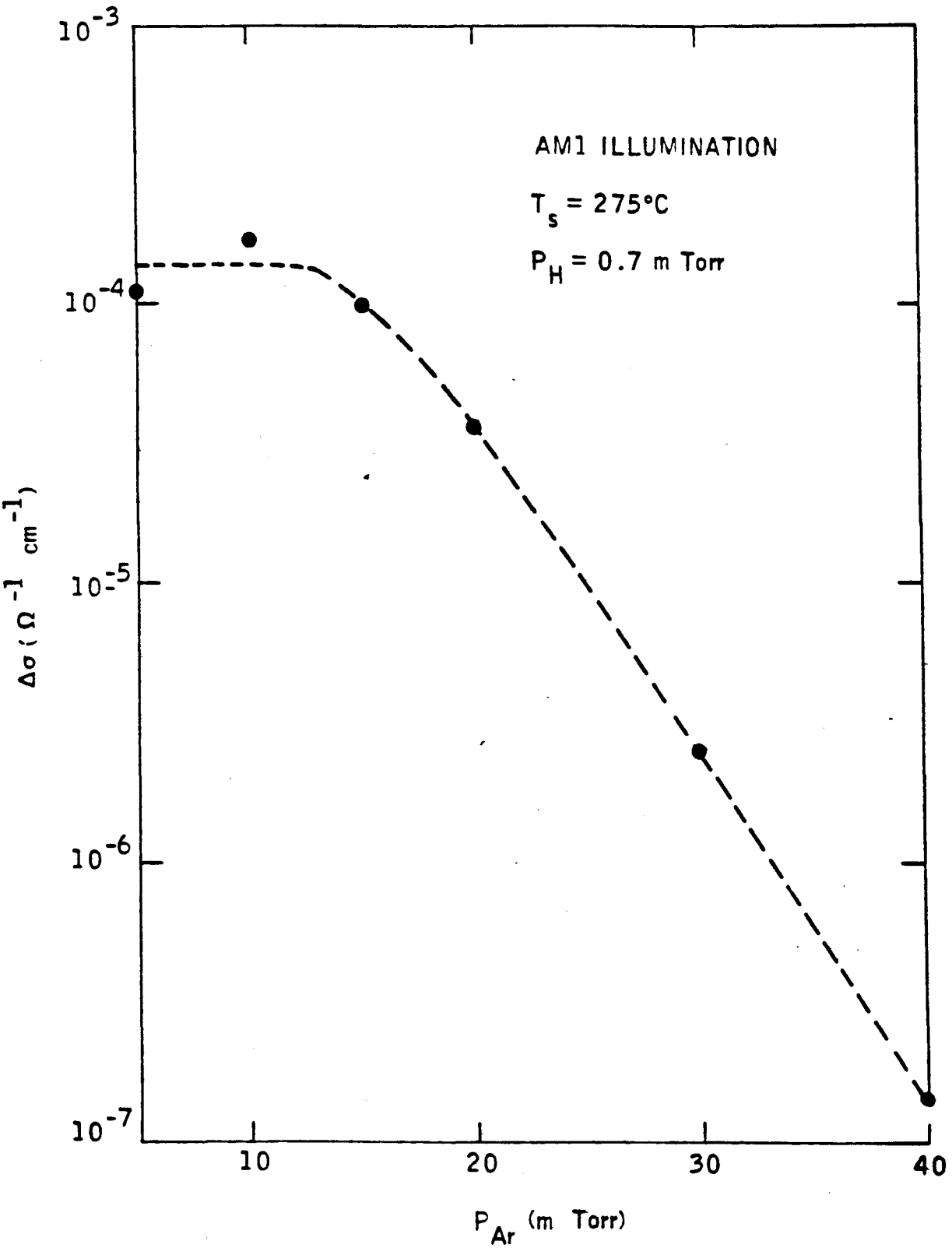
AM1 ILLUMINATION
T_s = 275°C
P_H = 0.7 m Torr
10^{-3}
10^{-4}
10^{-5}
10^{-6}
10^{-7}
$\Delta\sigma$ (Ω^{-1} cm^{-1})
10
20
30
40
P_{Ar} (m Torr)

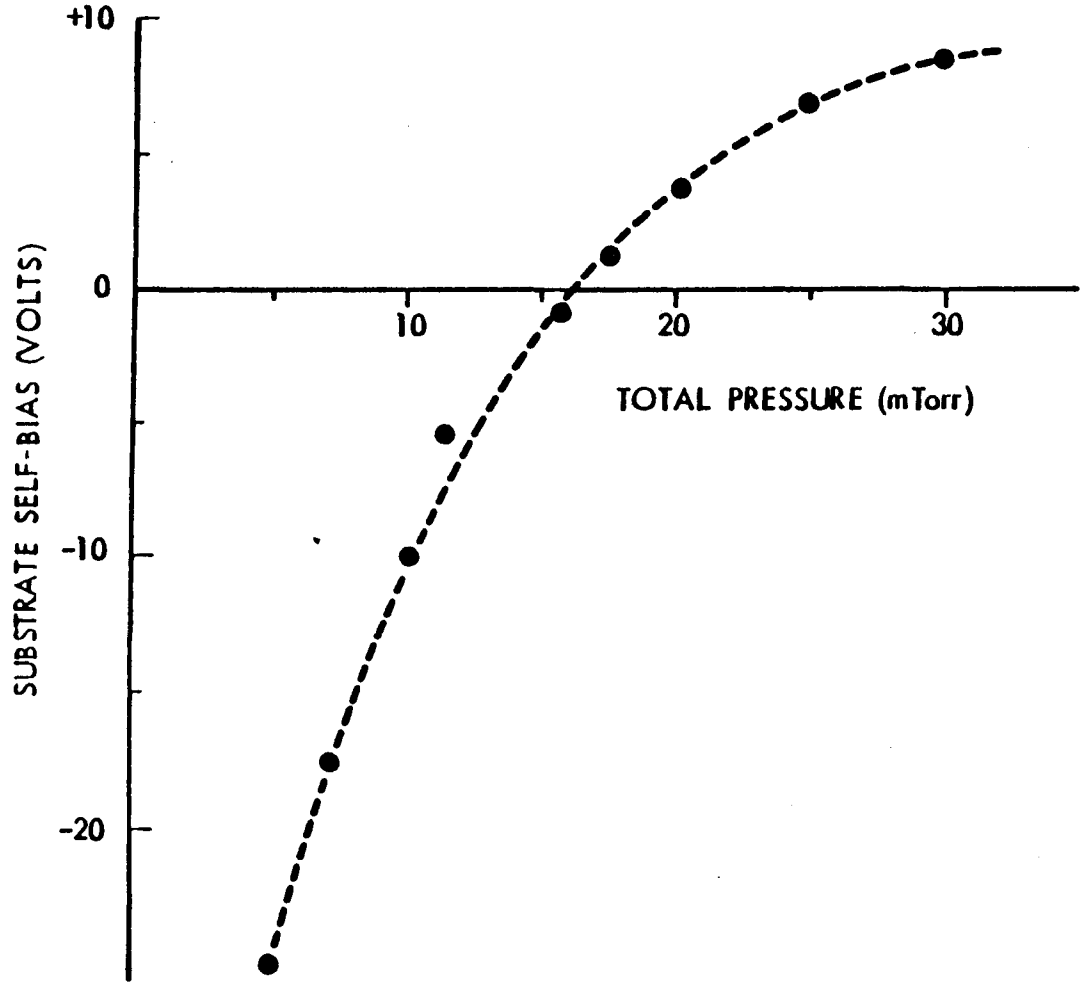
+10
0
-10
-20
10
20
30
SUBSTRATE SELF-BIAS (VOLTS)
TOTAL PRESSURE (mTorr)

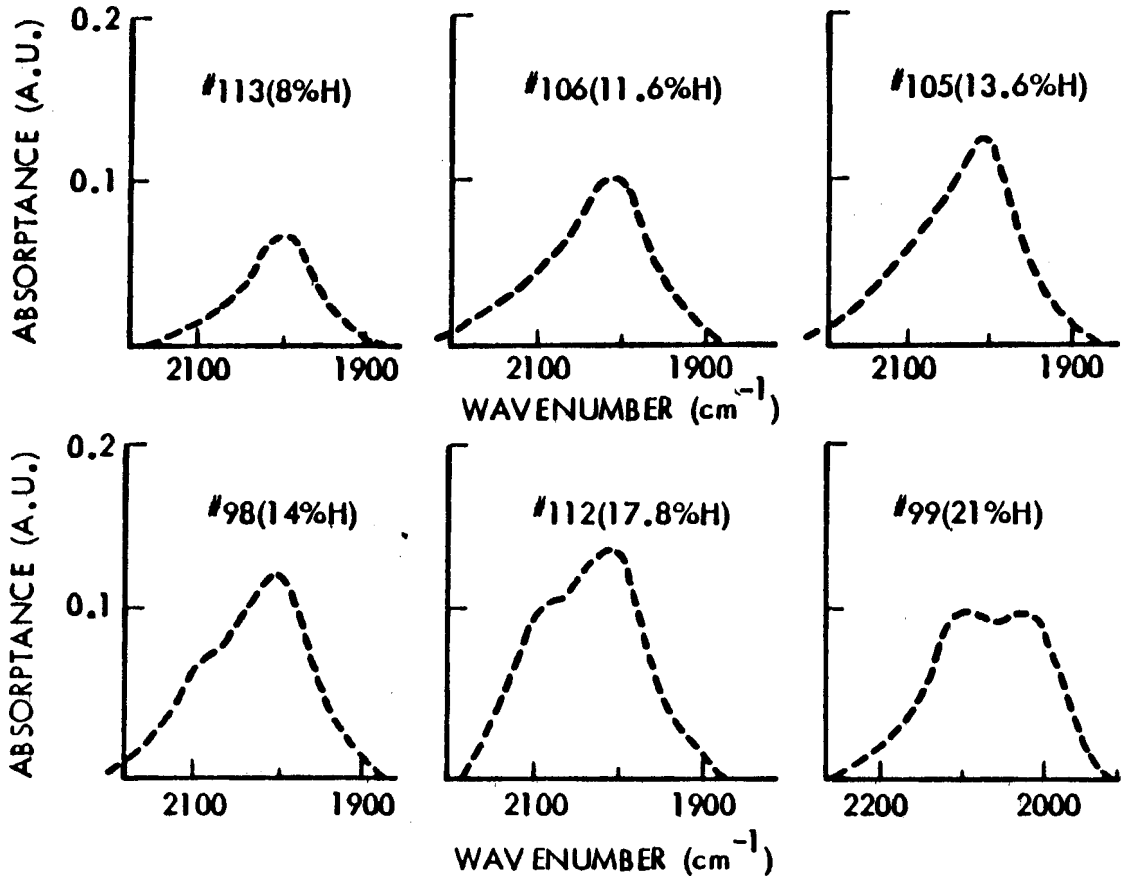
0.2
0.1
ABSORPTANCE (A.U.)
#113(8%H)
#106(11.6%H)
#105(13.6%H)
2100
1900
WAVENUMBER (cm-1)
#98(14%H)
#112(17.8%H)
#99(21%H)
2200
2000
WAVENUMBER (cm-1)

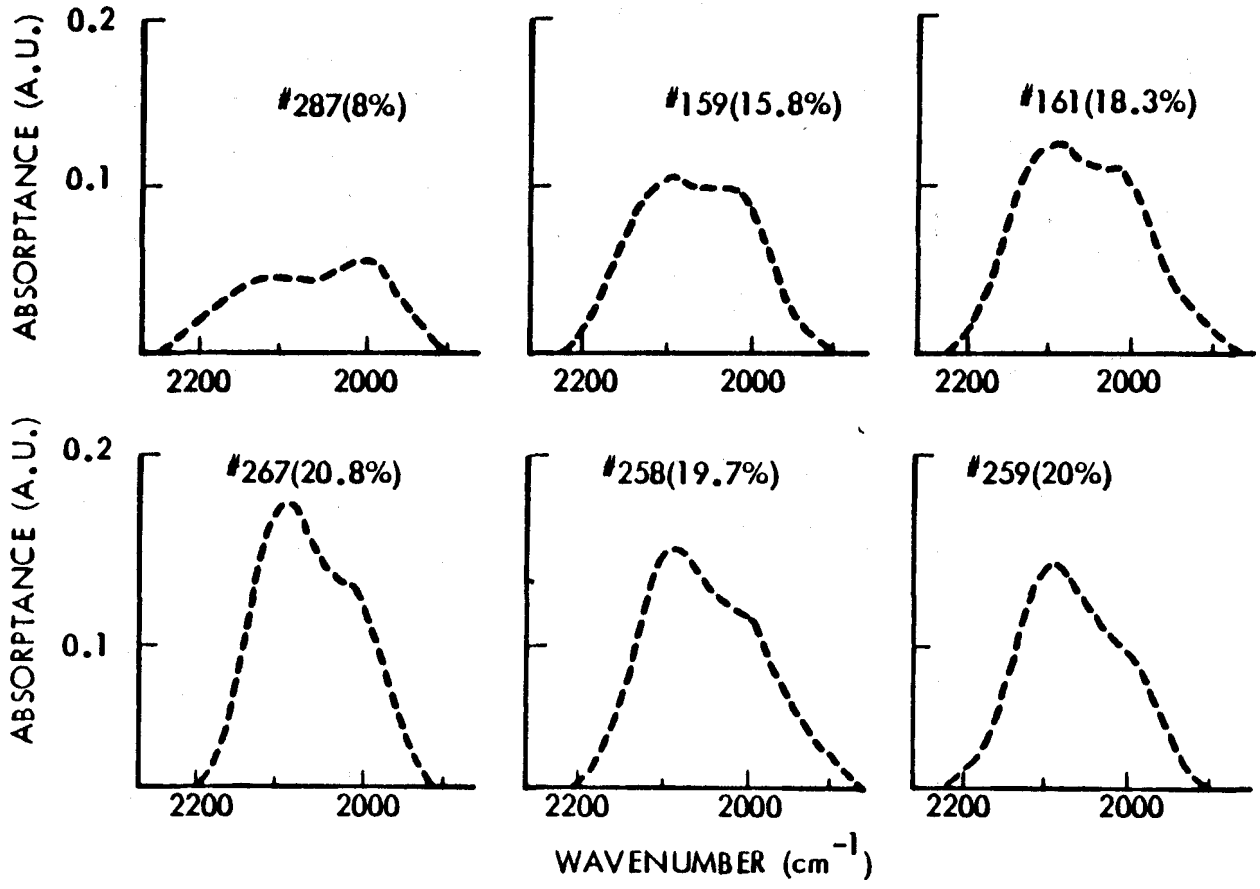
ABSORPTANCE (A.U.)
0.2
0.1
#287(8%)
#159(15.8%)
#161(18.3%)
#267(20.8%)
#258(19.7%)
#259(20%)
2200
2000
WAVENUMBER (cm^{-1})

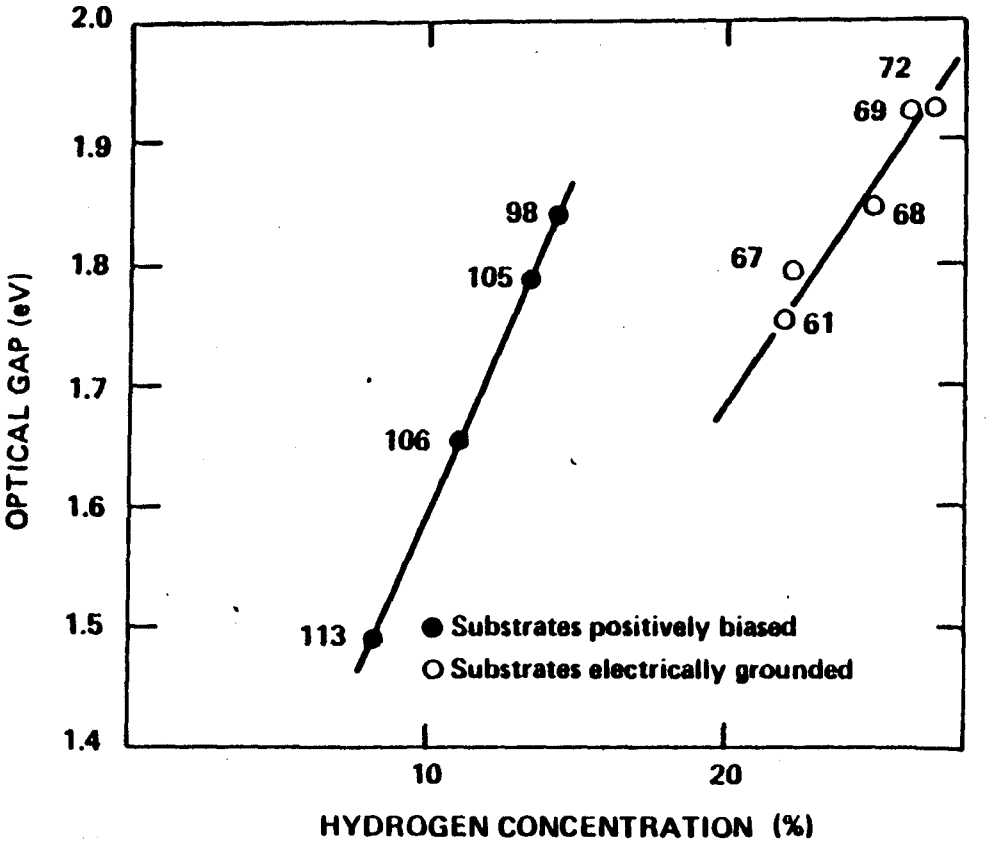
2.0
1.9
1.8
1.7
1.6
1.5
1.4
OPTICAL GAP (eV)
10
20
HYDROGEN CONCENTRATION (%)
72
69
68
67
61
98
105
106
113
● Substrates positively biased
○ Substrates electrically grounded

APPENDIX C. Electronic Properties and Applications of Micrystalline Silicon Films Prepared by Reactive Sputtering

ELECTRONIC PROPERTIES AND APPLICATIONS OF MICROCRYSTALLINE SILICON FILMS PREPARED BY REACTIVE SPUTTERING

T. D. Moustakas and H. Paul Maruska
Corporate Research Laboratory
Exxon Research and Engineering Company
Linden, N.J. 07036

ABSTRACT

The electronic properties of undoped, phosphorus doped and boron doped microcrystalline silicon films, prepared by reactive sputtering, were investigated through structural, optical and transport measurements. The data indicate the effect of structural ordering in the transition from the amorphous to the crystalline phase. The merits of microcrystalline versus amorphous doped films for solar cell applications have been demonstrated.

Hydrogenated microcrystalline silicon thin films ($\mu c\text{-}SiH_x$) were first prepared in 1968 by Veprek and Maracek [1] by H_2 plasma assisted silicon transport. Since then similar films have been produced in other laboratories.[2,3] In the past two years a number of groups have been developing methods to deposit such films by the glow discharge decomposition of silane, in order to use them as highly conductive and transparent P and N contacts in amorphous silicon ($a\text{-}SiH_x$) PIN solar cells.[4-6] Some progress has also been made in depositing intrinsic microcrystalline films by sputtering methods. One paper[7] reports on properties of such films produced by sputtering in a $He+H_2$ atmosphere, and another[8] on photoelectron spectroscopy studies of films produced by DC sputtering. However, the best sputtered PIN solar cell structures have been fabricated by RF sputtering in our $Ar+H_2$ atmosphere[9]. It is, therefore, important to identify deposition conditions for the formation of doped $\mu c\text{-}SiH_x$ by RF sputtering in $AR+H_2$, which can be used to improve the performance of PIN solar cells. In this paper we report for the first time the deposition of phosphorus doped, boron doped, and undoped $\mu c\text{-}SiH_x$ films produced by RF sputtering in an $Ar+H_2$ atmosphere. We have also fabricated sputtered PIN solar cells having μc-P and N layers. The films have been investigated by studying their structural characteristics and their optical and transport properties. The object of the study is to probe the effect of structural ordering in the transition from the amorphous to the crystalline phase, and to demonstrate the merits of using μc-P and N contacts in sputtered PIN solars cells.

The films were prepared at a substrate temperature of 325°C in an RF diode system having a water cooled polycrystalline Si target 5" in diameter. The target was supplied with an RF power of 100 watts which results

in a dc bias of -1200 volts. The sputtering gas consists of a 40 mTorr mixture of hydrogen and argon, whose flow rates were adjusted upstream with the help of mass flow controllers to be 100 and 10 sccm correspondingly. The phosphorus and boron doped layers were produced by premixing the argon with 2000 ppm of PH_3 or B_2H_6. The films for the structural studies, optical absorption, and conductivity measurements were deposited on quartz substrates and films for infrared absorption measurements on high purity polished single crystal silicon wafers.

The films were characterized for evidence of crystallinity by X-ray diffraction, for surface morphology by optical microscopy, and for evidence of hydrogen incorporation and bonding configuration by infrared absorption spectroscopy. The optical properties of the films were investigated by studying their optical densities in a Cary 17 spectrophotometer, using a 2mm aperture to eliminate the possibility of thickness gradients. The amplitude of the interference fringes, which are displayed at wavelengths below the absorption edge, was used to calculate the refractive index at a given wavelength. The interference fringes were also used to calculate the film thickness. The optical absorption coefficient was calculated by an interactive procedure from the optical transmission measurements.[10] Samples were cut into standard six contact bars for Hall Effect and conductivity measurements. The applied field during these measurements was kept below 10^2 volts/cm, well within the ohmic regime.

The deposition rate of the films was found to depend on the dopant gases in the discharge. The deposition rate of the undoped films was found to be 30Å/min, of the phosphorus doped films 25Å/min and of the boron doped films 45Å/min. The doped films show a certain characteristic surface morphology, while the undoped layers are smooth. Fig. 1A shows the

surface morphologies of the three types of films, deposited on quartz substrates, as viewed in an optical microscope under 1000 times magnification. The X-ray diffraction spectra (Cu-Ka, 40KeV) shown in Fig. 1B reveal weak and relatively broad peaks which correspond to the (111), (220) and (311) orientation of crystalline silicon. From the half-width of the (111) diffraction peak we infer an average grain size of about 60A. Infrared absorption spectra indicate vibrations of 2100, 900 and 640cm^{-1}, with hydrogen content of between 4 to 5 at%

The index of refraction vs. photon energy for the undoped, the phosphorus doped and the boron doped μc-SiH$_x$ films is shown in Fig. 2. For comparison we show in the same figure the index of refraction of single crystalline Si[11] and the index of refraction of an undoped and a boron doped a-SiH film. It is obvious from these results that doping of the μc-SiH$_x$ films results in a significant reduction in the index of refraction, while doping of the a-SiH$_x$ films does not have a similar effect on the index of refraction.

The optical absorption constant vs. photon energy of an undoped, a phosphorus doped and a boron doped μc-SiH$_x$ film is shown in Fig. 3. For comparison we show in the same Figure the optical absorption constant of single crystalline Si[12] as well as that of an undoped and a boron doped a-SiH$_x$ film.[13] The optical absorption constant of the undoped and the doped μc-SiH$_x$ layers merge together at photon engergies larger than 2.5eV and the doped films show higher optical absorption than the corresponding undoped film at lower energies.

The conductivity type of the three types of films was checked by measuring the sign of the thermoelectric power. The undoped and the boron doped films were found to be p-type and the phosphorus doped films are

n-type. Hall effect measurements on the doped films indicate that there is no sign anomaly between thermoelectric power and Hall coefficient. The carrier concentrations are in the range of $1\text{-}10\times10^{19}cm^{-3}$, while the Hall mobility for both n- and p- films is around unity. The temperature dependence of the conductivity for the three types of films is shown in Fig. 4. Indicated in the same figure are the conductivity activation energies. The boron-doped sample has an activation energy less than kT, which implies that the conductivity process is actually not activated (the semiconductor is degenerate).

These experimental results can now be accounted for in the following way. We agree with Veprek et al[2] that the growth of the $\mu c\text{-}SiH_x$ requires the establishment of chemical equilibrium at the plasma/film interface in order to form stable nuclei. These conditions are accomplished when the atomic hydrogen in the discharge leads to a significant etching of the weak Si-Si bonds of the growing film. We have shown in another paper[14] that the growth of the $a\text{-}SiH_x$ film takes place under conditions far away from chemical equilibrium at the plasma/film interface. The observation that the doped layers are deposited at different rates and that they have a rougher surface morphology than the undoped films is in agreement with the suggestion by Matsuda et al[4] that a high concentration of boron dopants can enhance crystallization due to the formation of stable nuclei. Finally, the infrared vibrational data agree with the finding of Richter and Ley[3], who studied $\mu c\text{-}SiH_x$ films produced by H_2-plasma assisted transport, that the hydrogen is bonded in the grain boundary regions in the form of SiH_2 or $(SiH_2)_x$ units.

The optical absorption data of Fig. 3 show the gradual progression from the crystalline to the amorphous phase. We believe that these

data are characteristic to the crystallite size produced under the conditions described in this paper. Under other conditions leading to material with larger crystallites, the optical absorption should move closer to the values of crystalline silicon, and for smaller crystallites should move closer to the absorption of the a-SiH_x. This tentative conclusion is under current investigation. The higher optical absorption of the doped layers in the infrared region is evidence of free carrier absorption. This is a reasonable assumption in view of the fact that the free carrier densities of these films at room temperature are as high as $10^{20}cm^{-3}$. The reduction of the index of refraction in the infrared region upon doping (see Fig. 2) is also consistent with interaction of the radiation with free carriers.[15] However, caution should be exercised in quantitatively interpreting these data since the contribution by scattering due to the observed surface morphology has not been taken into account.

Finally, the conductivity results of Fig. 4 are in general agreement with the suggestions by Spear et al.[5], who have studied the transport properties of glow discharge μc-SiH_x films. These authors suggest that the increase in conductivity in the μc-phase as compared to the amorphous phase can be associated with a higher free carrier concentration. The order associated with the microcrystalline phase should be sufficient to delocalize an appreciable range of the band tail states: Indeed, the weak dependence of the conductivity on temperature, observed in our P and N-type films, suggests that the Fermi level was able to move close to the corresponding band edges. The origin of the type of conductivity of the undoped films is not yet understood.[17]

The high conductivity and reduced optical absorption in the visible spectral region of the doped microcrystalline films make them ideal

candidates for contacts in PIN solar cells. Figure 5 shows the significant increase in the collection efficiency in the blue portion of the spectrum afforded by using a microcrystalline P-layer for the front contact and a microcrystalline N-layer as the rear contact in an all-sputtered cell (Si-485). For comparison, the spectral response of one of our best cells made with amorphous N- and P- layers (Si-403) is also shown. The amorphous cell had an AM1 engineering efficiency of 4.0% (9), while the cell with the microcrystalline contacts now has an improved efficiency of 4.6%. It is noteworthy that cells with microcrystalline contacts show larger open circuit voltages, by about 0.10V, than entirely amorphous cells. We attribute this to the larger separation in the N- and P- Fermi levels that are achieved with $\mu c\text{-}SiH_x$ films.

In conclusion, we have investigated a number of structural properties related to the film growth of sputtered $\mu c\text{-}SiH_x$ films, as well as their optical and transport properties. These data, together with the works of Spear et al.[6] and Richter and Ley[3] clearly indicate the effect of structural ordering in the transition from the crystalline to the amorphous phase. In addition we have demonstrated the merits of using microcrystalline P and N contacts in PIN solar cells.

Acknowledgements

The authors are grateful to Drs. B. Abeles, G. Cody, M. Cohen, A. Ghosh, J. Shropshire and B. Weinberger for a number of discussions and to R. Friedman, M. Hicks and J. Haberman for technical assistance. The work was supported partly by the U.S. Department of Engergy through a Solar Energy Institute grant (Contract No. XZ-0-9219).

References

1. S. Veprek and V. Marecek, Solid State Electronics 11, 683 (1968).
2. S. Veprek, Z. Iqbal, H.R. Oswald, F.A. Sarott and J.J. Wagner, Journal De Physique Colloque C4, Supplement Un No 10, Tome 42, Oct. 1981 P.(C4-251).
3. H. Richter and L. Ley, J. Of Appl. Phys. 52, 7281 (1981).
4. A. Matsuda, S. Yamasaki, K. Nakagawa, H. Okushi, K. Tanaka, S. Izima, M. Matsummura and H. Yamamoto, Jap. J. Appl. Phys. 19, L305 (1980).
5. T. Hamasaki, H. Kurata, M. Hirose and Y. Osaka, Jap. J. of Applied Phys. 20, L84 (1981).
6. W. E. Spear, G. Willeke, P.G. LeComber and A.G. Fitzgerald, Ref. 2, P.(C4-257).
7. T. Imura, K. Mogi, A. Hiraki, S. Nakashima and A. Mitsuishi, Solid State Commun. 40, 161 (1981).
8. H. Richter and L. Ley, Ref. 2 P.(C4-261).
9. T.D. Moustakas and R. Friedman, Appl. Phys. Lett. 40., 515 (1982).
10. J.P. deNeufville, T.D. Moustakas and A.F. Ruppert, J. of Non-Crystall. Solids 35&36, 481 (1980).
11. T. Huen, Appl. Opt. 18, 1927 (1979).
12. W.C. Dash and R. Newman Phys. Rev. 99, 1151 (1955).
13. T.D. Moustakas, H.P. Maruska and R. Friedman (unpublished).
14. T.D. Moustakas, T. Tiedje and W.A. Lanford, Tetrahedrally Bonded Amorphous Semiconductors, R.A. Street, D.K. Biegelsen and J.C. Knights Eds., (AIP Conference Proceedings No. 73, 1981) p. 20.
15. G. Lubberts, B.C. Burkey, F. Moser and E.A. Trabka, J. Appl. Phys. 52 6870 (1981).
16. It could be due to P-type impurities from the target or particular structural defects.

FIGURE CAPTIONS

Fig. 1 (A) The surface morphology of the undoped (a), the phosphorus doped (b), and the boron doped (c) films, viewed in an optical microscope under 1000 magnification.

(B) X-ray diffraction spectra of the $\mu c\text{-}SiH_x$ films.

Fig. 2 The index of refraction vs. photon energy of the three types of $\mu c\text{-}SiH_x$ films. For comparison we show also the index of refraction of crystalline silicon and of an undoped and a boron doped $a\text{-}SiH_x$ film.

Fig. 3 The optical absorption constant of the three types of $\mu c\text{-}SiH_x$ films. For comparsion we show also the optical absorption of crystalline silicon and of an undoped and a boron doped $a\text{-}SiH_x$ film.

Fig. 4 The dark conductivity vs. 1/T of the three types of $\mu c\text{-}SiH_x$ films. Sample Si-438 is doped with Boron, the Si-440 is doped with phosphorus and the Si-454 is not doped intentionally.

Fig. 5 Improvement in the collection efficiency of sputtered PIN cells in the blue portion of the spectrum, which is obtained by using a microcrystalline P-layer in place of a highly absorbing amorphous P-layer; ---Si-403 (amorphous P-layer), ——Si-485 (microcrystalline P-layer).

(A)

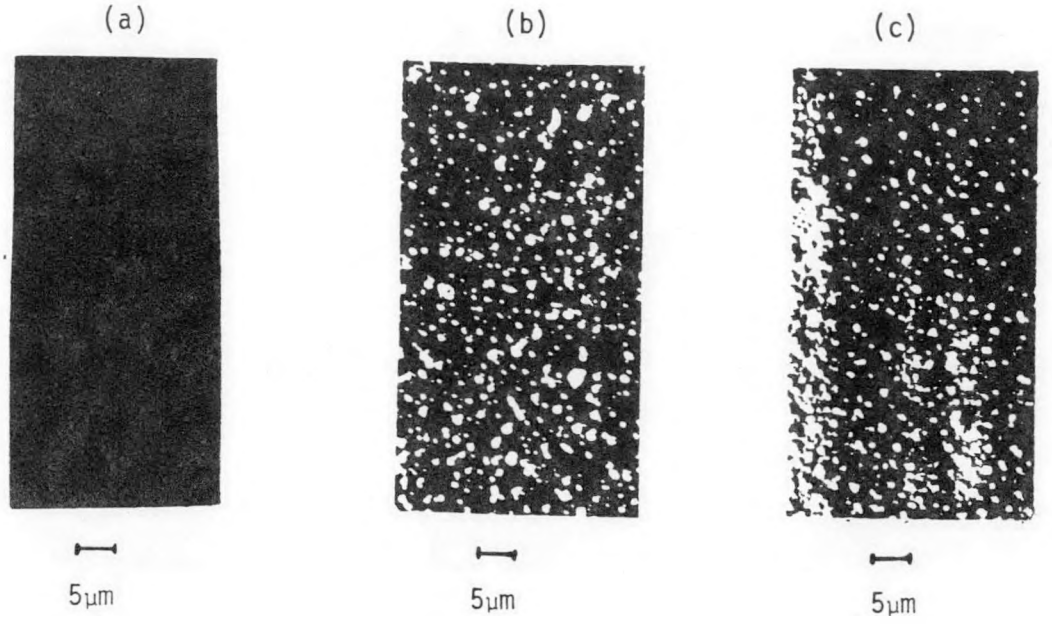
(a)
(b)
(c)
5μm
5μm
5μm

3)

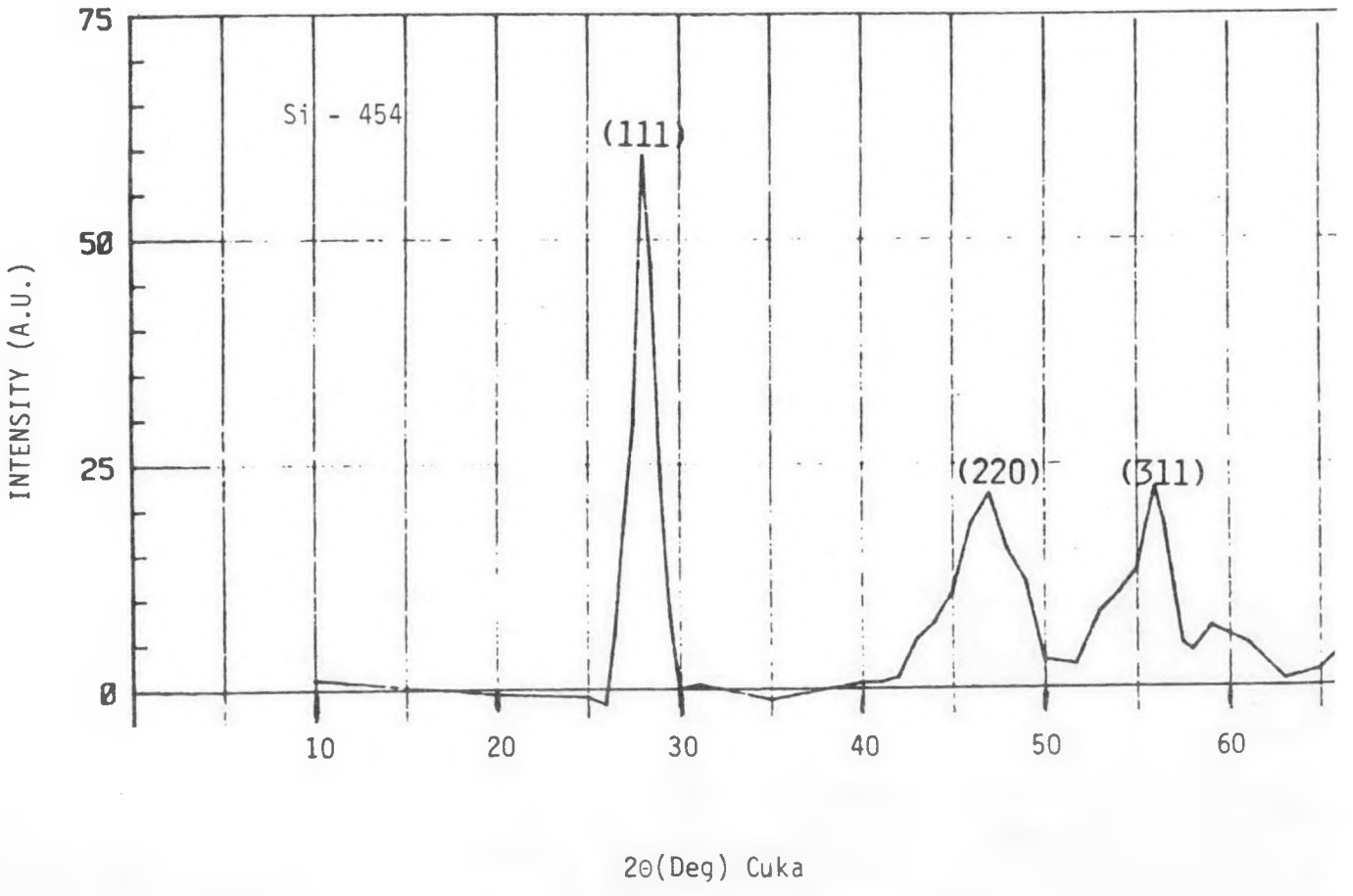
75
50
25
0
Si - 454
(111)
(220)
(311)
INTENSITY (A.U.)
10
20
30
40
50
60
2θ(Deg) Cuka

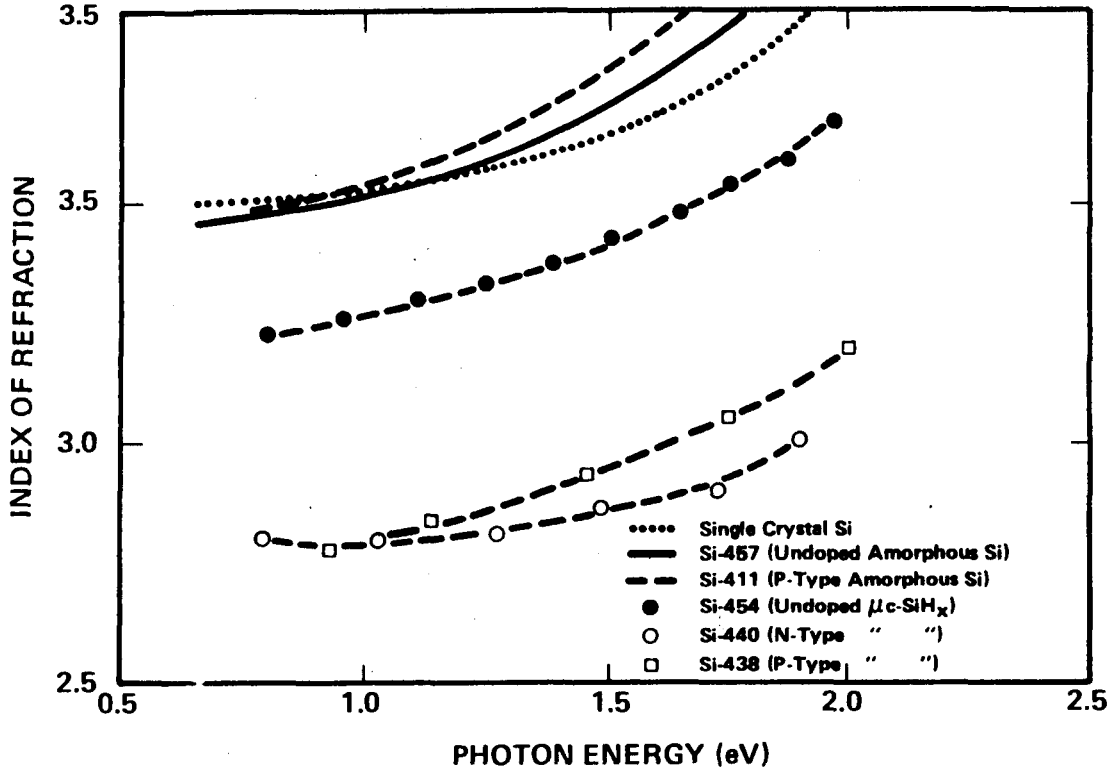
INDEX OF REFRACTION
3.5
3.5
3.0
2.5
0.5
1.0
1.5
2.0
2.5
PHOTON ENERGY (eV)
Single Crystal Si
Si-457 (Undoped Amorphous Si)
Si-411 (P-Type Amorphous Si)
Si-454 (Undoped μc-SiH$_x$)
Si-440 (N-Type " ")
Si-438 (P-Type " ")

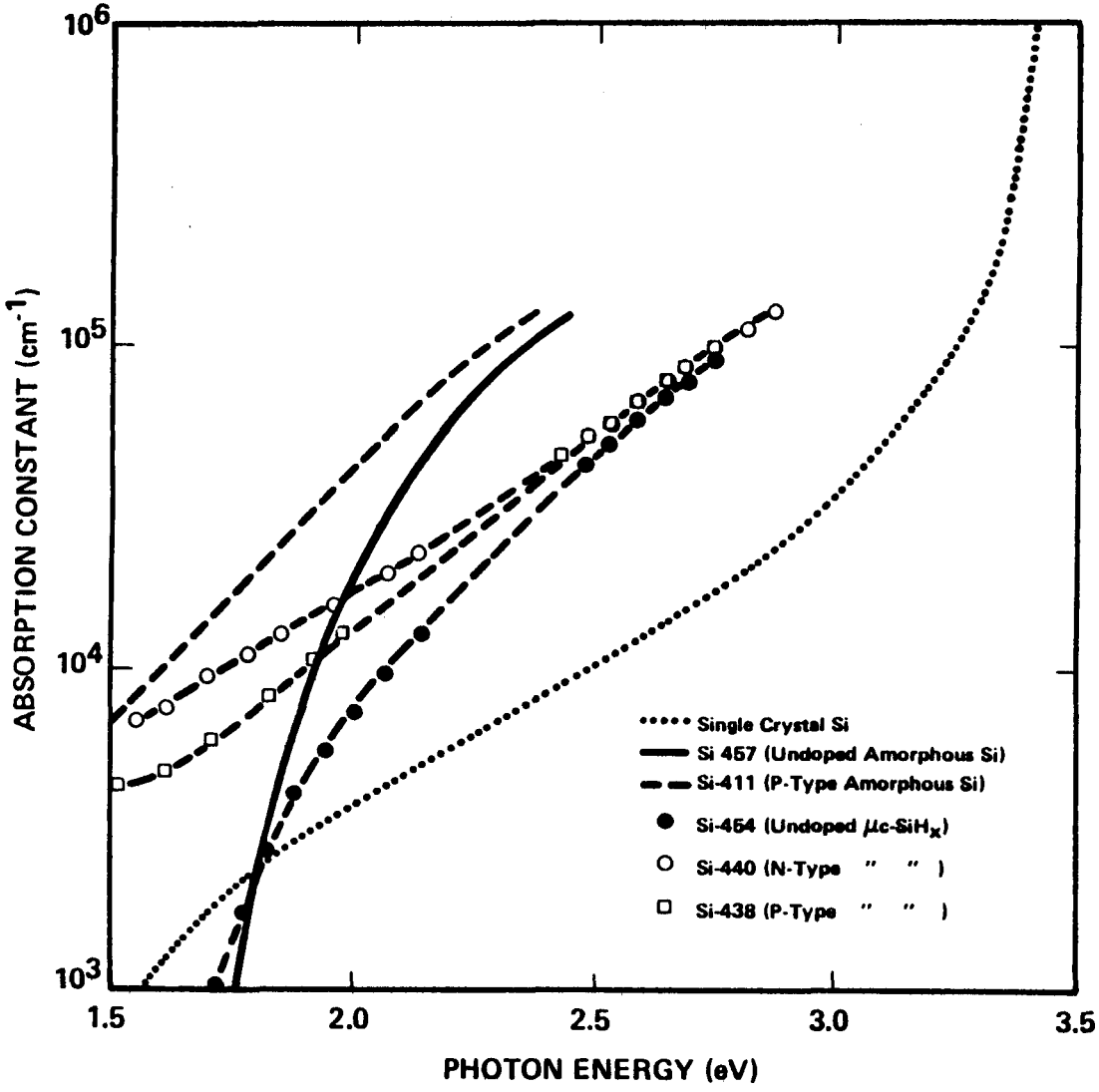
10^6
10^5
10^4
10^3
ABSORPTION CONSTANT (cm^{-1})
1.5
2.0
2.5
3.0
3.5
PHOTON ENERGY (eV)
Single Crystal Si
Si 457 (Undoped Amorphous Si)
Si-411 (P-Type Amorphous Si)
Si-454 (Undoped μc-SiH$_X$)
Si-440 (N-Type " ")
Si-438 (P-Type " ")

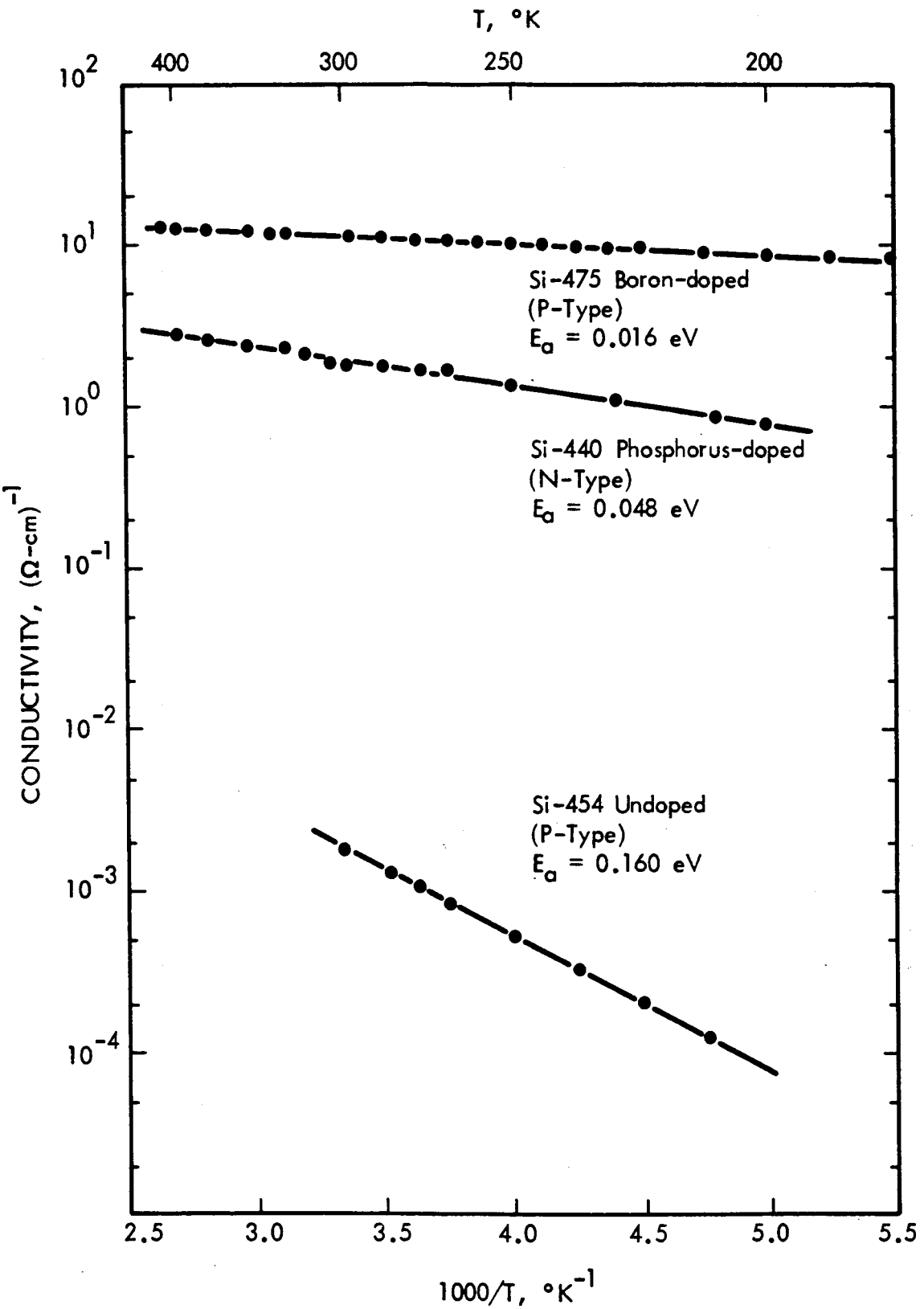
T, °K
400
300
250
200
10^2
10^1
10^0
10^{-1}
10^{-2}
10^{-3}
10^{-4}
CONDUCTIVITY, $(\Omega\text{-cm})^{-1}$
Si-475 Boron-doped
(P-Type)
E_a = 0.016 eV
Si-440 Phosphorus-doped
(N-Type)
E_a = 0.048 eV
Si-454 Undoped
(P-Type)
E_a = 0.160 eV
2.5
3.0
3.5
4.0
4.5
5.0
5.5
1000/T, $°K^{-1}$

FIGURE IMPROVEMENT IN THE COLLECTION EFFICIENCY OF SPUTTERED PIN CELLS IN THE BLUE PORTION OF THE SPECTRUM, WHICH IS OBTAINED BY USING A MICROCRYSTALLINE P-LAYER IN PLACE OF A HIGHLY ABSORBING AMORPHOUS P-LAYER; - - -Si-403 (AMORPHOUS P-LAYER), ——Si-485 (MICROCRYSTALLINE P-LAYER)

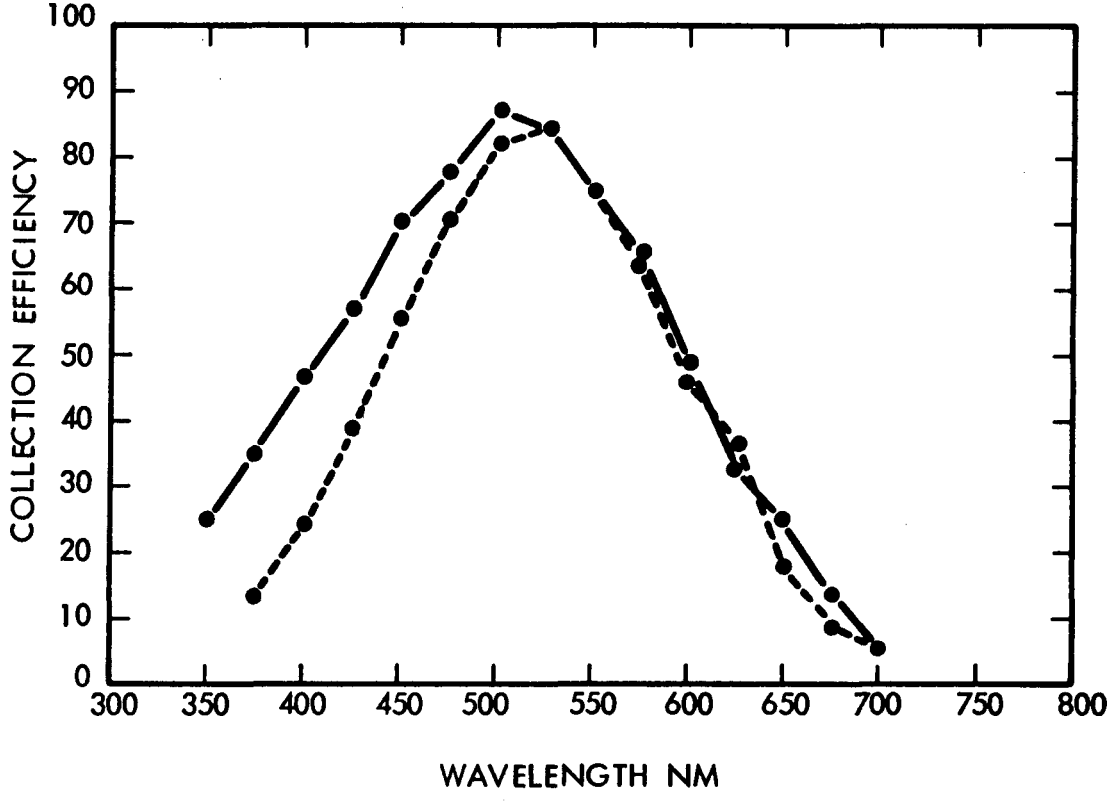

APPENDIX D. Optical and Transport Properties of Boron Doped Reactively Sputtered Amorphous Silicon Films

OPTICAL AND TRANSPORT PROPERTIES OF BORON DOPED REACTIVELY SPUTTERED AMORPHOUS SILICON FILMS

T.D. Moustakas, H. Paul Maruska, R. Friedman and M.C. Hicks
Corporate Research Laboratory
Exxon Research and Engineering Company
Linden, N.J. 07036

ABSTRACT

The optical and transport properties of boron doped films produced by reactive sputtering under a variety of deposition conditions have been investigated. A direct relation between the magnitude of the conductivity and the optical absorption constant has been found. This result suggests that boron doping broadens the valence band tail which increases the absorption, and that conduction in these states makes a substantial contribution to the current. It appears that the efficiency of B-doping is decreased by raising the level of hydrogen incorporation.

Trace impurity doping in hydrogenated a-SiH_x has been demonstrated in films produced either by glow discharge decomposition of silane[1] or by reactive sputtering[2]. There is both direct[3] and indirect[4] evidence that only a small fraction of the impurity atoms are 4-fold coordinated, and that the great majority of them are in non-doping configurations and thus introduce additional defects in the material. Although the nature and origin of these defects are not well understood[5] it is known that doped a-SiH_x films have poor photoelectronic properties, and their primary use in device applications has been in the formation of either ohmic or blocking contacts to the undoped a-SiH_x. One such application, for example, is the PIN solar cell structure. The performance of such a device depends greatly on both the optical losses in the doped layer through which the light must enter the device, as well as the relative displacement of the Fermi levels in the P and N layers. In this paper we report on the optical and transport properties of boron doped P-layers produced by reactive sputtering. The primary objective of this study is to evaluate these layers as "windows" in PIN solar cell structures, and to gain insights as to how boron doping modifies the electronic structure of a-SiH_x films.

The a-SiH_x films were prepared by RF sputtering of a polycrystalline target 5" in diameter. The sputtering gas was a 5 mTorr mixture of argon with variable amounts of hydrogen and diborane. The deposition parameters of all investigated samples are given in Table I. The films for the optical absorption measurements were deposited on quartz substrate, and those for the conductivity measurements were deposited on 7059 glass, coated first with four strips of NiCr thin films 8mm long and spaced 1 mm apart. The film thickness was between 0.5 to 1.0μm.

The optical densities of the films were measured in a Cary 17 Spectrophotometer, using a 2mm aperture to eliminate the possibility of thickness gradients. The amplitude, ΔOD, of the interference fringes in the wavelength region below the optical absorption edge was used to calculate the refractive index, n_f, for a given substrate index at a given wavelength. The interference fringes were also used to calculate the film thickness. The optical absorption coefficient was calculated by an iterative procedure from optical transmission measurements.[6] The applied field during the measurements of the conductivity was kept below 10^3 volts/cm, well within the ohmic regime.

The film's deposition rate, which was varied from 1 to 3A/sec depending on the power in the discharge, was found to be independent of the amount of the B_2H_6 in the sputtering gas. The index of refraction in the infrared wavelength region ($\lambda \approx 2.0\mu m$) was found to have values of between 3.4 to 3.5 for all B-doped films that were investigated.

The optical absorption constants vs photon energy for four of the samples, produced at 325°C with a power of 1.5 W/cm^2 are shown in Fig. 1. These data indicate clearly the effect of the concentration of B_2H_6 in the discharge on the optical absorption constant. Note that boron incorporation modified the optical absorption both in the high photon energy region (band-to-band transitions), and in the Urbach edge region[7]. The activation energy of the Urbach edge changes from 0.066 eV for the intrinsic film to 0.26 eV for the film deposited at 2000 ppm of B_2H_6.

The values of E_{04}, the energy at which the absorption constant becomes $10^4 cm^{-1}$, are listed in Table 1 for all of the samples. From Table 1 we may note the effects of power in the discharge and deposition temperature on the optical absorption constant. It is apparent that the

optical absorption spectrum is shifted towards the blue (while the Urbach edge actually becomes sharper) if either the power is raised (compare Si-411 with Si-415) or the substrate temperature is lowered (compare Si-416 with Si-340).

Fig. 2 shows the room temperature conductivity vs concentration of B_2H_6 in the discharge for the same samples shown in Fig. 1. According to these data, the doping efficiency of the sputtered films is equivalent to that of the films produced by glow discharge decomposition of silane.[1] Fig. 3 shows the temperature dependence of the conductivity for a number of boron doped films. These data can be fitted to an expression of the form $\sigma = \sigma_0 \exp(-E_a/kT)$. All of these curves intersect at $T = \infty$ with $\sigma_0 = 4.5$ $(\Omega\text{-cm})^{-1}$. Note that as the Fermi level moves closer to the valence band the magnitude of σ_0 remains invariant, and thus the typical behavior of the Meyer-Neldel Rule[8] is not followed. The implication here is that in this range the Fermi levels of the samples are located in a large density of gap states and thus do not move differently with temperature. In contrast, Rehm et al[9] found a large variation of σ_0 with E_a for boron doped films produced by the glow discharge method; their value of $\sigma_0 = 5(\Omega\text{-cm})^{-1}$ at the lowest activation energy, however, agrees with our results.

The room temperature conductivity and the optical gap (defined as the photon energy at which the optical absorption has a value of $10^4 cm^{-1}$) are related by a universal relation independent of the film's deposition parameters. This relation is shown in Fig. 4.

These experimental results can now be accounted for in the following way. The finding that the deposition rate of our films is independent of the amount of B_2H_6 in the sputtering gas is contrary to the observation by Street et al[5] that for glow discharge decomposition of

silane, boron doping substantially enhances the deposition rate. This difference can be attributed largely to the different growth processes of the two types of films. For example, there is ample evidence that reactions in the gas phase are far more important in the glow discharge decomposition of silane than in reactive sputtering.[10] The insensitivity of deposition rate to the amount of B_2H_6 in the discharge during sputtering suggests that B incorporates into the growing film through surface reactions at the substrate.

The modification of the optical absorption in the band, as well as in the Urbach edge region, is consistent with the notion that boron incorporation affects both the Si network as well as the defect structure. Street et al[5] have produced experimental evidence that both boron and phosphorous incorporation introduce dangling bond-type defects. If indeed boron incorporation introduces dangling bond related defects, then changes in the network may partly be associated with hydrogen bonding to these defects. The data relating to changes in power and temperature can be accounted for along these lines as follows. Films produced either at higher power in the discharge or lower deposition temperatures are expected to have more hydrogen incorporated into the network. Some of this extra hydrogen may remove dangling bond type defects introduced by the boron incorporation, and this results in a blue-shifted, sharper optical absorption.[7] The observation that the conductivity decreases as the concentration of hydrogen increases may be due to the formation of excess non-tetrahedrally bonded boron in the presence of hydrogen. If this hypothesis is correct, the material with the lowest density of states would not be the most dopable.[11]

The introduction of tetrahedrally coordinated boron impurities, which act as acceptors, leads to a concentration of holes at the Fermi level in the valence band tail. These holes must be thermally activated to allow conductivity, either into the extended states, or else into a set of localized states through which hopping can occur. The Fermi level moves slightly closer to the valence band as the boron concentration increases, but the position of the Fermi level for any of these samples is independent of temperature.

The broadening of the Urbach edge with boron incorporation can be interpreted as due either to broadening of the band tails[7] or to the introduction of internal electric fields due to charged impurities.[12] However, the poor doping efficiency indicated by the conductivity results suggests that the concentration of charged impurities is not sufficient to account for the large potential fluctuations that would be required to cause the large shifts in optical absorption that were measured. The observed correlation (Fig. 4) between the optical gap (which was measured at the onset of the Urbach edge) and the conductivity, indirectly supports the first mechanism. It appears, therefore, that boron incorporation broadens the valence band tail and that conduction in these states by a hopping process makes a substantial contribution to the current.

In conclusion, we have investigated the optical and transport properties of a number of boron-doped films produced under a variety of deposition conditons. The results suggest that boron-doping broadens the valence band tail, and that hole transport is dominated by conduction in these states. Therefore, p-layers with good "window" properties suffer from lower conductivity.

Acknowledgments

The authors are indebted to George Cody, Amal K. Ghosh, Joseph A. Shropshire for a number of technical discussions. This work was partially supported by the U.S. Department of Energy through a Solar Energy Research Institute contract (Contract # XZ-0-9219)

References

1. W. Spear and P.G. LeComber, Solid State Commun. 17, 1193 (1975).

2. W. Paul, A.J. Lewis, G.A.N. Connel and T.D. Moustakas, Solid State Commun. 20, 969 (1976).

3. J.C. Knights, T.M. Hayes and J.C. Mikkelsen, Phys. Rev. Lett. 39, 712 (1977).

4. A. Madan, P.G. LeComber and W. Spear, J. Non-Cryst. Solids 20, 239 (1976).

5. R.A. Street, D.K. Biegelsen and J.C. Knights (to be published).

6. O.S. Heavens, Optical Properties of Thin Solid Films (Dover, New York, 1965).

7. G. Cody, T. Tiedje, B. Abeles, T.D. Moustakas, B. Brooks and Y. Goldstein. J. De Physique, Colloque C4, Supplement au n^{o} 10, Tome 42, Octobre 1981, page C4-301.

8. W. Meyer and H. Neldel, Z. Tech. Phys. 18, 588 (1937).

9. W. Rehm, R. Fischer, J. Stuke and H. Wagner, Phys. Stat. Solid; 76b, 539 (1977).

10. T.D. Moustakas, T. Tiedje and W.H. Lanford, Tetrahedrally Bonded Amorphous Semiconductors, R.A. Street, D.K. Biegelsen and J.C. Knights Eds., (AIP Conference Proceedings No. 73, 1981) p. 20.

11. T. Tiedje, T.D. Moustakas and J.M. Cebulka, Phys. Rev. B, 23, 5634 (1981).

12. J.D. Dow and D. Redfield, Phys. Rev. B5, 594 (1972).

TABLE I: Deposition Parameters and Value of E_{04} for the Investigated Samples

Sample	B_2H_6(ppm)	T_s(°C)	Power(W/cm^2)	H/Ar	E_{04}(eV)
Si-405	0	325	1.5	0.40	2.03
Si-410	500	325	1.5	0.40	1.89
Si-408	1000	325	1.5	0.40	1.72
Si-411	2000	325	1.5	0.40	1.60
Si-414	2000	325	1.5	0.20	1.58
Si-415	2000	325	3.0	0.40	1.76
Si-416	2000	375	3.0	0.40	1.70
Si-340	2000	275	3.0	0.40	1.80

Figure Captions

Fig. 1 Optical absorption vs photon energy for an intrinsic and several B-doped films.

Fig. 2 Conductivity measured at 300°C vs the amount of B_2H_6 in the sputtering gas.

Fig. 3 Conductivity vs 1/T for a number of B-doped films.

Fig. 4 Conductivity (measured at 300°C) vs optical gap E_{04} (defined as the photon energy at which the optical absorption has a value of $10^4 cm^{-1}$) for all the investigated films.

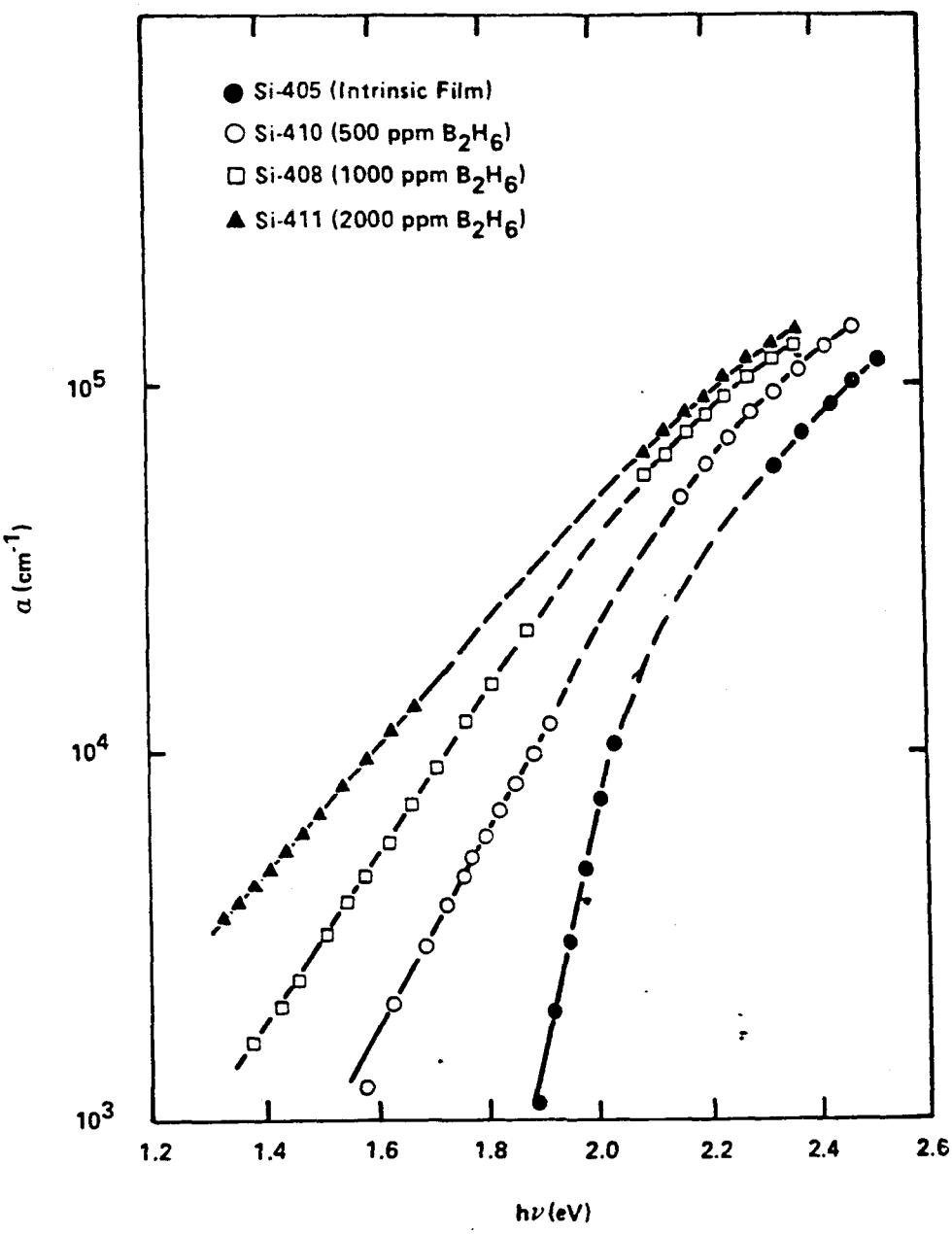
● Si-405 (Intrinsic Film)
○ Si-410 (500 ppm B_2H_6)
□ Si-408 (1000 ppm B_2H_6)
▲ Si-411 (2000 ppm B_2H_6)
10^5
10^4
10^3
α (cm^{-1})
1.2
1.4
1.6
1.8
2.0
2.2
2.4
2.6
$h\nu$ (eV)

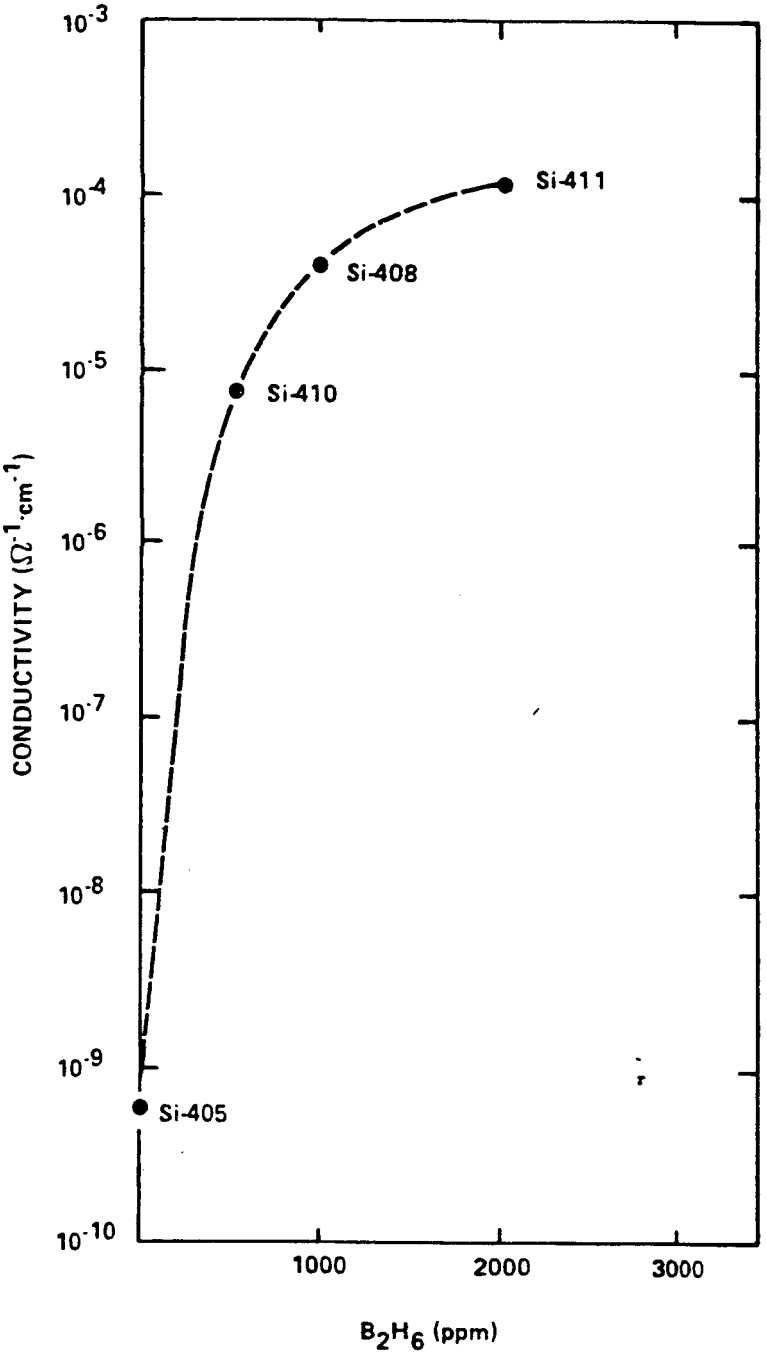
10^{-3}
10^{-4}
10^{-5}
10^{-6}
10^{-7}
10^{-8}
10^{-9}
10^{-10}
CONDUCTIVITY ($\Omega^{-1}\cdot cm^{-1}$)
Si-411
Si-408
Si-410
Si-405
1000
2000
3000
B_2H_6 (ppm)

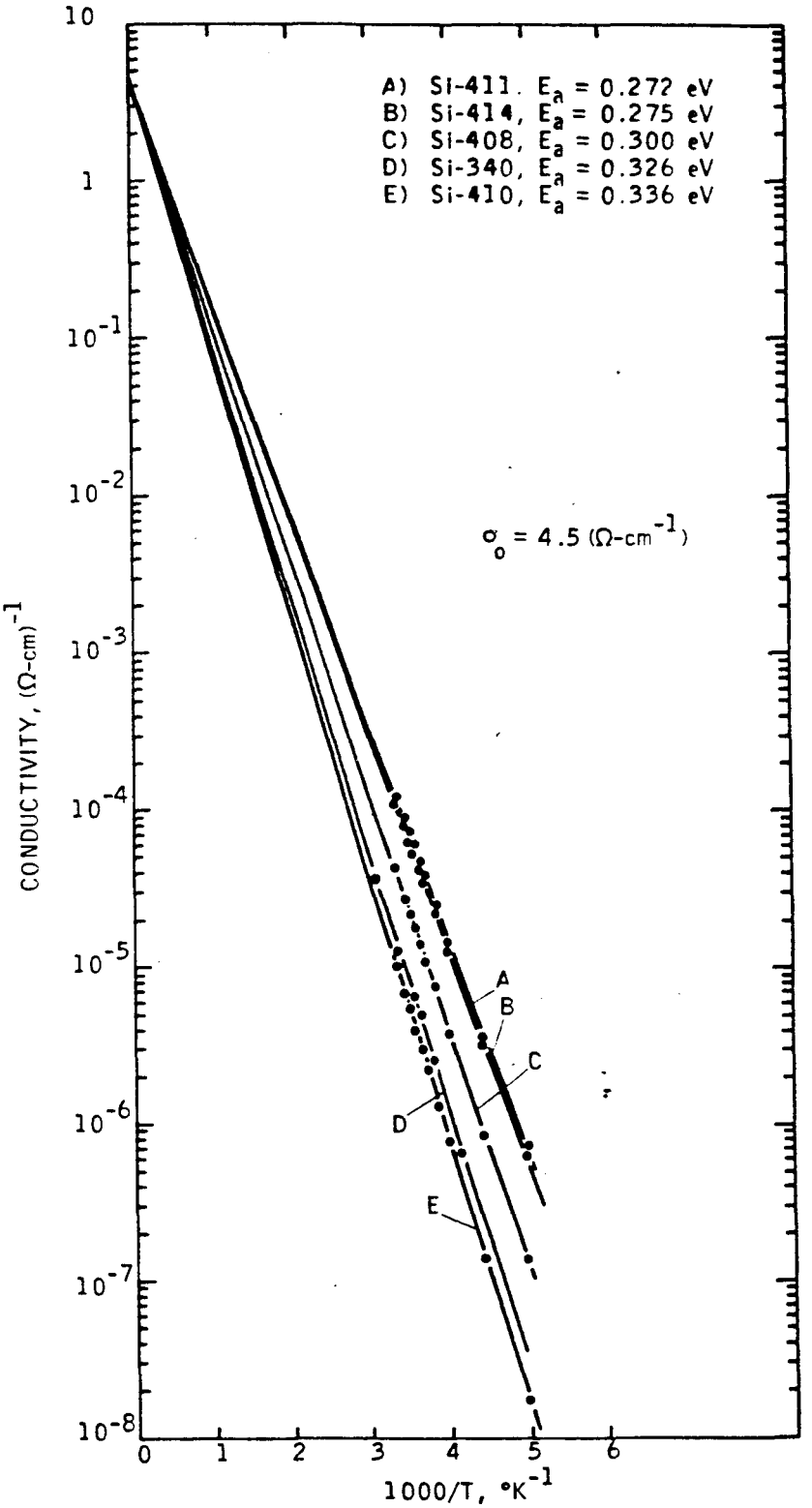
A) Si-411. E_a = 0.272 eV
B) Si-414, E_a = 0.275 eV
C) Si-408, E_a = 0.300 eV
D) Si-340, E_a = 0.326 eV
E) Si-410, E_a = 0.336 eV
σ_o = 4.5 (Ω-cm^{-1})
CONDUCTIVITY, (Ω-cm)$^{-1}$
1000/T, °K^{-1}
10
1
10^{-1}
10^{-2}
10^{-3}
10^{-4}
10^{-5}
10^{-6}
10^{-7}
10^{-8}
0
1
2
3
4
5
6
A
B
C
D
E

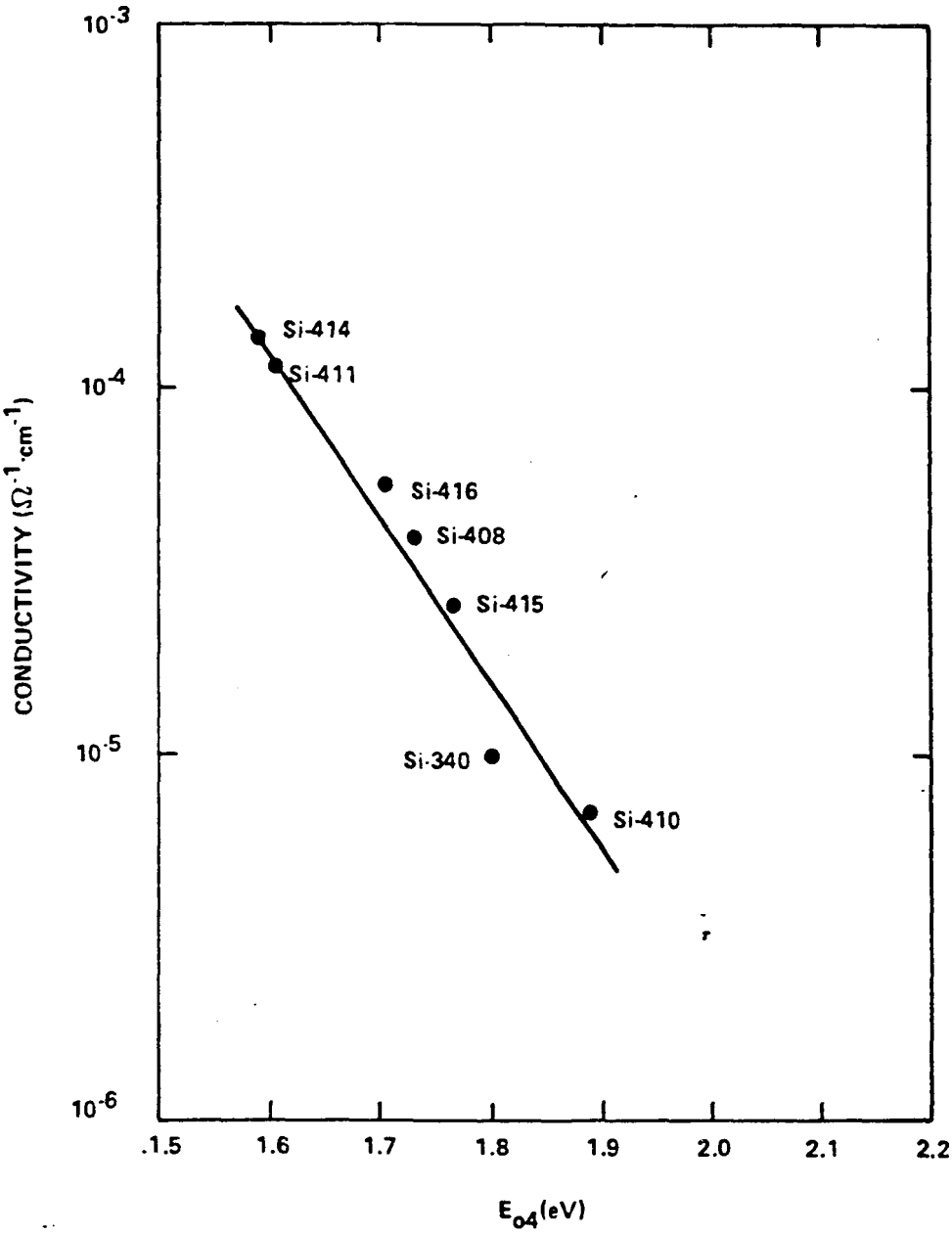
10^{-3}
10^{-4}
10^{-5}
10^{-6}
CONDUCTIVITY ($\Omega^{-1}\cdot cm^{-1}$)
Si-414
Si-411
Si-416
Si-408
Si-415
Si-340
Si-410
1.5
1.6
1.7
1.8
1.9
2.0
2.1
2.2
E_{o4}(eV)

APPENDIX E. Doping of Amorphous Silicon by Sputtering From Boron Doped Targets

0201-R-TDM

DOPING OF AMORPHOUS SILICON BY SPUTTERING FROM BORON DOPED TARGETS

T. D. Moustakas, H. P. Maruska,
R. Friedman and M. C. Hicks

Corporate Research Laboratory
Exxon Research and Engineering Company
Linden, New Jersey 07036

ABSTRACT

The doping of amorphous silicon by sputtering from boron doped targets has been investigated. Films produced at low total pressure and $H_2/Ar<1$ are amorphous with doping efficiency decreasing with the amount of hydrogen in the discharge. Films produce at high total pressure and $H_2/Ar>>1$ appear to be microcrystalline. The optical and transport properties of both types of films have been investigated.

I. INTRODUCTION

Trace impurity doping in hydrogenated amorphous silicon (α-SiHx) has been demonstrated in films produced either by glow discharge decomposition of silane[1] or by reactive sputtering[2]. In both of these methods doping by phosphorous or boron is accomplished by mixing certain percentages of PH_3 or B_2H_6 in the silane or $Ar+H_2$ discharges. This method of gas phase doping is highly undesirable, since it requires the handling of toxic gases.

In this paper we report for the first time boron doping of amorphous silicon by sputtering from boron doped targets. The emphasis of the study is to develop an understanding of the various physical and chemical effects occuring during sputtering from a (Si+B) target in an $Ar+H_2$ plasma, and thus be able to identify deposition parameters for efficient doping of amorphous silicon from boron doped targets. Films having amorphous or microcrystalline structure have been fabricated and the role of hydrogen in affecting the doping efficiency has been identified. The films have been characterized through structural, optical and transport measurements.

II. EXPERIMENTAL METHODS

The target used in this study was fabricated by hot pressing fine powders (-325 mesh, i.e. 5 to 10 μm) of 97 at % Si (99.999%) and 3 at % B (99.5%). The size of the target is 5" in diameter and $\frac{1}{4}$" thick.

Films have been produced by varying the substrate temperature, the substrate bias, the target voltage, the ratio of the flow rates of hydrogen to argon and the total pressure of $Ar+H_2$. The films have been deposited on a variety of substrates, such as quartz for optical measurements, 7059 glass (coated first with four strips of NiCr thin films) for conductivity measurements and high purity single crystal silicon for infrared vibrational and impurity concentration studies. The experimental techniques of measuring these properties have been described in another paper[3].

III. EXPERIMENTAL RESULTS

The deposited samples can be classified into two categories: The one type of samples were depositied at low total pressure ($Ar+H_2$=5m Torr) and $H_2/Ar<1$. The deposition conditions of these samples are summarized in Table I. The second type of samples were deposited at high total pressure ($Ar+H_2$>20mTorr) and $H_2/Ar=10$. The deposition conditions of these samples are summarized in Table II. In each class of samples we additionally investigated the effect of other deposition parameters, such as substrate temperature, substrate bias and power in the discharge. Certain trends in transport and optical properties have been observed upon varying these deposition parameters.

We first discuss the samples of Table I. Figure 1 shows the room temperature conductivity of all the investigated samples. Films produced at the lowest hydrogen content show the highest conductivity. The conductivity decreases by several orders of magnitude as the hydrogen content in the discharge increases from 1% to 40%. The temperature dependence of the conductivity of the samples deposited at 230℃ is shown in Figure 2. Note that the conductivity in the investigated temperature range is thermally activated with the same pre-exponential factor ($\sigma_0 \sim 3.5 \Omega^{-1} cm^{-1}$) and activation energies, which increase with the hydrogen content from 0.21eV to 0.5eV. Figure 3 shows the optical absorption constant vs. photon energy for all investigated samples. The optical absorption shifts to higher photon energies and becomes sharper with the hydrogen content in the discharge. Correspondingly, the index of refraction decreases. Figure 4 shows the correlation between the index of refraction, measured at 1.8μm, and the optical gap, defined as the photon energy at which te optical absorption has a value of $10^4 cm^{-1}$.

The conditions described in Table II were chosen to lead to microcrystalline films in analogy with gas phase doping[4]. Although x-rays analysis of representative samples does not indicate that the films described in Table II are microcrystalline, certain trends in conductivity and optical absorption suggest that the films are microcrystalline, but with crystallite size too small to be detected by x-rays (<30Å). One parameter, which was found to have a signficant effect in the conductivity is the total pressure of the sputtering gas. Figure 5 shows the room temperature conductivity vs. the total pressure for a number of films. The conductivity increases abruptly at pressures higher than 20mTorr. Figure 6 shows the temperature dependence of the conductivity for some of these samples. Note, that films produced at higher $Ar+H_2$ pressures have progressively weaker temperature dependence. However, the apparent thermally activated form of these data leads to pre-exponential factors of between 10^{-1} to 10^{-3}, which is considerably smaller than the values calculated from the data of Figure 2. Besides the total pressure, other parameters which were found to affect the conductivity are the substrate bias and the target voltage. These variations are shown in Table II. To illustrate the optical properties of these films, we plot in Figure 7 the optical absorption constant of one conductive film (#493) and one resistive film (#492). Note, that the optical absorption of sample #492 is remarkably similar to that of sample #491 of Figure 3. On the contrary, the optical absorption of #493 is not as sharp in the investigated photon energy.

IV. DISCUSSION

The results of the samples produced at low total pressure and $H_2/Ar<1$ can be accounted for in two different models: The one model assumes that incorporation probability of boron into the films is not influenced by the amount of hydrogen in the discharge. Then, the reduction of the conductivity as more hydrogen incorporates into the films (Figures 1 and 2) could result from the fact that less boron incorporates into sites which are tetrahedrally coordinated. A similar suggestion has recently been made by Magarino et al[5], who investigated doping effects on post-hydrogenated CVD-amorphous silicon. The optical data of Figures 3 and 4 can be easily accounted for in this model, since it is known that more hydrogen incorporation into the Si network results in larger optical gap and smaller index of refraction.

The second model assumes that hydrogen reacts with the boron at the surface of the target or the surface of the growing film and forms boron hydrides. These hydrides are pumped out, and thus less boron incorporates into the film. Direct measurements of the boron incorporated into the films is underway to differentiate between the two models. However, it appears that the second model cannot account for the optical data of Figures 3 and 4. If hydrogen is consumed in etching boron from either the target or the film, then the optical gap should not increase with the amount of hydrogen in the discharge.

The results of the samples produced at high total pressure and $H_2/Ar>>1$ can be accounted for in a model which assumes that the films undergo a transition from the amorphous to the microcrystalline phase. However, the size of the crystallites are too small to be detected by x-rays in films with thicknesses less than 5000Å. The abrupt transition

with the total pressure is believed to be due to bombardment effects by neutral or charded particles[6]. Such bombardment effects, which prevail at low total pressures, could introduce more disorder due to adatom diffusion. Such bombardment effects could also account for the observed conductivity changes in films produced under different substrate biasing conditions and target voltages. Further evidence for transition from the amorphous to the crystalline phase is provided by the optical data of Figure 7. The more conductive film (#493) has an optical absorption which begins to resemble that of microcrystalline films[4].

V. CONCLUSIONS

Boron doped films by sputtering from a Si+B target have been produced. Films deposited at low argon pressure (P_{Ar} = 5mTorr) and $H_2/Ar<1$ are amorphous, and are more efficiently doped at zero or low hydrogen concentration in the discharge ($H_2/Ar<2\%$). Two models regarding the effect of hydrogen in the doping of the films have been discussed.

Films produced at high total pressure and $H_2/Ar>>1$ appear to indicate a transition from the amorphous to crystalline phase. Further optimization of the parameters is required in order to produce microcrystalline films similar to those produced from gas phase doping[4].

References

1. W. Spear and P. G. LeComber, Solid State Commun. 17, 1193 (1975).

2. W. Pau, A. J. Lewis, G. A. N. Connel and T. D. Moustakas, Solid State Commun. 20, 969 (1976).

3. T. D. Moustakas, H. P. Maruska, R. Friedman and M. C. Hicks, Phys. Rev. B (Submitted for publication).

4. T. D. Moustakas and H. P. Maruska (to be published).

5. J. Magarino, D. Kaplan, A. Friederich and A. Deneuville, Philos. Mag. B., 45, 285 (1982).

6. T. D. Moustakas, Solar Energy Mater. (Nov. 1982).

TABLE I

Sample	T_S (°C)	V_S (Volts)	V_T (Volts)	Ar+H_2 (mTorr)	H_2/Ar	R(A/min)
#518	300	0	1000	5	0	92
#519	300	0	1000	5	0.0106	94
#520	300	0	1000	5	0.02	91
#494	230	0	1000	5	0.01	75
#490	230	0	1000	5	0.05	83
#487	230	0	1000	5	0.10	79
#491	230	0	1000	5	0.40	83

TABLE II

Sample	T_s (°C)	V_s (Volts)	V_T (Volts)	Ar+H_2 (mTorr)	H_2/Ar	R(A/min)	$6(\Omega \cdot cm)^{-1}$
#492	230	0	1000	20	10	38	1.0×10^{-7}
#493	230	0	1000	40	10	16.7	1.4×10^{-3}
#522	300	0	800	40	10	12.3	6.1×10^{-4}
#527	300	0	800	60	10	8.7	7.5×10^{-3}
#526	300	0	800	80	10	9.6	1.23×10^{-2}
#521	300	0	1200	40	10	34	1.3×10^{-9}
#523	300	+50	800	40	10	13.5	2.8×10^{-3}
#524	300	+100	800	40	10	14	1.5×10^{-2}
#525	300	+150	800	40	10	13.5	6.4×10^{-3}
#529	300	+50	800	80	10	9.75	2.8×10^{-3}
#528	300	+100	800	80	10	9	4.36×10^{-3}

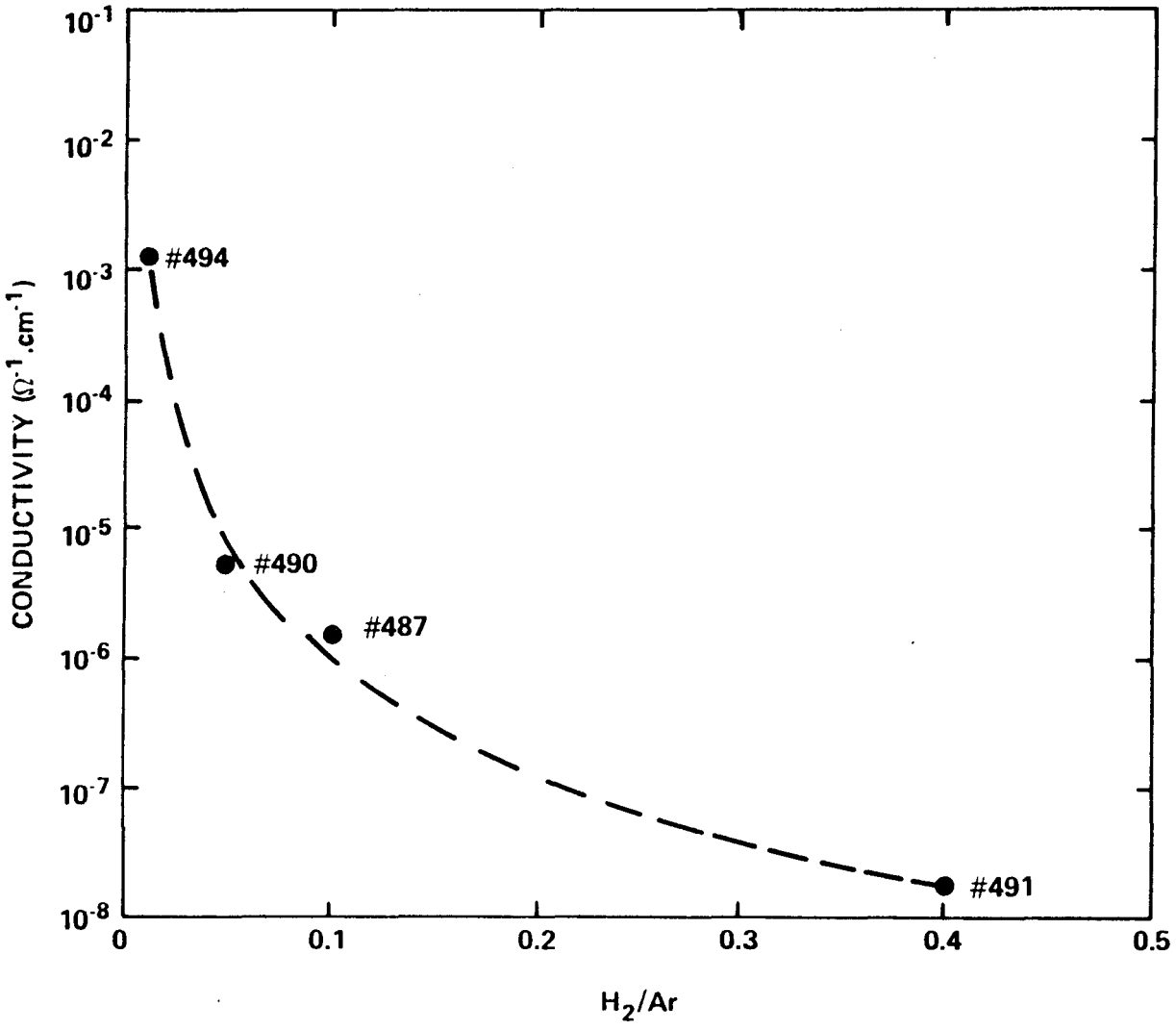
CONDUCTIVITY ($\Omega^{-1}.cm^{-1}$)
10^{-1}
10^{-2}
10^{-3}
10^{-4}
10^{-5}
10^{-6}
10^{-7}
10^{-8}
#494
#490
#487
#491
0
0.1
0.2
0.3
0.4
0.5
H_2/Ar

FIGURE 1

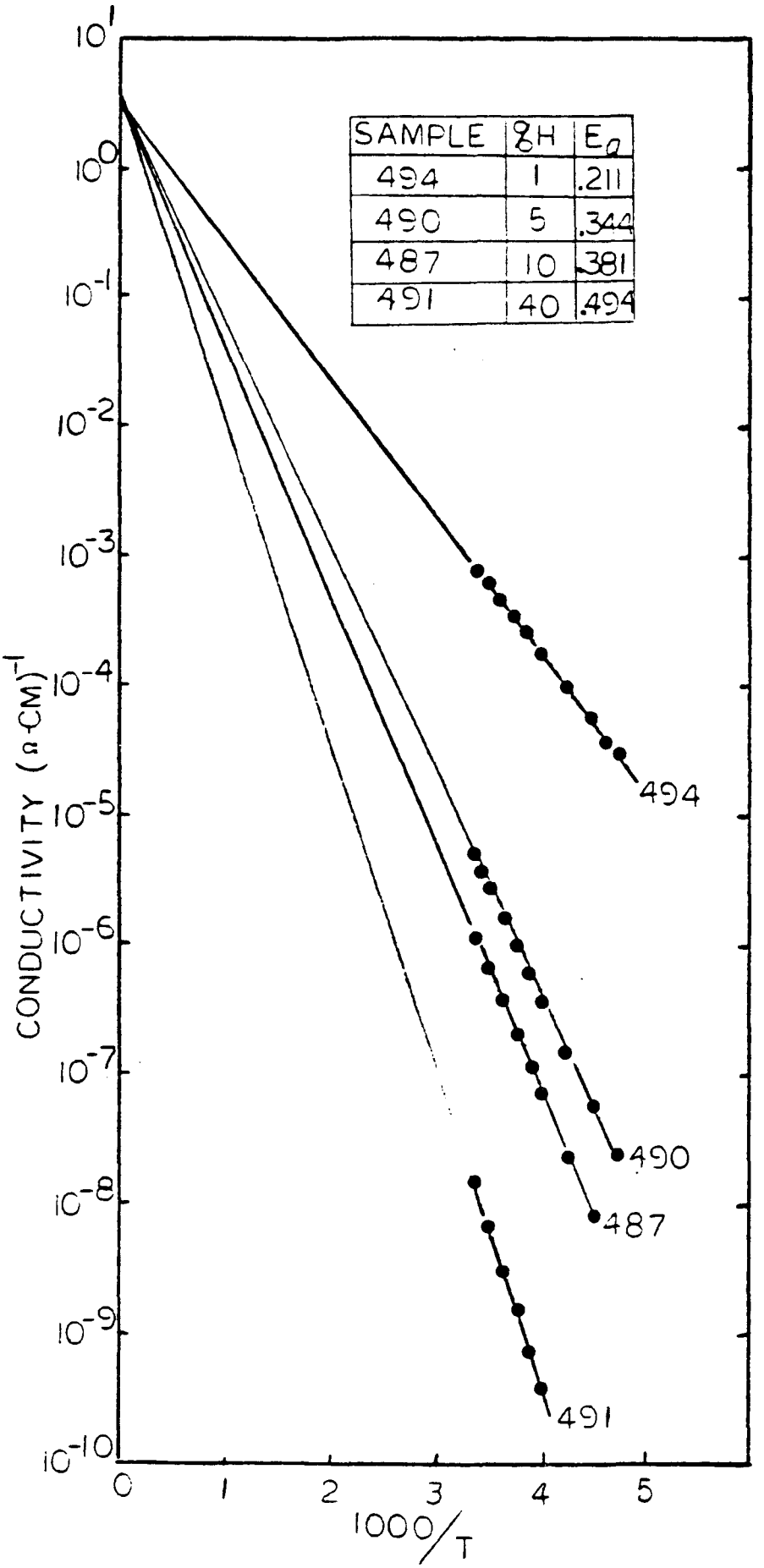
SAMPLE | %H | E_a
494 | 1 | .211
490 | 5 | .344
487 | 10 | .381
491 | 40 | .494
494
490
487
491
CONDUCTIVITY (Ω-CM)$^{-1}$
10^{1}
10^{0}
10^{-1}
10^{-2}
10^{-3}
10^{-4}
10^{-5}
10^{-6}
10^{-7}
10^{-8}
10^{-9}
10^{-10}
0
1
2
3
4
5
1000/T

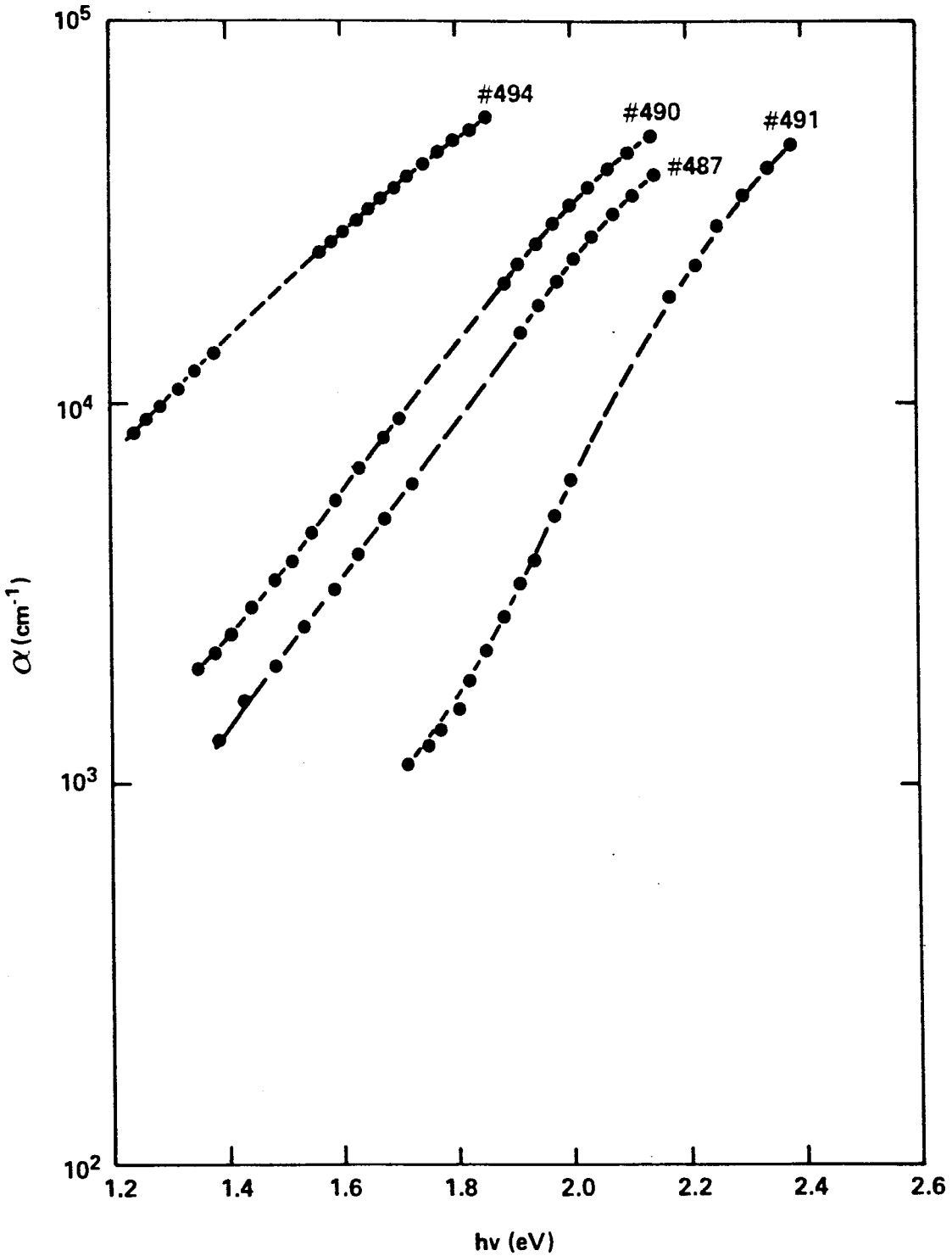
10^5
10^4
10^3
10^2
α (cm^{-1})
#494
#490
#487
#491
1.2
1.4
1.6
1.8
2.0
2.2
2.4
2.6
hv (eV)

FIGURE 3

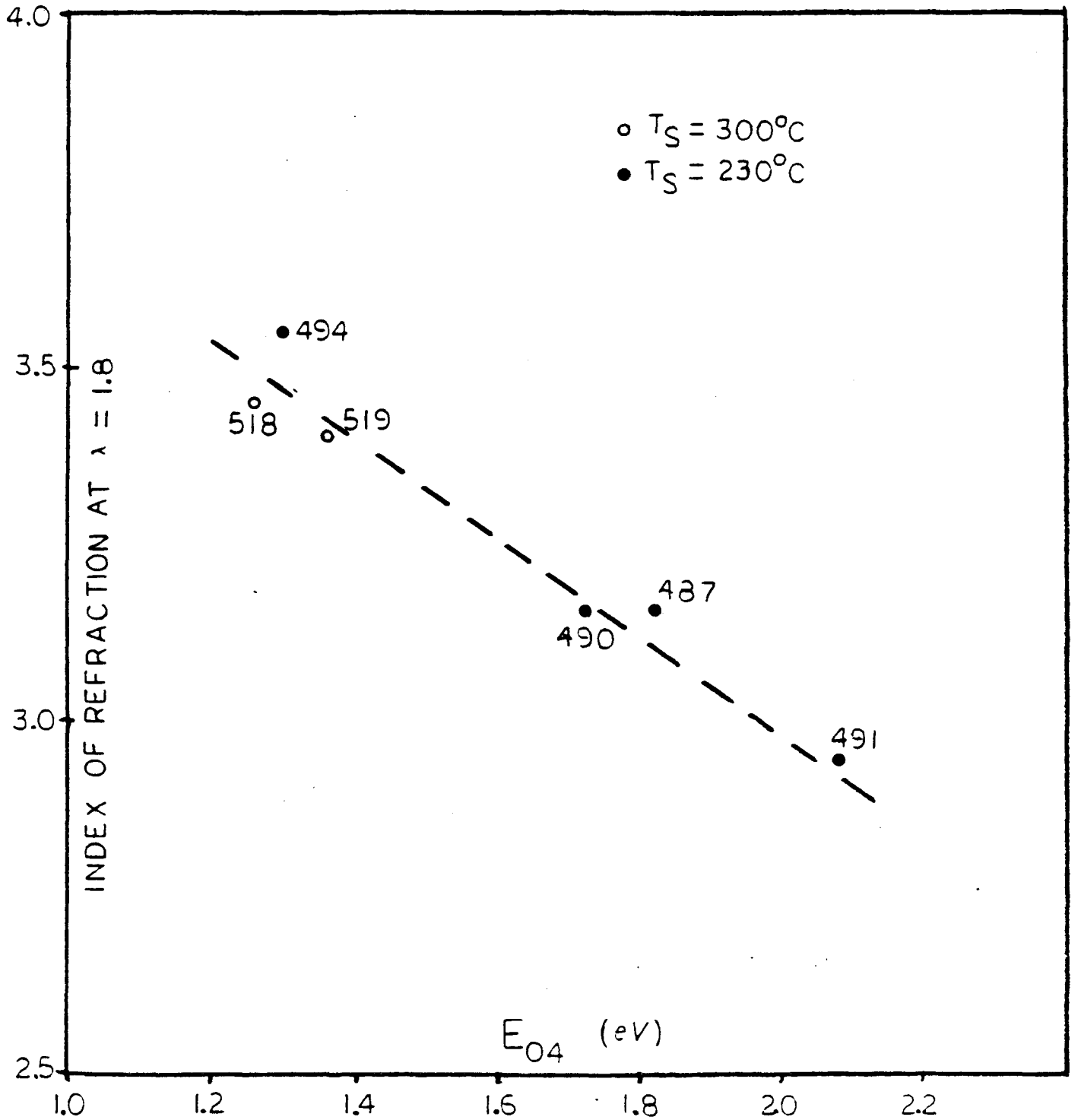
4.0
3.5
3.0
2.5
INDEX OF REFRACTION AT λ = 1.8
o T_S = 300°C
• T_S = 230°C
494
518
519
487
490
491
E_{04} (eV)
1.0
1.2
1.4
1.6
1.8
2.0
2.2

FIGURE 4

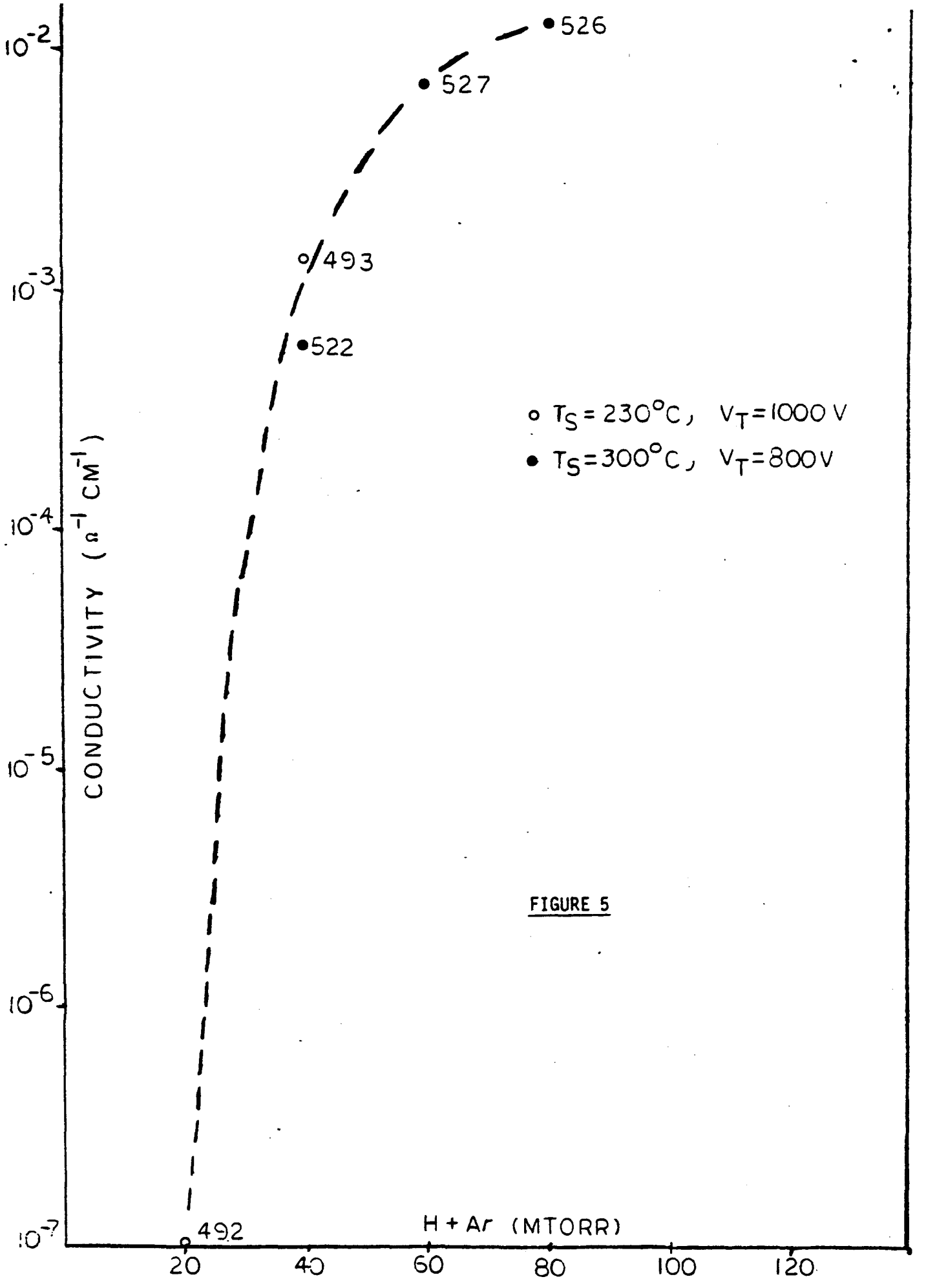
526
527
493
522
492
$T_S = 230°C$, $V_T = 1000$ V
$T_S = 300°C$, $V_T = 800$ V
CONDUCTIVITY (Ω^{-1} CM^{-1})
10^{-2}
10^{-3}
10^{-4}
10^{-5}
10^{-6}
10^{-7}
H + Ar (MTORR)
20
40
60
80
100
120

FIGURE 5

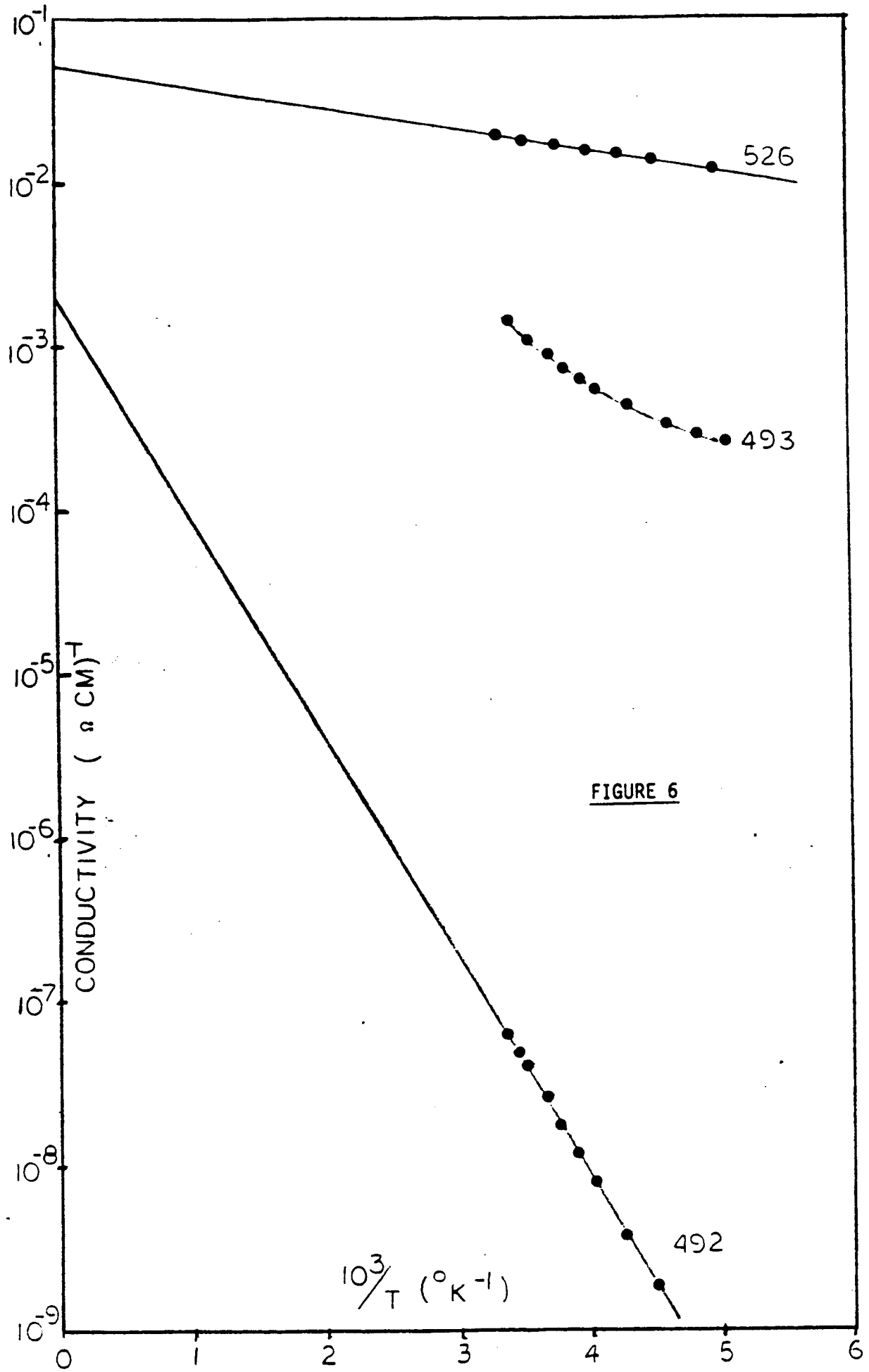
10^{-1}
10^{-2}
10^{-3}
10^{-4}
10^{-5}
10^{-6}
10^{-7}
10^{-8}
10^{-9}
CONDUCTIVITY (Ω CM)$^{-1}$
526
493
492
$10^3/T$ ($^\circ K^{-1}$)
0
1
2
3
4
5
6

FIGURE 6

FIGURE 7

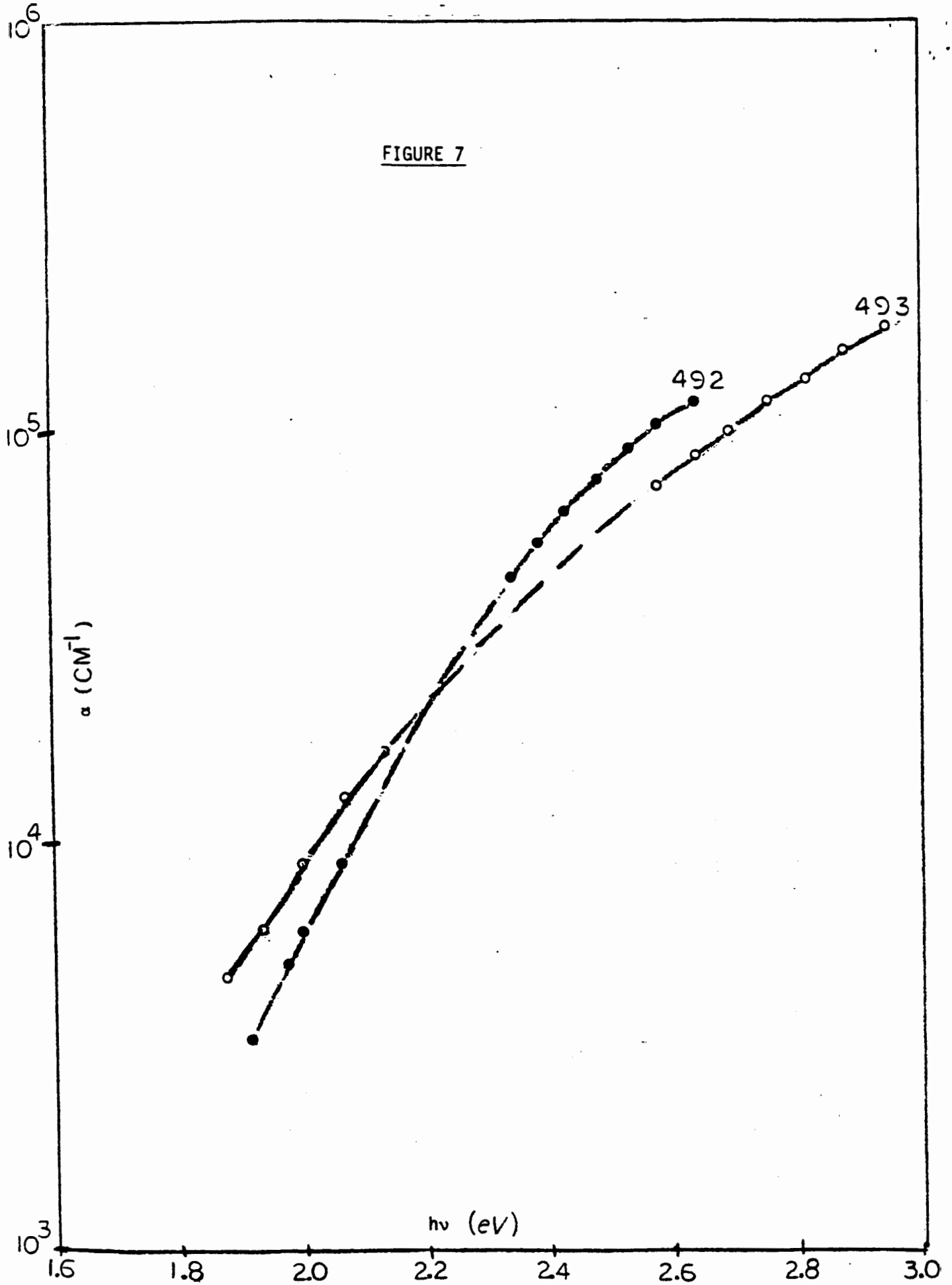

APPENDIX F. Properties of Phosphorus Doped Amorphous Silicon Films Deposited by Reactive Sputtering From Phosphorus Doped Silicon Targets

PROPERTIES OF PHOSPHORUS DOPED AMORPHOUS SILICON FILMS DEPOSITED BY REACTIVE SPUTTERING FROM PHOSPHORUS DOPED SILICON TARGET

T. D. Moustakas
Corporate Research Laboratories
Exxon Research and Engineering Company
P. O. Box 45
Linden, New Jersey 07036

ABSTRACT

Methods of depositing amorphous silicon films from phosphorus doped Si targets have been developed. The doping efficiency in these films decreases with the hydrogen content in the discharge.

The doping of amorphous silicon with phosphorus from the gas phase has been demonstrated in a number of laboratories. In this paper, we report for the first time the deposition of amorphous as well as microcrystalline phosphorus doped films by reactive sputtering in an $Ar+H_2$ atmosphere from a heavily phosphorus doped silicon target.

The phosphorus doped target was fabricated in single crystal form with 2.5×10^{19} phosphorus atoms/cm^3.

Films have been produced at 230°C by varying the H_2/Ar ratio in the discharge and maintaining all other deposition parameters the same.

We find that as the ratio H_2/Ar varies from 0 to 40% the transport and optical properties of the films vary dramatically. Figure 1 shows the room temperature conductivity for all the investigated samples. Preliminary temperature dependence data suggest that the decrease in the conductivity is associated with an increase in activation energy. Figure 2 shows the optical absorption constant vs photon energy for the same films. The optical gap increases monotonically with the hydrogen in the discharge.

The decrease of the doping efficiency with hydrogen content is under current study.

FIGURE 1

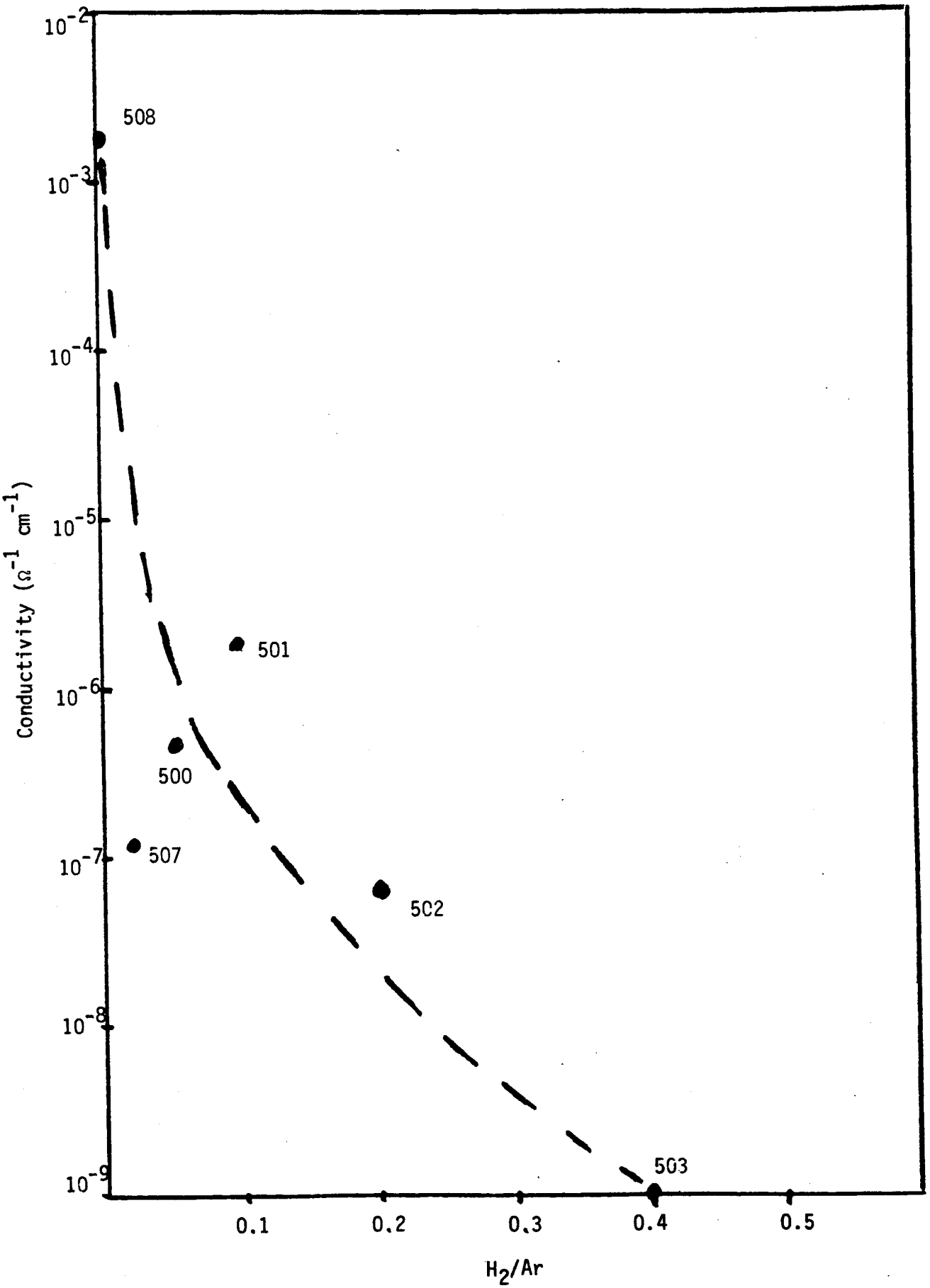
10^{-2}
10^{-3}
10^{-4}
10^{-5}
10^{-6}
10^{-7}
10^{-8}
10^{-9}
Conductivity (Ω^{-1} cm^{-1})
508
501
500
507
502
503
0.1
0.2
0.3
0.4
0.5
H_2/Ar

FIGURE 2

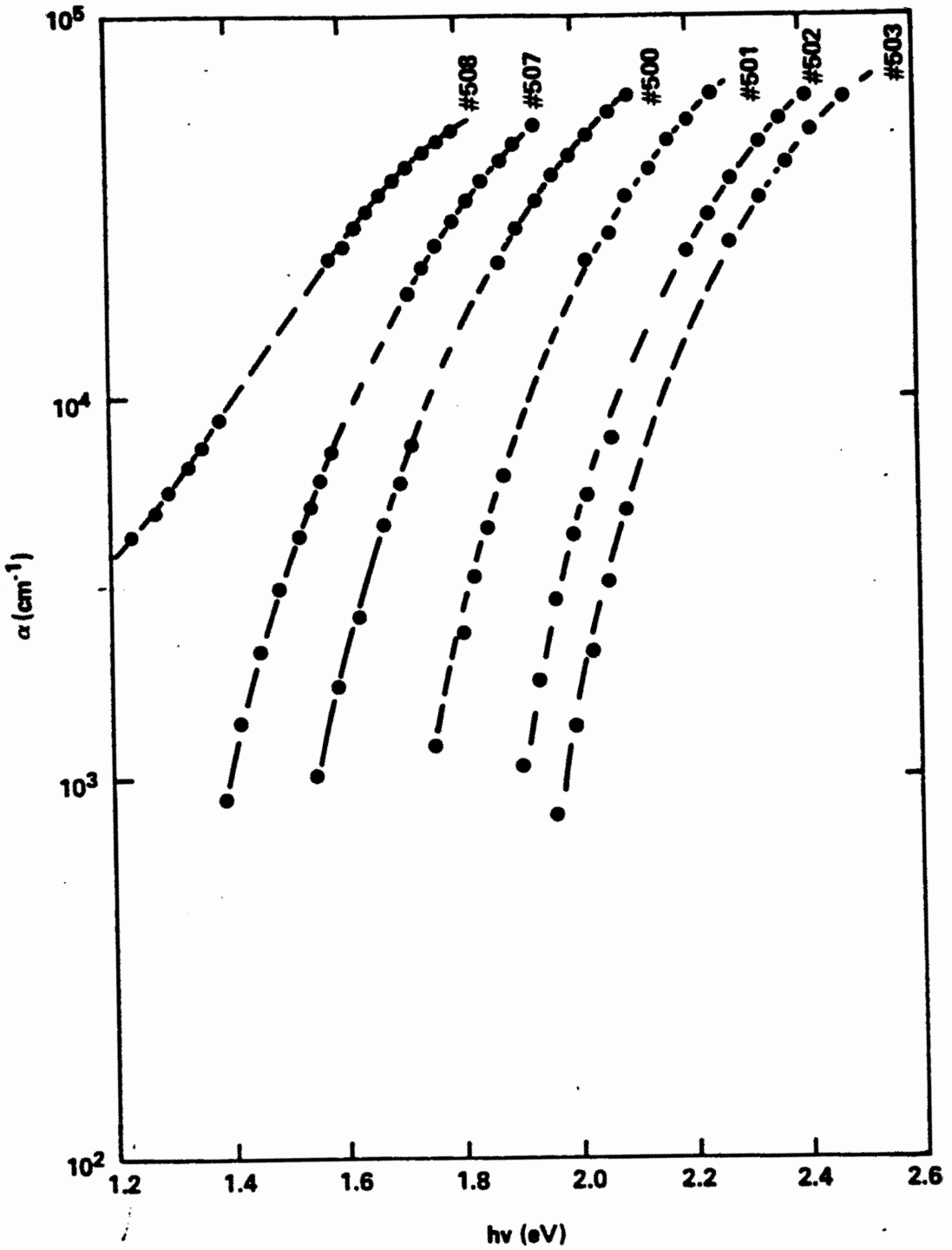
10^5
10^4
10^3
10^2
α (cm^{-1})
#508
#507
#500
#501
#502
#503
1.2
1.4
1.6
1.8
2.0
2.2
2.4
2.6
hv (eV)

APPENDIX G. Effect of Boron Compensation on the Photovoltaic Properties of Amorphous Silicon Solar Cells

Effect of boron compensation on the photovoltaic properties of amorphous silicon solar cells

J. D. Moustakas, H. P. Maruska, R. Friedman, and M. Hicks
Corporate Research Laboratory, Exxon Research and Engineering Company, Linden, New Jersey 07036

(Received 12 April 1983; accepted for publication 10 June 1983)

Intrinsic amorphous silicon films are normally slightly *n* type. As a result, in n^+-*i*-metal and n^+-*i*-p^+ solar cell structures the major potential barrier is at the *i*-*m* or *i*-p^+ interfaces. Low levels of boron compensation of the *i* layer move the Fermi level down to midgap. Further increases in boron render the *i* layer slightly *p* type, and move the major barrier to the *i*-n^+ interface. Therefore, it becomes possible to tailor the level of boron doping throughout the *i* layer so as to achieve high electric fields in all regions of the layer, and thus maximize the short circuit current.

PACS numbers: 84.60.Jt, 72.40. + w, 61.70.Tm

In a recent publication,[1] we described the effects of phosphorus contamination on the properties of sputtered amorphous silicon solar cells. Briefly, we determined that as the degree of phosphorus contamination in the *i* layer of the Schottky barrier structures (n^+-*i*-*m*) was reduced, the peak of the spectral response of the collection efficiency shifted towards the red. This red shift led to a pronounced increase in the short circuit current. The increase in the red response was held to be due to a decrease in the defect density in the *i* layer as phosphorus contamination was minimized. The consequent improved electronic structure of the *i* layer is responsible for a longer diffusion length and greater depletion width. On the other hand, the greater depletion width results in a decrease in the magnitude of the electric field at the *i*-*m* interface, and for this reason there was a slight concomitant decrease in the blue response, due to back diffusion of electrons to the metal.[2]

We also observed[1] that further improvement in the red response of the collection efficiency can be accomplished by compensating the phosphorus donors in the *i* layer through purposefully introducing low levels of boron during the growth of the *i* layer. The compensated sample that was discussed had 0.1 ppm of B_2H_6 added to the sputtering gas during the deposition of the *i* layer. The addition of boron tends to move the Fermi level, initially located at about 0.6 eV below the conduction-band edge, towards the center of the gap. We will now present data to show the effects of increasing the boron concentration beyond the value of total compensation.

The effect of boron incorporation in the *i* layer on the photovoltaic properties of amorphous silicon solar cells was investigated using Schottky barrier and n^+-*i*-p^+ structures. The device configurations employed were glass/SnO_2/n^+-*i*-Pt and glass/SnO_2/n^+-*i*-p^+/ITO. The substrates were Corning 7059 glass, coated with approximately 1-μm-thick SnO_2. The n^+ amorphous silicon, 250 Å thick, was produced by adding 0.2% PH_3 to the sputtering gas. The intrinsic amorphous silicon films were grown by rf sputtering from a polycrystalline target at a power density of 1 W/cm^2. The total pressure of the sputtering gas (argon + hydrogen) was 5 mTorr with the hydrogen concentration set at 20%. The substrate temperature was held at 325 °C. These layers were grown in the presence of variable amounts of B_2H_6 (between 0 and 1 ppm) and their thickness was varied between 0.5 to 1 μm. The sputtering system was cleaned between the n^+ and *i* depositions to reduce phosphorus contamination.[1] To complete the devices, a final film of either p^+-amorphous silicon (doped with 0.2% of B_2H_6 in the discharge) or else 50Å of Pt was deposited.

These devices were evaluated by studying both their *I*-*V* characteristics and their collection efficiency spectra, under illumination through either the top contact or the glass substrate. The *I*-*V* characteristics were measured using a calibrated xenon solar simulator. The collection efficiency was measured following the technique described by Wronski *et al.*[3] The short circuit current can be calculated by integrating the spectral response with the AM1 solar spectrum.[4] The transmission of the contact is determined by applying sufficient reverse bias to the cell so as to achieve 100% collection of carriers generated by photons actually absorbed in the *i* layer.

Figure 1 shows the spectral dependence of the collection efficiency for a number of n^+-*i*-Pt devices, which had been deposited at progressively higher amounts of B_2H_6 in the discharge during the formation of the *i* layer. The collection efficiency spectra were taken by illuminating the devices through the top Pt contact. Note that as the level of B_2H_6 in the discharge increased to more than 0.1 ppm, the quantum

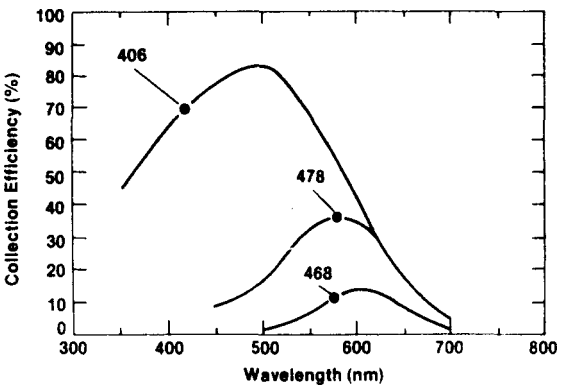

FIG. 1. Spectral dependence of the collection efficiency for a number of n^+-*i*-Pt devices, whose *i* layer was grown at progressively higher amounts of B_2H_6 in the discharge (sample 406 was grown with 0.02 ppm, sample 478 with 0.2 ppm, and sample 468 with 0.4 ppm of B_2H_6 in the discharge). These spectra were taken by illuminating the devices through the Pt contact.

 0003-6951/83/160368-03$01.00

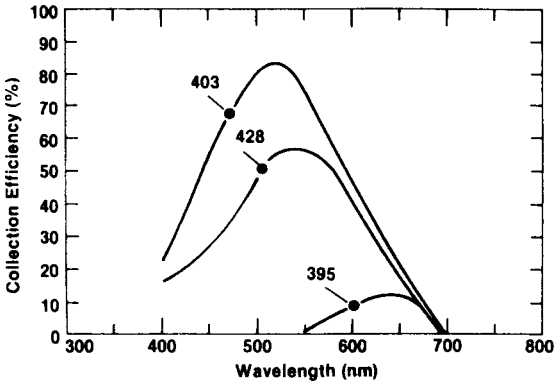

FIG. 2. Spectral dependence of the collection efficiency for a number of n^+-i-p^+ devices, whose i layer was grown at similar levels of B_2H_6 in the discharge as in samples of Fig. 1. These spectra were taken by illuminating the devices through the p^+ contact.

efficiency for blue-green light decreases significantly. These spectra were found to be independent of whether or not white bias illumination was present during the measurement. The internal short circuit currents calculated from these collection efficiency spectra are 11.8, 4.57, and 1.5 mA/cm^2 for the three devices. Exactly the same loss of blue-green response was found for n^+-i-p^+ devices, whose i layers were grown at progressively higher amounts of B_2H_6 in the discharge. Figure 2 shows the spectral dependence of the collection efficiency for three n^+-i-p^+ devices. These spectra were taken by illuminating the devices through the top p^+ contact.

In order to understand these changes, we further investigated the collection efficiency of the Schottky barrier device No. 468 by illuminating it through the glass substrate. The results are shown in Fig. 3. Note that the collection efficiency taken without dc white bias illumination shows good response in the red portion of the spectrum, but poor response in the blue portion of the spectrum. However, contrary to the findings in Fig. 1, when the dc white bias illumination is present, the blue response is restored. The short circuit current under bias illumination, calculated from this spectrum, was 6.8 mA/cm^2. The percent of light transmitted through the SnO_2 and n^+-amorphous silicon was found to be 65%, and thus the device is capable of generating an internal current of 10.5 mA/cm^2, which is considerably higher than

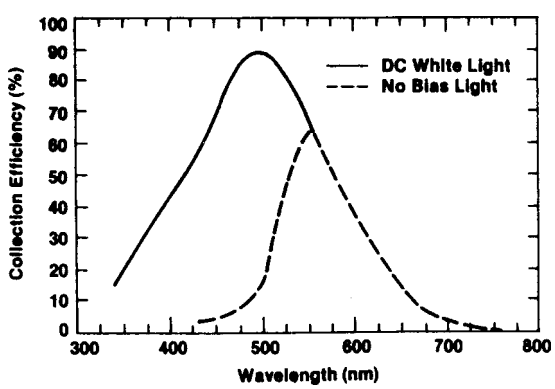

FIG. 3. Collection efficiency of one overcompensated sample (No. 468) taken under illumination from the glass substrate.

the current generated when the device was illuminated from the Pt side.

The I-V characteristic of device No. 468 show the same asymmetry, depending on whether it is illuminated from the Pt or the glass side. The results are shown in Fig. 4. Illumination from the glass side leads to considerably higher values of short circuit current and open circuit voltage than were found with illumination through the Pt contact. Not only that, but the value of $V_{oc} = 0.765$ V is remarkably higher than the V_{oc} value of a typical Schottky barrier device, which is about 0.55 V (Ref. 1). The short circuit current, measured with simulated AM1 sunlight (100 mW/cm^2) incident from the glass side, is slightly smaller ($J_{sc} = 4.9$ mA/cm^2) than that calculated from the collection efficiency measurements due to series resistance effects.

These results can now be accounted for in the following way. A small amount of boron (<0.1 ppm of B_2H_6 in the discharge) is needed to compensate residual donor states in the intrinsic amorphous silicon films, and thus to shift the Fermi level towards the middle of the gap. As the boron level increases (>0.1 ppm of B_2H_6 in the discharge) overcompensation occurs and the Fermi level moves below the middle of the gap, rendering the i layer slightly p type. Under such circumstances, the Pt (a high work function metal) or the heavily doped p^+ amorphous silicon will form only a small barrier with the slightly p-type i layer, while the major barrier will occur at the i-n^+ interface. In fact, this junction is essentially a p-n junction. We have therefore achieved the reverse of the conventional n^+-i-m (or n^+-i-p^+) structures, which have the i layer slightly n type and the major barrier at the i-m (or i-p^+) interfaces.

From such a model the results of Figs. 1–3 can be easily understood. Illumination through the front contact (Pt or p^+-type α-SiH$_x$), for the overcompensated samples, leads to poor blue-green spectral response because light of these wavelengths is absorbed in a region where there is only a very

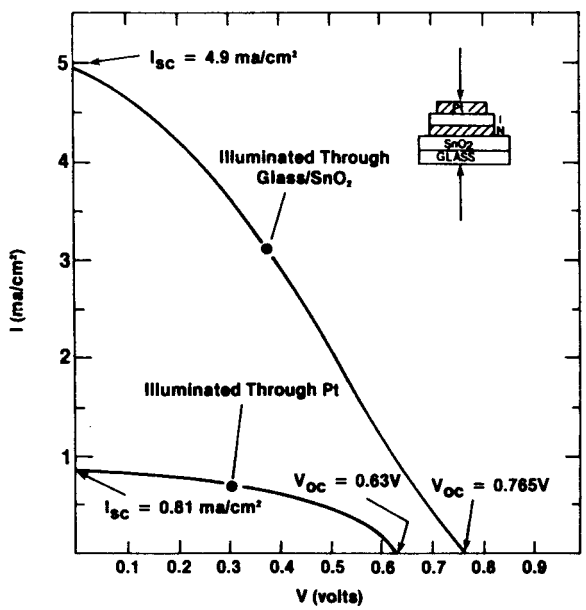

FIG. 4. I-V characteristics of one overcompensated sample (No. 468) taken under illumination with 100 mW/cm^2 of simulated light from the Pt or the glass side.

weak field. Illumination from the glass side, on the other hand, leads to a significantly increased spectral response in the blue as well as in the red spectral regions as long as dc white bias light is present during the collection efficiency measurement. In the absence of white bias illumination, the blue spectral response is very poor for the following reason: the thickness of the intrinsic layer is larger than the width of the space-charge region that is now present at the rear i-n^+ junction. Thus, the region of the i layer between the front contact and the end of the space-charge region contributes a series resistance to the cell, which impedes current flow. When the collection measurement involves the red portion of the spectrum, or else is performed in the presence of white bias illumination, red light can penetrate throughout the sample and reduce this series resistance, because amorphous silicon is a photoconductor. The results of Fig. 4 are also consistent with this interpretation. Illumination from the glass side leads to higher J_{sc}, since most of the light is then absorbed in the barrier region. (The poor FF has its origin in the poor Ohmic contact in the i-Pt interface.)

In conclusion, we have shown that by controlling the level of boron concentration in the i layer we can move the major barrier from the m-i (or p^+-i) to the n^+-i interface. Therefore, using this technique, it becomes possible to tailor the boron concentration throughout the i layer in order to achieve cells with high levels of electric field across the entire device, thereby attaining higher J_{sc}.

We thank B. Abeles, G. Cody, T. Tiedje, and C. Wronski for helpful suggestions. This work was sponsored in part by the Solar Energy Research Institute under contract No. XZ-0-9219.

[1]T. D. Moustakas, R. Friedman, and B. R. Weinberger, Appl. Phys. Lett. **40**, 587 (1982).
[2]Dina Gutkowicz-Krusin, J. Appl. Phys. **52**, 5370 (1981).
[3]C. R. Wronski, B. Abeles, and G. D. Cody, Solar Cells **2**, 245 (1980).
[4]R. Bird, "Terrestrial Solar Spectral Standards and Data Sets," SERI/TR-642-1149, 1981.

APPENDIX H. Effect of Power and Hydrogen in the Discharge on the Photovoltaic Properties of Sputtered Amorphous Silicon

Effects of power and hydrogen in the discharge on the photovoltaic properties of sputtered amorphous silicon

T. D. Moustakas and H. P. Maruska
Corporate Research Laboratory, Exxon Research and Engineering Company, Annandale, New Jersey 08801

(Received 1 August 1983; accepted for publication 15 September 1983)

The photovoltaic properties of amorphous silicon films produced by reactive sputtering have been investigated as a function of power level and hydrogen concentration in the discharge. We find that raising the power in the discharge leads to films with better bulk properties but poorer surface properties. Increasing the hydrogen concentration in the discharge affects the photovoltaic properties of the films by increasing the optical gap of the film and simultaneously decreasing the density of states in the middle of the gap. Because of this dual role of hydrogen, films with optical gaps of 1.7–1.85 eV are capable of generating the same magnitude of short circuit current in sunlight. However, the large gap material is capable of providing a higher open circuit voltage and therefore results in solar cells with better overall performance.

PACS numbers: 81.15.Cd, 72.40 + w, 73.60.Fw, 61.40.Df

The electronic properties of hydrogenated amorphous silicon depend sensitively on film inhomogeneities due to the microstructure of the silicon network, and on defect and network modification due to hydrogen incorporation. It is known, for example, that films with columnar morphology have poor electronic properties[1,2] and that hydrogen incorporation can affect both the density of states in the middle of the gap[3,4] as well as the optical properties of the films.[5] Therefore, identification of the deposition parameters which affect the film's microstructure and hydrogen incorporation is very important in the quest of improving the quality of the material for electronic applications. In the case of glow discharge decomposition of silane, Knights and Lujan[1] have reported that low power in the discharge leads to films with an indistinguishable columnar morphology that have the best electronic properties. Control of the hydrogen incorporation in this method of film deposition can only be accomplished either through the variation of the power in the discharge or the deposition temperature. However, since both of these parameters have a significant effect on the silicon network, the effect of hydrogen on the electronic properties of these films has not been fully established.

In this letter we examine how power in the discharge and pressure of hydrogen can separately affect the electronic properties of reactively sputtered amorphous silicon films. In this method of film deposition these two parameters can be controlled independently, and it is expected that the power in the discharge would affect the microstructure of the silicon network while the pressure of hydrogen would affect the defect structure and the optical properties.

To investigate these effects we deposited two series of films by rf sputtering from a polycrystalline Si target at deposition temperature $T_s = 325$ °C. In the one series of films the target bias voltage was maintained at -800 V and in the other at -1000 V. In both series the total pressure of the sputtering gas (argon + hydrogen) was 5 mTorr and the hydrogen content in the discharge was varied from 10% to 20%. The substrates in each run consisted of a stainless steel plate, precoated with approximately 400 Å of N^+ amorphous silicon, and a quartz plate. The layer of the N^+ amorphous silicon was deposited in a different run by mixing 0.2% of PH_3 in the sputtering gas. The predeposition of the N^+ layer was found to be necessary, since phosphorus contamination of the intrinsic layer was found to affect the quality of the intrinsic films.[6] After the deposition of the intrinsic films, Schottky barrier devices, having the configuration *SS* / N^+-*I*-Pt, were formed by sputtering 8.5 mm^2 Pt dots on the top of the intrinsic layers. The sample identification, the thickness of the intrinsic layer, and the values of the target voltage and ratios of H/Ar in the discharge are given in Table I.

These films were characterized by studying their optical absorption constant, and the *I-V* characteristics and collection efficiencies of the Schottky barrier devices. The optical absorption coefficient was calculated by an interactive procedure[7] from optical transmission measurements made in a Carey 17 spectrophotometer. The *I-V* characteristics were measured using a calibrated xenon solar simulator. The collection efficiency was measured following the technique described by Wronski *et al.*[8] The short circuit current was calculated by integrating the spectral response with the AM1 solar spectrum.[9] The transmission of the Pt contact was determined by applying sufficient reverse bias to the cell so as to achieve 100% collection of carriers generated by photons actually absorbed in *I* layer.

TABLE I. Film deposition parameters and photovoltaic constants of the investigated Schottky barrier structures.

Sample	Thickness (μm)	V_T (V)	H/Ar	J_{sc} (int)	V_{oc}	FF
470	0.55	800	0.10	9.5	0.49	0.54
461	0.54	800	0.125	9.8	0.51	0.57
462	0.54	800	0.15	9.7	0.53	0.57
465	0.54	800	0.20	9.4	0.54	0.58
436	0.50	1000	0.10	10.8	0.49	0.48
456	0.72	1000	0.125	11.0	0.51	0.49
435	0.48	1000	0.15	11.0	0.53	0.52
437	0.52	1000	0.20	10.9	0.56	0.51

 0003-6951/83/231037-03$01.00

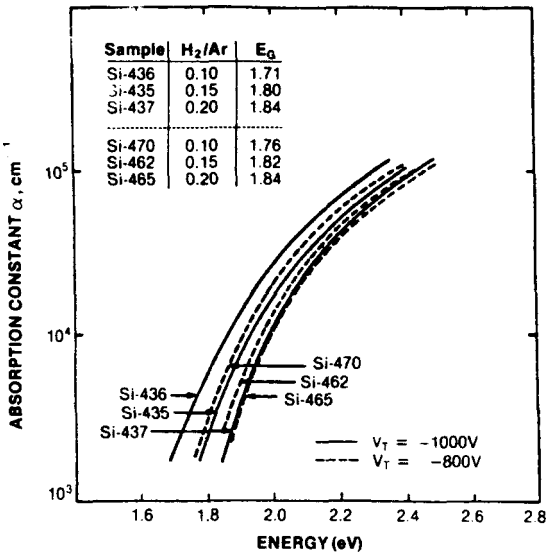

FIG. 1. Optical absorption constant vs photon energy for two series of films produced under target voltages of − 1000 and − 800 V.

Figure 1 shows the optical absorption constant versus photon energy for three samples from each series. The sample identification, the H/Ar ratios in the discharge, and the optical gap[10] of each film are given in the insert of the figure. The optical gaps in the one series vary from 1.71 to 1.84 eV and in the other from 1.76 to 1.84 eV. The optical absorption constants of samples 456 and 461 have been omitted for clarity. The optical gaps of these films are 1.78 and 1.80 eV, respectively.

Figure 2 shows the spectral dependence of the collection efficiency for the two series of films. Note that these spectra fall into two distinct groups, which correlate with the target voltage but not with the hydrogen content in the discharge. For the − 800 V samples the collection efficiency peaks at 450 nm, while for the − 1000 V samples it peaks at 500 nm. Table I shows the internal short circuit current of each device, as well as the V_{oc} and FF as measured under illumination of 100 mW/cm^2 from a xenon solar simulator. Note that while the J_{sc} is smaller for the − 800 V samples, the fill factors are in all cases larger for these films than for the − 1000 V samples. The V_{oc} in both series of films increases systematically with the hydrogen in the discharge.

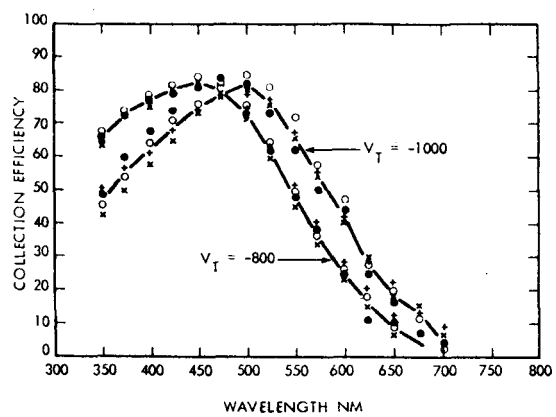

FIG. 2. Spectral dependence of the collection efficiency of two series of *N-I*-Pt Schottky barrier devices made at the indicated target voltages.

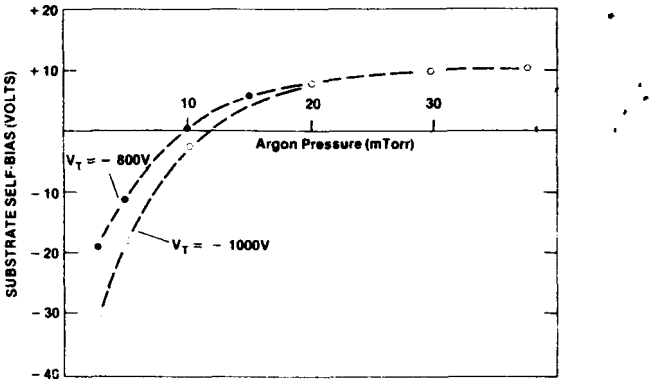

FIG. 3. Substrate potential, measured with respect to the ground, vs the argon pressure for target voltages − 800 and − 1000 V.

These results can now be accounted for in the following way. The shift of the peak of the collection efficiency towards the red, as the power in the discharge increases, suggests that the electronic quality of the films improves with the power in the discharge. This is contrary to the finding by Knights and Lujan,[1] who determined that the quality of the glow discharge amorphous silicon films improved with decreasing power in the discharge. The improvement of the sputtered material with the power in the discharge is believed to have originated in more perfect coalescence of the island structure due to mild bombardment by charged particles.[2] Indication of this is provided in Fig. 3. Here, we show the substrate potential, measured with respect to the ground,versus the argon pressure, for target voltages − 800 and − 1000 V. These data suggest[2] that films produced at low argon pressures and high target voltages are subjected to more charged particle bombardment. The fact that the power in the discharge has an opposite effect for films grown by glow discharge decompositions of silane and by reactive sputtering signifies that the film growth process in these two methods of film deposition is different. Sputtering is a physical vapor deposition technique and the critical parameter in the network formation is the ratio of the substrate temperature to the melting point of the evaporant (T_s / T_m.) If this ratio is less than 0.45 the growth mode is columnar.[11,12] Charged particle bombardment is equivalent to an increase in substrate temperature. The adverse effect of power in the discharge on the FF is associated with recombination at the interface. Bombardment by charged particles, such as electrons or Ar^+ ions, in addition to facilitating the coalescence of the island structure may also create point defects. Such point defects may be healed during the growth of the bulk of the film due to the presence of atomic hydrogen. However, similar defects at the interfaces may not be easily healed after the termination of the discharge. According to such a model the interfaces of films grown at higher power should have more recombination centers. In another paper we show how such a model can account for the differences in the FF of the two series of films.[13]

The insensitivity of the collection efficiency to hydrogen in the discharge can be qualitatively understood as follows: we have shown in previous publications[3,4] that the density of states in the middle of the gap, the collection width,

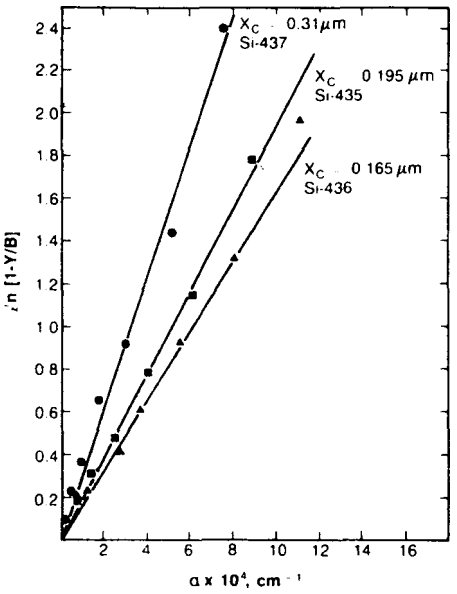

FIG. 4. Plot of $-\ln(1 - Y/B)$ vs α for three samples deposited at target voltage of -1000 V. The indicated values of X_c were obtained from the slopes of the straight line fits.

and the diffusion length of the minority carriers improves with increases in the concentration of hydrogen in the discharge. The insensitivity of the collection efficiency to hydrogen concentration suggests that the improvements in the electronic properties are counterbalanced by the optical losses due to the increases of the optical gap (from 1.71 to 1.84 eV). To illustrate this point we modeled the collection efficiency of the samples produced at target voltage of 1000 V according to the relation[8]

$$Y = B\,[1 - \exp(-\alpha X_c)], \tag{1}$$

where Y is the internal yield and X_c is the collection width. Figure 4 show that the collection width increases with the hydrogen content from 0.165 to 0.31 μm. Thus, the larger gap material has a wider space-charge region and the optical losses are counterbalanced by the better collection characteristics of these films. In addition since the open circuit voltage increases with the optical gap of the material, there is a advantage of using the larger gap material for photovolta applications since it will produce the same current and higher open circuit voltage.

In conclusion, we have investigated the effects of pow and hydrogen content in the discharge on the photovolta properties of sputtered amorphous silicon. The results su gest that raising the power in the discharge leads to film with better bulk properties but poorer surface propertie Films, whose optical gap varies through hydrogen incorpo ation from 1.71 to 1.84 eV, are capable of generating th same J_{sc}. However, the large gap material is capable of pr viding a higher open circuit voltage and results in solar cel with better overall performance.

We thank B. Abeles, G. Cody, T. Tiedje, and C Wronski for helpful suggestions. The technical assistance o R. Friedman and M. Hicks is gratefully acknowledged. Th work was sponsored in part by the Solar Energy Researc Institute under contract No. ZB-3-02166-01.

[1]J. C. Knights and R. A. Lujan, Appl. Phys. Lett. **35**, 244 (1979).
[2]T. D. Moustakas, Solar Energy Mater. **8**, 187 (1982).
[3]T. Tiedje, T. D. Moustakas, and J. M. Cebulka, Phys. Rev. **B23**, 56 (1981).
[4]T. D. Moustakas, C. R. Wronski, and T. Tiedje, Appl. Phys. Lett. **39**, 72 (1981).
[5]Eva C. Freeman and W. Paul, Phys. Rev. B **20**, 716 (1979).
[6]T. D. Moustakas, R. Friedman, and B. R. Weinberger, Appl. Phys. Let **40**, 587 (1982).
[7]J. P. deNeufville, T. D. Moustakas, A. F. Ruppert, and W. A. Lanford, Non Cryst. Solids **35–36**, 481 (1980).
[8]C. R. Wronski, B. Abeles, and G. D. Cody, Solar Cells **2**, 245 (1980).
[9]R. Bird, "Terrestrial Solar Spectral Standards and Data Sets," SERI/TF 642-1149 (1981).
[10]The optical gap is defined by the relation $(\alpha h\nu)^{1/2} = C(h\nu - E_g)$.
[11]J. A. Thornton, J. Vac. Sci. Technol. **11**, 666 (1974).
[12]T. D. Moustakas, *Semiconductors and Semimetals* (Academic, Ne York, 1983), Vol 21A.
[13]H. P. Maruska and T. D. Moustakas, IEEE Trans. Electron Devices (to b published).

APPENDIX I. Correlation Between Deposition Parameters and Performance of Sputtered Amorphous Silicon Solar Cells

A Reprint from the

PROCEEDINGS

Of SPIE-The International Society for Optical Engineering

Volume 407

Photovoltaics for Solar Energy Applications II

April 5-6, 1983
Arlington, Virginia

Correlation between deposition parameters and performance of sputtered amorphous silicon solar cells

T. D. Moustakas
Corporate Research Laboratory, Exxon Research and Engineering Company
Linden, New Jersey 07036

Correlation between deposition parameters and performance of sputtered amorphous silicon solar cells

T. D. Moustakas

Corporate Research Laboratory, Exxon Research and Engineering Company
Linden, New Jersey 07036

Abstract

This paper describes correlations between deposition parameters and photovoltaic properties of intrinsic amorphous silicon films produced by RF sputtering. We present data showing strong dependence between photovoltaic properties and structural and compositional inhomogeneity of the films. Studies on films produced at different hydrogen concentrations show that the ones with larger optical gaps have better photovoltaic potential. Small concentration of dopant impurities in the intrinsic films has significant effect on their photovoltaic properties. These optimization studies lead to intrinsic material, which when incorporated in a P-I-N solar cell generates external currents up to 13 mA/cm^2 and open circuit voltages of between 0.85 to 0.95 volts.

Introduction

Of the two plasma methods of depositing hydrogenated amorphous silicon (glow discharge decomposition of silane, and sputtering from a silicon target in an Ar+H_2 plasma), the former has attracted considerably more attention. The extensive investigation of this material through structural, optical transport and recombination studies has led to the fabrication of solar cell structures with efficiencies up to 10%.[1]

The alternative technology of sputtering from a silicon target in an Ar+H_2 plasma, inherently has many advantages as a deposition process. Principal among these is the ability to uncouple the two source materials, Si and H, and to independently optimize the role that each plays in forming the network and in determining the ensuing electro-optical properties. This type of control is not possible for glow discharge decomposition of silane in that the source materials are initially chemically bonded in the feed gas, SH_4. In addition, sputtered films, in general, are mechanically strong and adhere very well on a variety of substrates, a necessary requirement for photovoltaic applications. Besides these considerations, sputtering is a widely practiced fabrication technique for a number of large area thin film applications. Despite these advantages, this technology has attracted much less attention for amorphous silicon deposition, primarily because early work suggested that sputtered α-SiH_x films are inferior to those produced by the glow discharge technique.[2,3] In addition there is a widespread belief that sputtering is an unsuitable technology for surface sensitive devices.[4]

In this paper we review progress made in our laboratory over the past few years in exploring the photovoltaic potential of sputtered intrinsic hydrogenated amorphous silicon. The effects of doped layers on the solar cell performance will be reported in other papers.[5,6] We first explore the correlation between structural and compositional inhomogeneities and photovoltaic properties of the films, by studying a number of deposition parameters which affect the silicon network. Then we investigate the effect of hydrogen incorporation on the optical and electronic properties of the films, and their combined effect on the photovoltaic properties. The effects of small concentrations of dopant impurities, such as phosphorus and boron, on the photovoltaic properties of the intrinsic films are also addressed. Finally, we show that these optimization studies lead to intrinsic material, which when incorporated in P-I-N solar cell structures, generate external currents up to 13 mA/cm^2 and open circuit voltages of between 0.85 to 0.95 volts.

Deposition system and experimental methods

The deposition system used in this study has been described in more detail in another paper.[7] Here we briefly review only the most important features and emphasize primarily the methods of device fabrication. The deposition system has stainless steel walls, held at ground potential, and electrically insulated cathode and anode assemblies. The water cooled target is a polycrystalline silicon disk, 5" in diameter and 1/4" thick and is supplied with an RF power at a frequency of 13.56 MHz. The anode assembly was held 5 cm below the target and can be either grounded, floated or supplied with RF or DC electrical bias. The system was evaluated by a combination of turbomolecular and mechanical pumps, to a total leak rate of approximately 1-2x10^{-5} Torrls^{-1}.

Primarily we used Schottky Barrier structures for the purpose of studying the photovoltaic potential of the intrinsic films. The device configurations employed were I-Pt (or Pd) and the substrate was stainless steel or Corning 7059 glass coated with approximately 1μm thick SnO_2. The N amorphous silicon, 250 Å thick, was produced by adding 0.2% PH_3 to the sputtering gas. The intrinsic film was produced by varying a number of deposition parameters. Such parameters include, argon and hydrogen partial pressures, target and substrate bias voltage and variable amounts of PH_3 or B_2H_6. The sputtering system was cleaned between N and I depositions to reduce phosphorus contamination.[8] To complete the devices, a final film of 50 Å of Pt or 100 Å or Pd was deposited on the top of the intrinsic film.

These devices were evaluated by studying both their I-V characteristics and the collection efficiency spectra, under illumination through either the top contact or the glass substrate. The I-V characteristics were measured using a calibrated Xenon Solar Simulator. The collection efficiency was measured following the technique described by Wronski et al.[9] The short circuit current can be calculated by integrating the spectral response with the AM1 solar spectrum.[10] The transmission of the contact is determined by applying sufficient reverse bias to the cell so as to achieve 100% collection of carriers generated by photons actually absorbed in the I-layer.

Relation between photovoltaic properties and structural inhomogeneities of the films

Amorphous silicon films are known to grow with different types of structural inhomogeneities. For example, the structural studies of Knights and Lujan[11] and Ross and Messier[12] led to the the discovery that plasma deposition of α-SiH_x films proceeds via nucleation and growth of island structures (average lateral dimensions ≈100 Å). The coalescence of these islands, if imperfect, leads to columnar morphology in subsequent growth. Another type of structural inhomogeneity are microvoids of about 10 Å in diameter, which have been observed in small angle scattering experiments.[13]

Structural inhomogeneities in amorphous silicon films may be controlled in different ways, depending on the method of deposition. Knights and co-workers[11] report that growth of glow discharge films in pure silane, at low deposition rates, at large substrate negative bias, and deposition temperature between 200 and 300°C leads to much more perfect coalescence of the islands. Bagley and co-workers[14] report that LPCVD films, grown at temperatures of about 600°C, have the highest density and thus are more homogeneous. In the case of sputtered films, it has been shown[7,12] that there is strong correlation between structural and compositional inhomogeneities of the films and charged particle bombardment during the growth of the film.

The present author[7] proposed that the microstructural changes of the sputtered films, induced by the charged particle bombardment, can be accounted for in the following way. The coalescence of the island structure is correlated with secondary electron bombardment which enhances adatom surface mobility through local heating. On the other hand, energetic argon ion bombardment may introduce inhomogeneities through resputtering. This is because the growth habit of these films is columnar and therefore resputtering by Ar^+ ions is likely to be anisotropic, with higher sputtering yields at the low density intercolumnar regions. Incomplete regrowth of these regions could lead to microvoid formations.

Structural inhomogeneities may affect the photovoltaic properties of the films in a variety of ways. An example of this is the introduction of defects which control recombination, and another is the introduction of additional disorder which affects the extent of the band tails thereby affecting carrier transport and optical properties. In this section we explore such correlations by studying the photovoltaic properties of sputtered films, grown under deposition conditions which affect film inhomogeneity through charged particle bombardments. Such deposition parameters are, for example, the pressure of the sputtering gas and the target voltage.

Effect of pressure of the sputtering gas

Structural studies[12] of amorphous silicon sputtered films, produced with the pressure of argon as the variable, showed no evidence of columnar morphology at low argon pressure and strong evidence of columnar morphology at high argon pressure. The transition from the one regime to the other, depends on the apparatus geometry, cathode-anode distance and power in the discharge. These microstructural changes have been correlated with charged particle bombardment effects.[7,12]

To investigate whether correlation exists between these microstructural changes and the photovoltaic properties of the films, we studied a number of films deposited at fixed

hydrogen partial pressure (P_H=0.7 mTorr) and argon partial pressure varying between 5 to 30 mTorr. All films were deposited at 275°C and at constant forward power of 200 watts. The choice of this mode of operation resulted in a small but monotonic increase of the deposition rate from 2.1 to 2.6 Å/sec, because the ion current increases as the argon pressure increases. As a result of that, the hydrogen content in the films was found to decrease with the argon pressure from 21.5 to 19.5 at. %. Correspondingly, the optical gap of the films were found to decrease from 1.84 eV to 1.78 eV. Structural studies of these films indicate that the transition between the non-columnar to columnar regimes occurs between 15 to 20 mTorr of argon.

The photovoltaic properties of these films correlate remarkably with the observed microstructural changes. Figure 1 shows the secondary photoconductivity of the films, measured under AM1 illumination. Note that the photoconductivity is reduced rather abruptly for argon pressures higher than 15 mTorr. Figure 2 shows the I-V characteristics of N-I-Pd Schottky barrier structures. The I-layer in these devices was deposited at 5, 10, 20 and 30 mTorr of argon. Note that the films produced at argon pressures of 20 and 30 mTorr have poorer photovoltaic properties than those produced at 5 and 10 mTorr of argon. Therefore, films grown under some charged particle bombardment have less structural inhomogeneity and the best photovoltaic properties.

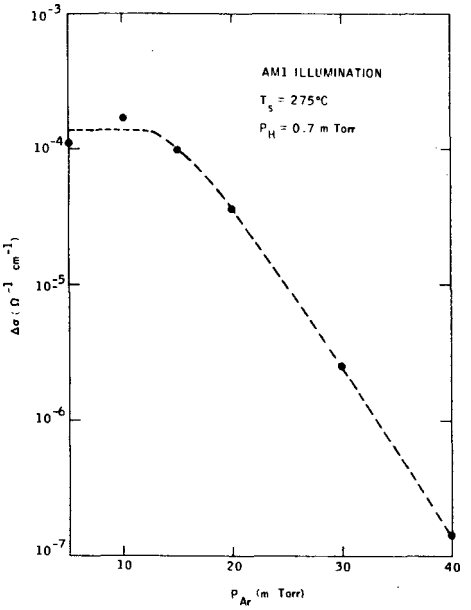

Figure 1. Photoconductivity, measured under AM1 illumination, vs. the argon pressure in the discharge.

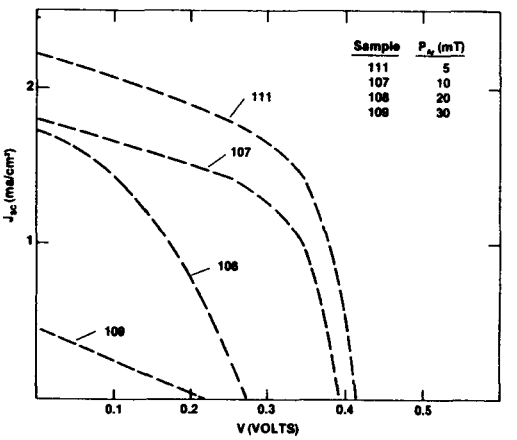

Figure 2. I-V characteristics of a number of N-I-Pd Schottky barrier structures, whose I-layer was produced at different argon pressure

Effect of target voltage

The target voltage is also expected to affect film homogeneity through charged particle bombardment. Both the substrate floating potential (measured with respect to the ground) and the plasma potential are influenced by the target voltage. In addition, in RF discharge the relation between target potential and plasma potential may also be influenced by the geometry of the system.[15]

To investigate the effect of target voltage on the photovoltaic properties, we deposited two series of films with the target voltage as the variable. In one series the induced target DC bias voltage was maintained at -800 Volts, and in the other at -1000 volts. All samples were deposited at fixed temperature (325°C) and total sputtering gas pressure (argon + hydrogen = 5mTorr). In each series the flow rates of H_2/Ar were varied from 10 to 20%. The Schottky barrier devices employed had the configuration N-I-Pt.

Figure 3 shows the spectral dependence of the collection efficiency of the two series of films. Note that these spectra fall into two distinct groups. For the -800 volts samples, the collection efficiency peaks at 450 nm, while for the -1000 volts samples it peaks at 500 nm. This red shift leads to an increase in the internal short circuit from

9.5 mA/cm^2 to 11 mA/cm^2. Greater details of the effect of target voltage on the photovoltaic properties have been reported in another paper.[16]

The fact that the collection efficiency of the devices produced at each target voltage is independent of hydrogen content is significant, and suggests that the observed effect is unrelated to the changes of the opto-electronic properties of the films due to the hydrogen incorporation. These changes are going to be discussed in more detail later. Therefore, the shift of the peak of the collection efficiency towards the red part of the spectrum, as the target voltage (power in the discharge) increases, suggests that the electronic equality of the films improves with the power in the discharge. This is contrary to the findings by Knights and Lujan that the quality of the glow discharge amorphous silicon films improves with decreasing power in the discharge. This discrepancy signifies that the film growth process in these two methods of film deposition is different. We attribute the improvement in the quality of the sputtered material, as the target voltage increases, to improvements in film homogeneity due to additional bombardment by charged particles. Indication of this is provided in Figure 4. Here we show the substrate potential, measured with respect to the ground, vs. the argon pressure for target voltages -800 and -1000 volts. These data suggest that films produced at higher target voltages are subjected to more charged particle bombardment.

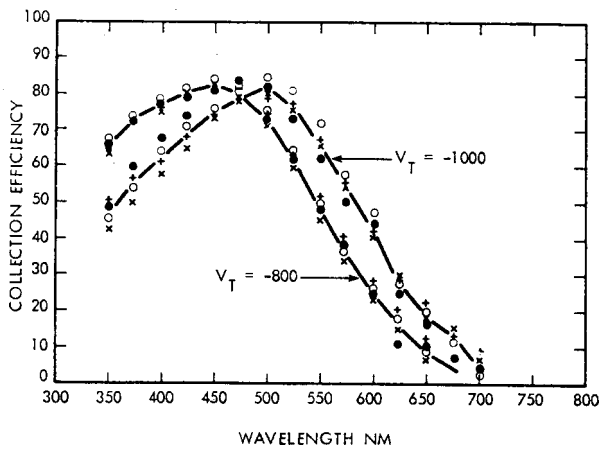

Figure 3. Collection efficiency of two series of N-I-Pt devices, whose I-layer was deposited at voltages of -800 and -1000 volts. In each series, the ratio of the flow rates of hydrogen to argon were respectively 10, 12, 15 and 20%.

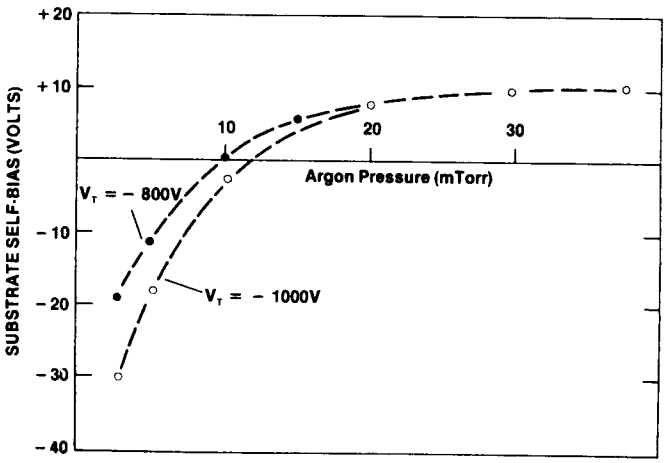

Figure 4. Substrate potential, measured with respect to the ground, vs. the argon pressure for target voltages -800 and -1000 volts.

Relation between photovoltaic properties and compositional inhomogeneities of the films

Structural inhomogeneities in the silicon network are also expected to lead to compositional inhomogeneities upon alloying the material with hydrogen or other impurities. Such inhomogeneities have been observed both in glow discharge and sputtered amorphous silicon through NMR, neutron scattering and infrared vibrational studies.[17-19] In reactively sputtered amorphous silicon, for example, the work of Freeman and Paul [20] and that of Brodsky and co-workers [21] reveal that the Si-H stretching vibration, of films produced under a variety of deposition conditions, is always a doublet. Although there are multiple opinions[22] as to the type of local environments which give rise to this doublet, it is evident that its existence indicates that these films are compositionally inhomogeneous.

Compositional inhomogeneities introduce compositional disorder, which together with other types of disorder, for example thermal and structural[23], should in principle determine the extent of the band tails. Therefore, compositional inhomogeneities are expected to affect carrier transport, optical properties and possibly carrier recombination and thus the photovoltaic characteristics of the films.

In order to investigate whether there is a correlation between compositional inhomogeneities and photovoltaic properties of sputtered amorphous silicon films we developed methods to control the degree of compositional inhomogeneities in these films. These methods have been described in another paper,[7] in which we have shown that, positive substrate bias favors the 2000 cm^{-1} Si-H stretching mode, while negative bias favors the 2100 cm^{-1} Si-H stretching mode. Utilizing this technique we deposited two series of films; in one series the substrates were electrically biased at +50 volts and in the other were electrically grounded. The hydrogen partial pressure in each series was adjusted so that to produce films with optical gaps in the range of 1.6 to 1.9 eV. All other deposition parameters were fixed. Namely the deposition temperature was 275°C, the argon pressure 15 mTorr and the power in the discharge 200 watts. The hydrogen content in these films was determined by the ^{15}N nuclear reaction[24] and the Si-H bonding configuration was determined by studying the IR vibrational spectra. The Si-H stretching vibration for the biased samples centers at 2000 cm^{-1}, while for the grounded samples is a doublet with the 2100 cm^{-1} mode becoming progressively stronger as the hydrogen content increases. On the basis of these data, it is evident that the first series of films are compositionally and structurally more homogeneous than the second series of films. Therefore, the films of the first series should have sharper band tails.

To test this conclusion we studied the optical properties of both series of films. Figure 5 shows the optical gap[25] vs. the hydrogen content in the films. These data clearly indicate that structurally and compositionally inhomogeneous films require more hydrogen to attain the same optical gap. The fact that the more homogeneous films have larger gaps for the same amount of hydrogen, is consistent with the model proposed by Cody and co-workers[23] that the optical gap is related to disorder. Our data suggest that in addition to structural and thermal disorder, which was proposed by Cody, compositional disorder is also important in determining the optical properties of amorphous SH_x alloys.

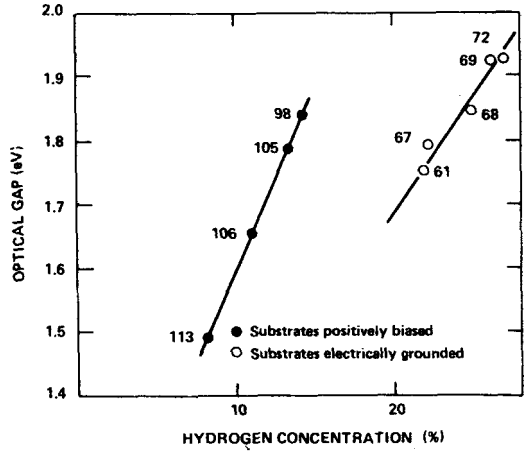

Figure 5. Optical Gap vs Hydrogen Content for Two Series of Films, Produced on Electrically Grounded and Postively Biased Substrates. In the First Series of Films the Si-H Stretching Vibration is a Doublet, while in the Second is a Singlet Centered at 2000 cm^{-1}.

These studies demonstrated that compositional inhomogeneities affect the optical properties of hydrogenated amorphous silicon films. The effect of such inhomogeneities on carrier transport and recombination and their combined effect on the photovoltaic properties is under current study.

Relation between photovoltaic properties and hydrogen content of the films

Hydrogen incorporation in the amorphous silicon network influences the opto-electronic properties of the films more than any other deposition parameter. Despite that, the effect of hydrogen on the photovoltaic properties of amorphous silicon produced by the method of glow discharge decomposition of silane, has not been fully established. This is because hydrogen incorporation can only be controlled indirectly by varying deposition parameters, such as power in the discharge and substrate temperature. However, such deposition parameters can also influence the photovoltaic properties through the modification of the silicon network. In reactive sputtering, on the other hand, one can fix the deposition parameters, which control the microstructure of the silicon network, (deposition temperature, total pressure of the sputtering gas, target and substrate voltage), and vary the hydrogen content in the films by varying the partial pressure of

hydrogen in the discharge. In the following we briefly review the results of our study regarding the role of hydrogen in amorphous silicon.

It is known since 1974[26] that dangling bond related defects, whose energy states lie in the middle of the gap, can be eliminated through hydrogen incorporation. In our laboratory we were able to show,[27] through Capacitance-Voltage and ESR measurements, that the density of states in the middle of the gap depends exponentially on the partial pressure of hydrogen in the discharge. These results are reproduced in Figure 6, and show that amorphous silicon produced by reactive sputtering can be made to have mid-gap density of states less than 10^{15} cm^{-3} eV^{-1}. We have also shown [28] that the states in the middle of the gap control the electron-hole recombination in amorphous silicon solar cells. These results are reproduced in Figure 7, and show clearly that the $\mu\tau$ product of the minority carriers is inversely proportional to the density of states in the middle of the gap. Since the states in the middle of the gap determine both the width of the space charge region and electron-hole recombination (diffusion length of minority carriers), we concluded that the photovoltaic properties of the films should improve systematically with the hydrogen content.

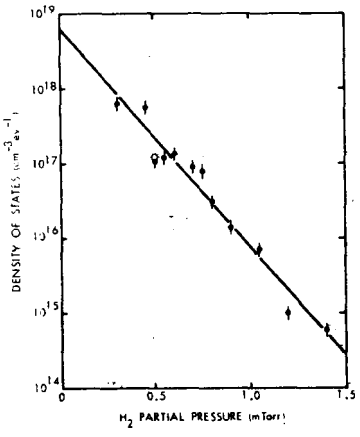

Figure 6. Density of States in the Middle of the Gap as a Function of Hydrogen Partial Pressure in the Discharge. The Point Indicated by the Symbol (o) is the ESR Spin Density (1.1×10^{17} cm^{-3}).

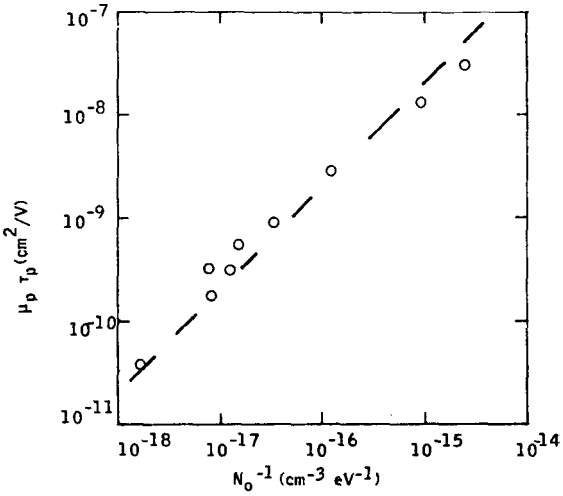

Figure 7. $\mu\tau$ Products vs the Inverse of the Density of States in the Middle of the Gap for the Films Shown in Figure 6.

Besides reducing the states in the middle of the gap, hydrogen incorporation also affects the optical absorption constant of the films. As an illustration, we show in Figure 8 the optical absorption constant vs. photon energy for the films reported in Figures 6 and 7. The results of Figures 6-8 suggest that hydrogen incorporation improves the electronic quality of the films while simultaneously increasing their optical band gap. This is an unfortunate tradeoff since the photovoltaic properties of a semiconductor depend both on its ability to absorb a significant fraction of the solar spectrum and its ability to collect the photogenerated electron-hole pairs. To illustrate this point we refer to the collection efficiency data of Figure 3. The optical gaps of the films, produced at target voltage of -1000 volts, were increased from 1.71 to 1.84 eV, as the hydrogen content increased, but the collection efficiency remained unchanged. The insensitivity of the collection efficiency to hydrogen suggests that the improvements in the electronic properties are counter balanced by the optical losses due to the increase in the optical gap. It should be noted, however, that the open circuit voltage increases with the optical gap of the material.[29] Therefore, the larger gap material has a better photovoltaic potential because it produces the same current and higher open circuit voltage.

Cody and co-workers[23] have reached the same conclusion by studying the effect of hydrogen on the structural disorder of the films. These authors correlated the increase of the optical gap to the removal of structural disorder by hydrogen incorporation. This should result in material with sharper band tails, which is expected to have better transport and possibly better recombination properties.

Effect of phosphorus and boron impurities on the photovoltaic properties of intrinsic amorphous silicon films

The effects of phosphorus and boron contamination on the photovoltaic properties of intrinsic films have been published elsewhere.[8,30] Here, we only give a brief account of these results. To probe the effects of these impurities we used N-I-Pt Schottky barrier structures, whose I-layer was contaminated intentionally with small amounts of PH_3 or B_2H_6 (<1 ppm). We found that as the degree of phosphorus contamination was reduced, the peak of the spectral response of the collection efficiency shifted towards the red. This red shift led to a pronounced increase in the short circuit current. The increase in the red response was held to be due to a decrease in the density of the defects which determine the space charge region. The consequent improved electronic structure of the I-layer is responsible for a longer diffusion length and greater depletion width.

To study the effects of boron contamination we fabricated a number of N-I-Pt devices, whose I-layer was grown at progressively higher amounts of B_2H_6 in the discharge. Figure 9 shows the spectral dependence of the collection efficiency for three such devices. These spectra were taken by illuminating the devices through the top Pt contact. Note that, as the level of B_2H_6 in the discharge increases the quantum efficiency for blue-green light decreases significantly. The internal short circuit currents, calculated from these collection efficiency spectra, are 11.8 mA/cm^2, 4.57 mA/cm^2 and 1.5 mA/cm^2 for the three devices.

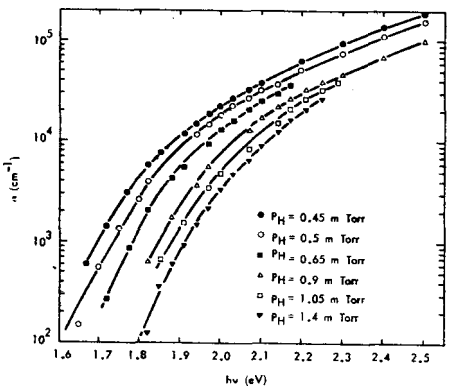

Figure 8. Optical Absorption Constant vs Photon Energy for Some of the Films of Figure 6.

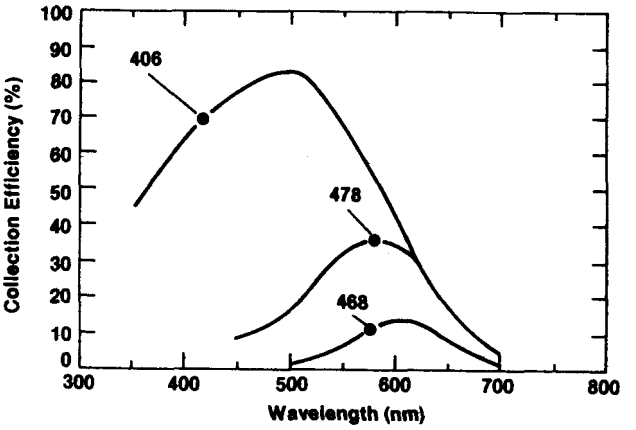

Figure 9. Spectral dependence of the collection efficiency for a number of N-I-Pt devices, whose I-layer was grown at progressively higher amount of B_2H_6 in the discharge (sample 406 was grown with 0.02 ppm, Sample 478 with 0.2 ppm and sample 468 with 0.4 ppm)

In order to understand these changes, we further investigated the collection efficiency of the Schottky barrier device #468 by illuminating it through the glass substrate. In this case, we found that the blue-green response of the quantum efficiency was restored and the device generates on internal current of 10.5 mA/cm^2.

These results can be accounted for as follows: The intrinsic amorphous silicon films are normally slightly N-type. As a result, in N-I-Metal and N-I-P solar cell structures the major potential barrier is at the I-M or I-P interface. Low levels of boron compensation moves the Fermi level close to the middle of the gap and improves the photovoltaic performance of the device. Further increases in boron render the I-layer slightly P-type, and move the major barrier to the I-N interface. Therefore, in such devices, illumination from the N-side gives better photovoltaic performance.

These data suggest that small amounts of dopant impurities as well as compensational effects are important in sputtered hydrogenated amorphous silicon and separate process chambers are required for reproducible fabrication of P-I-N solar cells.[31]

Performance of P-I-N solar cells

The studies outlined in the previous sections have led to the fabrication of P-I-N solar cell structures, which generate short circuit currents up to 13 mA/cm^2 and V_{oc} of between 0.85 to 0.95 volts. As an example, we give in Figure 10 the I-V characteristics of one solar cell structure, which has the configuration SS/NIP/ITO. The efficiency of this device, 5.5%, is limited by the small FF. Details of the device fabrication and the possible causes for the poor FF are discussed in another paper.[32]

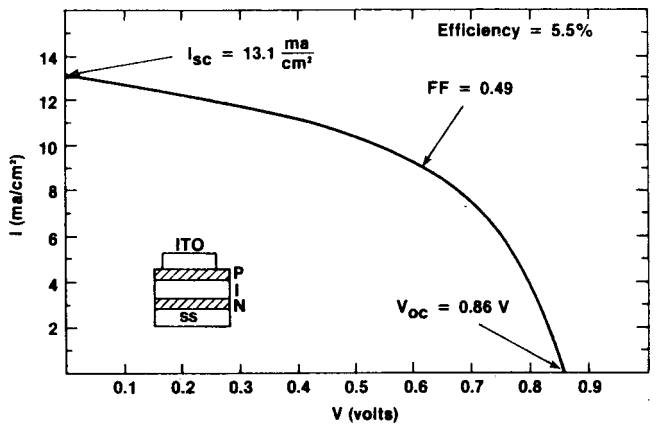

Figure 10. I-V characteristics of a P-I-N solar cell structure. The device design and the photovoltaic parameters are shown in the insert of the figure.

Conclusions

The experimental results presented in this paper show strong correlations between photovoltaic properties and structural and compositional inhomogeneities, amount of incorporated hydrogen and contamination by low level of dopant impurities. These results can be summrarized as follows.

Structural inhomogeneities in sputtered amorphous silicon films are correlated with bombardment of the growing film by charged particles. Deposition parameters, which were found to affect such inhomogeneities, are the pressure of the sputtering gas, and the target and substrate bias. Structural inhomogeneities influence the photovoltaic properties through the introduction of defects which control recombination and possibly through the modification of the structural disorder, which affects the width of the band tails, and thus carrier transport and optical properties. Compositional inhomogeneities were found to affect the optical properties, suggesting that such inhomogeneities introduce additional disorder, which broadens the band tails. Our studies[7-27] do not indicate that compositional inhomogeneities introduce defects in the middle of the gap.

Opto-electronic and photovoltaic studies of films produced at different hydrogen concentrations suggest that the dual role of hydrogen in removing dangling bond related defects and simultaneously increasing the optical gap is an unfortunate trade-off. We suggested that since the current is independent of hydrogen content the large gap material has an advantage for photovoltaic applications because it leads to solar cells with higher V_{oc}.

The introduction of low levels (<1 ppm) of PH_3 and B_2H_6 in the discharge has a significant effect on the photovoltaic properties of the films. Some of the effects may be related to the introduction of structural defects by these impurities or to the shift of the Fermi level towards the conduction or valance bands.

Careful optimization of these deposition parameters can lead to solar cells with reasonably high efficiencies.

Acknowledgements

The author is indebted to B. Abeles, J. Amick, G. Cody, M. Cohen, A. Ghosh, H. P. Maruska, A. Rose, T. Tiedje and C. Wronski for a number of technical discussions and to R. Friedman and M. Hicks for technical assistance. The work was partially supported by the U. S. Department of Energy through a Solar Energy Research Institute Contract (Contract #ZB-3-02166-01).

References

1. Catalano, A., D'Aiello, R. V., Dresner, J., Faughnan, B., Firester, A., Kane, J., Schade, H., Smith, Z. E., Swartz, G. and Triano, A. Proc. of 16th IEEE Photovoltaic Specialists Conference (in press).
2. Paul, W., Lewis, A. J., Connell, G.A.N., and Moustakas, T. D., Solid State Communications, Vol. 20, pp. 969-972 (1976).
3. Spear, W. E., Adv. Phys., Vol. 26, p. 811 (1977).
4. Amick, J. A., Schnable, G. L., Vossen, J. L., J. Vac. Sci. Technol., Vol. 14, pp. 1053-1063 (1977).
5. Moustakas, T. D., Maruska, H. P., Friedman, R., and Hicks, M. C., Phys. Rev. B (to be published).
6. Moustakas T. D. and Maruska, H. P. (to be published).
7. Moustakas, T. D., Solar Energy Materials, Vol. 8, pp. 187-204 (1982).
8. Moustakas, T. D., Friedman, R. and Weinberger, B. R., Appl. Phys. Lett. Vol. 40, pp. 587-588 (1982).
9. Wronski, C. R., Abeles, B., and Cody, G. D., Solar Cells, Vol. 2, p. 245 (1980).
10. Bird, R., Terrestrial Solar Spectral Standards and Data Sets, SERI/TR-642-1149 (1981).
11. Knights, J. C. and Lujan, R. A., Appl. Phys. Lett., Vol. 35, p. 244 (1979).
12. Ross, R. C., and Messier, R., J. Appl. Phys., Vol. 52, p. 5329 (1981).
13. Temkin, R. J., Paul, W., and Connell, G.A.N., Adv. Phys., Vol. 22, p. 581 (1973).
14. Bagley, B. (to be published).
15. Vossen, J. L. and Kern, W., Thin Film Processes, Academic Press, New York (1978).
16. Moustakas, T. D. and Maruska, H. P. (to be published).
17. Reimer, J. A., Vaughnan, R. W. and Knights, J. C., Phys. Rev. Lett., Vol. 44, p. 193 (1980).
18. Postol, T. A., Falco, C. M., Campwirth, R. T., Schuller, I. K., and Velon, W. B., Phys. Rev. Lett., Vol. 45, p. 648 (1980).
19. Knights, J. C., Japan. J. Appl. Phys., Vol. 18, p. 101 (1979).
20. Freeman, E. C. and Paul, W., Phys. Rev. B, Vol. 18, p. 4288 (1978).
21. Brodsky, M. H., Cardona, M., and Cuomo, J. J., Phys. Rev. B, Vol. 16, p. 3556 (1977).
22. Paul, W., Solid State Commun., Vol. 34, p. 283 (1980).
23. Cody, G. D., Tiedje, T., Abeles, B., Brooks, B. and Goldstein, Y., Phys. Rev. Lett., Vol. 47, p. 1480 (1981).
24. Moustakas, T. D., Tiedje, T. and Lanford, W. A., Tetrahedrally Bonded Amorphous Semiconductors, Eds., Street, R. A., Biegelsen, D. K., and Knights, J. C., AIP Conf. Proc. No. 73, p. 20 (1981).
25. The optical gap Eg, of the films was defined by the relation $(\alpha h\nu)^{1/2} \sim (h\nu - Eg)$.
26. Lewis, A. J., Connell, G.A.N., Paul, W., Pawlik, J. R. and Temkin, R. J., Tetrahedrally Coordinated Amorphous Semiconductors, Ed by Brodsky, Kirkpatrick and Weaire (AIP No. 20, 1974).
27. Tiedje, T., Moustakas, T. D., and Cebulka, J. M., Phys. Rev. B, Vol. 23, pp. 5634-5637 (1981).
28. Moustakas, T. D., Wronski, C. R., and Tiedje, T., Appl. Phys. Lett., Vol. 39, pp. 721-723 (1981).
29. Morel, D. L., Moustakas, T. D., Appl. Phys. Lett., Vol. 39, pp. 612-614 (1981).
30. Moustakas, T. D., Maruska, H. P., Friedman, R. and Hicks, M., Appl. Phys. Lett. (to be published).
31. Kuwano, Y., Ohnishi, M., Tsuda, S., Nakashima, Y., Nakamura, N., Japan. J. of Appl. Phys., Vol. 21, pp. 413-417 (1982).
32. Moustakas, T. D. (to be published).

APPENDIX J. High Efficiency Amorphous Sililcon Solar Cells Fabricated by Reactive Sputtering

Proc. of the Symposium on Material and New
Processing Technologies for Photovoltaics,
Proc. Vol. 83-11 p. 291. J. A. Amick, V. K. Kapur and J. Dietl Eds.
The Electrochemical Society, Pennington, NJ (1983)

HIGH EFFICIENCY AMORPHOUS SILICON SOLAR CELLS FABRICATED BY REACTIVE SPUTTERING

T. D. Moustakas

Exxon Research and Engineering Company
P.O. Box 45
Linden, New Jersey 07036

ABSTRACT

This paper describes the effect of a number of deposition parameters on the photovoltaic properties of intrinsic amorphous silicon films produced by RF sputtering. We find that the argon pressure and the power in the discharge affect the photovoltaic properties through the modification of the film's microstructure. Hydrogen incorporation and small levels of phosphorus and boron impurities affect the photovoltaic properties through reduction of residual dangling bond related defects and modification of their occupation. These optimization studies lead to intrinsic films, which when incorporated in P-I-N solar cell structures, generate external currents up to 13 mA/cm^2 and open circuit voltages of between 0.85 to 0.95 volts. The efficiency of these devices, 5.5%, is limited by the low FF, typically less than 50%.

INTRODUCTION

There are two plasma methods for depositing hydrogenated amorphous silicon; glow discharge decomposition of silane and reactive sputtering from a silicon target in a mixture of inert gas and hydrogen. Of the two, glow discharge has attracted considerably more attention. The extensive investigation of this deposition process, through structural, optical, transport, recombination and device studies, has led to the fabrication of solar cell structures with efficiency up to 10% (1). This breakthrough was due not only to the improvements of the quality of the amorphous silicon films but also to improvements in device design. The device configuration, glass/SnO_2/PIN/Ag, employs a highly transparent P-layer, made of silicon carbide alloys (2) and a highly reflective back contact made of silver. The solar cell parameters of this device are J_{sc} = 17.8 mA/cm^2, V_{oc} = 0.84 Volts and FF = 0.676.

The alternative method of film deposition has attracted much less attention because it was perceived as an unsuitable technology for surface sensitive devices. In addition it was widely assumed that sputtering leads to films with poorer optoelectronic properties. The photovoltaic potential of this material was initially tested through the fabrication of Schottky barrier and metal-insulator-semiconductor

structures (3,4). The moderate performance of such devices (conversion efficiency ~2%) reinforced the widespread belief that sputtered amorphous silicon films are inferior to those produced by glow discharge decomposition of silane. However, recent progress in identifying deposition parameters, which control the film growth (5), and progress in device studies (6,7) have led to the fabrication of multilayer P-I-N solar cell structures with efficiency 4% (8).

In this paper we report that the photovoltaic properties of the intrinsic films can be improved even further, by optimizing deposition parameters, which affect the silicon network, and by adjusting the hydrogen content and level of boron compensation. These optimization studies lead to intrinsic material, which when incorporated in P-I-N solar cell structures, generate external currents up to 13 mA/cm^2 and open circuit voltages of between 0.85 to 0.95 volts. The efficiency of these devices, 5.5%, is limited by the low FF, typically less than 50%. These structures have the configuration stainless steel/NIP/ITO. The structural, optical and transport properties of the P and N-layers will be reported in another paper (9).

EXPERIMENTAL METHODS

The deposition system has stainless steel walls, held at ground potential and electrically insulated cathode and anode assemblies. The water cooled target is a polycrystalline silicon disk, 5" in diameter and 1/4" thick and is supplied with an rf power at a frequency 13.56 MHz. The anode assembly, 26" in diameter, is held 2" below the target and can be grounded, floated or supplied with rf or dc electrical bias. The substrates (quartz glass and polished stainless steel plates) were fastened with a stainless steel frame and molybdenum springs on the top fo the anode assembly. The substrates were heated with quartz radiation heaters to temperatures between 200 to 400°C.

The system was pumped by a combination of turbomolecular and mechanical pumps to a base pressure of about 1-2 x 10^{-7} Torr and routinely checked for atmospheric leaks with a mass spectrometer. The systems total leak rate was approximately 1-2 x 10^{-5} Torr ℓ s^{-1}, with H_2O being the principal impurity. The total pressure of argon and hydrogen was monitored with a MKS-310 capacitance monometer and the partial pressures of the two gases were measured with a UTI-100C mass spectrometer. The flow rates of the two gases were determined by a combination of Tylan FM-360 mass flow meters and Brooks 5835 control valves. The ratio of H_2/Ar was regulated by a MKS-254 mass flow controller.

Primarily we used Schottky barrier structures for the purpose of studying the photovoltaic properties of the intrinsic films. The device configurations employed were N-I-Pt (Pd) and the substrate was stainless steel or Corning 7059 glass coated with approximately 1μm

thick SnO_2. The N amorphous silicon, 250 A thick, was produced by adding 0.2% PH_3 to the sputtering gas. The sputtering system was cleaned between N and I depositions to reduce phosphorus contamination (10).

Multilayer devices were fabricated in the configuration: stainless steel/NIP/ITO. The P-layer was produced by mixing 0.2% of B_2H_6 to the sputtering gas and has a thickness of approximately 100A.

These devices were evaluated by studying both their I-V characteristics and the collection efficiency spectra, under illumination through either the top contact or the glass substrate. The I-V characteristics were measured using a calibrated Xenon Solar Simulator. The collection efficiency was measured following the technique described by Wronski et al. (11). The optical absorption coefficient was calculated (12) from optical transmission measurements made in Cary 17 spectrophotometer.

EXPERIMENTAL RESULTS AND DISCUSSION

Effect of Pressure of the Sputtering Gas

Structural studies (13) of amorphous silicon sputtered films, produced with the pressure of argon as the variable, showed no evidence of columnar morphology at low argon pressure and strong evidence of columnar morphology at high argon pressure. The transition from the one regime to the other, depends on the apparatus geometry, cathode-anode distance and power in the discharge. These microstructural changes have been correlated with charged particle bombardment effects (5,13).

To investigate the correlation between these microstructural changes and the photovoltaic properties of the films, we studied a number of films deposited at fixed hydrogen partial pressure (P_H = 0.7 mTorr) and argon partial pressure varying between 5 to 30 mTorr. All films were deposited at 275°C and at constant forward power of 200 watts. The choice of this mode of operation resulted in a small but monotonic increase of the deposition rate from 2.1 to 2.6 A/sec, because the ion current increases as the argon pressure increases. As a result of that, the hydrogen content in the films was found to decrease with the argon pressure from 21.5 to 19.5 at %. Correspondingly, the optical gap of the films was found to decrease from 1.84 eV to 1.78 eV. Structural studies (5) of these films indicate that the transition between the non-columnar to columnar regimes occurs between 15 to 20 mTorr of argon.

The photovoltaic properties of these films correlate remarkably well with the observed microstructural changes. Figure 1 shows the I-V characteristics of N-I-Pd Schottky barrier structures. The I-layer in these devices was deposited at 5, 10, 20 and 30 mTorr of

argon. Note that the films produced at argon pressures of 20 and 30 mTorr have poorer photovoltaic properties than those produced at 5 and 10 mTorr of argon. Therefore, films grown under some charged particle bombardment have less structural inhomogeneity and the best photovoltaic properties.

Effect of Target Voltage

The target voltage is also expected to affect film homogeneity through charged particle bombardment. Both the substrate floating potential (measured with respect to the ground) and the plasma potential are influenced by the target voltage. In addition, in RF discharge the relation between target potential and plasma potential may also be influenced by the geometry of the system (14).

To investigate the effect of target voltage on the photovoltaic properties, we deposited two series of films with the target voltage as the variable. In one series the induced target DC bias voltage was maintained at -800 volts, and in the other at -1000 volts. All samples were deposited at fixed temperature (325°C) and total sputtering gas pressure (argon + hydrogen = 5mTorr). In each series the flow rates of H_2/Ar were varied from 10 to 20%. The Schottky barrier devices employed had the configuration N-I-Pt.

Figure 2 shows the spectral dependence of the collection efficiency of the two series of films. Note that these spectra fall into two distinct groups. For the -800 volts samples, the collection efficiency peaks at 450 nm, while for the -1000 volts samples it peaks at 500 nm. This red shift leads to an increase in the internal short circuit from 9.5 mA/cm^2 to 11 mA/cm^2. Greater details of the effect of target voltage on the photovoltaic properties have been reported in another paper (15).

The fact that the collection efficiency of the devices produced at each target voltage is independent of hydrogen content is significant, and suggests that the observed effect is unrelated to the changes of the opto-electronic properties of the films due to the hydrogen incorporation. These changes are going to be discussed in more detail later. Therefore the shift of the peak of the collection efficiency towards the red part of the spectrum, as the target voltage (power in the discharge) increases, suggests that the electronic quality of the films improves with the power in the discharge. This is contrary to the findings by Knights and Lujan (16) that the quality of the glow discharge amorphous silicon films improves with decreasing power in the discharge. This discrepancy signifies that the film growth process in these two methods of film deposition is different. We attribute the improvement in the quality of the sputtered material, as the target voltage increases, to improvements in film homogeneity due to additional bombardment by charged particles. Indication of this is provided in Figure 3. Here we show the substrate potential, measured with respect

to the ground, vs. the argon pressure in the discharge for target voltages -800 and -1000 volts. These data suggest (5) that films produced at higher target voltages are subjected to more charged particle bombardment.

Effect of Hydrogen Content

Hydrogen incorporation in the amorphous silicon network influences the opto-electronic properties of the films more than any other deposition parameter. Despite that, the effect of hydrogen on the photovoltaic properties of amorphous silicon produced by the method of glow discharge decomposition of silane, has not been fully established. This is because hydrogen incorporation can only be controlled indirectly by varying deposition parameters, such as power in the discharge and substrate temperature. However, such deposition parameters can also influence the photovoltaic properties through the modification of the silicon network. In reactive sputtering, on the other hand, one can fix the deposition parameters, which control the microstructure of the silicon network, (deposition temperature, total pressure of the sputtering gas, target and substrate voltage), and vary the hydrogen content in the films by varying the partial pressure of hydrogen in the discharge. In the following we briefly review the results of our study regarding the role of hydrogen in amorphous silicon.

It has been shown (6,7) that the density of states in the middle of the gap depends exponentially on the partial pressure of hydrogen in the discharge and that these states control electron-hole recombination in amorphous silicon solar cells. Since the states in the middle of the gap determine both the width of the space charge region and electron-hole recombination (diffusion length of minority carriers), we concluded that the photovoltaic properties of the films should improve systematically with hydrogen content.

Besides reducing the states in the middle of the gap, hydrogen incorporation also affects the optical absorption constant of the films. As an illustration we show in Figure 4 the optical absorption constant vs. photon energy of the films whose collection efficiencies are shown in Figure 2. Note that the optical gap (17) of the films produced at -1000 volts has increased from 1.71 to 1.84 eV.

This dual role of hydrogen in reducing the states in the middle of the gap while simultaneously increasing the optical gap is an unfortunate trade-off, since the photovoltaic properties of a semiconductor depend both on its ability to absorb a significant fraction of the solar spectrum and its ability to collect the photogenerated electron-hole pairs. This trade-off explains the insensitivity of the collection efficiency to hydrogen content. According to the data of Figures (2 and 4) films having optical gaps between 1.71 to 1.84 eV generate the same J_{sc}. Therefore, the larger

gap material has a better photovoltaic potential because it produces the same current and higher open circuit voltage (18).

Effect of Phosphorus and Boron Impurities

The effects of phosphorus and boron contamination on the photovoltaic properties of intrinsic films have been published elsewhere (10,19). Here, we only give a brief account of these results. To probe the effects of these impurities we used N-I-Pt Schottky barrier structures, whose I-layer was contaminated intentionally with small amounts of PH_3 or B_2H_6 (<1 ppm). We found that as the degree of phosphorus contamination was reduced, the peak of the spectral response of the collection efficiency shifted towards the red. This red shift led to a pronounced increase in the short circuit current. The increase in the red response was held to be due to a decrease in the density of the defects which determine the space charge region. The consequent improved electronic structure of the I-layer is responsible for a longer diffusion length and greater depletion width.

To study the effects of boron contamination we fabricated a number of N-I-Pt devices, whose I-layer was grown at progressively higher amounts of B_2H_6 in the discharge. Figure 5 shows the spectral dependence of the collection efficiency for three such devices (Sample 406 was grown with 0.02 ppm, Sample 478 with 0.2 ppm and Sample 468 with 0.4 ppm of B_2H_6 in the discharge). These spectra were taken by illuminating the devices through the top Pt contact. Note that, as the level of B_2H_6 in the discharge increases the quantum efficiency for blue-green light decreases significantly. The internal short circuit currents, calculated from these collection efficiency spectra, are 11.8 mA/cm^2, 4.57 mA/cm^2 and 1.5 mA/cm^2 for the three devices.

In order to understand these changes, we further investigated the collection efficiency of the Schottky barrier device #468 by illuminating it through the glass substrate. In this case, we found that the blue-green repsonse of the quantum efficiency was restored and the device generates an internal current of 10.5 mA/cm^2.

These results can be accounted for as follows: The intrinsic amorphous silicon films are normally slightly N-type. As a result, in N-I-Metal and N-I-P solar cell structures the major potential barrier is at the I-M or I-P interface. Low levels of boron compensation moves the Fermi level close to the middle of the gap and improves the photovoltaic performance of the device. Further increase in boron render the I-layer slightly P-type, and moves the major barrier to the I-N interface. Therefore, in such devices, illumination from the N-side gives better photovoltaic performance.

These data suggest that small amounts of dopant impurities as well as compensational effects are important in sputtered hydrogenated

amorphous silicon and separate process chambers are required for reproducible fabrication of P-I-N solar cells (20).

Performance of P-I-N Solar Cells

The studies outlined in the previous sections have led to the fabrication of P-I-N solar cell structures, which generate short circuit currents up to 13 mA/cm^2 and V_{oc} of between 0.85 to 0.95 Volts. As an example, we give in Figure 6 the I-V characteristics of one solar cell structure which has the configuration SS/NIP/ITO. The I-layer of this device was produced at 5mTorr of Ar + H_2 (H_2/Ar = 0.18), at target voltage of -800 volts and deposition temperature of 325°C. The efficiency of this device is 5.5%. Figure 7 shows the collection efficiency of this device. The short circuit current, which is calculated by integrating this spectral response with the AM1 solar spectrum (21), agrees reasonably well with the value found by illuminating the sample with the solar simulator. Details of the device fabrication and possible causes for the poor FF are discussed in another paper (22).

CONCLUSIONS

The experimental results presented in this paper show strong correlations between photovoltaic properties and structural inhomogeneities, amount of incorporated hydrogen and contamination by low levels of dopant impurities. These results can be summarized as follows:

Structural inhomogeneities in sputtered amorphous silicon films are correlated with bombardment of the growing film by charged particles. Deposition parameters, which were found to affect such inhomogeneities, are the pressure of the sputtering gas and the target voltage.

Opto-electronic and photovoltaic studies of films produced at different hydrogen concentrations suggest that the dual role of hydrogen in removing dangling bond related defects and simultaneously increasing the optical gap is an unfortunate trade-off. We suggested that, since the current is independent of hydrogen content, the large gap material has an advantage for photovoltaic applications because it leads to solar cells with higher V_{oc}.

The introduction of low levels (<1 ppm) of PH_3 and B_2H_6 in the discharge has a significant effect on the photovoltaic properties of the films. Some of these effects may be related to the introduction of structural defects by these impurities or to the shift of the Fermi level towards the conduction or valance bands.

Careful optimization of these deposition parameters can lead to solar cells with reasonably high efficiencies.

ACKNOWLEDGMENTS

The author is indebted to H. P. Maruska and C. Wronski for a number of technical discussions and to R. Friedman and M. Hicks for technical assistance. The work was partially supported by the U.S. Department of Energy through a Solar Energy Research Institute Contract (Contract #ZB-3-02166-01).

REFERENCES

1. A. Catalano, R. V. D'Aiello, J. Dresner, B. Faughnan, A. Firester, J. Kane, h. Schade, Z. E. Smith, G. Swartz and A. Triano, 16th IEEE Photovoltaic Specialist Conference, 1421 (1982).

2. Y. Tawada, M. Kondo, H. Okamoto and Y. Hamakawa, Solar Energy Materials, 6, 299 (1982).

3. J. M. Thompson, J. Allison, M. M. Al-Kaisi and I. P. Thomas, Revue de Phys. Appl., 13, 625 (1978).

4. P. Victorovitch, D. Jousse, A. Chenevas-Paul and L. Lieuz-Rocherz, Revue de Phys. Appl., 14, 204 (1979).

5. T. D. Moustakas, Solar Energy Materials, 8, 187 (1982).

6. T. Tiedje, T. D. Moustakas and J. M. Cebulka, Phys. Rev. B., 23, 5634 (1981).

7. T. D. Moustakas, C. R. Wronski and T. Tiedje, Appl. Phys. Lett., 39, 721 (1981).

8. T. D. Moustakas and R. Friedman, Appl. Phys. Lett., 40, 515 (1982).

9. T. D. Moustakas and H. P. Maruska (to be published).

10. T. D. Moustakas, R. Friedman and B. R. Weinberger, Appl. Phys. Lett., 40, 587 (1982).

11. C. R. Wronski, B. Abeles and G. D. Cody, Solar Cells, 2, 245 (1980).

12. J. P. deNeufville, T. D. Moustakas and A. F. Ruppert, J. of Noncrystall. Solids, 35-36, 481 (1980).

13. R. C. Ross and R. Messier, J. Appl. Phys., 52, 5329 (1981); Tetrachedrally Bonded Amorphous Semiconductors, eds. R. A. Strect, D. K. Biegelsen and J. C. Knights, AIP Conf. Proc. No. 73 (1981) 53.

14. J. L. Vossen and J. J. Cuomo, "Thin Film Processes", (J. L. Vossen and W. Kern, Eds.) Chapter 2, Academic Press, New York (1978).

15. T. D. Moustakas and H. P. Moruskas (to be published).

16. J. C. Knights and R. A. Lujan, Appl. Phys. Lett., 35, 244 (1979).

17. The Optical Gap Eg of the Films, is defined by the relation $(\alpha h\nu)^{1/2} = B(h\nu-Eg)$.

18. D. L. Morel and T. D. Moustakas, Appl. Phys. Lett., 39, 612 (1981).

19. T. D. Moustakas, H. P. Maruska, R. Friedman and M. Hicks (to be published).

20. Y. Kuwano, M. Ohnishi, S. Tsuda, Y. Nakashima and N. Nakamura, Japan J. of Appl. Phys., 21, 413 (1982).

21. R. Bird, Terrestial Solar Spectral Standards and Data Sets, SERI/TR-642-1149 (1981).

22. T. D. Moustakas (to be published).

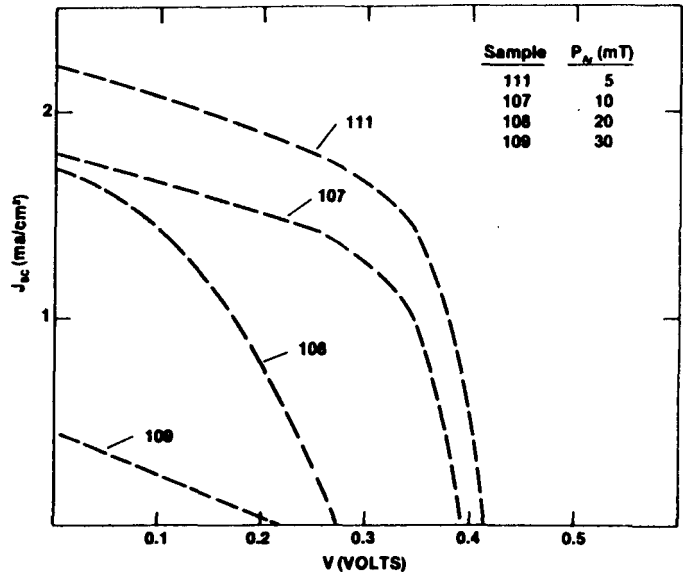

Figure 1. I-V Characteristics of N-I-Pd Schottky Barrier structures.

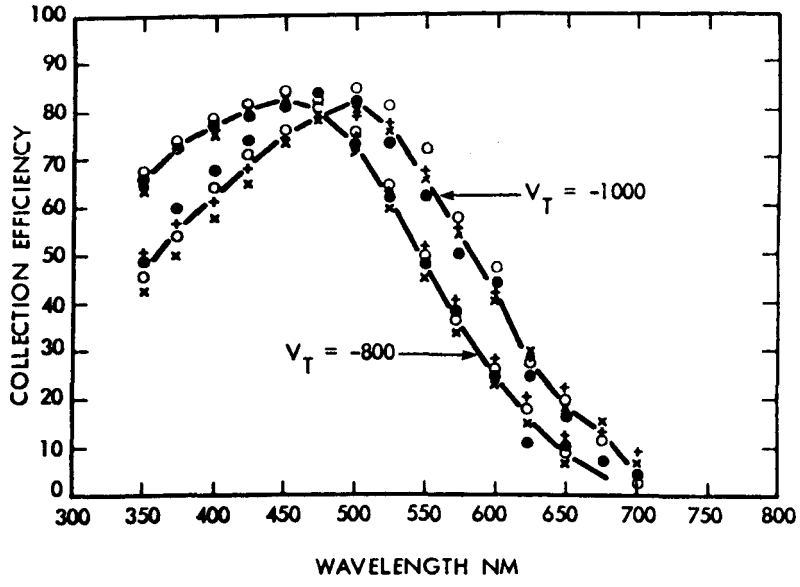

Figure 2. Spectral Dependence of the Collection Efficiency of two Series of N-I-Pt Devices, Made at Indicated Voltages.

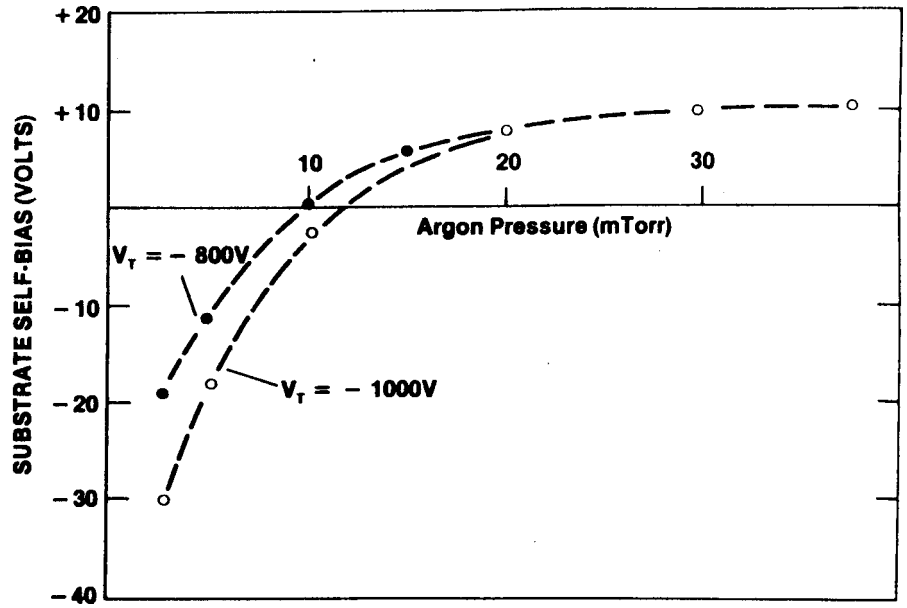

Figure 3. Substrate Potential, Measured with Respect to the Ground, vs. the Argon Pressure for Target Voltages −800 and −1000 Volts

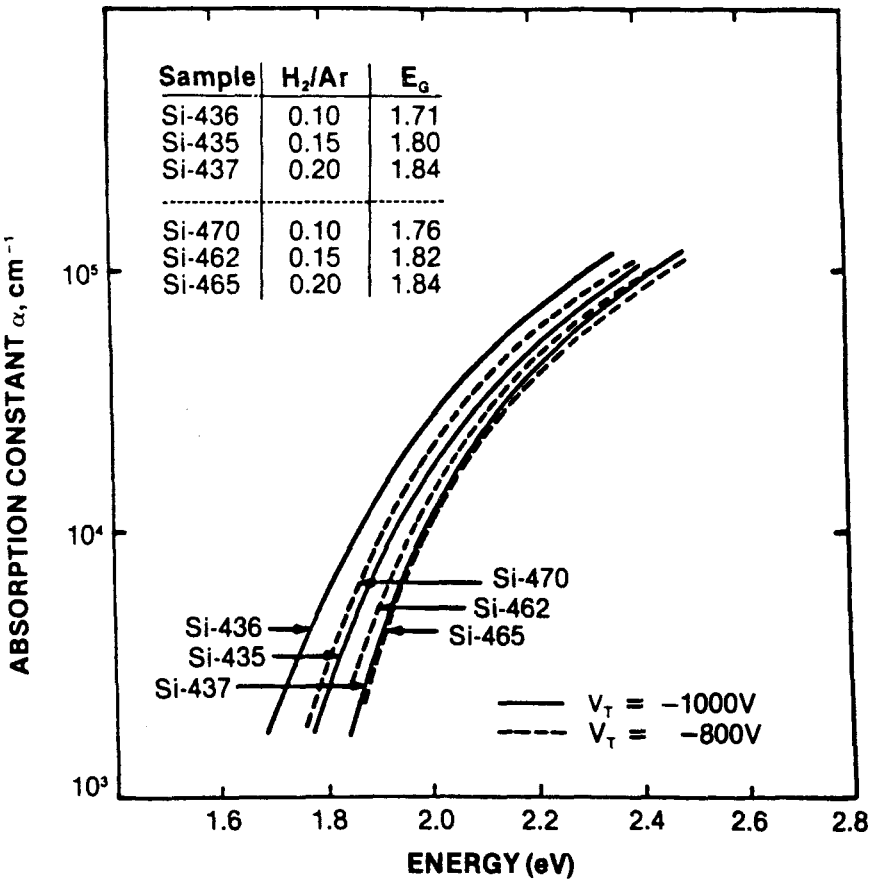

Figure 4. Optical Absorption Constant vs. Photon Energy for Two Series of Films Produced under Target Voltage of −1000 V and −800 V

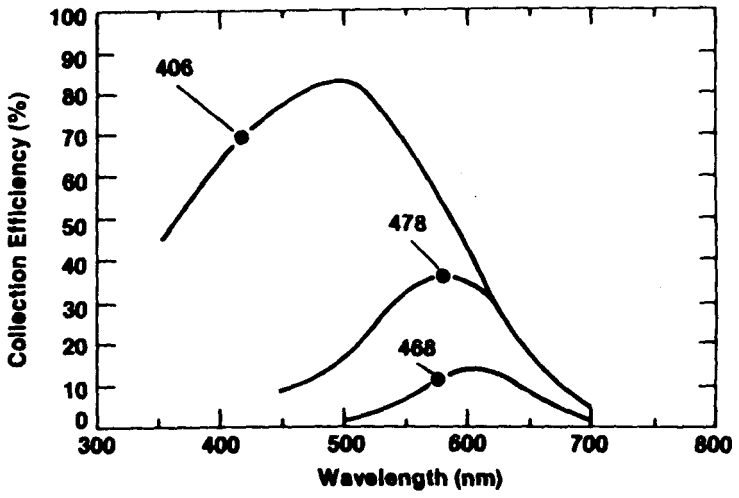

Figure 5. Effect of Boron Compensation on Spectral Dependence of Collection Efficiency of N-I-Pt Devices.

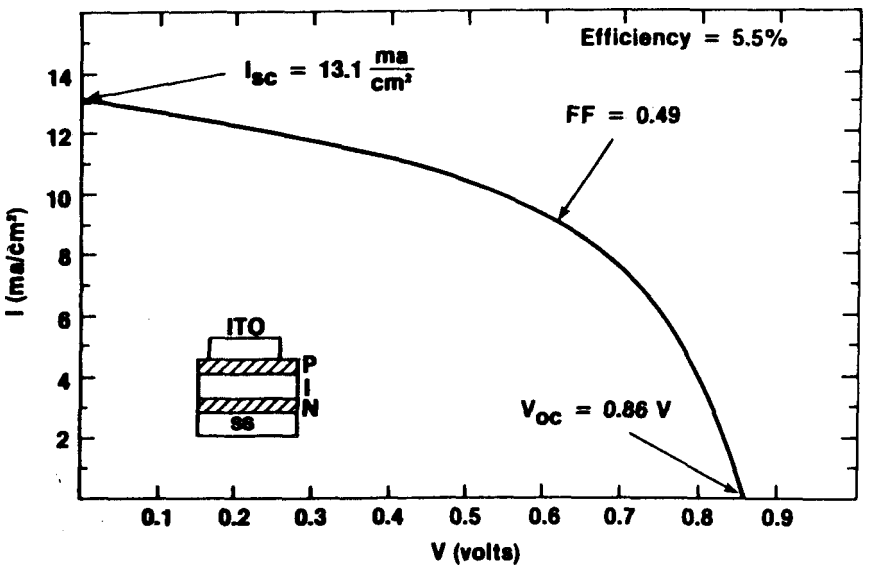

Figure 6. I-V Characteristics of a Sputtered SS/NIP/ITO Solar Cell Structure.

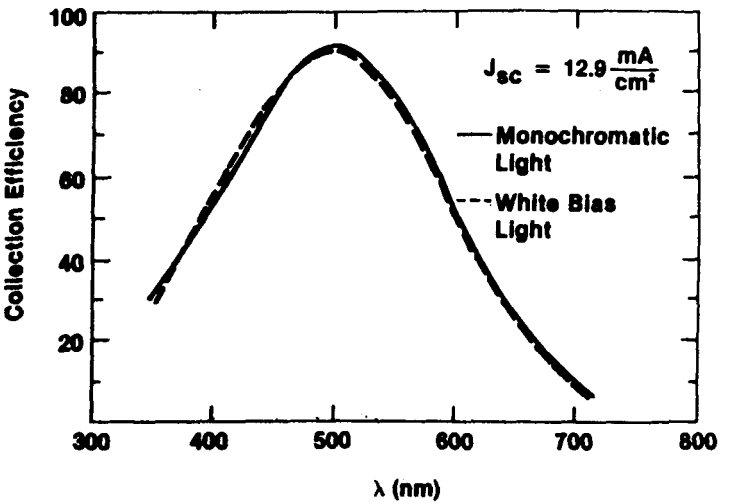

Figure 7. Spectral Dependence of the Collection Efficiency of the Device Shown in Figure 6.

APPENDIX K. Progress in Amorphous Silicon Solar Cells Produced by Reactive Sputtering

PROGRESS IN AMORPHOUS SILICON SOLAR CELLS PRODUCED BY REACTIVE SPUTTERING

T. D. MOUSTAKAS
Corporate Research Laboratory
Exxon Research and Engineering Company
Clinton Township
Route 22 East
Annandale, New Jersey 08801

Summary

In this paper we review the photovoltaic properties of reactively sputtered amorphous silicon and show that efficient PIN solar cells can be fabricated by the method of sputtering. The photovoltaic properties of the intrinsic films correlate with their structural and compositional inhomogeneities. Hydrogen incorporation and small levels of phosphorus and boron impurities also affect the photovoltaic properties through reduction of residual dangling bond related defects and modification of their occupation. The optical and transport properties of the doped P and N-films were found to depend sensitively on the amount of hydrogen and boron or phosphorus incorporation into the films as well as on their degree of crystallinity. Combination of the best intrinsic and doped films leads to PIN solar cell structures generating J_{SC} of 13 mA/cm^2 and V_{OC} of between 0.85 to 0.95 volts. The efficiency of these devices, 5 to 6%, is limited by the low FF, typically about 50%. As a further test to the potential of this technology we fabricated efficient tandem solar cell structures and tested device design concepts, such as the incorporation of optically reflective back contacts.

1. INTRODUCTION

Of the two plasma methods for depositing hydrogenated amorphous silicon the glow discharge decomposition of silane has attracted considerably more attention, and this led to the fabrication of solar cells with efficiencies up to 10% (1). This breakthrough resulted partly through progress in the thin film growth process (2) and partly through improvements in the device design (3).

The alternative technology of reactive sputtering has attracted much less attention, primarily because early work suggested that sputtered amorphous silicon solar cells are inferior to those produced by the glow discharge process (4,5). In addition there is a wide-spread belief that sputtering is an unsuitable technology for surface sensitive devices (6).

In this paper we show that the properties of both the intrinsic and doped sputtered amorphous silicon films can be optimized to lead to solar cell structures with high efficiencies. Correlations between the photovoltaic properties and structural and compositional inhomogeneities, hydrogen content, and small levels of phosphorus and boron impurities in the intrinsic films have been studied. The doped films were optimized for maximum transparency and conductivity, through the variation of the amount of hydrogen and phosphorus or boron incorporation. The role of degree of crystallinity in the transport and optical properties of the doped films

was also investigated. The photovoltaic potential of the sputtered amorphous silicon films was assessed through the fabrication and evaluation of single and tandem PIN solar cell structures. Device design concepts such as the incorporation of optically reflective back contacts have been tested.

2. EXPERIMENTAL METHODS

The deposition system used in this study has been described in more detail in another paper (7). Here we briefly review only the most important features and emphasize primarily the methods of device fabrication. The deposition system has stainless steel walls, held at ground potential and electrically insulated cathode and anode assemblies. The water cooled target, a polycrystalline silicon disk 5" in diameter and 1/4" thick, is supplied with an RF power at a frequency 13.56 MHz. The anode assembly, 26" in diameter, is held 2" below the target and can be grounded, floated or supplied with RF or DC electrical bias.

The main deposition variables were the partial pressures of argon and hydrogen, the concentrations of PH_3 and B_2H_6 in the sputtering gas and the target and substrate bias voltages.

The investigated devices have the configurations: substrate/N-I/Pt (or Pd), substrate/N-I-P/ITO, and substrate/P-I-N/ITO. All active layers (N,I,P) were deposited in the same deposition chamber but not sequentially. The deposition system was scrupulously cleaned between N and I or P and I layers.

The films were characterized for evidence of crystallinity by x-ray diffraction, and for hydrogen incorporation and bonding by infrared absorption spectroscopy. The optical absorption coefficient was calculated from optical transmission measurements. The conductivity was measured on samples deposited on quartz substrates.

Each device was characterized by measuring its I-V characteristics with a calibrated Xenon simulator and the spectral dependence of the collection efficiency (8). The short circuit current was calculated by integrating the spectral response with the (AM)1 solar spectrum (9).

3. EXPERIMENTAL RESULTS AND DISCUSSION

3.1 Photovoltaic properties of intrinsic films

The photovoltaic properties of the intrinsic films were found to depend sensitively on deposition parameters which affect their structural and compositional inhomogeneities as well as the amount of incorporated hydrogen and traces of phosphorus and boron impurities. Some of these properties have been described in a number of recent papers (10-17). In this article we present a comprehensive summary of these results.

3.1.1 Effect of Structural and compositional inhomogeneities

Structural studies on glow discharge and sputtered amorphous silicon films (2,18) revealed that the deposition of these films proceeds via nucleation and growth of island structures (average lateral dimensions $\sim$100Å). The coalescence of these islands if imperfect, leads to columnar morphology in subsequent growth. Another type of structural inhomogeneities are microvoids of about 10Å in diameter, which have been observed in small angle scattering experiments (19). The existence of such structural inhomogeneities in the silicon network are also expected to lead to compositional inhomogeneities upon alloying the material with hydrogen or other impurities. Such types of inhomogeneities have been observed

through NMR, neutron scattering and infrared vibrational studies (20-22). It has been shown that these type of structural and compositional inhomogeneities in sputtered material are controlled by charged particle bombardment during the growth of the film (7,18,23). Deposition parameters which affect charged particle bombardment are the pressure of sputtering gas, the target voltage and the substrate bias.

Structural and compositional inhomogeneities may affect the photovoltaic properties of the films in a variety of ways. An example of this is the introduction of dangling bond related defect, which control recombination, and another is the introduction of structural and compositional disorder, which affects the extend of the band tails and therefore influences carrier transport and optical properties (24). To illustrate this correlation we show in Figs. 1 and 2 the effect of argon pressure and target voltage respectively on the photovoltaic properties of the sputtered films.

Fig. 1 shows the I-V characteristics of a number of Schottky barrier structures having the configuration SS/N-I-Pd. The I-layer in these devices was deposited at 5, 10, 20 and 30 mTorr of argon and constant all other deposition parameters. Note that the films produced at argon pressures of 20 and 30 mTorr have poorer photovoltaic properties than those produced at 5 and 10 mTorr of argon. This result correlates fairly well with structural studies (7,18), which reveal no evidence of columnar morphology for films produced at low argon pressures and strong evidence of columnar morphology for films produced at high argon pressures.

Fig. 2 shows the spectral dependence of the collection efficiency for two series of Schottky barrier structures (SS/N-I-Pt) produced with the target voltage of the only variable. In one series the induced DC target voltage was maintained at -800 volts and in the other at -1000 volts. In each series the flow rates of H_2/Ar were varied from 0.1 to 0.2. Note that these spectra fall into two distinct groups, which correlate with the target voltage but not with the hydrogen content in the discharge. For the -800V samples the collection efficiency peaks at 450nm, while for the -1000V samples it peaks at 500nm. The fact that the collection efficiency of the devices produced at each target voltage is independent of hydrogen content is significant, and suggests that the observed effect is not related to changes of the optoelectronic properties of the films due to the hydrogen incorporation. Therefore, the shift of the peak of the collection efficiency towards the red part of the spectrum, as the target voltage (power in the discharge) increases, suggests that the electronic quality of the films improves with the power in the discharge. This is contrary to the findings (2) that the quality of the glow discharge amorphous silicon films improves with decreasing power in the discharge. The improvement of the sputtered material with the power in the discharge is believed to have originated in more perfect coalescence of the island structure due to additional bombardment by charged particles (11).

The substrate bias was found to have a significant effect on compositional inhomogeneities (bonding configuration of hydrogen) and on the optical properties of the films (7,10,23). The effect of such inhomogeneities on carrier transport and recombination and their combined effect on the photovoltaic properties is under current study.

3.1.2 Effect of hydrogen content

It has been shown (12,13) that the density of states in the middle of the gap depends exponentially on the partial pressure of hydrogen in the discharge and that these states control the electron-hole recombination in amorphous silicon solar cells. Since the states in the middle of the gap

determine both the width of the space charge region and electron hole recombination (diffusion length of the minority carriers), one would expect that the photovoltaic properties of the amorphous silicon films should improve with the amount of incorporated hydrogen. However, besides reducing the density of states in the middle of the gap, hydrogen incorporation also affects the optical properties of the films. As an illustration we show in Figure 3 the optical absorption constant vs. photon energy of the films whose collection efficiencies are shown in Figure 2. Note that the optical gap (26) of the films produced at -1000 volts has increased from 1.71 to 1.84 eV. This dual role of hydrogen in reducing the states in the middle of the gap while simultaneously increasing the optical gap is an unfortunate trade-off, since the photovoltaic properties of a semiconductor depend both on its ability to absorb a significant fraction of the solar spectrum and its ability to collect the photogenerated electron-hole pairs. This trade-off explains the insensitivity of the collection efficiency to hydrogen content. According to the data of Figures 2 and 3 films having optical gaps between 1.71 to 1.84 eV generate the same J_{sc}. Therefore, the larger gap material has a better photovoltaic potential because it produces the same current and higher open circuit voltage (14).

3.1.3 Effects of Phosphorus and boron impurities

The effects of phosphorus and boron impurities on the photovoltaic properties of the intrinsic films were investigated by studying N-I-Pt Schottky barrier structures, whose I-layer was contaminated intentionally with small amounts of PH_3 or B_2H_6 or both (16,17). The effects of phosphorus contamination and boron compensation of the intrinsic layer are shown in Fig. 4. Samples 295, 384 and 385 were prepared under the same deposition conditions for the I-layer but with progressively longer evacuation times between N and I depositions (20 min, 2h and 24h). Sample 387 was prepared under the same pumping mode as sample 385 but the I-layer was intentionally doped by adding 0.1 ppm of B_2H_6 in the sputtering gas. The improvement in the collection efficiency with evacuation time between N and I depositions is related to the decrease in phosphorus incorporation into the I-layer. The additional improvement in Sample 387 is related to boron compensation of residual phosphorus donors in the I-layer.

The effect of increasing the boron concentration in the I-layer beyond the value of total compensation is shown in Fig. 5. This figure shows the spectral dependence of the collection efficiency for three Schottky barrier structures having the configuration glass/SnO_2/N-I-Pt. The N-layer in all three samples was deposited in a different deposition run and the sputtering chamber was thoroughly cleaned before the deposition of the I-layer. The amount of B_2H_6 in the discharge during the growth of the I-layers was 0.02, 0.2 and 0.4 ppm for the samples 406, 478 and 468 respectively. Note that as the level of B_2H_6 in the discharge increased to more than about 0.1 ppm the quantum efficiency for blue-green light decreases significantly. However, the blue-green response is restored when the devices are illuminated from the glass side.

These results can be understood along the lines of recent doping models of amorphous silicon (27,28), which predict that substitutional doping can only occur in the presence of localized gap states and that the density and nature of these localized states is influenced by the position of the Fermi level. Overcompensation by boron renders the I-layer P-type and moves the major barrier to the I-N interface. Therefore, in such devices, illumination from the N-side gives better photovoltaic performance.

3.2 Properties of doped films

Phosphorus and boron doped films have been fabricated either in amorphous or microcrystalline form. We find that the critical parameter for the transition from the one regime to the other is the relative concentrations of hydrogen to argon in the discharge. Films produced under conditions of $H_2/Ar < 1$ were found by x-rays to be amorphous and those produced under $H_2/Ar >> 1$ were found to be partially crystallized. The mechanisms of crystallization and details of structural, optical and transport properties of both amorphous and microcrystalline films are discussed elsewhere (29,30). Here we give only a brief summary of the results which affect the performance of solar cell structures.

Fig. 6 shows the optical absorption constant vs photon energy for one amorphous boron doped film and two microcrystalline films one doped with phosphorus and the other with boron. The amorphous film was deposited at 325°C with H_2 + Ar = 5mT (H_2/Ar = 0.4) and 0.2 at.% of B_2H_6 in the discharge. The microcrystalline films were also deposited at 325°C with H_2 + Ar = 40 mT (H_2/Ar = 10) and 0.2 at.% of B_2H_6 or PH_3 in the discharge respectively. Note that for the same level of doping the microcrystalline films are far more transparent in the visible part of the spectrum than the amorphous films.

Besides the difference in their optical properties these films have also different transport properties. The amorphous film has room temperature conductivity of $10^{-4}\Omega^{-1}cm^{-1}$ and conductivity activation energy of 0.27eV. The microcrystalline films have room temperature conductivities of between 1 to 10 $\Omega^{-1}cm^{-1}$ and the weak temperature dependence suggests degenerate conduction. The microcrystalline doped films are therefore more suitable for photovoltaic applications than amorphous doped films.

3.3 Solar cells

Solar cell structures were fabricated in the configurations: SS/N-I-P/ITO and SS/P-I-N/ITO. The deposition chamber was cleaned between N and I or P and I depositions to minimize the phosphorus and boron contamination effects, which were discussed previously. Since boron contamination was found to be far more severe than phosphorus contamination the most efficient cells were fabricated with the first configuration. Besides contamination effects, the optical and transport properties of the doped layers were found to have a significant effect on the device performance. For example, devices fabricated with amorphous P and N layers were reported to have an efficiency of about 4% (31). This performance can be improved significantly upon using microcrystalline P and N layers, due to their high conductivity and reduced optical absorption in the visible spectral region. As an example, we show in Figs. 7 and 8 the I-V characteristics and the spectral dependence of the collection efficiency of one such device. The I-layer of this device was produced at 5 mTorr of Ar + H_2 (H_2/Ar = 0.18), at target voltage of -800 volts and deposition temperature of 325°C. The P and N layers were deposited under the conditions described in section 3.2. This solar cell structure generates a J_{sc} of $13^{mA}/cm^2$ and V_{oc} of 0.86 Volts. The efficiency of this device, 5.5%, is limited by the low FF of 0.49. In the following we discuss the factors which limit the efficiency of these devices and suggests methods for further improvments.

The low value of the FF is partly due to the degradation of the N-I interface which results from the need to clean the chamber between N and I depositions. It has been shown in another paper (16) that the FF increases from 0.49 to 0.57 as the evacuation time between N and I depositions decreases from 24h to 20 min. Also studies of the wavelength dependence of the FF were accounted for in terms of surface recombination at the N-I

interface (32). Therefore, the low value of the FF is not inherent, to the sputtered devices. Sequential deposition of all layers in interlocked, dedicated sputtering chambers should lead to FF's equivalent to those found in cells prepared by the glow discharge decomposition of silane process (1).

The J_{SC} can be increased by further improvements in the film's structural and compositional homogeneity and by improvements in the device design. As an example, we show in Fig. 9 how the incorporation of back reflective contacts can improve the red portion of the spectrum. The two devices have the configurations: substrate/N-I-P/ITO. In the one device the substrate is SS and in the other is SS/Ag/TiO_2. The TiO_2 layer, approximately 30 Å thick, acts to prevent diffusion of silver into the amorphous silicon. Incorporation of highly transparent a-SiC heterocontact should result in significant improvement in the blue part of the spectrum (1). Therefore, upon implementation of these device design concepts the J_{SC} should approach the values of cells produced by the glow discharge process.

The V_{OC} value is also expected to increase upon minimizing cross contamination and improving the device design. Values of V_{OC} as high as 0.95 Volts have already been observed in devices having the configuration: SS/N-I-P/ITO.

To further test the potential of this technology we fabricated tandem solar cell structures having the configuration: SS/N-I-P-N-I-P/ITO. The I-layers in both solar cells was made under the same conditions, and their thickness was not adjusted for current matching. The P and N layers were microcrystalline. The I-V characteristics of this device, shown in Fig. 10, suggests good junction characteristics. In particular, the tunneling between the microcrystalline P and N layers appears to be satisfactory. These initial results suggest that high efficiency tandem cells can be fabricated by the method of sputtering if a smaller gap material, made for example from α-SiGe alloys, is used as a back solar cells.

4. CONCLUSIONS

The studies presented in this paper showed that the properties of both the intrinsic and doped sputtered amorphous silicon films can be optimized to produce high efficiency solar cells.

The photovoltaic properties of the intrinsic films were found to depend sensitively on structural and compositional inhomogeneities, amount of incorporated hydrogen and low levels of dopant impurities.

Conditions for deposition of both amorphous as well as microcrystalline phosphorus and boron doped films have been identified. These films were characterized through studies of their optical and transport properties and the superiority of the microcrystalline films for photovoltaic applications has been demonstrated.

The combination of the best intrinsic and doped films led to the fabrication of P-I-N solar cell structures with efficiency 5.5%. We showed that this efficiency can be improved even further by depositing the three layers in sequential dedicated chambers and by implementing device design concepts such as back reflective contacts and highly transparent a-SiC front contacts. Finally, the photovoltaic potential of this technology was demonstrated through the fabrication of efficient tandem solar cell structures.

ACKNOWLEDGMENTS

The author is indebted to B. Abeles, G. Cody, P. Maruska, A. Rose, T. Tiedje and C. Wronski for a number of technical discussions and to R. Friedman and M. Hicks for technical assistance. The work was partially supported by the U.S. Department of Energy through a Solar Energy Research Institute Contract (Contract #ZB-3-02166-01).

REFERENCES

1. Catalano, A., D'Aiello, R. V., Dresner, J., Faughnan, B., Firester, A., Kane, J., Schade, H., Smith, Z. E., Swartz, G., and Triano, A. (1982). IEEE Photovoltaic Spec. Conf. 16, 1421.
2. Knights, J. C., and Lujan, R. A. (1979). Appl. Phys. Lett. 35, 244.
3. Hamakawa, Y., Fujimoto, K., Okuda, K., Kashima, Y., Nonomura, S., and Okamoto, H. (1983) Appl. Phys. Lett. 43, 644.
4. Thompson, M. J., Allison, J., Al-Kaisi, M. M., and Thomas, I. P. (1978). Rev. Phys. Appl. 13, 625.
5. Victorovitch, P., Jousse, D., Chenevas-Paule, A., and Licuz-Rocherz, L. (1979). Rev. Phys. Appl. 14, 204.
6. Amick, J. A., Schnable, G. L., Vossan, J. L. (1977). J. Vac. Sci. Technol. 14, 1053.
7. Moustakas, T. D. (1982). Sol. Energy Mater. 8, 187.
8. Wronski, C. R., Abeles, B., and Cody G. D. (1980) Solar Cells, 2, 245.
9. Bird, R., (1981). Terrestrial Solar Spectral Standards and Data Sets, SERI/TR-642-1149.
10. Moustakas, T. D. (1983). "Photovoltaics for Solar Energy Applications II", D. Adler, Ed., Proc. SPIE 407, 56.
11. Moustakas T. D., and Maruska, H. P. (1983) Appl. Phys. Lett. 43.
12. Tiedje, T., Moustakas, T. D. and Cebulka, J. M. (1981). Phys. Rev. B 23, 5634.
13. Moustakas, T. D., Wronski, C. R. and Tiedje, T. (1981). Appl. Phys. Lett. 39, 721.
14. Morel, D. L., and Moustakas, T. D. (1981). Appl. Phys. Lett. 39, 612.
15. Moustakas, T. D., Wronski, C. R., and Morel, D. L. (1980). J. Non-Crystall. Solids, 35-36, 719.
16. Moustakas, T. D., Friedman, R., Weinberger B. R. (1982). Appl Phys. Lett. 40, 587.
17. Moustakas, T. D., Maruska, H. P., Friedman, R., and Hicks M. (1983). Appl. Phys. Lett. 43, 368.
18. Ross, R. C., and Messier, R. (1981). J. Appl. Phys. 52, 5329.
19. D'Andonio, P., and Konnert, J. H. (1979). Phys. Rev. Lett. 43, 1161.
20. Jeffrey, F. R., Lowry, M. E., Garcia, M. L. Barnes, R. G., and Torgeson, D. E. (1981) In "Tetrahedrally Bonded Amorphous Semiconductors" (R. A. Street, D. K. Biegelsen, and J. C. Knights, eds) p. 83, Am. Inst. Phys. New York.
21. Postol, T. A., Falco, C. M., Campuirth, R. T., Schuller, I. K. and Yelon W. B. (1980) Phys. Rev. Lett. 45, 648.
22. Freeman, E. C., and Paul, W. (1978). Phys. Rev. B 18, 4288.
23. Moustakas, T. D. (1984). In "Hydrogenated Amorphous Silicon/Semiconductors and Semimetals", Ed. by J. Pankove (Academic Press, New York).
24. Cody, G. D., Tiedje, T., Abeles, B., Brooks, B., and Goldstein, Y. (1981). Phys. Rev. Lett. 47, 1480.
25. Movchan, B. A., and Demshishin, A. V. (1969). Fiz. Met Metalloved, 28 653.

26. The optical gap, Eg., is defined by the relation: $(ahv)^{1/2} = B(hv-Eg)$.
27. Adler, D., (1978). Phys. Rev. Lett. 41, 1755.
28. Street, R. A. (1982). Phys. Rev. Lett. 49, 1187.
29. Moustakas, T. D., Maruska, H. P., Friedman R., and Hicks, M. (To be published).
30. Moustakas, T. D., and Maruska, H. P. (To be published).
31. Moustakas, T. D., and Friedman, R. (1982). Appl. Phys. Lett. 40, 515.
32. Maruska, H. P., and Moustakas, T. D. (To be published).

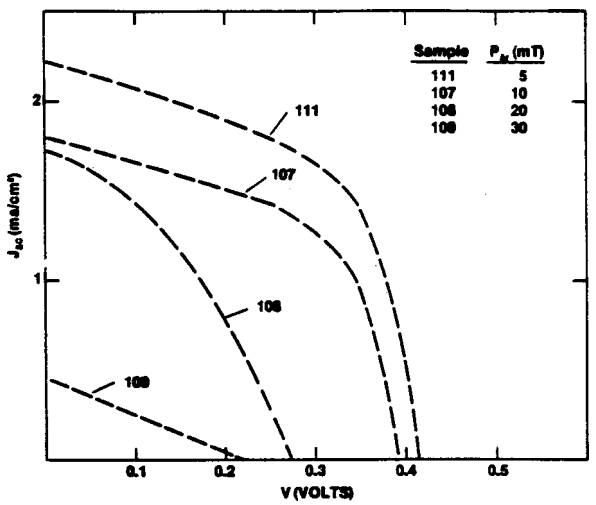

Figure 1. I-V Characteristics of N-I-Pd Schottky Barrier structures.

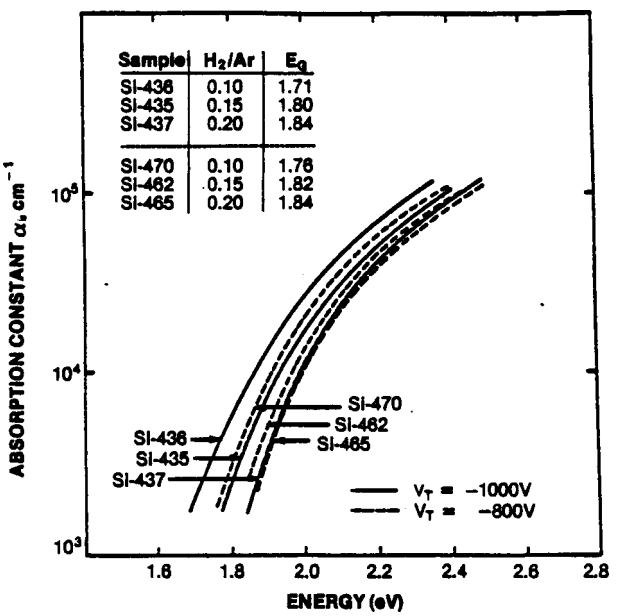

Figure 3. Optical Absorption Constant vs. Photon Energy for Two Series of Films Produced under Target Voltage of −1000 V and −800 V

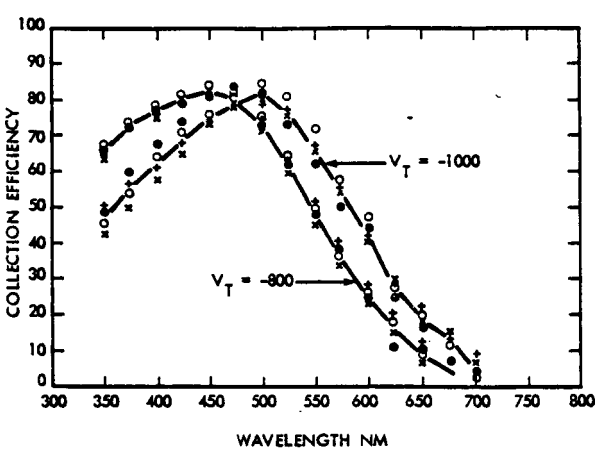

Figure 2. Spectral Dependence of the Collection Efficiency of two Series of N-I-Pt Devices, Made at Indicated Voltages.

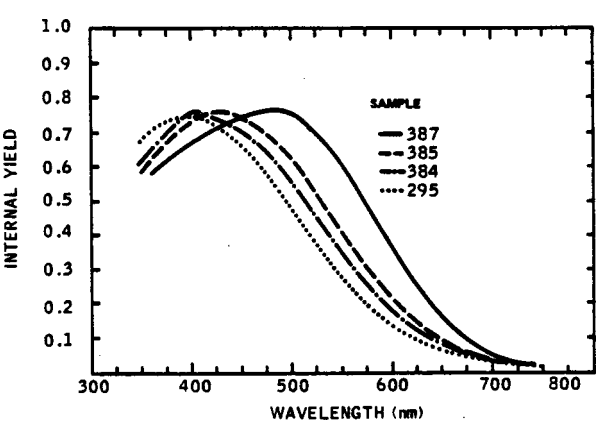

Figure 4. Effect of Phosphorus Contamination and Boron Compensation on the Collection Efficiency of N-I-Pt Devices

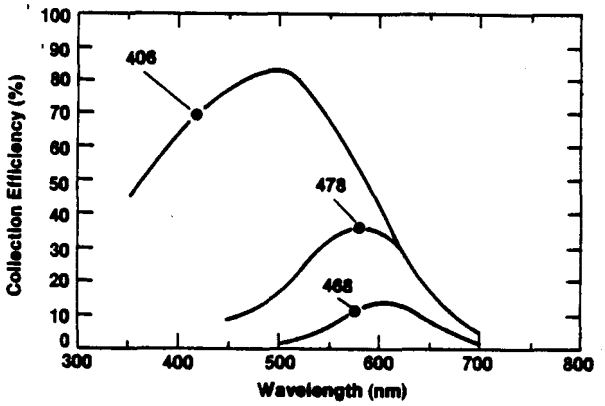

Figure 5. Effect of Boron Compensation on Spectral Dependence of Collection Efficiency of N-i-Pt Devices.

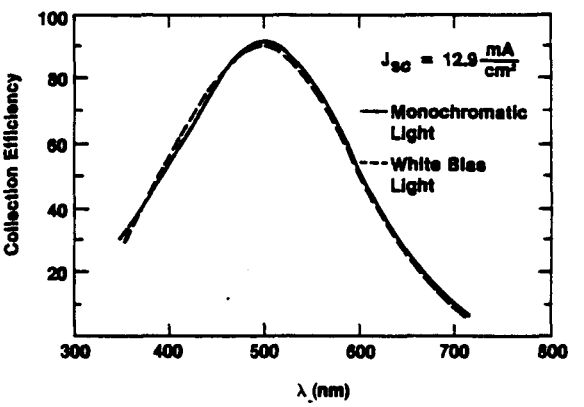

Figure 8. Spectral Dependence of the Collection Efficiency of the Device Shown in Figure 7.

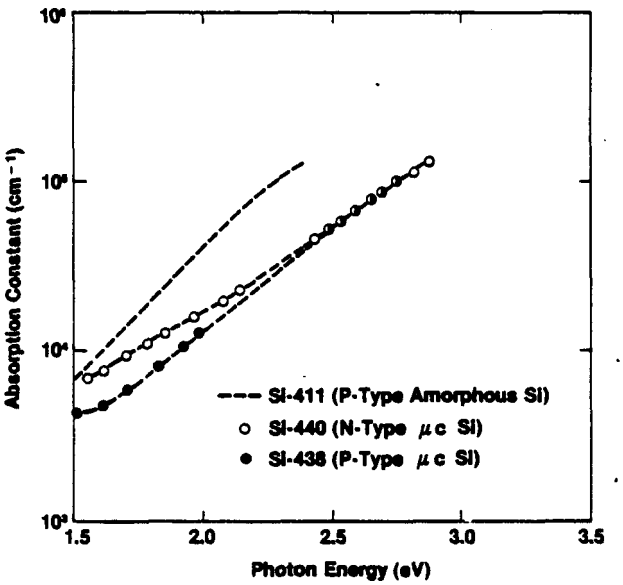

Figure 6. Optical Absorption Constant vs. Photon Energy for Amorphous and Microcrystalline Silicon Doped Films

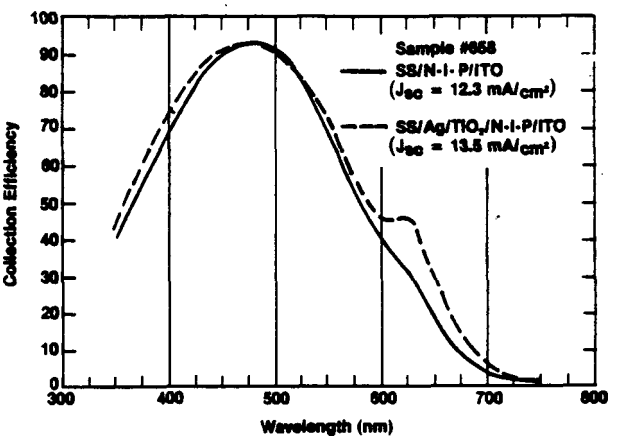

Figure 9. The Effect of Substrate Reflectivity on the Spectral Dependence of the Collection Efficiency of Sputtered Solar Cells

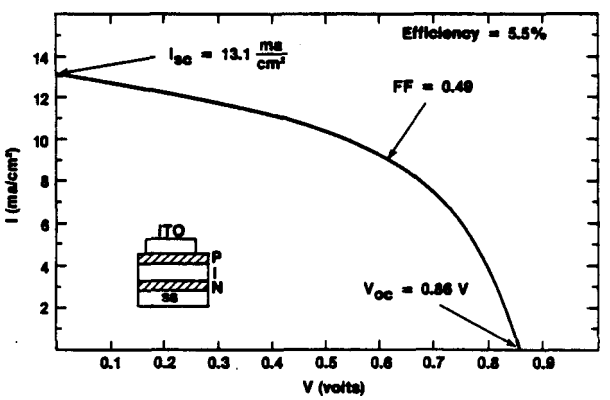

Figure 7. I-V Characteristics of a Sputtered SS/NIP/ITO Solar Cell Structure.

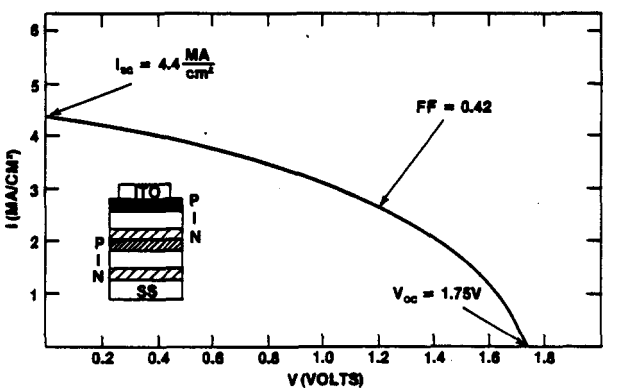

Figure 10. I-V Characteristics of a Sputtered SS/NIP NIP/ITO Solar Cell Structure

APPENDIX L. Influence of the Wavelength of Incident Light on Shunt Conductance and Fill Factor in Amorphous Silicon Solar Cells

INFLUENCE OF THE WAVELENGTH OF INCIDENT LIGHT ON SHUNT CONDUCTANCE AND FILL FACTOR IN AMORPHOUS SILICON SOLAR CELLS

H. Paul Maruska and T. D. Moustakas
Exxon Research and Engineering Company
Clinton Township
Route 22 East
Annandale, New Jersey 08801

ABSTRACT

A variety of a-Si solar cells (n-i-m and n-i-p structures) were prepared by the method of sputtering. The photoconductive shunt resistance was obtained from the light I-V characteristics in far reverse bias, and the influence of this parameter on the fill factor was studied. Correlations were sought between fill factors, diffusion lengths, collection widths and the hydrogen concentration in the i-layer. The fill factors were found to vary with the wavelengths of the light under which an I-V curve was measured, and for certain cells with poorer overall fill factors, lower values were obtained in both the red and the blue portions of the spectrum. The decreased values at the ends of the spectrum were ascribed to recombination of the photo-generated carriers at both the front and the back contacts to the i-layer.

1. INTRODUCTION

RF Sputtering has been demonstrated to be a viable technique for fabricating high efficiency a-Si solar cells (1). However, a problem remains in that the Fill Factors tend to be somewhat low. Fill Factor is determined by (a) shunt and series resistance, (b) any voltage dependence of the photocurrent and (c) the "dark" I-V characteristic. The work reported herein takes a closer look at the parameters influencing the Fill Factor in a-Si devices.

The solar cells used in this study were of both the n-i-m (Schottky Barrier) and n-i-p types. Preparation conditions for these Sputtered devices have been described earlier (1,2). All of the layers were deposited in the same deposition chamber, but not sequentially. We have shown that unless the system is scrupulously cleaned between the n and i-layer depositions, phosphorus contamination degrades the performance of the i-layer.(3) However, one must be concerned that stopping the discharge and removing the sample to clean the system may have adverse effects on the quality of the n-i interface. The same concern applies to the i-m interface because the metal film is formed in a separate run also. The illuminated current-voltage characteristics (in simulated AM1 sunlight) and the spectral dependence of the collection efficiency were measured for each sample. The devices which are included in this paper where chosen to illustrate various facets of the Fill Factor problem, and do not necessarily portray our highest efficiencies.

2. LIGHT I-V CHARACTERISTICS: GENERAL CONSIDERATIONS OF SERIES AND SHUNT RESISTANCES

2.1 Series and Shunt Resistance

The shape of the light I-V characteristic, and thus, the magnitude of the maximum power, can be adversely affected by series and shunt resistances

which may be present in the cell. A current flowing through a shunt resistor is in parallel with the photocurrent, but of opposite sign, and, therefore, causes the I-V curve to slope downward in the low voltage section. Shunt resistance also decreases the open circuit voltage. On the other hand, series resistance tends to increase the "dark current" because it forward biases the cell. This increase in "dark current" is substantial only at large voltages, near V_{OC}, so R_S will generally influence the high voltage portion of the curve. However, a large R_S will also reduce I_{SC}, and, in fact, can make the I-V characteristic a straight line, according to

$$V = IR_S + \frac{kT}{q} \ln \left(\frac{I-I_L}{I_o}\right), \qquad (1)$$

where I_L is the photogenerated current and I_o is the dark saturation current. If $I << I_L$, then the second term is essentially V_{OC}, and this is the equation of a straight line. This condition is met for large R_S.

In the case where both shunt and series resistance are present simultaneously, then even small values of R_S can lead to a decrease in I_{SC}, well before the characteristic becomes a straight line. This will happen because the forward bias developed across R_S will cause a shunt current to flow in opposition to the photocurrent.

The values of shunt resistance in illuminated cells (white light) were measured for a number of sputtered a-Si cells and are listed in Table I. All of the values have been normalized to an area of 1 cm^2. Measurements were taken at reverse biases greater than 3 or 4 volts, where the characteristic becomes completely linear. For Schottky barrier cells, R_{SH} is between 2000-4000Ω, while for most N-I-P cells it falls between 3000-5000Ω, although one cell was as high as 9000Ω. The results are quite different in the dark. Most cells have dark shunt resistances >1 megohm, and, thus, are essentially free

of mechanical shunts (i.e. pin holes which allow the front and back contacts to touch). Occasionally there are cells with such mechanical shunts, but these cells then have poor characteristics and we will not discuss them further. It is seen, therefore, that the shunting that we are concerned with turns out to be photoconductive.

We have also measured the series resistance as the slope of the linear portion of the light I-V at far forward bias. As a check of this technique, we remeasured each device with a fixed resistor of known value in series with it, whereupon the slope of the line was found to be the sum of the internal (cell) and external (fixed) resistances. These data are also presented in Table I. It is seen that the series resistance of all of these cells falls between 15-25Ω.

2.2 Applicability of the Shifting Approximation

Generally one can attempt to describe the current in an illuminated solar cell as the sum of the dark current-voltage characteristic (the forward bias diode current) and the photogenerated current. The basis for this is the superposition principle. If the use of the superposition principle is valid, then the total current is the sum of the response to several excitations applied independently, one at a time. In the case in question, one excitation would be the optical generation rate G of free carriers due to sunlight, while the other would be the excess injected carrier concentration N due to the applied voltage across the terminals. For superposition to apply, control of these excitations must be independent. That is, one must be able to set the generation rate G=0 and determine N due to the terminal voltage (by darkening the cell), and then set N=0 (by shorting the cell) while having an optical excitation G. At least three conditions must be

met: (a) the junction space charge region must not control both the photocurrent and the dark current, (b) there must be no series resistance, (c) all material parameters must be independent of illumination level. (4)

A solar cell with significant R_S can be treated analytically by separating the series resistance from the intrinsic junction system. (4) When the applied voltage V_a is set equal to 0, the intrinsic device voltage $V_I = V_a + IR_S$ is not zero due to R_S, and, thus, $N \neq 0$. In fact,

$$N = N_o[\exp(qV_a kT)\exp(qIR_S/kT) - 1] \qquad (2)$$

To obtain the condition N = 0, one must apply a reverse voltage to the device with magnitude equal to IR_S.

Rothwarf (5) has pointed out that in certain types of devices, especially amorphous silicon and Cu_2S/CdS cells, the photocurrent is voltage dependent, and the forward bias diode current is modified by light. These cases can be treated (5) by the following generalized form of the superposition principle:

$$J(V) = J'_D(V) - J_L(V) \qquad (3)$$

Here $J'_D(V)$ is the diode forward bias current that would exist in the dark if the conditions present in the light could be maintained in the dark, and $J_L(V)$ is the voltage dependent photocurrent. That is, a functional form for $J'_D(V)$ can be found such that the measured illuminated current-voltage characteristics can be generated from Equation (3).

2.3 Simulated I-V Characteristics for Sputtered Cells

Calculations were made to simulate I-V characteristics which are consistent with the limitations just discussed. The model started with a current generator of assumed fixed magnitude, I_L, and with shunt conductance G_{SH} ($G_{SH} = 1/R_{SH}$) and series resistance R_S, both of constant magnitude. Then one can write,

$$I = I_0 \exp\left(\frac{q}{nkT}(V-IR_S)\right) + (V-IR_S)G_{SH} - I_0 + I_L \ , \qquad (4)$$

where the values of I_0 and n must correspond to $J'_D(V)$, not the measured dark current. Here we are taking $I_L = -10mA/cm^2$, $I_0 = 5 \times 10^{-12}A/cm^2$, $K = q/nkT = 26.6$ volts^{-1}. The results for R_S=20Ω and R_{SH} between 100 and 500Ω are shown in Figure 1. The fill factors vary from 0.33 with R_{SH}=100Ω to 0.57 for R_{SH}=500Ω. Notice how the short circuit current is reduced by lowering the shunt resistance: this will only occur if series resistance is simultaneously present.

In our cells we commonly encounter fill factors between 0.40 and 0.60. Figure 1 then indicates that $125 < R_{SH} < 550\Omega$. However, we noted above that the photoconductive shunt measured in far reverse bias (Table 1) is typically several thousand ohms, and is, therefore, much too large to account for fill factors in the range of 0.40-0.60. The assumption of constant I_L consequently is in doubt.

We compare the computer simulation with the measured data for nip cell Si-403 in Figure 2. The cell current was normalized (actual J_{SC}=9.8 mA/cm^2) for comparison. A very close fit to the data is achieved by using R_S=20Ω and R_{SH}=200Ω, while Table I shows the actual R_{SH} for this device to be 5100Ω. We suggest that the "shunt resistance" of 200Ω might be represented

by an equivalent "resistor" related to the voltage dependence of the photocurrent. Accordingly, we can write,

$$I_L(V) = I_{LO} - V/R_{SH}, \tag{5}$$

where I_{LO} is the uncompensated photocurrent. The origin of this closely linear dependence of $I_L(V)$ on V is discussed in detail below.

As a further indication that the photoconductive shunt that we measured under reverse bias is not the major determinant of the fill factor, we show in Figure 3 experimental data for cells made under different conditions which exhibit no correlation between fill factor and the slope of the I-V curve in far reverse bias.

2.4 Voltage-Dependent Photocurrent

Recently, Crandall (6) has obtained an approximate solution for the voltage dependence of the photocurrent. He considered the case of a P-I-N device with a low density of gap states, so that the electric field E is constant (a Mott barrier). He neglected diffusion and assumed long wavelength, uniformly-absorbed light. Then the transport equations become

$$-\mu_p E \frac{dp}{dx} - R + G = 0 \tag{6}$$

$$\mu_n E \frac{dn}{dx} - R + G = 0 \tag{7}$$

where R is the recombination and G is the generation term. The boundary conditions were $p(o) = n(L) = 0$. The I-layer had a thickness L, and light was incident through the N-layer at x=o.

To account for recombination, a regional approximation was used. From x=o to $x=X_c$, it was assumed that $R = p/\tau_p$, which is to say that

the recombination is dominated by the low hole concentration in the vicinity of the N-type contact. From $x=X_c$ to $x=L$, $R=n/\tau_n$, so that electrons dominate. The solution of the equations is

$$\text{Region 1:} \quad p = G\tau_p[1-\exp(-x/\ell_p)] \tag{8}$$

$$\text{Region 2:} \quad n = G\tau_n[1-\exp(x-L)/\ell_n] \tag{9}$$

AT $x=X_c$, $p/\tau_n = n/\tau_n$ so that

$$X_c = L/(1+\ell_n/\ell_p) \tag{10}$$

Here, $$\ell_n = \mu_n\tau_n E, \quad \ell_p = \mu_p\tau_p E \tag{11}$$

Since

$$J = q(\mu_n nE + \mu_p pE), \tag{12}$$

when this is evaluated at $x=X_c$, it yields

$$J=qG(\ell_n+\ell_p)[1-\exp\{-L/(\ell_n+\ell_p)\}] \tag{13}$$

If the sum of the drift lengths is taken, so that $\ell=\ell_n+\ell_p$, and using equations (11), then

$$J=qG\left(\frac{\mu T}{L}\right)V\left[1-\exp\left(-\frac{L^2}{\mu\tau V}\right)\right] \tag{14}$$

We will now show that this equation can be approximated as linear when the applied voltage is small. Let V_a = applied voltage and V_o = built-in voltage of the junction, so that

$$V = V_o - V_a, \tag{15}$$

and let $V_T = L^2/\mu\tau$. Thus,

$$J=qGL\left(\frac{V_o-V_a}{V_T}\right)\left[1-\exp\left(\frac{-V_T}{V_o-V_a}\right)\right] \tag{16}$$

As long as $(V_o-V_a) >> V_T$, this can be expanded to give

$$J \approx qGL \left[\left(1 - \frac{1}{2} \frac{V_T}{V_o} \right) - \left(\frac{1}{2} \frac{V_T}{V_o^2} \right) V_a \right] \qquad (17)$$

This equation has the form $J=J_L + G_{SH}V_a$, which was equation (5) above. It should be stressed that this equation gives only the photocurrent, not the total cell current. However, at low forward voltages where the dark current is very small, and if true shunt currents are negligible, then it will indicate the initial slope of an illuminated I-V curve as well. This treatment can be generalized to more complex forms of the electric field. One must keep in mind that equation (17) was derived only for uniformly absorbed light, not for the case of sunlight shown in Figure 3. However, it will be shown below that the overall fill factor of a device is often governed by the spectral portion of the absorbed light which has the poorest fill factor.

3. INFLUENCE OF WAVELENGTH ON THE LIGHT I-V CHARACTERISTICS

3.1 Depletion width, diffusion length, collection width

Two series of Schottky barrier devices were made with varying concentrations of hydrogen in the discharge between 10 and 20%,[2] the first series using a target voltage V_T=-1000 and the second V_T=-800.[7] It was found that the illuminated current-voltage characteristics and the spectral responses fell into two distinct groups, so that the fill factor (FF) and the peak of the response for any sample was correlated with V_T, but was essentially independent of the hydrogen content.[7] For any of the 800 Volt samples the peak response was at 450nm and FF was around .55, while for the 1000 Volt samples the peak was at 500nm and FF was around 0.50. The spectral responses are shown in Figure 4. The difference in the red response of the two series can be related to differences in the collection width X_C.

Optical absorption measurements indicated that for both sets of samples, the optical band gap increased to higher energies as the hydrogen content of the samples was increased, as shown in Table II. Thus, one would have expected the peak of the spectral response in either series to shift to shorter wavelengths with increased hydrogen content, unless the collection width also increased proportionately with hydrogen content. Furthermore, one could expect that the larger blue response of the 800V samples would be related to the presence of lower values of the depletion width X_o. To see this, recall that the electric field in a-Si devices is given by[8]

$$E = - \frac{V_o}{X_o} \exp (-x/X_o), \tag{18}$$

so that a larger value of X_o will lower the field at the front contact and thus reduce the force driving electrons into the bulk and away from recombination centers at the m-i interface.

Using the measured values of optical absorption and spectral response, the value of the hole diffusion length L_p as well as X_o were calculated according to the formulation of Dina Gutkowicz-Krusin[9]. In that work, exact solutions for the photogenerated carrier densities and carrier collection efficiencies in a-Si Schottky barrier cells were produced, and the dependence of the collection efficiency on device thickness, hole diffusion length, absorption constant, and depletion width was determined. The theory can be used to determine these parameters from experimental measurements. (The boundary condition at the front contact was taken to be infinite recombination velocity, so that values of X_o found from this treatment may be underestimated). The results for the samples

in our study are listed in Table II. (Lengths are given in microns, energies in eV).

It is relatively straightforward to determine the collection width X_C for all the cells by using the long wavelength response and the optical absorption data that is available. Basically, X_C should be the sum of X_O and L_p, because it represents the distance over which photogenerated carriers can be collected, either by drift or diffusion processes. The collection efficiency in the long wavelength range can be represented by[10]

$$Y = B[1-\exp(-\alpha X_C)] \tag{19}$$

where α is the absorption constant and B is an adjustable parameter.

We have plotted the quantity $-\ell n[1-Y/B]$ vs α for all of the samples, and from the slopes of the lines, values of X_C were determined. The values of X_C are plotted against the bandgaps of the respective devices in Figure 5. It is clear from this figure that as the hydrogen content is increased, and hence the bandgap is increased, so is the collection width increased. Furthermore, the 1000V samples always have a larger collection width at any hydrogen concentration than the corresponding 800V sample. Thus we now find that the shift in the peak position towards the blue is not only due to the higher bandgaps of the 800V samples, but is also due to their poorer collection widths. However, the 1000V samples all exhibit a larger magnitude of the depletion region width X_O, which causes a lowering of the electric field at the front surface and thus leads to a loss in blue response. Thus the half-width of all the responses remains the same.

3.2 Determination of Fill Factor

It was noted above that for these two sets of samples, the fill factors (FF) from the illuminated current-voltage characteristics also fell into two distinct groups, with FF around 0.50 for the cells made at 1000V, and around 0.55 for those made at 800V. Let us explore this in more detail. We will concentrate on two samples which were both made with 20% hydrogen in Argon in the discharge,[11] but the results apply to the other sample as well. Sample Si-437 was made at 1000V, while Si-465 was made at 800V.

The illuminated I-V characteristics for these two cells are shown in Figure 6. Here we see that Si-437 has the larger AM1 short circuit current (10.7 mA/cm^2 as opposed to 8.7 mA/cm^2 for Si-465), but it has a fill factor of 0.51 in contrast to 0.57 for Si-465. We also show a calculated I-V characteristic (dotted line) which would have given FF=0.57 for Si-437. It is clear that most of the loss in FF for Si-437 occurs in the low voltage region: in fact, the two devices exhibit parallel characteristics near V_{OC}. This indicates that they have essentially the same series resistance.

The lower value of J_{SC} for Si-465 becomes apparent from an inspection of the spectral response curves shown in Figure 7. The quantum efficiency of cell Si-465 peaks at 450 nm, a region of the spectrum with decreased solar intensity. The incremental current J_{SCi} generated in each 25 nm of bandwidth for both devices is also presented in this figure. The values of current were obtained by integrating the quantum efficiency with the SERI Global Horizontal AM1 solar spectrum.[12] Calculated this way, the total current for Si-437 is 10.7 mA/cm^2 and that for Si-465 is 9.3 mA/cm^2, which is in fairly good agreement with the solar simulator results (Figure 6). Notice that although the two quantum efficiency curves have essentially the same half-width, and are just shifted from one another by 50 nm, the current gained by Si-465 in the blue is more than offset by the current gained by Si-437 in the red.

We have also measured a series of power curves for these cells which were generated in response to monochromatic light, and representative examples of the data for Si-437 are shown in Figure 8. At each wavelength where a measurement was taken, the intensity of the monochromatic light was adjusted so as to maintain a constant J_{SC}. At each chosen wavelength, the fill factor FF_i was calculated, and these values for the two devices in question are collected in Figure 7. There is a striking difference in the results for the two samples: Although they both have the same fill factor in the green portion of the spectrum (475-550 nm), the fill factor of Si-465 is definitely superior in both the red and the blue regions.

The fill factor can be used as a measure of how rapidly the photocurrent decreases with forward bias. (Refer to Section 2, above.) Thus, knowing the incremental short circuit current J_{SCi} for each 25 nm of bandwidth in the spectral response, and the corresponding fill factor FF_i in each appropriate wavelength range, we can make a summation over all wavelengths of interest and calculate what the current should be at the maximum power point. (This essentially neglects the effects of R_S.) By taking the ratio of the calculated total current at the maximum power point to the measured total short circuit current, we can determine the overall fill factor that will occur in response to the total spectrum. That is

$$FF = \frac{\Sigma_i FF_i \, J_{SCi}}{\Sigma \, J_{SCi}} \qquad (20)$$

Using this technique, we have obtained FF=0.55 for Si-437 and FF=0.59 for Si-465. Although both values are a little larger than the corresponding numbers for the AM1 measurements, (.51 and .57, respectively) they are in the correct order and have approximately the same ratio. The discrepancy probably indicates that the incremental FF's came out slightly too high because the

monochromatic measurements were made at intensities significantly below AM1, and the series resistance effects were neglected. Because both samples appear to have the same series resistance, the slight increase in FF that occurs as the light level is reduced should be the same in both samples.

We next investigated whether it is the red or the blue portions of the spectrum that contribute most to the lower overall FF in Si-437. First we substituted the FF_i values for the blue region, i.e., $350<\lambda<475$ nm, that were found for Si-465 in place of those measured for Si-437. We then proceded again to calculate the incremental currents at the maximum power point ($J_{SCi} \times FF_i$) and then to take the sum. In this case, the overall fill factor for Si-437 came out to be 0.57, as opposed to 0.55 earlier. We made this exchange of the values of FF_i for Si-465 in place of Si-437 again for wavelengths in the red, $550<\lambda<725$ nm. In this case again, the overall fill factor came out to be 0.57 for Si-437. When we used the entire set of FF_i from Si-465 in place of those from Si-437, we got FF=0.59, just the same as the actual value for Si-465, calculated by this method. Thus we see that the reduced values of incremental fill factor FF_i in both the red and the blue spectral regions share equally in the overall lowering of the total FF of Si-437, as compared to that of Si-465.

4. DISCUSSION

There is an apparent paradox here. The 1000V samples have poorer fill factors than the 800V samples, even though they have significantly larger values of collection widths and diffusion lengths. We previously noted that FF is around 0.50 for the 1000V samples and around 0.55 for the 800V samples. Furthermore, when the fill factors were examined monochromatically,

it was found that they agreed in the green portion of the spectrum for both types of samples, but the 1000V samples had consistently lower FF's in the blue and red portions. For a-Si solar cells, where the major portion of the current is generated in the depletion region, the fill factor indicates how rapidly the photocurrent decreases with increasing forward bias, i.e., with decreasing internal electric field, as shown earlier. Examples of I-V characteristics taken with 350, 450 and 650 nm light for the 1000V sample Si-437 were shown in Figure 8. Notice in this figure that the reduced fill factors with both violet and red light are mainly attributable to larger slopes in the I-V characteristic in the low voltage section: we would expect that if the problem with violet light were related to series resistance (lack of photoconductivi in the rear low-field region due to poor penetration of 350 nm light) then instead the slope of the high voltage portion would be significantly changing. The 650 nm curve has also a reduced V_{OC}, which is characteristic of "shunt-like" problems, as indicated earlier.

Notice now also the reverse-bias characteristics of Si-437 taken with monochromatic light, shown in Figure 9. The reverse-bias current is dramatically increased at negative voltages, (i.e., increased electric field) when the illumination is red light (600, 700 nm) or violet light (350, 400 nm). However, there is little increase for the curves generated with green light (450, 500 nm). Thus we see the importance of the electric field for the collection of carriers generated either near the front surface or deep in the bulk. For sample Si-465, there is no change in the reverse-bias characteristics taken at wavelengths below 500 nm, which is consistent with constant values of fill factor at these wavelengths. Also, the red light characteristics of Si-465 do not show as much of an increase in reverse bias as do those of Si-437.

Thus it appears that the lower fill factor shown by the 1000V sample with violet light may be due to back diffusion of photogenerated electrons, against the action of the field, into the front metal contact where they are lost. This problem becomes aggravated as the field is reduced (forward bias). The magnitude of this problem depends on the surface recombination velocity at the m-i interface. Next, one might be tempted to ascribe the low red light FF to poor diffusion lengths: as forward bias is applied the collection width decreases, and it becomes more difficult to collect at the front metal contact the holes generated deep in the sample by red light. But we found that the 800V samples had better overall fill factors inspite of having lower diffusion lengths, and especially, better incremental fill factors in the red. A more reasonable explanation is the loss of holes by back diffusion into the rear n-type contact. This problem is again aggravated by forward bias, which reduces the magnitude of the electric field and the depletion width. Once again, the surface recombination velocity, this time at the i-n interface, controls the situation. The samples made at the higher target voltage could have a greater surface recombination velocity at the m-i and the i-n interfaces due to the bombardment effects during the time between the actual depositions of the various layers. However, the structure of the i-layer itself is improved by having more energetic species impinging during the growth, which have greater surface mobility, and this leads to a longer diffusion length.

Furthermore, the problems of surface contamination and subsequent degradation of performance which can result from removing the samples from the chamber between the deposition of each layer, as described at the beginning of this work, may well be the cause for the generally lower Fill Factors we have encountered with sputtered a-Si cells. Sequential deposition of all layers in

interlocked, dedicated sputtering chambers should lead to Fill Factors equivalent to those found in cells prepared by other techniques.

5. CONCLUSION

The slope of the low voltage portion of the I-V characteristics of sputtered a-Si solar cells cannot be correlated with the shunt conductance which is determined from reverse bias. A voltage dependence of the photogenerated current is indicated, and this process lowers the fill factor.

Recombination at the front and rear surfaces of the i-layer in sputtered a-Si Schottky barrier devices affects the fill factor values obtained in response to blue and red light, respectively. The problem can be related to surface bombardment effects at high target voltages during the sputter deposition process. However, the higher voltage provides more energetic and hence more mobile species during the growth of the i-layer. Thus, the i-layer acquires a better structure, and the diffusion length improves. Unfortunately, the two processes are contradictory, so little overall improvements in efficiency is observed with this particular change in the deposition parameters. However, preparation of the layers in a sequential dedicated system is expected to lead to better interfaces and hence higher performance.

6. ACKNOWLEDGMENT

This work was sponsored in part by the Solar Energy Research Institute under contract No. XZ-0-9219. It is a pleasure to thank Dr. Christopher R. Wronski for many helpful discussions during the course of this work. We wish to thank Michael C. Hicks, Robert Friedman, and Collins Mikesell for excellent technical assistance.

REFERENCES

1. T. D. Moustakas and R. Friedman, "Amorphous silicon p-i-n solar cells fabricated by reactive sputtering", Appl. Phys. Lett., Vol. 40, No. 2, pp. 515-517, 1982.

2. D. L. Morel and T. D. Moustakas, "Effect of hydrogen on the diode properties of reactively sputtered amorphous silicon Schottky barrier structures", Appl. Phys. Lett., Vol. 39, No. 8, pp. 612-614, 1981.

3. T. D. Moustakas, R. Friedman and B. R. Weinberger, "Effect of phosphorus and boron impurities on amorphous silicon solar cells", Appl. Phys. Lett. Vol. 40, No. 7, pp.587-588, 1982.

4. F. A. Lindholm, J. F. Fossum and E. L. Burgess, "Basic corrections to predictions of solar cell performance required by nonlinearities", Proc. 12th Photovoltaic Specialists Conf. (Baton Rouge, LA), New York: IEEE Press, 1976, pp. 33-39.

5. Allen Rothwarf, "The superposition principle for current in solar cells", Proc. 13th Photovoltaic Specialists Conf. (Washington, DC), New York: IEEE Press, 1978, pp. 1312-1317.

6. Richard S. Crandall, "Transport in hydrogenated amorphous silicon p-i-n solar cells", J. Appl. Phys., Vol. 53, No. 4, pp. 3350-3352, 1982.

7. T.D. Moustakas and H. P. Maruska, "Effect of power and hydrogen in the discharge on the photovoltaic properties of sputtered amorphous silicon", Appl. Phys. Lett., Vol. 43, No. 11, pp. 1037-1039, 1983.

8. T. D. Moustakas, C. R. Wronski and T. Tiedje, "Electron-hole recombination in reactively sputtered amorphous silicon solar cells," Appl. Phys. Lett., Vol. 39, no. 9, pp. 721-723, 1981.

9. Dina Gutkowicz-Krusin, "On the carrier collection efficiency of amorphous silicon hydride Schottky barrier solar cells: Effect of recombination," J. Appl. Phys. vol. 52, no. 8, pp. 5370-5376, 1981.

10. T. D. Moustakas, C. R. Wronski, and D. L. Morel, "Photovoltaic properties of reactively sputtered a-SiH_x films," Journal of Non-Crystalline Solids, Vols. 35 & 36, pp. 719-724, 1980.

11. T. D. Moustakas, J. T. Tiedje, and W. A. Lanford, "Experimental Evidence for a kinetic model of hydrogen incorporation into sputtered a-Si", Proc. Conf. on Tetrahedrally Bonded Amorphous Semiconductors, in AIP Conf. Proc. 73, 20, 1981.

12. R. Bird, "Terrestrial Solar Spectral Standards and Data Sets", SERI/TR-642-1149 (1981).

TABLE I

Shunt and Series Resistance of Sputtered a-Si Cells, Normalized to 1 cm^2 Area

a. Schottky Barrier Cells (nim)

Cell #	R_{SH}, Ω	R_S, Ω
295	5500	--
380	4200	--
384	6200	25
385	5200	--
386	6800	--

b. nip Cells

Cell #	R_{SH}, Ω	R_S, Ω
274	3700	13
390	3200	--
397	4800	16
399	4600	21
400	4250	--
401	3150	
403	5100	15
424	9000	22
425	7000	21

TABLE II

PARAMETERS FOR SCHOTTKY BARRIER CELLS

Sample	Target Voltage	% H_2	Band Gap	FF	X_o	L_p	X_c
Si-436	1000	10	1.71	.47	.13	.045	.165
Si-435	1000	15	1.80	.52	.14	.052	.195
Si-437	1000	20	1.84	.51	.33	.110	.32
Si-470	800	10	1.76	.54	.10	.032	.13
Si-462	800	15	1.82	.55	.11	.043	.17
Si-465	800	20	1.84	.57	.12	.043	.185

FIGURE 1: Calculated light IV characteristics, using $R_s = 20\,\Omega$, $I_L = -10\ mA/cm^2$, $I_o = 5 \times 10^{-12}\ A/cm^2$, $n = 1.5$.

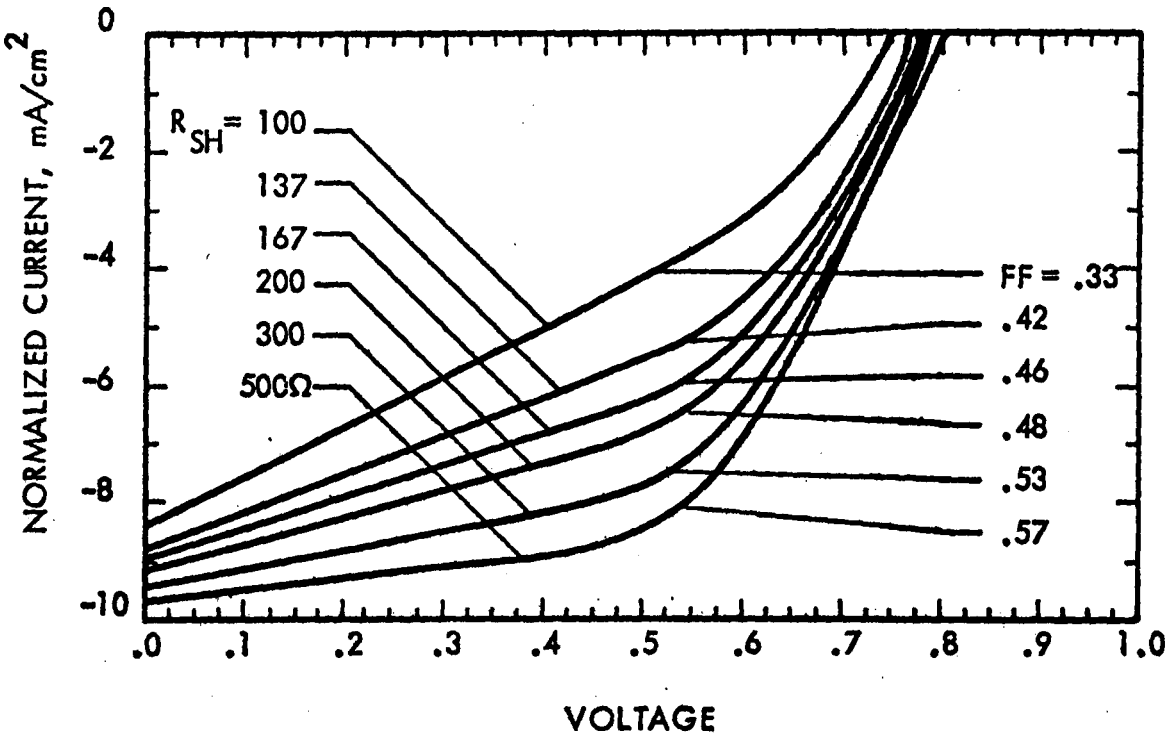

FIGURE 2. CALCULATED LIGHT IV COMPARED WITH EXPERIMENTAL DATA

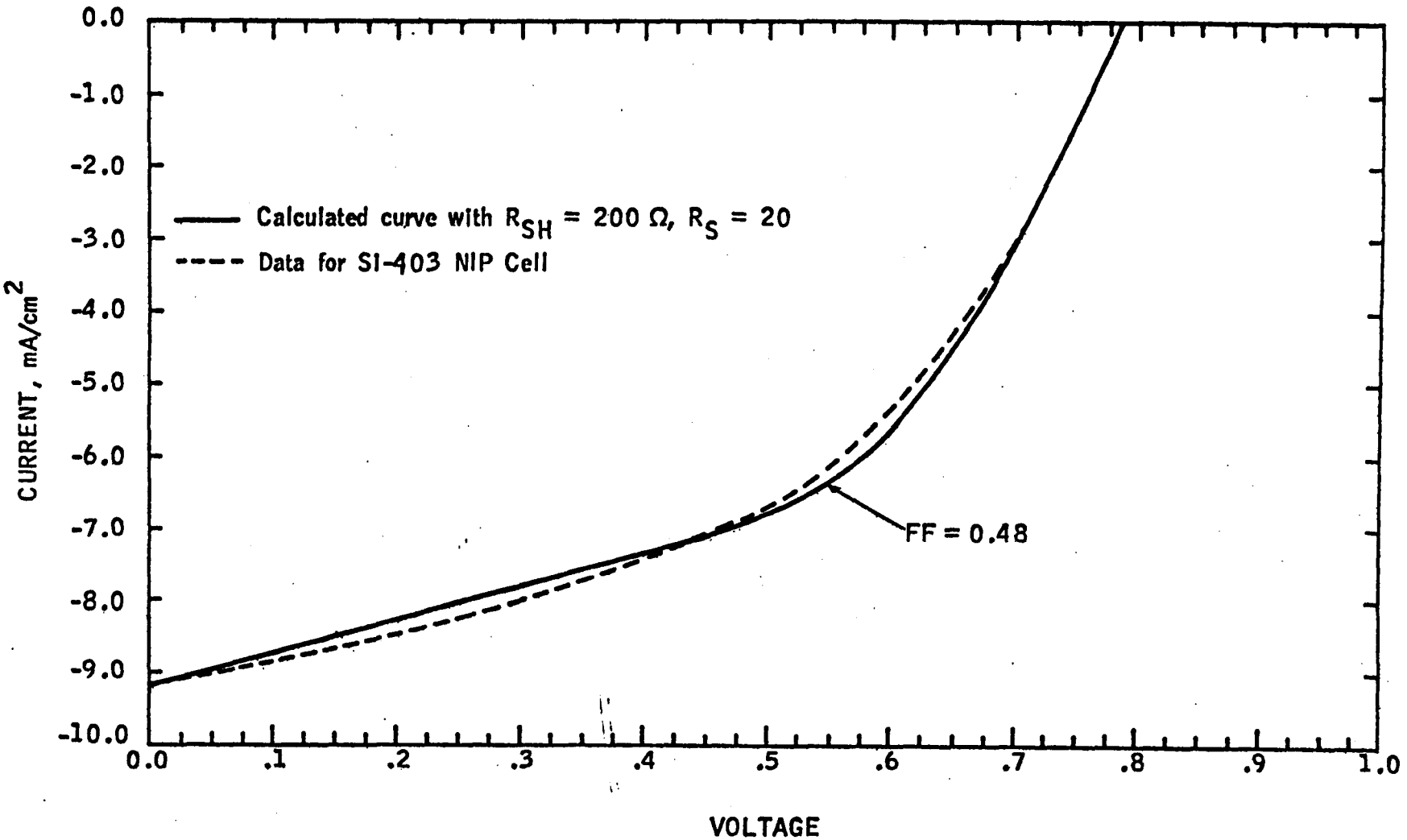

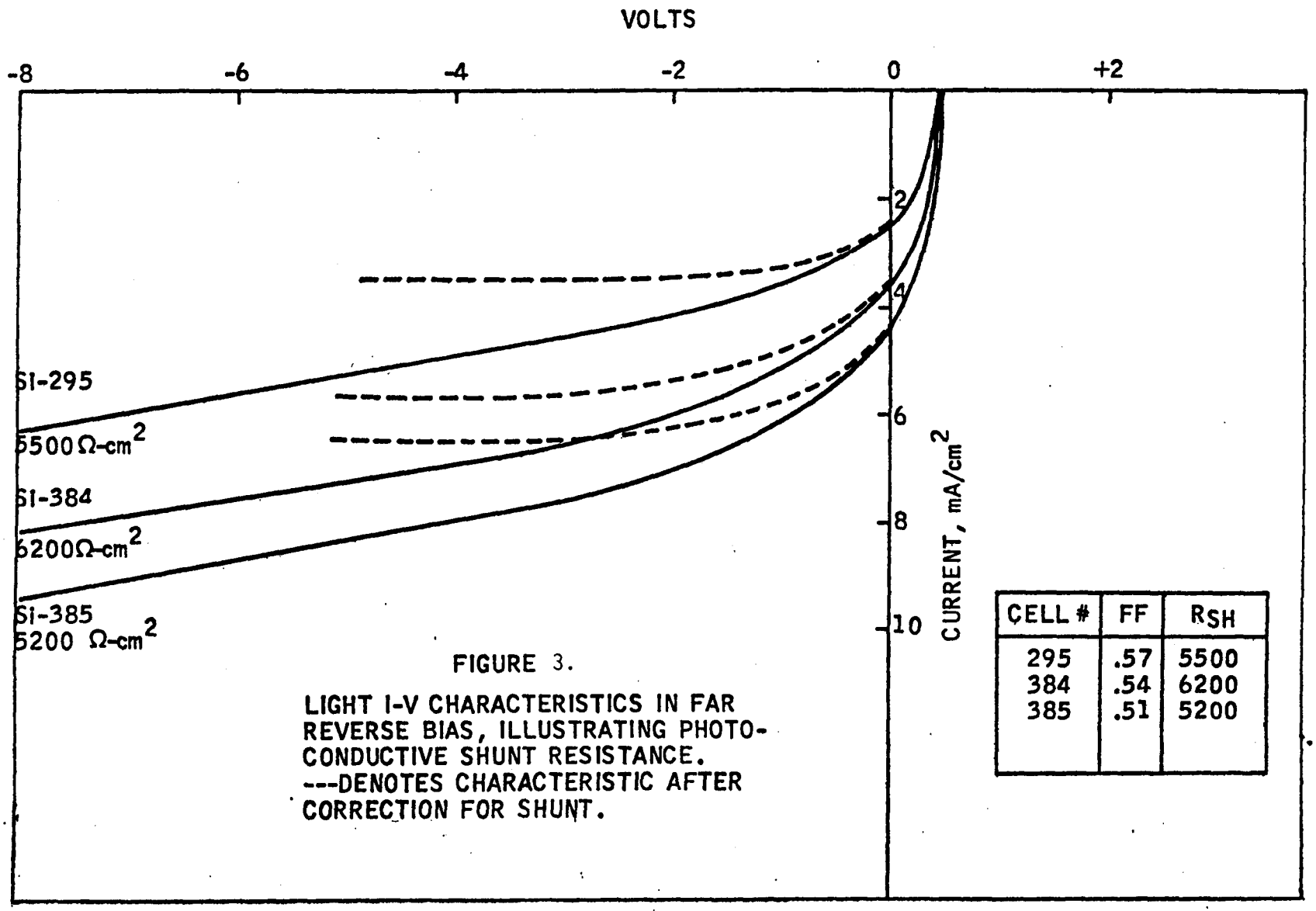

CELL #	FF	R_{SH}
295	.57	5500
384	.54	6200
385	.51	5200

FIGURE 3.

LIGHT I-V CHARACTERISTICS IN FAR REVERSE BIAS, ILLUSTRATING PHOTO-CONDUCTIVE SHUNT RESISTANCE.
---DENOTES CHARACTERISTIC AFTER CORRECTION FOR SHUNT.

FIGURE 4. Comparison of the collection efficiency of two sets of devices made at target voltages of -800V and -1000V. In each set, the hydrogen concentrations in the discharge were, respectively, 10, 12, 15 and 20 percent.

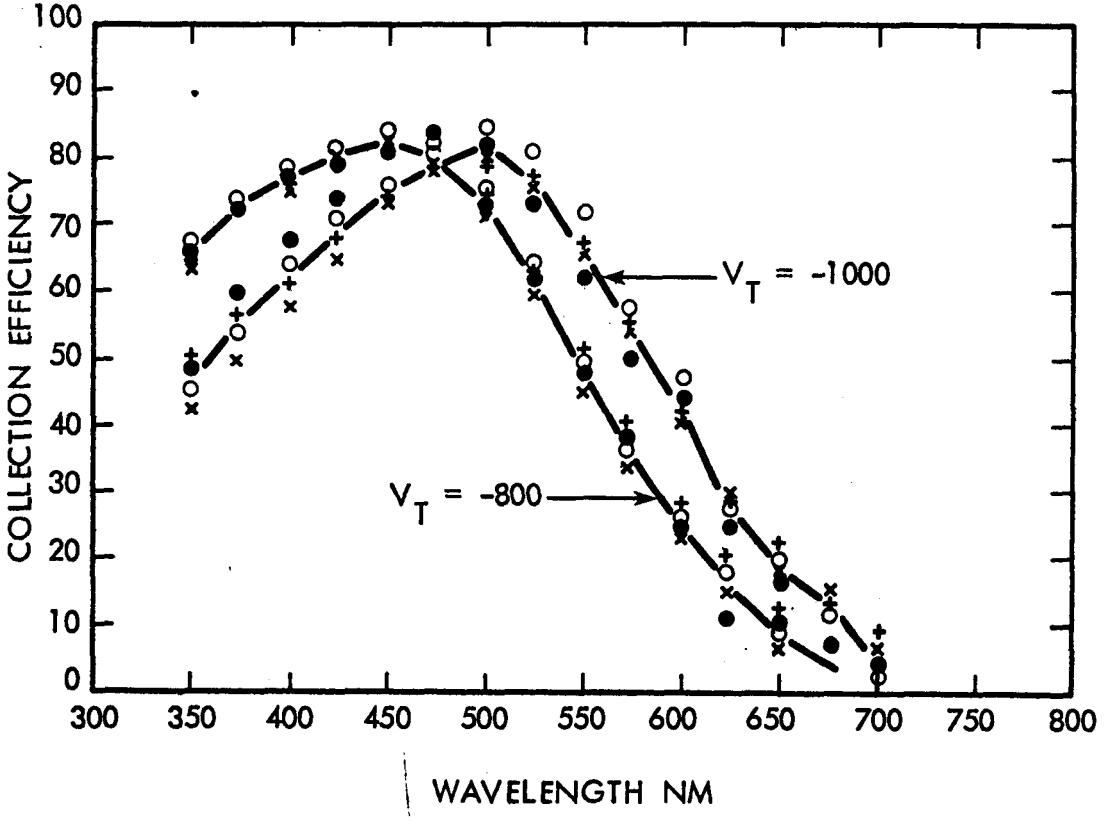

FIGURE 5. The collection width increases as the hydrogen content, and hence the band gap, increases. ● V_T = -1000, ■ V_T = -800.

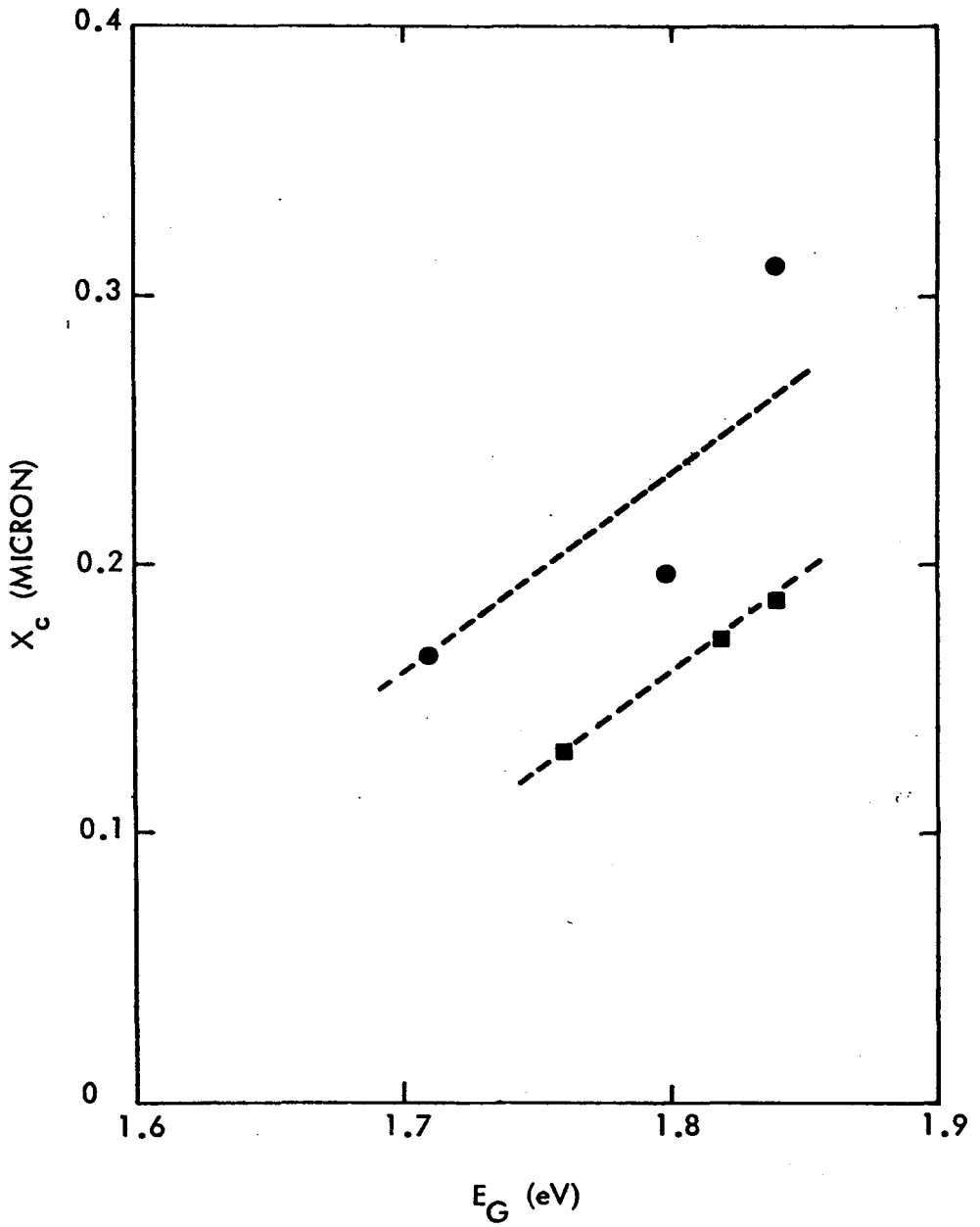

FIGURE 6. Comparison of the current-voltage characteristics of Si-437 (V_T = -1000) and Si-465 (V_T = -800)

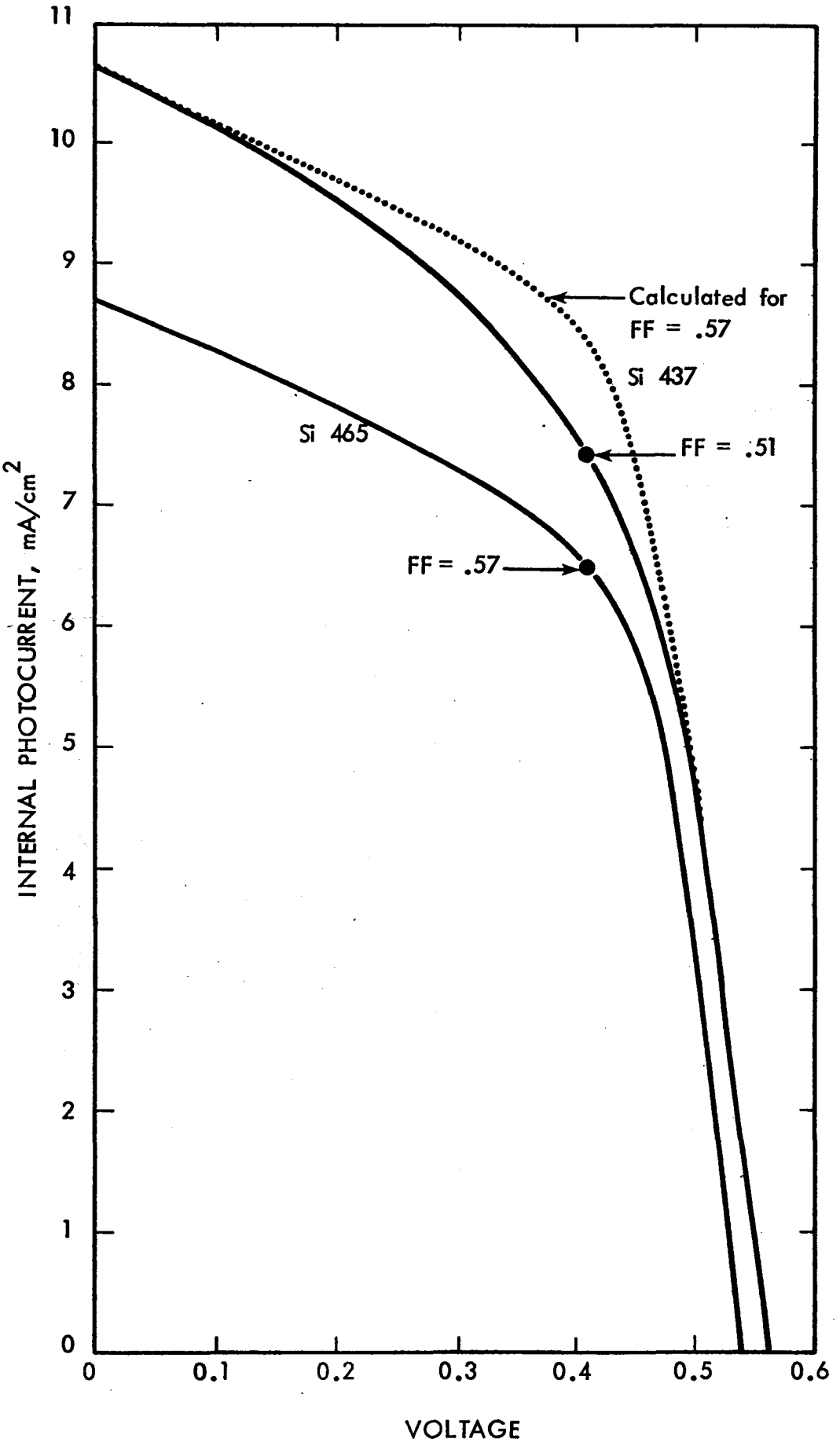

FIGURE 7. Wavelength dependences of the spectral response and of the incremental fill factor for two schottky devices.

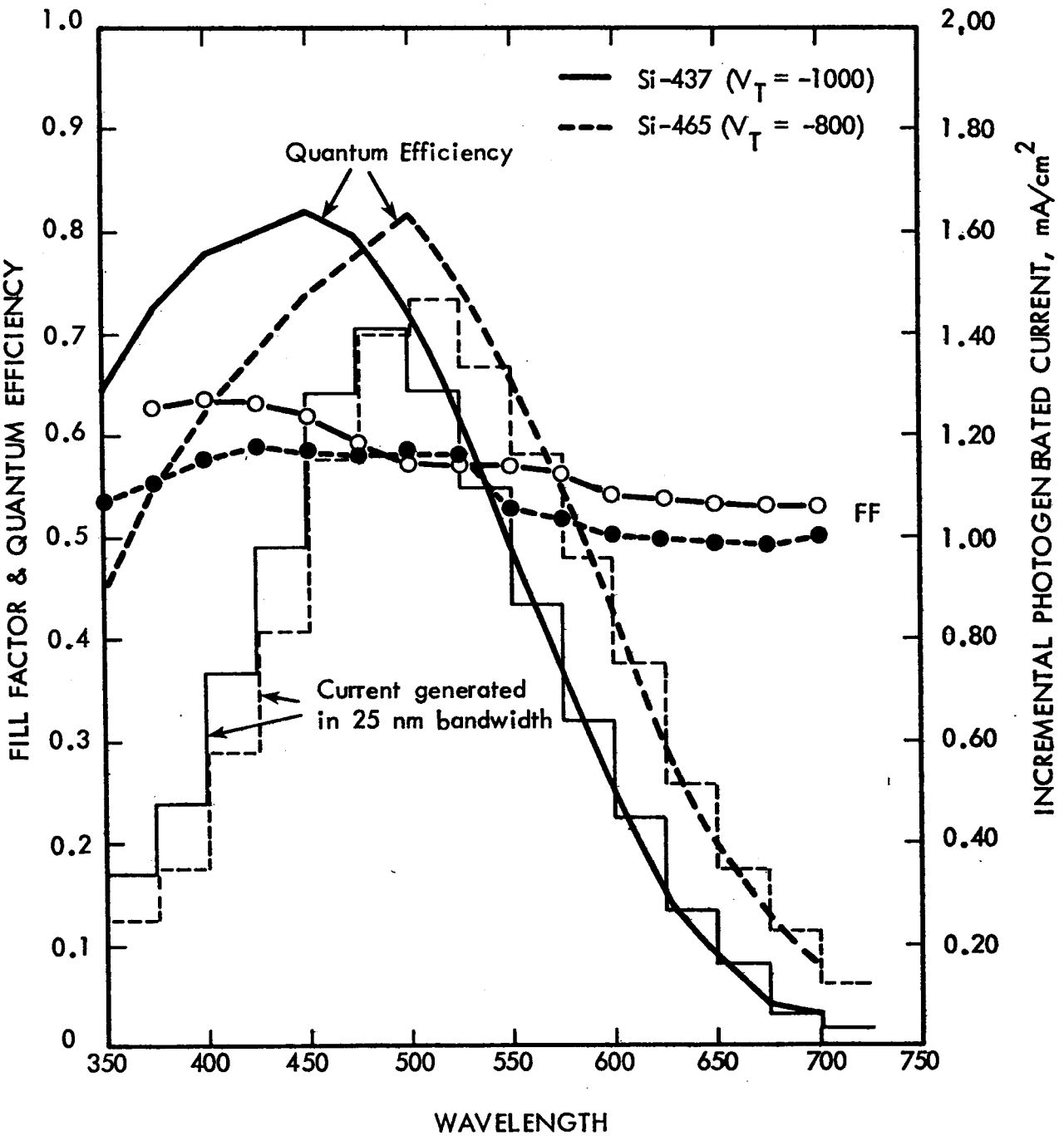

FIGURE 8. Incremental I-V Characteristics taken with Monochromatic Light

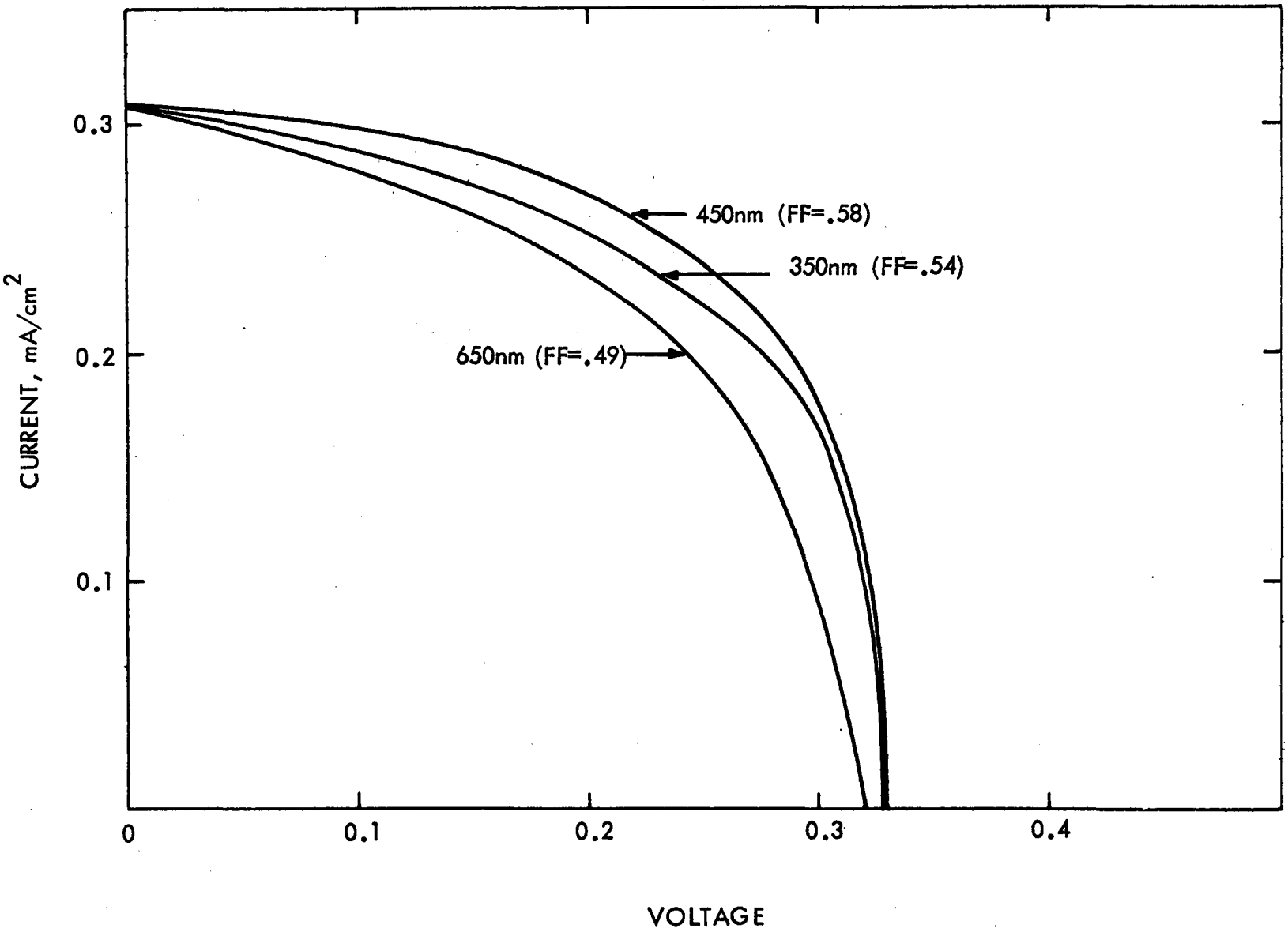

FIGURE 9. Current-voltage characteristics taken with monochromatic light

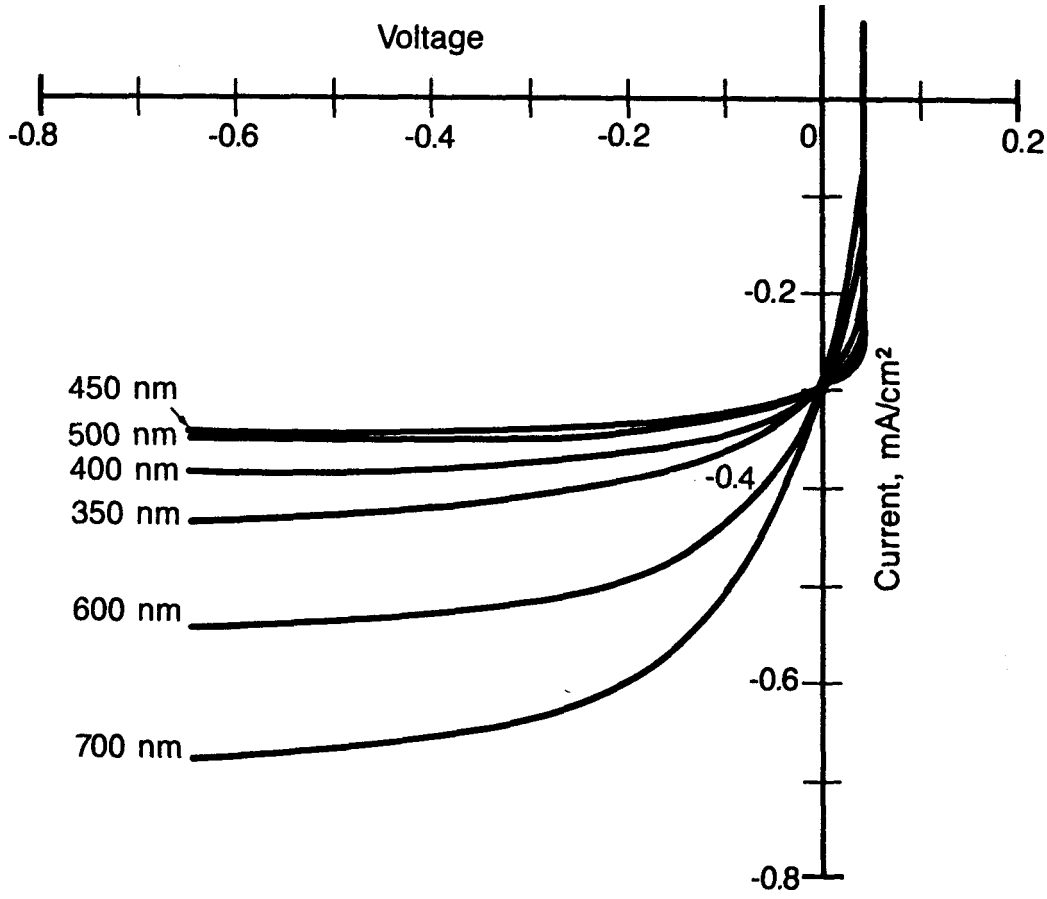

APPENDIX M. Opto-electronic Properties of Boron Compensated Amorphous Silicon Solar Cells

Optoelectronic Properties of Boron Compensated Amorphous Silicon Solar Cells

T. D. Moustakas and C. R. Wronski
Corporate Research Laboratory
Exxon Research and Engineering Company
Clinton Township
Route 22 East
Annandale, New Jersey 08801
(201) 730-3023

The doping of the "intrinsic" region of hydrogenated amorphous silicon (a-Si:H) solar cells with low levels of boron has a large effect on the cell performance. It is generally found that mnominal doping of the intrinsic film with less than 1 ppm of boron has beneficial effects but that higher levels of boron lead to the rapid deterioration of cell performance. This behavior is not currently understood. To obtain insights into the mechanisms responsible for this, the optoelectronic properties have been studied in reactively sputtered a-Si:H films and solar cell structures deposited with less than 1 ppm of B_2H_6 in the Ar-H_2 discharge. Two series of films were investigated because the density of defects and the doping efficiency of a-Si:H films depends on both the hydrogen and the B_2H_6 concentration in the discharge. In one series the level of B_2H_6 was kept constant and the pressure of hydrogen was changed; in the other series, the pressure of hydrogen was kept constant and the level of B_2H_6 was changed.

The doping effect of boron incorporation was determined by the temperature dependence of the dark conductivity. The density of defect states and their role in determining the photovoltaic properties of the material were determined through optical transmission, dual beam photoconductivity[1] and carrier collection efficiency measurements on solar cell structures.

It has been shown[2] that hydrogen incorporation in the undoped amorphous silicon films reduces the density of states in the middle of the gap from about 10^{19} to below 10^{15} states/cm^3 eV. We find, however, that the

presence of small amounts of B_2H_6 iin the Ar-H_2 discharge dramatically affects such a reduction of states in the middle of the gap. This is illustrated in Figure 1 where the optical adsorption is shown for films deposited with 0.4 ppm of B_2H_6 and variable amounts of hydrogen in the discharge. It can be seen in Figure 1 that the optical absorption below approximately 1.3 eV is virtually independent of hydrogen content. This optical absorption is directly related to the densities of deep gap states which have a value of approximately 1×10^{17} states/cm^3 eV. In addition the samples of Figure 1 have a photoconductive mobility-lifetime products for holes of approximately 1×10^{-6} cm^2/V which is also consistent with a density of defects states that is constant and independent of hydrogen. This is in contrast to the optical absorption at high photon energies where the increased hydrogen concentration brings about the same changes as in the case of undoped a-Si:H films.[3] The samples produced at constant hydrogen pressure and variable amounts of B_2H_6 exhibit densities of deep lying defects that increase with B_2H_6 and have a marked effect on both the photo-conductive and ambipolar mobility-lifetime products.

We find that the introduction of boron into the a-Si:H films has two effects on solar cell performance. One is the introduction of acceptor states which compensate residual defect states. This effect is beneficial because it extends the width of the space charge region. The second effect is the introduction of deep lying gap states which act as free carrier recombination centers and hinder carrier collection. The nature and energy distribution of these defects introduced by boron doping is discussed and the relation between doping and hydrogen concentration is identified.

References

1. C. R. Wronski, B. Abeles, T. Tiedje and G. D. Cody, Solid State Comm., 44, 1423, (1982).

2. T. Tiedje, T. D. Moustakas and J. M. Cebulka, Phys. Rev. B, 23, 5634 (1981).

3. T. D. Moustakas, C. R. Wronski and T. Tiedje, Appl. Phys. Lett. 39, 721 (1981).

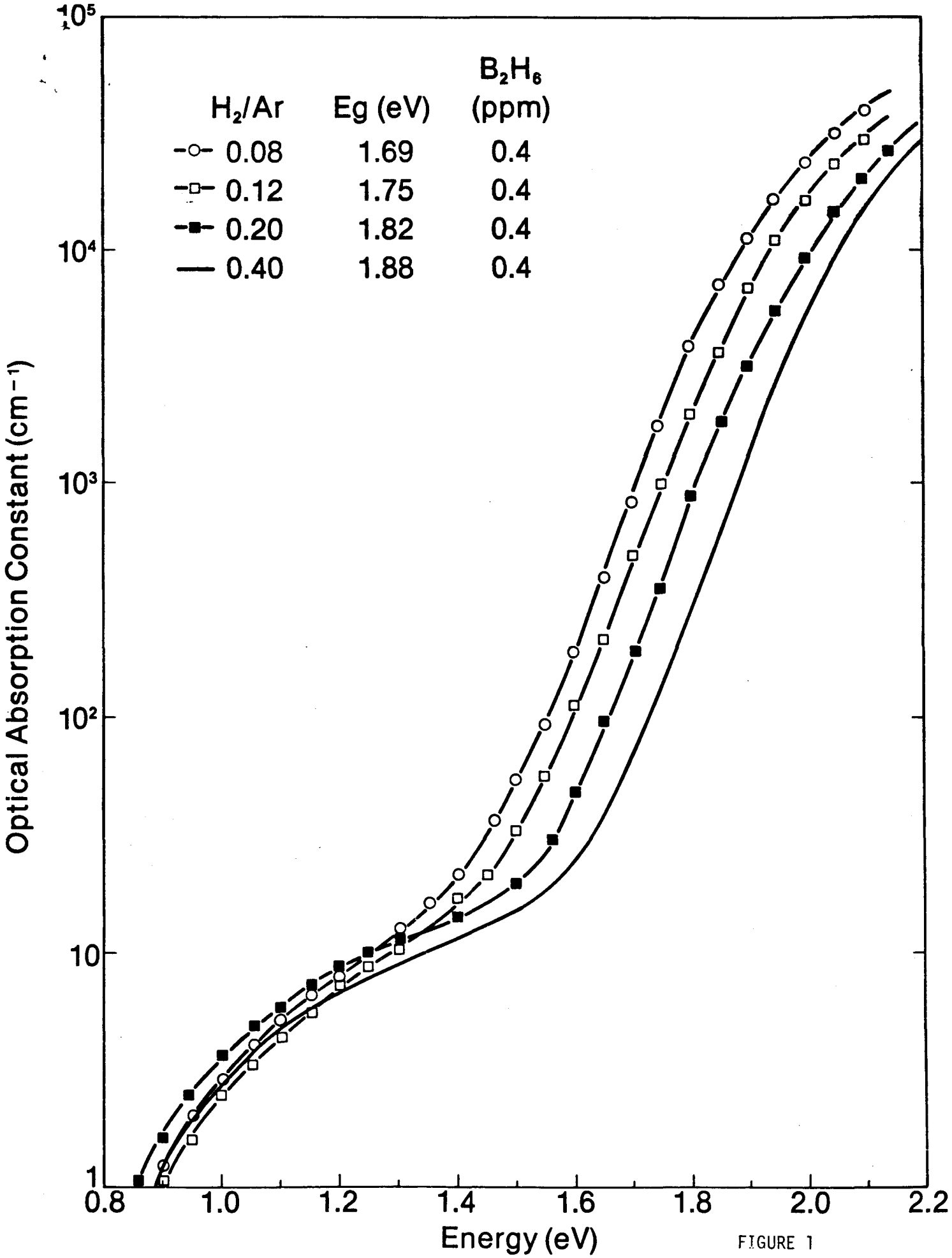
B_2H_6
H_2/Ar
Eg (eV)
(ppm)
0.08
1.69
0.4
0.12
1.75
0.4
0.20
1.82
0.4
0.40
1.88
0.4
Optical Absorption Constant (cm^{-1})
10^5
10^4
10^3
10^2
10
1
0.8
1.0
1.2
1.4
1.6
1.8
2.0
2.2
Energy (eV)

FIGURE 1

Document Control Page	1. SERI Report No. SERI/STR-211-2363	2. NTIS Accession No.	3. Recipient's Accession No.

4. Title and Subtitle
Sputtered Amorphous Silicon Solar Cells

5. Publication Date
September 1984

6.

7. Author(s)
T. D. Moustakas, H. P. Maruska, C. R. Wronski

8. Performing Organization Rept. No.

9. Performing Organization Name and Address
Exxon Research and Engineering Company
Route 22 East
Annandale, New Jersey 08801

10. Project/Task/Work Unit No.
3432.10

11. Contract (C) or Grant (G) No.
(C) ZB-3-02166-01
(G)

12. Sponsoring Organization Name and Address
Solar Energy Research Institute
1617 Cole Boulevard
Golden, Colorado 80401

13. Type of Report & Period Covered
Technical Report

14.

15. Supplementary Notes
Technical Monitor: Ed Sabisky

16. Abstract (Limit: 200 words)

This document reports on research conducted to further develop reactive sputtering of amorphous silicon for solar cell applictions. The major goals of the program were to develop intrinsic material capable of tenerating a short-circuit current density of 12 to 13 mA/Cm^2 and an open-circuit voltage of 0.9; to investigate the mechanism of doping of sputtered a-SiH$_x$ and c-SiHx films and develop methods to dope these layers; to investigate the origin of the low fill factor; to demonstrate a complete p-i-n solar cell structure fabricated totally from silicon targets, without any gas-phase toxic dopants; and to fabricate p-i-n solar cells having efficiencies of 6% or larger. Results showed that the properties of intrinsic and doped sputtered amorphous silicon films can be optimized to produce high-efficiency cells. The photovoltaic properties of the intrinsic films depended on structural and compositional inhomogeneities, amount of incorporated hydrogen, and low levels of dopant impurities. Amorphous and microcrystalline phosphorus- and boron-doped films were characterized through studies of their optical and transport properties; the superiority of the microcrystalline films for photovoltaic applications has been demonstrated. The 5.5% efficiency obtained with the p-i-n solar cell structures can be improved by depositing the three layers in sequential dedicated chambers and by such device design concepts as back reflective contacts and transparent a-SiC front contacts.

17. Document Analysis
a. Descriptors
Amorphous State; Crystal Doping; Crystal Growth; Deposition; Silicon Solar Cells; Sputtering; Thin Films
b. Identifiers/Open-Ended Terms
Photovoltaic Properties

c. UC Categories
63

18. Availability Statement
National Technical Information Service
U.S. Department of Commerce
5285 Port Royal Road
Springfield, Virginia 22161

19. No. of Pages
233

20. Price
A11

Form No. 0069 (3-25-82)